

BIODIESEL FUEL TECHNOLOGY FOR MILITARY APPLICATION

**INTERIM REPORT
TFLRF No. 317**

**By
E.A. Frame
G.B. Bessee
H.W. Marbach, Jr.
U.S. Army TARDEC Fuels and Lubricants Research Facility (SwRI)
Southwest Research Institute
San Antonio, Texas**

**Under Contract to
U.S. Army TARDEC
Petroleum and Water Business Area
Warren, Michigan 48397-5000**

Contract No. DAAK70-92-C-0059

Approved for public release; distribution unlimited

December 1997

DTIC QUALITY INSPECTED 4

19971218 053

Disclaimers

The findings in this report are not to be construed as an official Department of the Army position unless so designated by other authorized documents.

Trade names cited in this report do not constitute an official endorsement or approval of the use of such commercial hardware or software.

DTIC Availability Notice

Qualified requestors may obtain copies of this report from the Defense Technical Information Center, Attn: DTIC-OCC, 8725 John J. Kingman Road, Suite 0944, Fort Belvoir, Virginia 22060-6218.

Disposition Instructions

Destroy this report when no longer needed. Do not return it to the originator.

REPORT DOCUMENTATION PAGE			Form Approved OMB No. 0704-0188	
Public reporting burden for this collection of information is estimated to average 1 hour per response, including the time for reviewing instruction, searching existing data sources, gathering and maintaining the data needed, and completing and reviewing the collection of information. Send comments regarding this burden estimate or any other aspect of this collection of information, including suggestions for reducing this burden, to Washington Headquarters Services, Directorate for Information Operations and Reports, 1215 Jefferson Davis Highway, Suite 1204, Arlington, VA 22202-4302, and to the Office of Management and Budget, Paperwork Reduction Project (0704-0188), Washington, DC 20503.				
1. AGENCY USE ONLY (Leave blank)		2. REPORT DATE December 1997	3. REPORT TYPE AND DATES COVERED Interim July 1994 to May 1996	
4. TITLE AND SUBTITLE Biodiesel Fuel Technology for Military Application			5. FUNDING NUMBERS DAAK70-92-C-0059; WD 34	
6. AUTHOR(S) Frame, Edwin A., Bessee, Gary B., and Marbach, Jr., Howard W.				
7. PERFORMING ORGANIZATION NAME(S) AND ADDRESS(ES) U.S. Army TARDEC Fuels and Lubricants Research Facility (SwRI) Southwest Research Institute P.O. Drawer 28510 San Antonio, Texas 78228-0510			8. PERFORMING ORGANIZATION REPORT NUMBER TFLRF No. 317	
9. SPONSORING/MONITORING AGENCY NAME(S) AND ADDRESS(ES) U.S. Army TARDEC Petroleum and Water Business Area Warren, MI 48397-5000			10. SPONSORING/MONITORING AGENCY REPORT NUMBER	
11. SUPPLEMENTARY NOTES				
12a. DISTRIBUTION/AVAILABILITY STATEMENT Approved for public release; distribution unlimited			12b. DISTRIBUTION CODE	
13. ABSTRACT (Maximum 200 words) This program addressed the effects of biodiesel (methyl soyate) and blends of biodiesel with petrofuels on fuel system component and material compatibility, fuel storage stability, and fuel lubricity. Biodiesel was found to have excellent lubricity properties and was effective at 1 volume percent (vol%) blend in improving the lubricity of Jet A-1 fuel. The following potential problem areas associated with methyl soyate use were identified: storage stability, compatibility with some metals, and compatibility with nitrile elastomers.				
14. SUBJECT TERMS Biodiesel Fuel Properties Storage Stability Materials Compatibility Elastomers Fuel Filters Fuel Lubricity			15. NUMBER OF PAGES 309	
			16. PRICE CODE	
17. SECURITY CLASSIFICATION OF REPORT Unclassified	18. SECURITY CLASSIFICATION OF THIS PAGE Unclassified	19. SECURITY CLASSIFICATION OF ABSTRACT Unclassified	20. LIMITATION OF ABSTRACT	

EXECUTIVE SUMMARY

Problem: Diesel fuel is essential for maintaining military ground equipment mobility. The supply of diesel fuel available to the military would be increased if agriculturally derived material such as methyl soyate (biodiesel) were found to be acceptable for use in military equipment.

Objective: The objective of this program was to investigate the application of methyl soyate-based biodiesel fuel as an alternative fuel component for military ground equipment.

Importance of Project: Use of methyl soyate as a diesel fuel component would reduce the use of imported refined fuels and crude oils and assist in developing an infrastructure for alternative fuels. Another potential benefit of biodiesel use is reduction of equipment exhaust emissions.

Technical Approach: The thrust of this investigation was directed towards assessing fuel system material compatibility, fuel stability, and lubricity effects of neat methyl soyate and blends with petrofuels.

Accomplishments: Results of the investigation showed acceptable performance of methyl soyate and petrofuel blends with elastomer compatibility (with respect to most elastomers), fuel lubricity, most physical properties, and fuel filter and coalescer performance. The following potential problem areas associated with methyl soyate use were identified: storage stability, compatibility with some metals, and compatibility with nitrile elastomer.

Military Impact: Successful fielding of biodiesel in CONUS operations will extend the fuel supply, support infrastructure for alternative fuel, and potentially reduce exhaust emissions.

Preceding Page Blank

FOREWORD/ACKNOWLEDGEMENTS

This work was performed by the U.S. Army TARDEC Fuels and Lubricants Research Facility (TFLRF) located at Southwest Research Institute (SwRI), San Antonio, TX, during the period July 1994 to May 1996 under Contract No. DAAK70-92-C-0059. The work was funded by the U.S. Department of Agriculture, USDA-CSRS-SP (Ms. Carmela Bailey), Washington D.C., U.S. Army Natick RD&E Center (Dr. H. Schreuder-Gibson), Natick MA, and U.S. Army TARDEC, Warren, MI. Mr. T.C. Bowen (AMSTA-RBFF) of MTCB served as the contracting officer's representative. Mr. M.E. LePera (AMSTA-RBF) of MTCB served as the project technical monitor.

The authors would like to acknowledge the assistance of Dr. P.I. Lacey and the efforts of the TFLRF chemistry staff, including Dr. G.E. Fodor, Mr. S.R. Westbrook, Mr. K.E. Hinton, and Ms. M.S. Voigt. Technical support was provided by Messrs. M.R. Gass, R.E. Grinstead, W.K. Groff, and J.P. Fey. Finally, the authors wish to thank Mr. J.H. Marshall for operations management in support of this project and Ms. M.M. Clark for report preparation.

TABLE OF CONTENTS

<u>Section</u>	<u>Page</u>
I. INTRODUCTION AND BACKGROUND	1
II. OBJECTIVES AND APPROACH	2
III. PROPERTIES OF TEN-FUEL MATRIX	2
IV. STORAGE STABILITY	12
A. Total Acid Number (TAN) by ASTM D 664	13
B. Color by ASTM D 1500	18
C. Steam Jet Gum by ASTM D 381	18
D. Jet Fuel Thermal Oxidation Test (JFTOT) by ASTM D 3241	20
E. Water Content by ASTM D 4928	22
V. STORAGE STABILITY CONCLUSIONS	25
A. Storage Stability by ASTM D 4625	25
B. Total Acid Number (TAN) by ASTM D 664	25
C. Color by ASTM D 1500	25
D. Steam Jet Gum by ASTM D 381	25
E. Jet Fuel Thermal Oxidation Test (JFTOT) by ASTM D 3241	26
F. Water Content by ASTM D 4928	26
VI. MATERIAL COMPATIBILITY	26
A. Elastomer Compatibility	27
1. Literature Search	27
2. Test Procedure and Results	28
B. Metal Compatibility	34
1. Literature Search	34
2. Storage Tests	35
C. Fuel Filters	54
1. Literature Search	54
2. Test Procedure and Results	54
D. Conclusions	58

TABLE OF CONTENTS, CONT'D

<u>Section</u>	<u>Page</u>
VII. ADDITIVE COMPATIBILITY	59
VIII. FUEL LUBRICITY EVALUATIONS WITH BIODIESEL	61
A. Laboratory Wear Tests	61
1. U.S. Army Scuffing Load Wear Test	61
2. High-Frequency Reciprocating Rig (HFRR) Tests	62
B. Results	63
C. Lubricity Effects With Storage Time	66
D. Pump Stand Evaluations	67
E. Procedure	68
F. Results of Pump Stand Evaluations	70
IX. CONCLUSIONS	79
A. Properties of Ten-Fuel Matrix	79
B. Storage Stability	79
C. Material Compatibility	79
1. Elastomers	79
2. Metals	80
3. Filters	80
D. Additive Compatibility (JP-8 Additives)	80
E. Fuel Lubricity	80
X. RECOMMENDATIONS	81
XI. LIST OF REFERENCES	81

APPENDICES

A. STATEMENT OF WORK for Biodiesel Fuel Evaluation	87
B. Elastomer Tensile Strength	95
C. Elastomer Elongation	129
D. Shore A Hardness and Swell of Evaluated Materials	163
E. Total Acid Number (TAN)	175

TABLE OF CONTENTS, CONT'D

<u>Section</u>	<u>Page</u>
F. 6.2L GM Single-Pass Filter Evaluation	189
G. HMMWV Single-Pass Filter Evaluation	225
H. SAE J1839 Coarse Droplet Fuel/Water Separation Evaluations	259
I. Fuel Properties	273
J. 200-Hour Pump Stand Evaluation of Stanadyne Fuel Injection Pumps Using Fuel AL-24252	277
K. 200-Hour Pump Stand Evaluation of Stanadyne Fuel Injection Pumps Using Fuel AL-24322	295

LIST OF ILLUSTRATIONS

<u>Figure</u>	<u>Page</u>
1 Effect of biodiesel on cloud point	8
2 Effect of biodiesel on freeze point	8
3 Effect of biodiesel on net heat of combustion	9
4 Effect of biodiesel on 50% distillation point	9
5 Effect of biodiesel on 90% distillation point	10
6 Microseparometer results for the ten fuels	11
7 Effect of biodiesel on cetane number	12
8 Total insolubles	15
9 Total acid number	17
10 Water content	23
11 Fuels and copper coupons after six-month storage at 51.6°C	39
12 Fuels and brass coupons after six-month storage at 51.6°C	41
13 Fuels and bronze coupons after six-month storage at 51.6°C	43
14 Fuels and steel coupons after six-month storage at 51.6°C	45
15 Fuels and cast aluminum coupons after six-month storage at 51.6°C	47
16 Fuels and aluminum coupons after six-month storage at 51.6°C	49
17 FTIR analysis of neat biodiesel	51
18 FTIR analysis of LSRD-4	51
19 FTIR analysis of Reference DF-2	52
20 FTIR analysis of JP-8	52
21 FTIR analysis of solid material recovered from 20% BD + 80% JP-8 blend stored in the presence of brass	53
22 FTIR analysis of 30% BD + 70% JP-8 blend stored in the presence of steel	53
23 High-frequency reciprocating rig	62
24 Scuffing load increase in SLWT	63
25 Wear decrease in HFRR	64
26 Fuel lubricity by SLWT	64
27 Fuel lubricity by HFRR	65
28 Lubricity improvement with biodiesel	65
29 Fuel system schematic	69
30 Transfer pump pressure percent decrease at 1,000 rpm	73
31 Transfer pump pressure percent decrease at 2,100 rpm	74
32 Injection advance decrease degrees at 1,000 rpm	74
33 Average visual pump wear rating	77

LIST OF TABLES

<u>Table</u>	<u>Page</u>
1 Ten-Fuel Matrix	5
2 Fuel Inspection Properties	6
3 Storage and Thermal Stability Properties by ASTM D 4625	14
4 Total Acid Number Results	17
5 Color Results	18
6 Steam Jet Gum Results	19
7 JFTOT Biodiesel Blends	21
8 Water Content Percent Results	22
9 Changes in Tensile Strength	30
10 Changes in Elongation	32
11 Summary of Hardness and Swell Characteristics	34
12 TAN Results, Six Months, at 51.6°C	36
13 Visual Ratings, Metal Coupons, Six Months	36
14 Additized Jet A Fuel Blends	60
15 TAN's for New JP-8 Blends	60
16 Ten-Fuel Matrix	61
17 U.S. Army Scuffing Load Wear Test Data	66
18 High-Frequency Reciprocating Rig Data	67
19 Description of 200-hr Pump Stand Tests	68
20 Biodiesel Blend Properties	68
21 Pre-Test Pump Delivery	71
22 Pre-Test Transfer Pump Pressure	71
23 Pre-Test Injection Advance Measurement	71
24 Pre-Test Sundry Measurements	71
25 Post-Test Pump Delivery	72
26 Post-Test Transfer Pump Pressure	72
27 Post-Test Injection Advance Measurement	72
28 Post-Test Sundry Measurements	72
29 Visual Wear Level on Critical Pump Components	76
30 Wear Volume on Selected Pump Components ($\text{mm}^3 \times 10^{-3}$)	77
31 Archard's Wear Coefficient	78

I. INTRODUCTION AND BACKGROUND

The use of agriculturally derived fuel components is of interest to the military for ground equipment applications. While the term "biodiesel" may refer to any of the bioderived diesel fuels, biodiesel (BD) within the content of this report will refer specifically to methyl soyate (MS), which is composed of methyl esters of soya bean-derived oil. Potential benefits associated with BD use include reduction in the use of imported refined fuels and crude oils, assistance in creating the demand for an alternate fuel infrastructure, and reduction in some engine exhaust emissions.

In October of 1993, an overall program for investigating the use of BD in military ground equipment was prepared. The overall program consisted of five phases and is presented in Section XII. This report covers Phase 1, Materials Compatibility, and most of Phase 2, Fuel Blend Characteristics. Phases 3 through 5 remain to be funded.

Technical literature was reviewed to ensure that the Army BD program did not duplicate previous work. Recent papers covered exhaust emission effects when using BD and BD blends with petrofuels. McDonald et al reported diesel exhaust particulate matter reduction when using neat BD and 30% BD blend in a Caterpillar 3304, prechamber, naturally aspirated engine.(1)* Scholl and Sorenson reported that "in terms of combustion behavior and exhaust emission characteristics, MS can basically be regarded as interchangeable with diesel fuel."(2) This work was conducted in a four-cylinder, four-stroke, naturally aspirated, direct-injected diesel engine, and use of BD resulted in lower hydrocarbon emissions and reduced smoke number than DF-2 at optimum operating conditions. Thus, both direct- and indirect-injected combustion chamber configurations showed improvement in reduced exhaust emissions when using BD. Holmberg and Peeples provided an excellent overall review and summary of previous research efforts with biodiesel fuels.(3) Research in the following areas was reviewed and abstracted:

* Underscored numbers in parentheses refer to the list of references at the end of this report.

- Exhaust emissions
- Engine materials compatibility
- Durability and impact on lubricants
- Maintenance recommendations
- Coking and injector tip fouling
- Torque and power output
- Fuel characteristics.

Areas of concern for military ground equipment use of BD were carefully reviewed. This review confirmed the need for additional research in the areas of storage stability, materials compatibility, fuel additive compatibility, and fuel lubricity effects.

II. OBJECTIVES AND APPROACH

The objective of this program was to investigate the application of methyl soyate-based BD fuel as an alternative fuel component for military ground equipment. The approach was to conduct investigations concerning the effect of neat BD and BD blends in the following technical areas:

- Storage stability
- Fuel system materials short-term compatibility
 - Elastomers
 - Metals
 - Filters
- Fuel lubricity
- Fuel additive compatibility

The methodology for investigating each of these technical areas will be presented and discussed in the respective sections of this report.

III. PROPERTIES OF TEN-FUEL MATRIX

The original fuel matrix was proposed that included methyl soyate blended into both low sulfur diesel fuel (on-highway applications) and high sulfur diesel fuel (off-highway applications such as construction equipment, etc) at both 20 and 30 volume percent.

The rationale for this fuel selection matrix was:

- Both low sulfur (0.05 % or less) and high sulfur (0.05-0.50%) diesel fuel were selected as potential markets for Biodiesel fuel within DoD and will include off-highway as well as on-highway applications. (Note: Defense Fuel Supply Center was procuring both types for DoD agencies.)
- High sulfur diesel fuel, with its somewhat lower degree of refinement processing, may surface more potential compatibility and blending problems.

The reasons for using both 20 and 30 percent blending ratios was:

- Actual ratio of methyl soyate to diesel fuel had not yet been standardized and regulated by EPA.
- Use of two blending ratios provides means to extrapolate between data points should some characteristics show marginal results.
- Initial results from emissions testing had shown 30 percent blends to give significant lowering of emissions over those 20 percent blends.

Initially, JP-8 was not included in the test fuel matrix. The reasons for not considering JP-8 in the fuel matrix were:

- A limitation existed on availability of resources for this Biodiesel Fuel Program.
- JP-8 is not a diesel/distillate fuel, but instead a kerosene.
- JP-8 is the single fuel on the battle field, intended only for forces operating in OCONUS forward areas once deployed.
- JP-8 will not be found in all Army installations within CONUS; only those relegated to training (k.e., Ft. Irwin CA) and those selected few locations where mobilization sites have been identified such as Ft. Hood TX, and Ft. Bliss TX.
- Primary fuels for powering diesel fueled vehicles/equipment within the CONUS post-camp-station DoD installations are both low and high sulfur diesel fuels.

- In those few locations where JP-8 is used as the single fuel, blending with methyl soyate would totally defeat the single fuel concept because the blend could not be used in Army aircraft. Hence, the whole purpose of "training with the fuel that is to be used in combat would be lost."

JP-8 fuel was eventually added to the test fuel matrix at the request of other U.S. Army organizations.

In this program, a ten-fuel matrix was used for the storage stability and materials compatibility investigations. Description of the ten-fuel matrix is presented in TABLE 1. The low-sulfur diesel fuel used was LSRD-4, a standard reference diesel fuel that is widely used to define diesel engine lubricant performance. It contains 0.04 wt% sulfur. The off-road diesel fuel used was reference DF-2, commonly referred to as "Cat fuel." Reference DF-2 is a straight-run, mid-range natural sulfur fuel. The JP-8 fuel was obtained from Kelly Air Force Base, San Antonio, TX. The neat biodiesel (methyl soyate) was supplied by Midwest Biofuels, Inc., Kansas City, KS. The initial drums received were analyzed and found to contain 0.08 wt% sulfur and 762 ppm water. Both values were greater than the maximum allowed for methyl soyate as stated in American Society of Agricultural Engineers draft engineering practice document.(4) Investigations by the biodiesel supplier revealed that an incorrect material had inadvertently been supplied. The drums were returned, and the replacement biodiesel (AL-23395-F) was found to be in specification for sulfur content. This sample was slightly higher in water content (639 ppm) than the specification requirement of 500 ppm water maximum; however, the decision was made to use the sample for the program.

TABLE 1. Ten-Fuel Matrix

<u>Fuel No.</u>	<u>Code</u>	<u>Description</u>
1	AL-23395-F	Biodiesel (Methyl Soyate)
2	AL-23403-F	Low-Sulfur Diesel Fuel, LSRD-4
3	AL-23404-F	Reference DF-2
4	AL-22363-F	JP-8
5	AL-23405-F	20%* Biodiesel + 80% Low-Sulfur Diesel Fuel
6	AL-23406-F	30% Biodiesel + 70% Low-Sulfur Diesel Fuel
7	AL-23407-F	20% Biodiesel + 80% Ref. DF-2
8	AL-23408-F	30% Biodiesel + 70% Ref. DF-2
9	AL-23409-F	20% Biodiesel + 80% JP-8
10	AL-23410-F	30% Biodiesel + 70% JP-8

* All blends were volume percent (vol%).

Inspection analyses of the ten fuels in the matrix are presented in TABLE 2. Compared to diesel fuel and kerosene, neat biodiesel has a higher flash point; slightly higher viscosity; higher cloud, pour and freeze points; lower heat of combustion; and a relatively narrow distillation range. These characteristics are carried over in the blends of biodiesel and petrofuel. Lubricity effects of biodiesel are discussed in a separate section of this report. Plots of selected key fuel properties are presented to illustrate the effect of 20 and 30 vol% biodiesel on blend properties in the three petrofuels. Figure 1 shows the cloud points of the ten-fuel matrix, while Fig. 2 shows freeze points. In both plots, it is evident that BD raises the cloud and freeze points of the petrofuel blends. Because biodiesel has a lower net heat of combustion than the petrofuels, the blends have correspondingly reduced net heat of combustion, as shown in Fig. 3. The effect of biodiesel in raising the 50 and 90 percent distillation points of the blends is illustrated in Figs. 4 and 5, respectively.

TABLE 2. Fuel Inspection Properties

Fuel No. AL- Code	1 23395	2 23403	3 23404	4 22363	5 23405	6 23406	7 23407	8 23408	9 23409	10 23410
Property	Method									
Gravity, API°	28.5	34.7	35.0	43.9	33.6	32.8	33.7	32.9	40.6	38.7
Density, 15°C, kg/L	0.8839	0.8509	0.8494	0.8064	0.8566	0.8613	0.8597	0.8603	0.8218	0.8310
Flash Point, °C	163.5	74	75.5	47.5	76	78.5	79.5	82.5	50	51.5
Cloud Point, °C	-4.2	-17.9	-9.4	-55.5	-16.1	-14.9	-8.7	-8.4	-27.2	-22.1
Pour Point, °C	-9	-27	-18	-69	-24	-30	-27	-30	-45	-33
Freeze Point, °C	+5.9	-14.8	-5.9	-53.2	-12.7	-11.3	-5.7	-5.2	-16.9	-11.1
Kinematic Viscosity, 40°C, cSt	4.00	2.48	2.90	1.30	2.77	2.92	3.11	3.20	1.62	1.87
Color	<0.5	<0.5	0.5	0.5	0.5	0.5	0.5	0.5	0.5	0.5
Cetane Number	49.3	51.3	52.0	47.7	52.5	53.6	52.9	54.1	52.3	53.0
Hydrogen, mass%	11.77	12.94	13.00	13.91	12.82	12.66	12.83	12.64	15.35	13.19
Carbon, mass%	76.99	86.84	86.33	85.97	84.64	83.86	84.38	83.27	83.96	82.75
Net Heat of Combustion										
MJ/kg	37.26	42.73	42.59	42.99	41.52	41.06	41.52	40.95	41.77	41.01
BTU/lb	16,017	18,372	18,309	18,481	17,851	17,651	17,852	17,605	17,956	17,632
Steam Jet Gum, mg/100 mL	1345.3	0.7	1.6	1.2	115.3	328.3	61.3	138.6	86.6	248.1
TAN	0.15	0.01	0.05	0.01	0.07	0.11	0.09	0.12	0.04	0.09
Total Water by Karl Fischer, ppm	639	46	104	44	122	167	147	206	114	157
Total Aromatics by SFC, wt%	*	29.9	27.6	20.2	29.9	30.0	28.0	27.7	20.3	20.4
Monoaromatics	*	20.4	16.3	17.7	20.5	20.6	16.6	16.7	17.8	17.9
Diaromatics	*	8.9	10.2	2.5	8.8	8.8	10.2	9.9	2.5	2.5
Polyaromatics	*	0.6	1.1	0.02	0.6	0.6	1.2	1.1	<0.1	<0.1
Total Sulfur, mass%	<0.01	0.04	0.37	0.05	0.03	0.03	0.28	0.23	0.04	0.03
HFRR, mm	0.270	0.195	0.450	0.685	0.190	0.175	0.135	0.135	0.260	0.190
Scuffing Load Wear Test, g	6000	3900	4700	1850	4175	6000	5100	5100	4950	6000
Standard BOCLE, mm	0.68	0.57	0.58	0.55	0.55	0.58	0.54	0.58	0.54	0.61
Microseparator	99	96	75	00	100	94	00	55	56	21
JFTOT Deposit Volume, mm ³	0.013	0.022	0.143	0.003	0.004	0.007	0.003	0.001	<0.001	0.001

TABLE 2. Fuel Inspection Properties, cont'd

Fuel No. AL- Code	1	2	3	4	5	6	7	8	9	10
	23395	23403	23404	22363	23405	23406	23407	23408	23409	23410
Property	Method									
Distillation, °C at % Off	D 86									
Initial	317	188	205	159	193	193	205	204	163	161
10	334	215	237	180	221	226	244	247	183	186
50	337	259	271	204	277	290	287	296	215	228
90	348	317	321	236	332	335	335	338	334	338
95	347	332	340	246	339	341	344	345	339	340
Final	347	344	357	260	346	346	352	350	343	343
Residue, wt%	0	1.9	1.5	1.0	1.3	1.3	1.3	2.1	1.2	1.2

* Unable to analyze

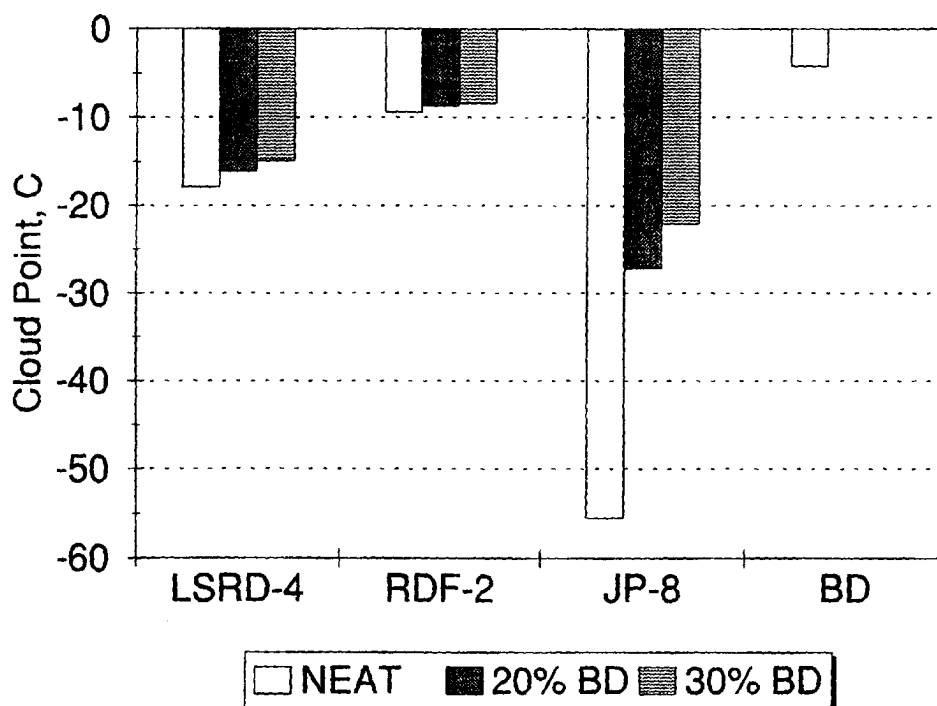


Figure 1. Effect of biodiesel on cloud point

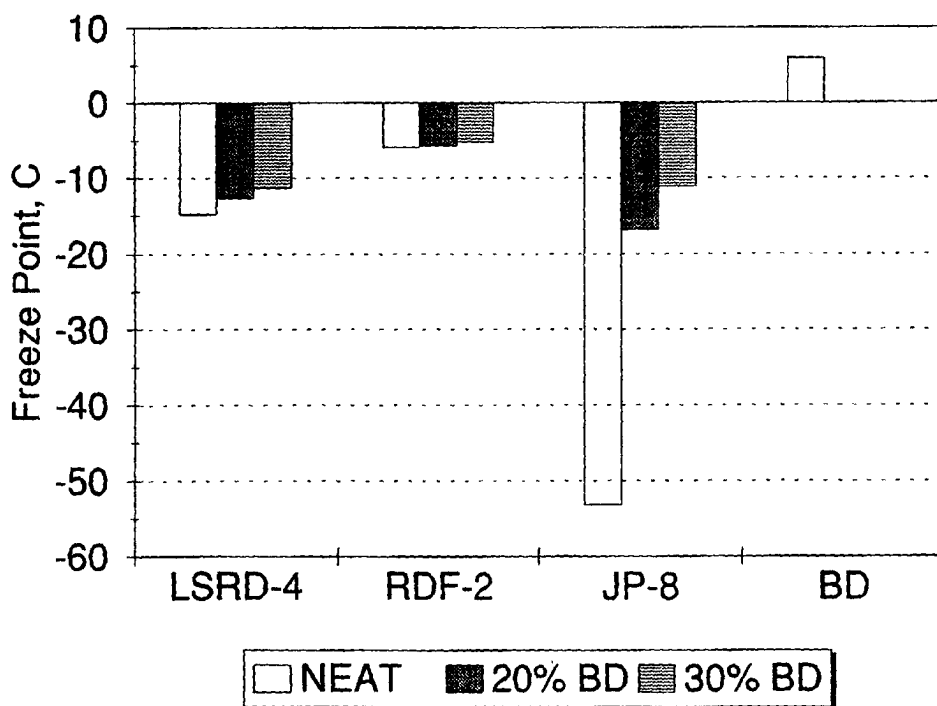


Figure 2. Effect of biodiesel on freeze point

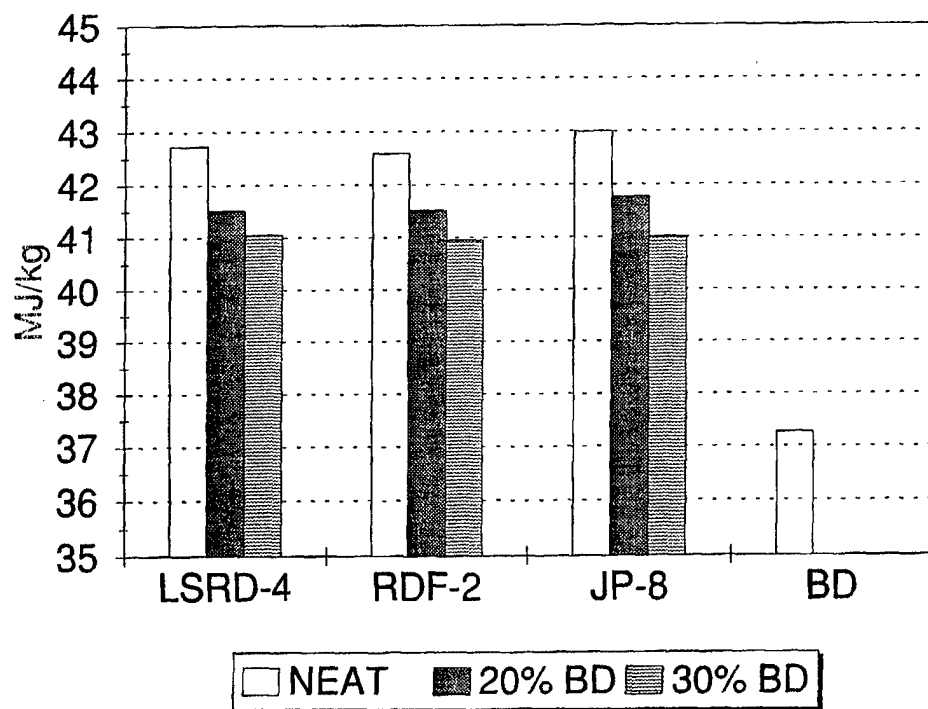


Figure 3. Effect of biodiesel on net heat of combustion

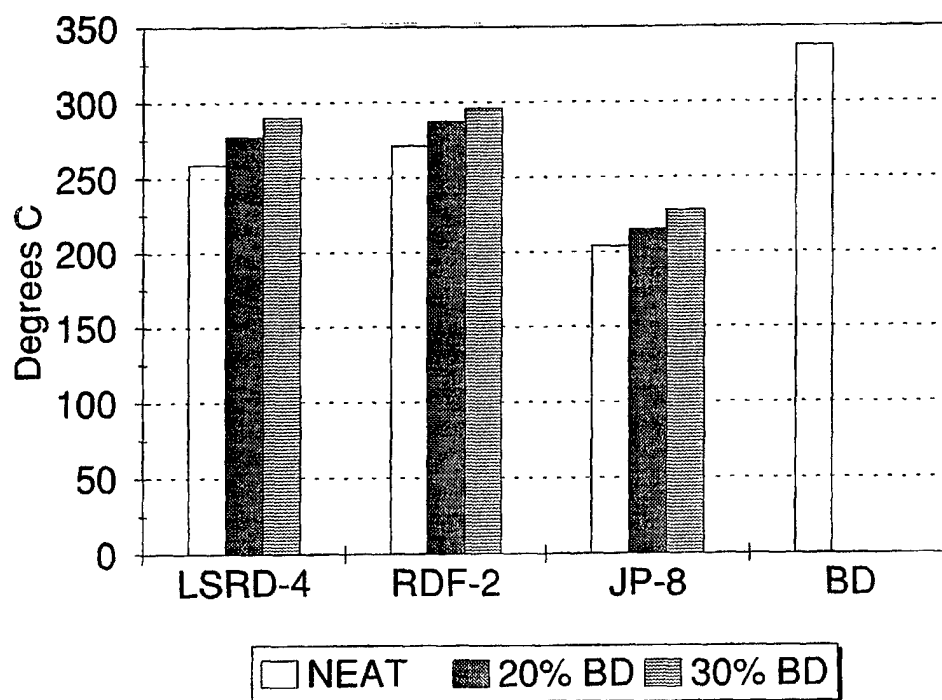


Figure 4. Effect of biodiesel on 50% distillation point

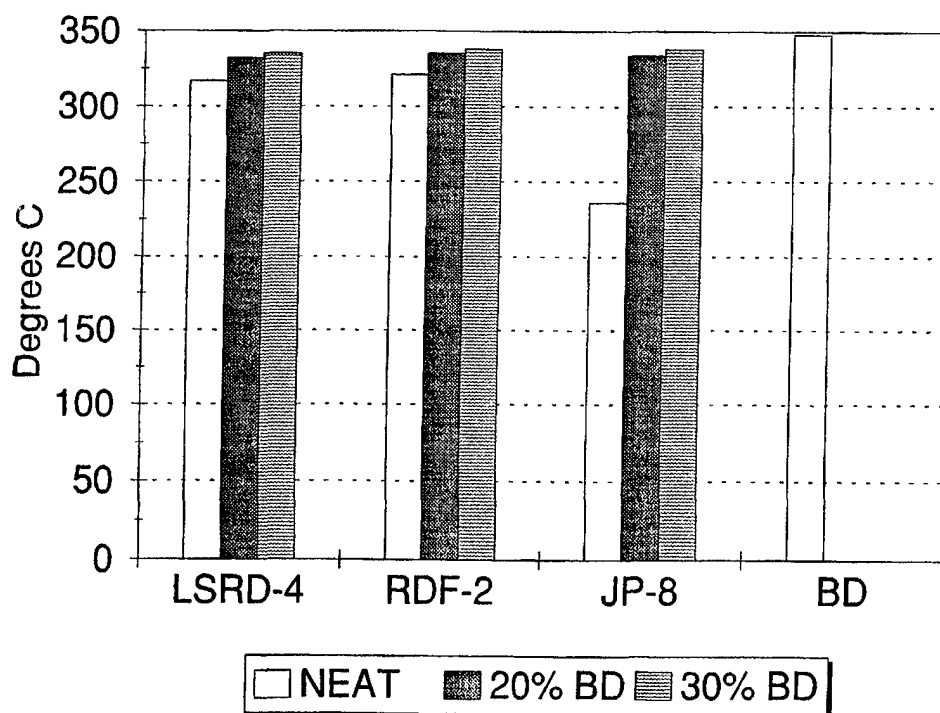


Figure 5. Effect of biodiesel on 90% distillation point

The water separation characteristics of neat biodiesel and the remaining fuels in the ten-fuel matrix were determined using the ASTM D 3948 (5) microseparometer test. This test method rates the ability of a fuel to release entrained or emulsified water when passed through fiberglass coalescing material. In this test, a water and fuel emulsion is created and sent through a standard fiberglass coalescer at a programmed rate. The effluent is analyzed for uncoalesced water by a light transmission method, with results reported as a rating between 0 and 100. The higher the rating, the more easily water is coalesced. Easily coalesced water implies that the fuel is relatively free of surfactant materials. Microseparometer results for the ten fuels in the matrix are presented in Fig. 6. The neat biodiesel had excellent water separation results, which was somewhat unexpected considering the amount of water contained in the neat biodiesel. The biodiesel blends in the low-sulfur fuel (LSRD-4) produced excellent microseparometer ratings. The biodiesel blends in the reference DF-2 had lower microseparometer ratings than neat reference DF-2. The neat JP-8 obtained a very low microseparometer rating, and the biodiesel blends had slightly better water

separation characteristics. Overall, biodiesel had positive or no effect on water separation of petrofuel blends, except for the reference DF-2.

The effect of biodiesel on fuel cetane number was investigated (Fig. 7). Neat biodiesel had a cetane number of 49.3. The biodiesel appeared to function as a cetane improver in the three petrofuels. Considering the repeatability of the cetane number procedure (± 0.9), the data still tend to indicate a synergistic cetane number improvement effect of biodiesel on petrofuel blends.

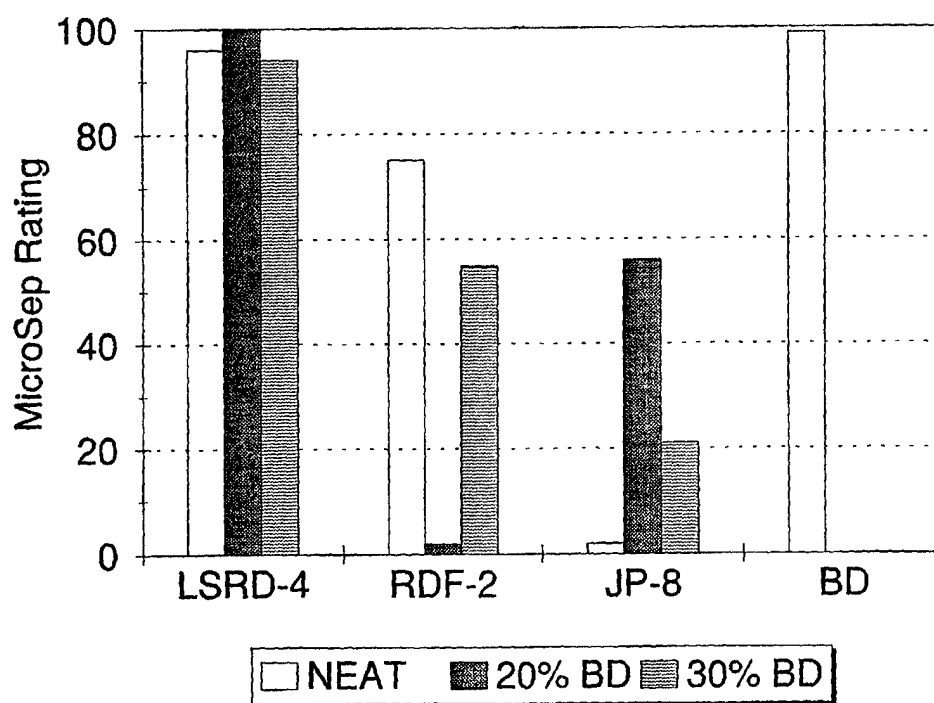


Figure 6. Microseparometer results for the ten fuels

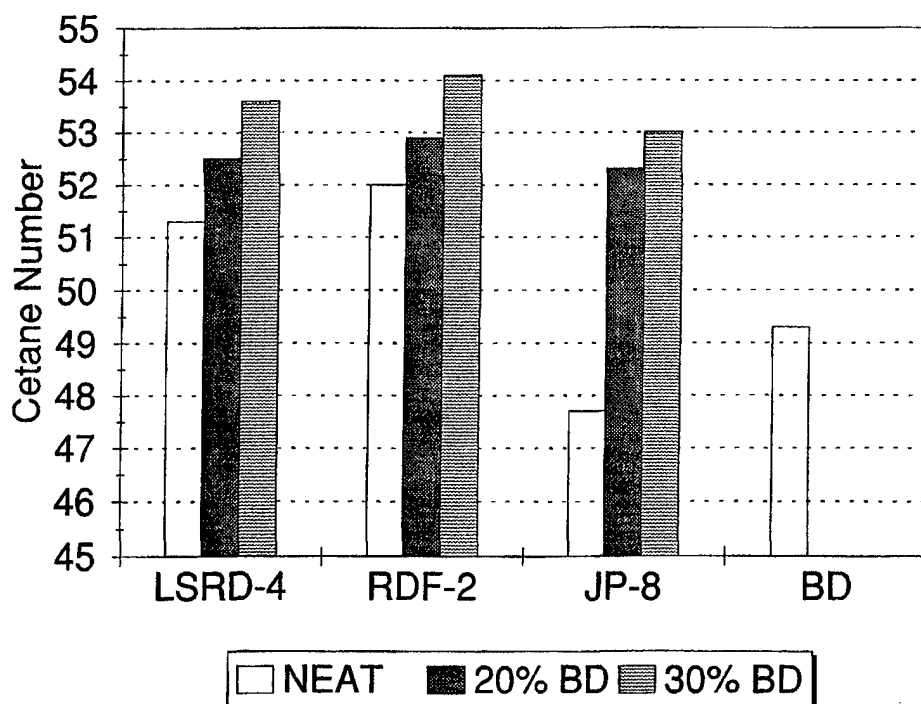


Figure 7. Effect of biodiesel on cetane number

IV. STORAGE STABILITY

Military fuel generally has a longer turnover time than commercial fuel, making storage stability an important concern for the military. Storage and thermal stability properties of the ten-fuel matrix were determined using ASTM D 4625 at 43°C (110°F) (6). This test method evaluates the inherent storage stability of distillate fuels. It has been shown that aging fuel at 43°C results in an approximately four-fold (4:1) acceleration of degradation compared to an ambient temperature of 21°C. Filtered fuel in 400-mL volumes is aged by storage in borosilicate glass containers at 43°C (110°F) for periods of 0, 4, 8, 12, and 18 weeks. After aging for a selected time period, a sample is removed from storage, cooled to room temperature, and analyzed for filterable insolubles, adherent insolubles, and total insolubles. Filterable insolubles are the solids formed during storage that can be removed from the fuel by filtration. Adherent insolubles are those that adhere to the sample containers and can be dissolved with a solvent of equal parts acetone, methanol, and toluene. Total insolubles represent the sum of the filterable insolubles plus the adherent insolubles, reported in mg/100 mL.

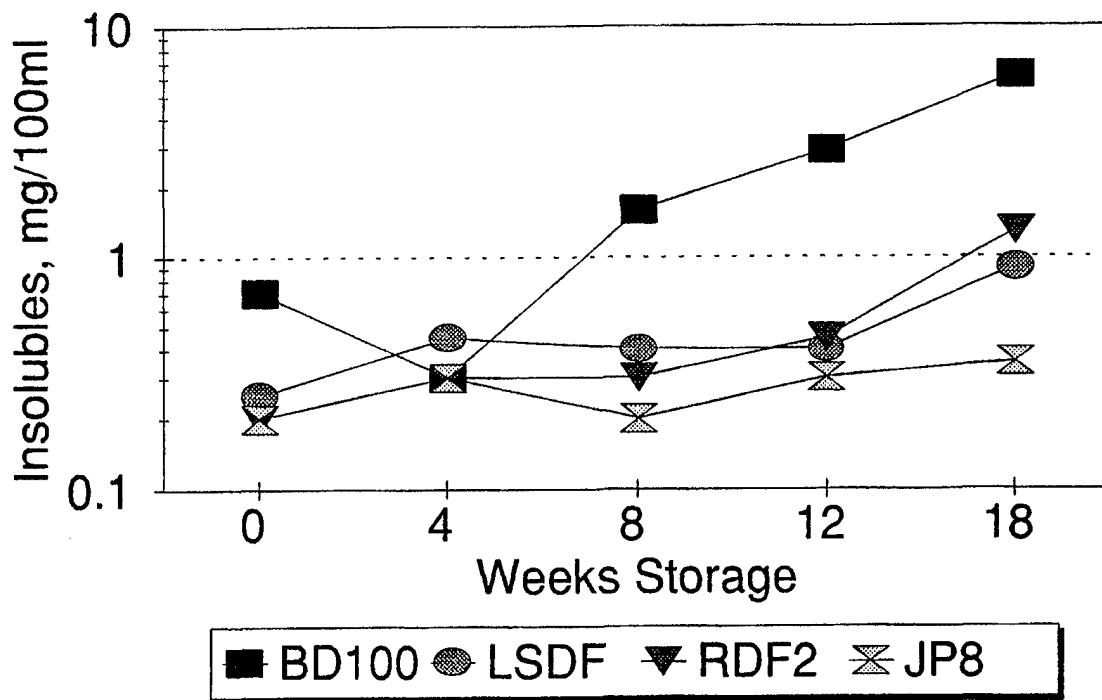
These results are presented in TABLE 3 and Fig. 8. In general, the storage samples experienced increased insolubles content with increased storage time. The biggest increase occurred in the 18-week samples, with two exceptions: 1) Reference DF-2 blended with 20 and 30 vol% biodiesel and 2) neat JP-8 fuel. The insolubles of these fuels remained approximately the same. In addition, the straight biodiesel had larger deposits than did the neat low-sulfur diesel fuel (LSDF), neat No. 2 Reference diesel fuel, and neat JP-8 fuel. The biodiesel blends generally had larger deposits than did the neat petrofuels with the possible exception of the Reference DF-2 blends, whose insoluble deposits remained essentially the same through the 18-week storage period. Starting with the eight-week storage period, additional tests were conducted, including the U.S. Army Scuffing Load Wear Test (SLWT) (7); the High-Frequency Reciprocating Rig (HFRR) test; total acid number determination by ASTM D 664 (8); color by ASTM D 1500 (9); steam jet gum by ASTM D 381 (10); and the Jet Fuel Thermal Oxidation Test (JFTOT) by ASTM D 3241 (11) to evaluate the effects of storage time. Determination of water content (Karl Fischer) by ASTM D 4928 (12) was added at the 12-week period because an emulsion appeared when the stored fuels were shaken.

A. Total Acid Number (TAN) by ASTM D 664

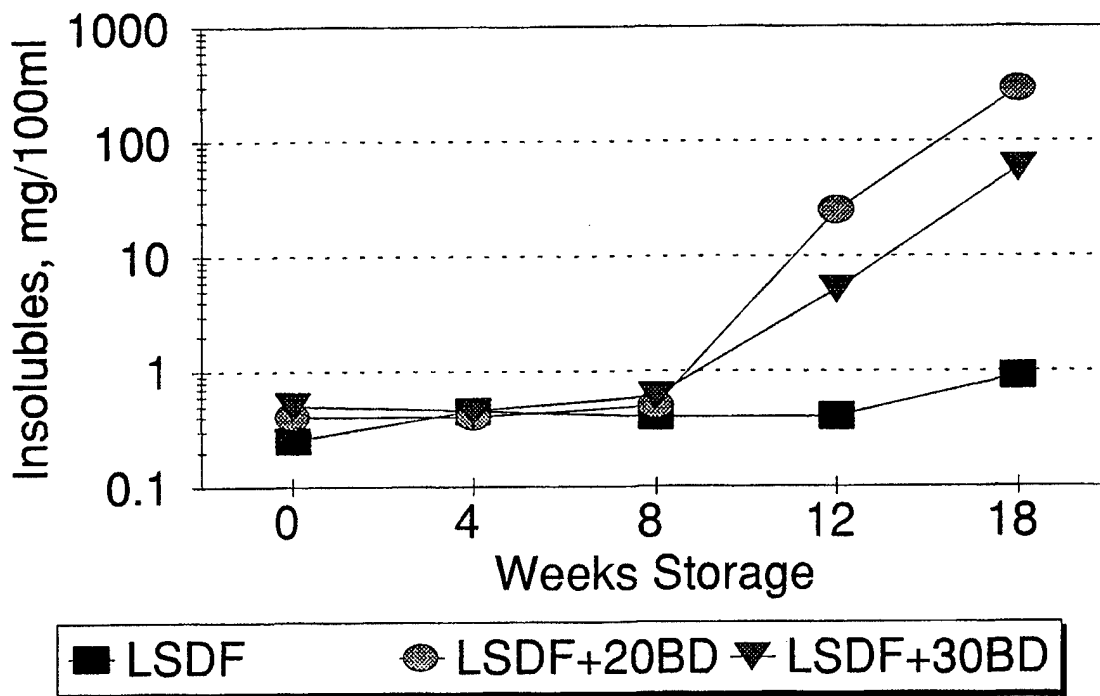
This method covers the determination of acid constituents in petroleum products and is used to indicate relative changes that occur in a petroleum product during use under oxidizing conditions, regardless of color or other properties. Data are reported in mg KOH/g (8), and the results from these tests are presented in TABLE 4 and Fig. 9. Neat low-sulfur diesel fuel, Reference No. 2 diesel fuel, JP-8, and the 20 and 30 vol% biodiesel blended in Reference No. 2 diesel fuel performed the best. These fuels did not show any significant increase in TAN during the 18 weeks of storage. A significant increase in TAN was observed in the remaining five fuels (i.e., the neat biodiesel and the 20 and 30 vol% blends in LSDF and JP-8 fuel) with the 12-week storage samples, continuing to increase in the 18-week samples.

TABLE 3. Storage and Thermal Stability Properties by ASTM D 4625

Fuel Code	Filterable Insolubles, mg					Adherent Insolubles, mg					Total Insolubles, mg/100 mL				
	0 wk	4 wk	8 wk	12 wk	18 wk	0 wk	4 wk	8 wk	12 wk	18 wk	0 wk	4 wk	8 wk	12 wk	18 wk
AL-23395-F 100% Biodiesel	2.5	1.0	5.6	10.3	20.0	0.3	0.2	0.9	1.1	4.6	0.7	0.3	1.6	2.9	6.1
AL-23403-F LSDf	0.7	0.9	0.7	0.9	1.6	0.2	0.9	0.9	0.8	2.1	0.25	0.45	0.4	0.4	0.9
AL-23404-F Ref. No. 2	0.7	0.9	0.7	1.0	3.8	0.1	0.2	0.5	0.8	1.5	0.2	0.3	0.3	0.45	1.3
AL-22363-F JP-8	0.7	1.0	0.5	0.6	0.8	0.1	0.1	0.4	0.6	0.6	0.2	0.3	0.2	0.3	0.35
AL-23405-F 20% BD + LSDf	1.4	1.2	1.2	6.0	220.4	0.3	0.3	0.9	94.0	915.6	0.4	0.4	0.5	25.0	284.0
AL-23406-F 30% BD + LSDf	2.0	1.5	1.6	12.4	66.5	0.1	0.3	0.8	7.9	265.6	0.5	0.45	0.6	5.1	58.0
AL-23407-F 20% BD + Ref. No. 2	2.6	1.8	2.1	1.6	1.7	0.7	0.5	0.9	0.8	0.7	0.8	0.5	0.75	0.6	0.6
AL-23408-F 30% BD + Ref. No. 2	2.0	1.0	1.5	14.0	1.3	0.5	0.4	0.6	0.9	0.4	0.6	0.4	0.5	3.7	0.4
AL-23409-F 20% BD + JP-8	0.8	0.5	1.2	276.2	211.7	0.4	0.3	0.4	1141.7	636.5	0.3	0.2	0.4	354.5	212.0
AL-23410-F 30% BD + JP-8	1.9	0.8	1.3	75.8	115.6	0.5	0.3	0.6	188.7	337.3	0.6	0.35	0.5	66.1	113.2

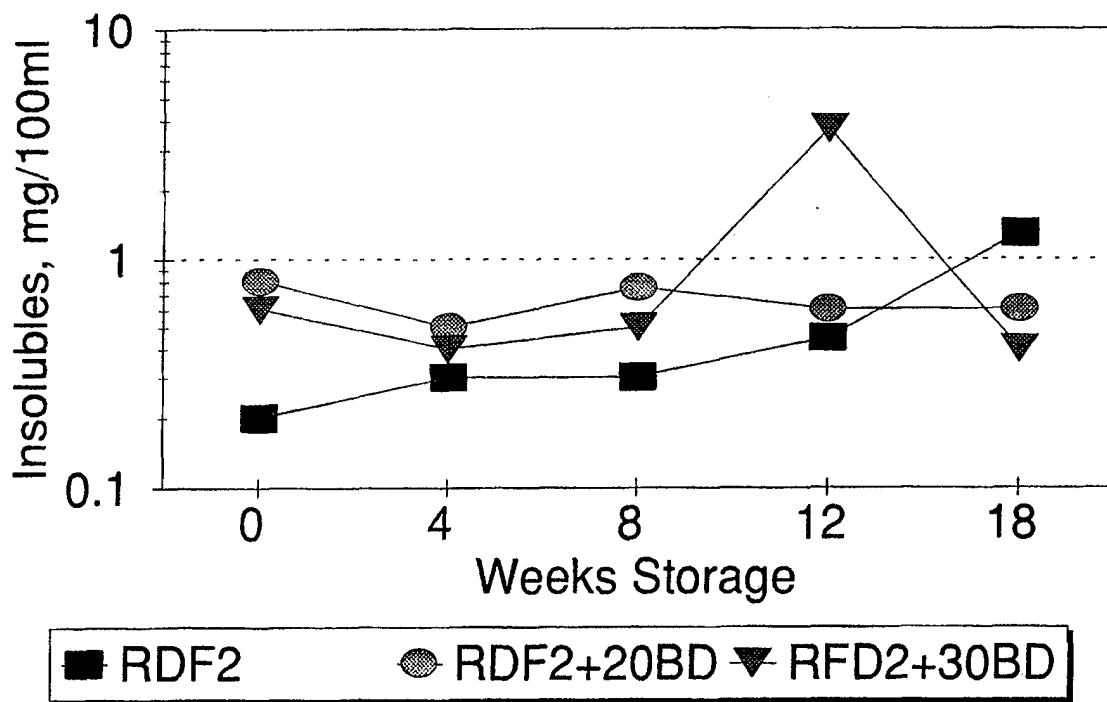


a. Neat base fuels

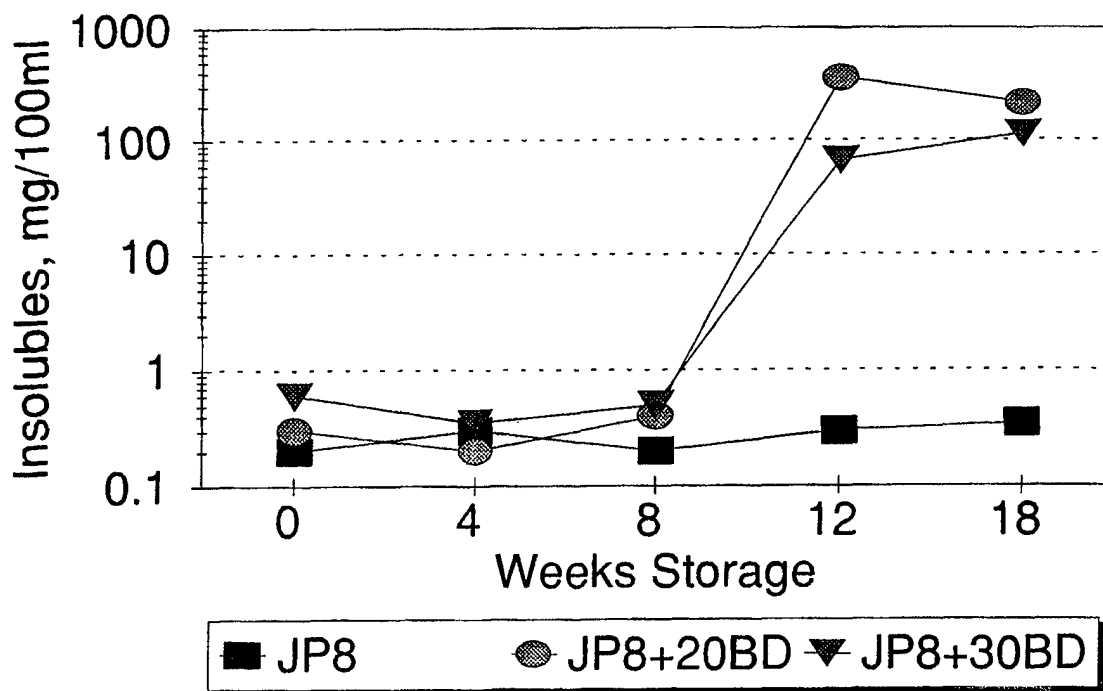


b. Biodiesel blends in LSDF

Figure 8. Total insolubles



c. Biodiesel blends in reference DF-2



d. Biodiesel blends in JP-8

Figure 8. Total insolubles

TABLE 4. Total Acid Number Results

Fuel No.	Fuel Code	TAN, mg KOH/g			
		0 wk	8 wk	12 wk	18 wk
1	AL-23395-F	0.15	0.96	1.97	4.63
2	AL-23403-F	0.01	0.01	0.01	0.01
3	AL-23404-F	0.05	0.06	0.07	0.07
4	AL-22363-F	0.01	0.01	0.01	0.01
5	AL-23405-F	0.07	0.26	0.83	3.56
6	AL-23406-F	0.11	0.65	3.82	4.22
7	AL-23407-F	0.09	0.09	0.11	0.11
8	AL-23408-F	0.12	0.13	0.14	0.14
9	AL-23409-F	0.04	0.16	1.46	3.52
10	AL-23410-F	0.09	0.67	2.26	6.63

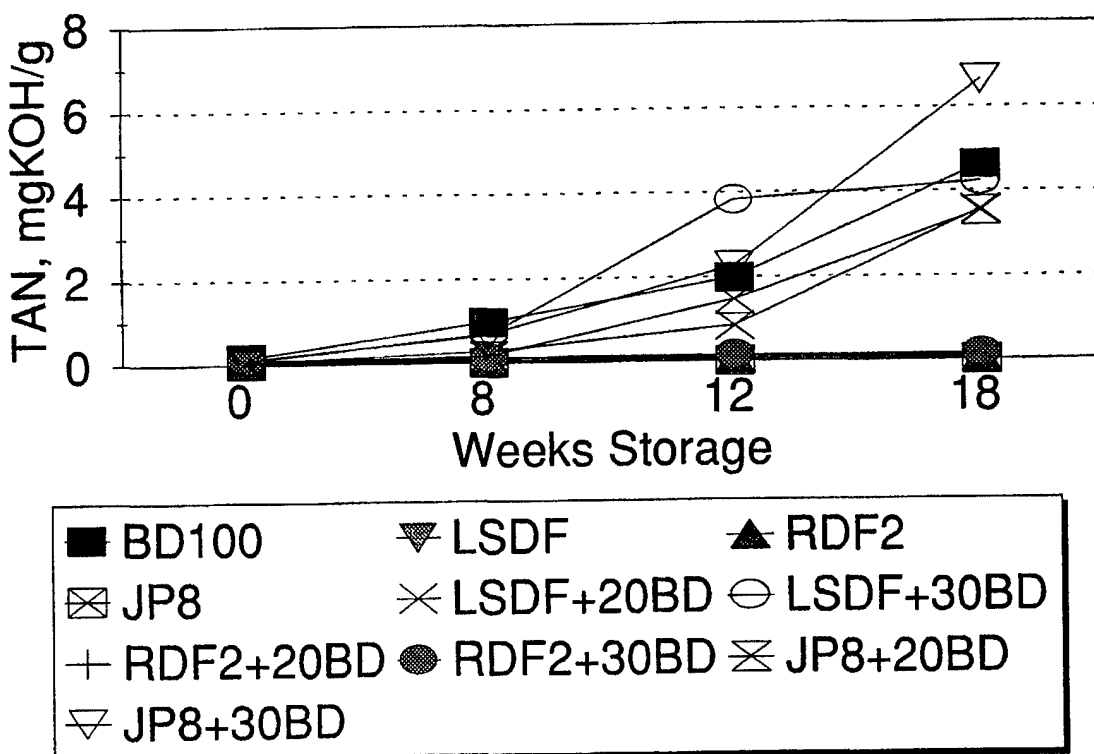


Figure 9. Total acid number

B. Color by ASTM D 1500

This method covers the visual determination of the color of a wide variety of petroleum products. Using a standard light source, a liquid is placed in a test container and compared with colored glass disks ranging in value from 0.5 to 8.0 (luminous transmittance ranging from 0.86 to 0.0025 T_w). (9) The neat biodiesel and JP-8 along with the 20 and 30 vol% biodiesel blends in JP-8 produced no increase in color over the 18-week storage period. The 20 and 30 vol% biodiesel blends in LSDF and Reference No. 2 diesel fuel produced lighter colors than did the neat LSDF and Reference No. 2 diesel fuel. These results are presented in TABLE 5.

TABLE 5. Color Results

Fuel No.	Fuel Code	Color, units			
		0 wk	8 wk	12 wk	18 wk
1	AL-23395-F	<0.5	<0.5	<0.5	<0.5
2	AL-23403-F	<0.5	1.0	1.5	1.5
3	AL-23404-F	0.5	0.5	<2.0	<2.0
4	AL-22363-F	0.5	0.5	0.5	0.5
5	AL-23405-F	<0.5	<1.0	<1.5	<1.5
6	AL-23406-F	0.5	1.0	<1.5	<1.5
7	AL-23407-F	0.5	1.0	1.0	1.0
8	AL-23408-F	0.5	<1.0	1.0	1.0
9	AL-23409-F	0.5	0.5	0.5	0.5
10	AL-23410-F	0.5	0.5	0.5	0.5

C. Steam Jet Gum by ASTM D 381

In this method, 100 mL of sample (in two glass containers of 50 mL each) is evaporated in controlled conditions of temperature and steam flow for 30 minutes. The unwashed gum consists of evaporated residue of existent gum and any nonvolatile additive components, reported in mg/100 mL. (10) Existent gum of distillate petroleum products should be low (typically <5 mg/100 mL) to ensure induction system cleanliness. The increase in existent gum over time is an indication of oxidative fuel degradation. Gum in all test fuels appeared to increase with storage time with the exception of JP-8, which decreased in gum residue. The 20 and 30 vol% biodiesel blends with Reference No. 2 diesel fuel had unusual results in that the zero- and eight-week gum

residue remained the same, but the 12-week samples experienced a large increase in gum residue, returning to the zero-week level at 18 weeks. The neat biodiesel and biodiesel blends all had heavy residue that was still wet or tacky at 30 minutes drying time. When the drying time of these samples was increased by 30 minutes for a total of 60 minutes, the gum weights decreased approximately 50 percent; however, the residue was still wet or tacky. The neat biodiesel and all biodiesel blends had larger deposits than the neat LSDF and Reference No. 2 diesel and JP-8 fuels. These results are presented in TABLE 6.

TABLE 6. Steam Jet Gum Results

Fuel No.	Fuel Code	Gum, mg/100 mL			
		0 wk	8 wk	12 wk	18 wk
1	AL-23395-F Biodiesel	1,345	19,591	28,467	30,105
2	AL-23403-F LSDF	0.7	2.2	3.5	4.0
3	AL-23404-F Ref. No. 2	1.6	2.7	3.0	6.4
4	AL-22363-F JP-8	1.2	7.4	0.6	0.2
5	AL-23405-F 20% BD + LSDF	115	896	1,475	4,073
6	AL-23406-F 30% BD + LSDF	328	1,704	5,869	6,445
7	AL-23407-F 20% BD + Ref. No. 2	61	76	2,733	72
8	AL-23408-F 30% BD + Ref. No. 2	139	147	9,245	131
9	AL-23409-F 20% BD + JP-8	87	434	2,467	3,985
10	AL-23410-F 30% BD + JP-8	248	2,911	4,469	7,253

D. Jet Fuel Thermal Oxidation Test (JFTOT) by ASTM D 3241

The Jet Fuel Thermal Oxidation Test (JFTOT) rates the tendencies of jet fuels to deposit decomposition products within the fuel system. The fuel is pumped at a fixed volumetric flow rate through an aluminum heated tube section, including a precision test filter together with associated equipment for controlling and measuring the heated tube temperature. After test completion, the tube is measured for deposits using the deposit measuring device (DMD). Maximum deposit volume and depth were measured. Deposit thickness appeared to show no specific trends, except that neat biodiesel had the least deposit thickness. Also, the JFTOT pump and some of the lines were coated with a gummy substance.

Reference No. 2 diesel showed the greatest total volume deposit at the zero hour, while the biodiesel and the 30% biodiesel + 70% LSDF blend ranked considerably lower. It would be expected that the deposits would increase or remain the same with increased storage time. However, the deposit volume results of these three fuels decreased with storage time. By mid-storage, they were below the minimum deposit limit and remained below through the end of the storage test. These results are presented in TABLE 7.

The LSDF, the 20% BD + 80% Ref. No. 2 blend and the 20% BD + 80% JP-8 blend, in that order, finished the storage test with the highest increase in volume deposits.

The following five fuels completed the storage test with total volume deposits below the minimum test limits: BD, Ref. No. 2, JP-8, 30% BD + 70% LSDF, and 30% BD + 70% Ref. No. 2. These two blends had the best volume deposit results by staying at or below the minimum deposit limits throughout the storage test. The biodiesel appeared to have the best long-term storage results in the JFTOT.

TABLE 7. JFTOT Biodiesel Blends

Fuel	0 wk		8 wk		12 wk		18 wk	
	Thickness, μm	Volume, mm^3	Thickness, μm	Volume, mm^3	Thickness, μm	Volume, mm^3	Thickness, μm	Volume, mm^3
AL-23395-F Biodiesel	0.037	0.012	0.019	<0.005	<0.005	<0.005	<0.005	<0.005
AL-23403-F LSDF	0.286	0.022	0.017	0.005	0.011	<0.005	0.359	0.066
AL-23404-F Ref. No. 2	1.332	0.143	0.656	0.089	0.017	<0.005	0.014	<0.005
AL-22363-F JP-8	0.009	<0.005	0.006	<0.005	0.038	0.012	0.031	<0.005
AL-23405-F 20% BD + LSDF	0.011	<0.005	0.008	<0.005	0.040	0.013	0.022	0.006
AL-23406-F 30% BD + LSDF	0.031	0.007	0.007	<0.005	0.006	<0.005	0.044	<0.005
AL-23407-F 20% BD + Cat 1-H (Ref. No. 2)	0.006	<0.005	0.050	0.006	0.029	0.009	0.557	0.046
AL-23408-F 30% BD + Ref. No. 2	<0.005	<0.005	0.054	<0.005	0.099	0.006	0.016	<0.005
AL-23409-F 20% BD + JP-8	<0.005	<0.005	0.006	<0.005	0.323	0.021	0.067	0.023
AL-23410-F 30% BD + JP-8	<0.005	<0.005	0.008	<0.005	0.010	<0.005	0.032	0.007

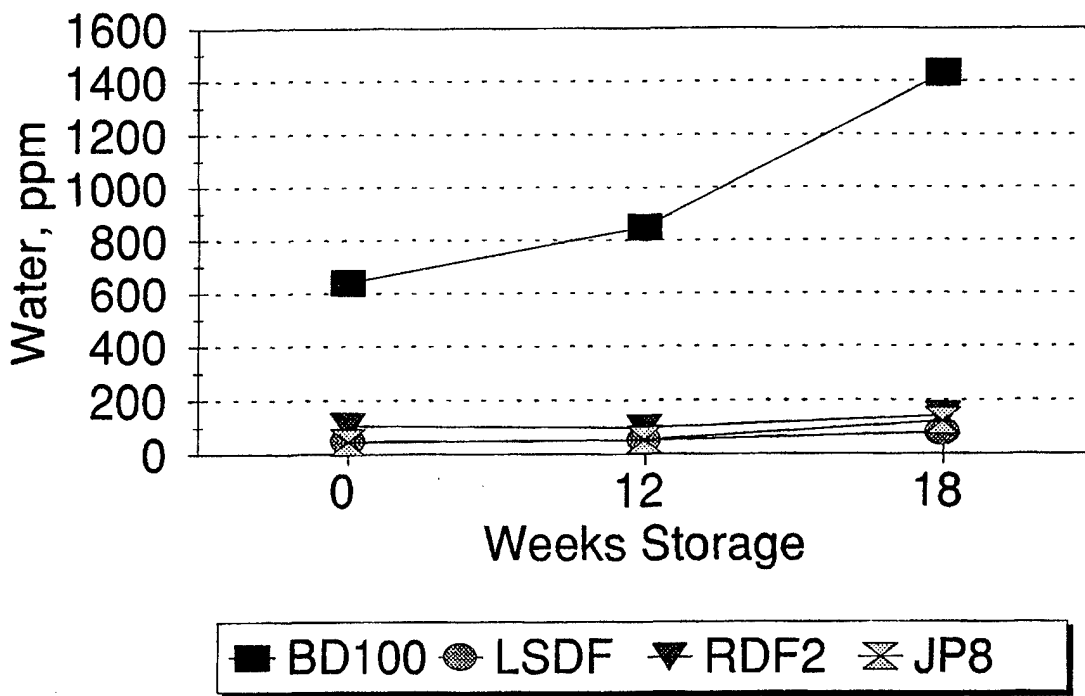
E. Water Content by ASTM D 4928

This method uses the Karl Fischer reagent and has a typical accuracy of one percent and a sensitivity of approximately 20 micrograms of water.(12)

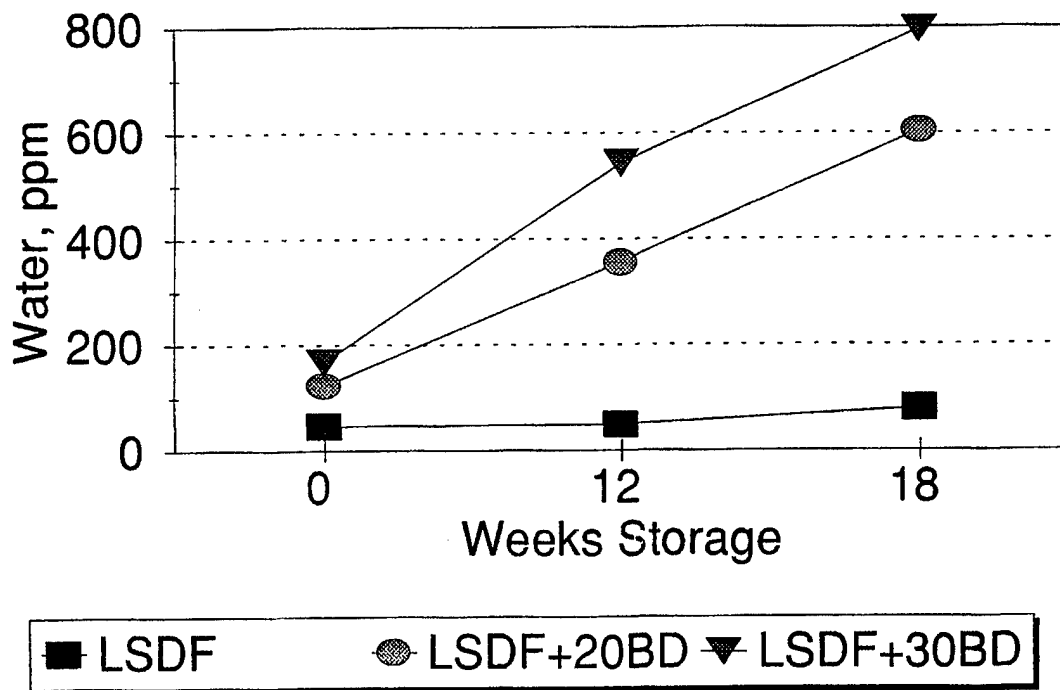
This test was started when a phase separation appeared in some of the blends at the 12-week storage period. The neat biodiesel had the highest water content at all test durations. The neat biodiesel and biodiesel blends had greater water content than did the neat LSDF and Ref. No. 2 and JP-8 fuels. The water content of all fuels increased with storage time. These results are presented in TABLE 8 and Fig. 10.

TABLE 8. Water Content Percent Results

Fuel No.	Fuel	<u>Water, ppm</u>		
		0 wk	12 wk	18 wk
1	AL-23395-F	639	848	1,430
2	AL-23403-F	46	49	80
3	AL-23404-F	104	97	142
4	AL-22363-F	44	53	123
5	AL-23405-F	122	355	604
6	AL-23406-F	167	543	796
7	AL-23407-F	147	161	188
8	AL-23408-F	206	151	280
9	AL-23409-F	114	466	562
10	AL-23410-F	157	613	769

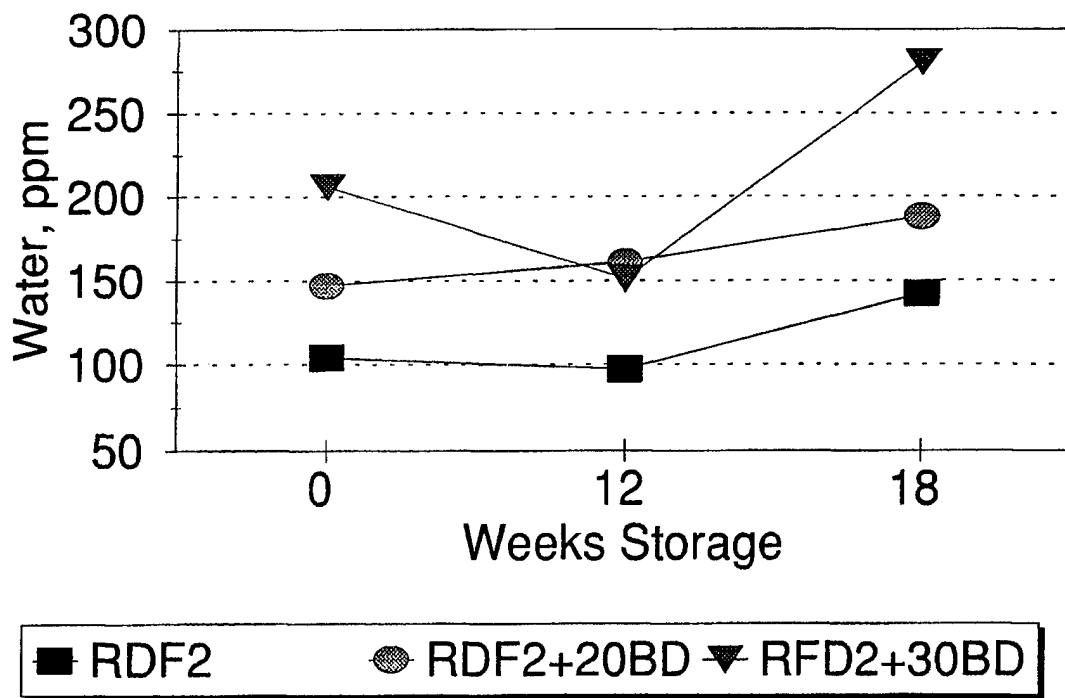


a. Neat base fuels

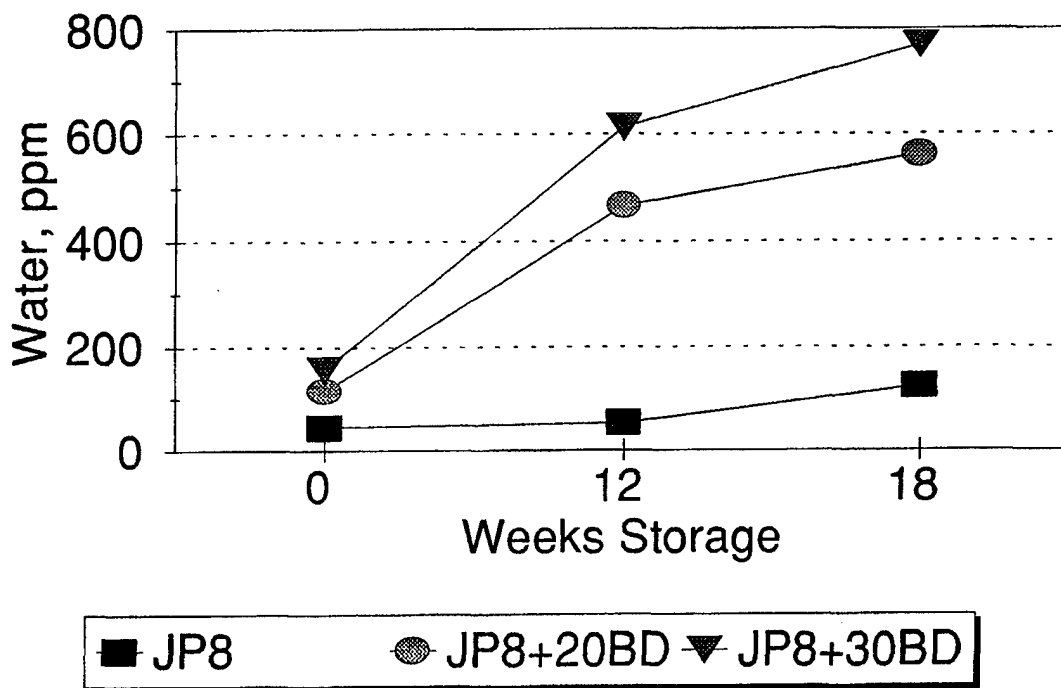


b. Biodiesel blends in LSDF

Figure 10. Water content



c. Biodiesel blends in reference DF-2



d. Biodiesel blends in JP-8

Figure 10. Water content

V. STORAGE STABILITY CONCLUSIONS

A. Storage Stability by ASTM D 4625

The biodiesel and the 20 and 30 percent BD blends with LSDF and JP-8 had higher insoluble contents than the neat LSDF and neat Ref. No. 2 and JP-8 fuels. The 20 and 30 percent BD blends with Ref. No. 2 fuel had insoluble deposits that were equivalent to the three neat petrofuels. The neat biodiesel had an increase in insolubles between 4 and 5 weeks, while the BD blends in LSDF and JP-8 had a large increase between 8 and 12 . Overall, the BD reduced storage stability in LSDF and JP-8.

B. Total Acid Number (TAN) by ASTM D 664

The neat BD, all LSDF and JP-8 blends had a steady increase in TAN with time, which indicates fuel instability. The neat petrofuels and the BD blends in DF-2 were stable.

C. Color by ASTM D 1500

Neat LSDF and DF2 increased in color with time as did their BD blends. BD, JP-8 and its BD blends did not darken with time.

D. Steam Jet Gum by ASTM D 381

The neat biodiesel produced the most gum, a large amount of gum initially, and increased in gum with time. Only the neat LSDF, Ref. No. 2, and JP-8 evaporated to dryness. The biodiesel and all the biodiesel blends had a wet residue at the end of 30- and 60-minute steam flow times. BD blends in petrofuels produced increased gum contents with time.

E. Jet Fuel Thermal Oxidation Test (JFTOT) by ASTM D 3241

BD and the neat petrofuels had decreasing JFTDT deposit with storage time. No major increases in JFTOT deposit were observed for any of the other fuels.

F. Water Content by ASTM D 4928

All fuels had increased water content with storage time. The biodiesel blends had more water than did the neat LSDF, Ref. No. 2, and JP-8 fuels. The neat biodiesel had the highest water content (1,430 ppm) at the end of storage time.

VI. MATERIAL COMPATIBILITY

Material compatibility is a major concern whenever fuel composition is changed in the fuel system. The design engineer incorporates materials that will facilitate the safest and most efficient operation possible. The consequence of changing the fuel composition is best illustrated by the state of California's reduction of aromatics in low-sulfur diesel fuel. This action resulted in the shrinkage of o-rings from their design swell, causing leakage in pumps and other fuel system components.⁽¹³⁾

A literature search was performed to determine the extent of material compatibility testing performed on biodiesel and biodiesel blends. The literature search also incorporated testing of other alternative fuels to identify the proper materials, elastomer, and metals for evaluation. Engine and elastomer manufacturers and fuel system designers were also contacted to discover if new materials were being used in recent engine designs.

A. Elastomer Compatibility

1. Literature Search

The National Biodiesel Board provided various contacts through which to obtain much of the preliminary biodiesel compatibility research. Reed, in his evaluation of ten common polymers, reported that only nitrile rubber and polyurethane form gave unsatisfactory results.(14) Holmberg, et al, stated "the principal bus engine manufacturers, Detroit Diesel Corporation (DDC), Cummins Engine Company, and Navistar, are cooperating with National Soydiesel Board (NSDB) in testing their engines. In blends of biodiesel of up to 30 vol%, no instances of fuel system degradation have been identified. It appears that possible material compatibility issues for higher blends can be easily resolved."(15)

Schumaker, et al, performed an evaluation utilizing a 1991 Dodge pickup fueled with methyl-ester soybean oil (then called soydiesel). It had been determined that the fuel storage and delivery system required modification, since the rubber-based components in the original equipment manufacturer fuel lines deteriorated when exposed to soydiesel. At the time of Schumaker's paper, Cummins Engine Company would not endorse or approve the use of soydiesel or biodiesel as a fuel in their products until further research had been performed.(16)

Schumaker's results were confirmed in a demonstration for the Federal Armed Forces (Germany). Rape seed methyl ester (RME) was deemed suitable for use in diesel engines when all elastomers used in the vehicle fuel system and refueling facilities had been replaced with materials resistant to RME.(17)

Literature detailing elastomer and plastics compatibility studies in automotive systems using other alternative fuels investigated a wide variety of materials. These compatibility studies were performed with raw sunflower oil and an ester of sunflower oil on various plastics and rubbers. The materials included polypropylene, high density polyethylene, Teflon®, Viton A®,

polvinylchloride, and nitrile rubber.(18) Other studies investigated the effects of alternative fuels with fluorosilicone, fluoroelastomers, fluoroplastics, nylon, and thermoplastics.(19-24)

Completion of the material compatibility matrix involved identifying those materials both commonly used in the automotive industry and in military applications. The selection process also took into consideration new materials used by engine manufacturers that may not have been included in other research.

The materials chosen for this investigation included Teflon®, nylon 6/6, nitrile rubber, Viton® A401C, Viton®GFLT, fluorosilicon, polyurethane, and polypropylene.

Teflon® was chosen for its widespread use in many fuel system designs and its inertness to most fluids. The fuel cell for the Bradley Fighting Vehicle is constructed of nylon 6/6. Nitrile rubber is the most common rubber used in automotive fuel systems. As previous studies had already illustrated problems with this material, it was used as a comparison. The two Viton® materials selected are the most common Viton® materials used by the automotive industry, according to a DuPont representative. Viton®A401C is a common, general-purpose fluoroelastomer, while the Viton® GFLT is a specialty Viton® that has the best combination of enhanced fluid resistance with improved low-temperature flexibility. Viton® F601C was also recommended due to its superior fluid resistance compared to Viton® A410C. However, the constraints of the program prevented use of this material. Fluorosilicon, polyurethane, and polypropylene are used in various configurations throughout the fuel system. These include o-rings, gaskets, and hoses.

2. Test Procedure and Results

Each material was stored in a glass container that was filled with a fuel used in the commercial and military market. The ten-fuel matrix is given below.

<u>Designation</u>	<u>Fuel/Fuel Blend</u>
A	100% JP-8
B	100% Biodiesel
C	100% ASTM Low-Sulfur Diesel Fuel (LSDF)
D	100% Reference No. 2 Diesel Fuel
E	20% Biodiesel + 80% ASTM LSDF
F	30% Biodiesel + 70% ASTM LSDF
G	20% Biodiesel + 80% Reference No. 2 Diesel Fuel
H	30% Biodiesel + 70% Reference No. 2 Diesel Fuel
I	20% Biodiesel + 80% JP-8
J	30% Biodiesel + 70% JP-8

Properties of the fuels are presented in TABLE 2. The elastomer compatibility study was performed as recommended by ASTM D 471 (25) and D 412 (26). Three tensile bars of each material were placed in sealed, glass containers and stored at 51.7°C (125°F) for 0, 22, 70, and 694 hours.

After the storage period was completed, the tensile strength, elongation, hardness, and swell were determined for each bar. Changes in tensile strength and elongation as a function of time are shown in Appendices A and B, respectively, for all materials and fuels. These results are summarized in TABLES 9 and 10, respectively.

Biodiesel severely affected the tensile strength of nylon 6/6. Tensile strength increased for the other base fuels and blends, whereas the tensile strength decreased immediately for nylon 6/6 in biodiesel. However, after 694 hours, the nylon 6/6 tensile strengths were very similar.

Although large changes in elongation occurred for nylon 6/6 in the base fuels, little or no change occurred in the fuel blends.

The Shore A hardness and percent swell of the materials are shown in Appendix C. A summary of the hardness and swell characteristics of these materials is presented in TABLE 11.

TABLE 9. Changes in Tensile Strength

<u>Fuel Blend</u>	<u>Material</u>	<u>Comments</u>
A	Teflon	More loss in tensile strength than other base fuels
B	Teflon	No significant change
C	Teflon	No significant change
D	Teflon	No significant change
E	Teflon	No significant change
F	Teflon	No significant change
G	Teflon	No significant change
H	Teflon	No significant change
I	Teflon	No significant change
J	Teflon	No significant change
A	Nitrile	No significant change
B	Nitrile	More loss in tensile strength than other base fuels
C	Nitrile	No significant change
D	Nitrile	No significant change
E	Nitrile	No significant change
F	Nitrile	Moderate loss in tensile strength
G	Nitrile	No significant change
H	Nitrile	Slight loss in tensile strength
I	Nitrile	Moderate loss in tensile strength
J	Nitrile	Slight loss in tensile strength
A	Nylon 6/6	No significant change
B	Nylon 6/6	Significant initial decrease in tensile strength
C	Nylon 6/6	No significant change
D	Nylon 6/6	No significant change
E	Nylon 6/6	No significant change
F	Nylon 6/6	No significant change
G	Nylon 6/6	694-hour data point appears to be an outlier
H	Nylon 6/6	No significant change
I	Nylon 6/6	No significant change
J	Nylon 6/6	No significant change
A	Viton A401-C	No significant change
B	Viton A401-C	No significant change
C	Viton A401-C	No significant change
D	Viton A401-C	No significant change
E	Viton A401-C	No significant change
F	Viton A401-C	Slight decrease in tensile strength
G	Viton A401-C	No significant change
H	Viton A401-C	No significant change
I	Viton A401-C	No significant change
J	Viton A401-C	No significant change

TABLE 9. Changes in Tensile Strength, cont'd

Fuel Blend	Material	Comments
A	Viton GFLT	No significant change
B	Viton GFLT	No significant change
C	Viton GFLT	No significant change
D	Viton GFLT	No significant change
E	Viton GFLT	No significant change
F	Viton GFLT	Slight decrease in tensile strength
G	Viton GFLT	No significant change
H	Viton GFLT	No significant change
I	Viton GFLT	No significant change
J	Viton GFLT	No significant change
A	Fluorosilicon	No significant change
B	Fluorosilicon	Significant initial increase in tensile strength
C	Fluorosilicon	Significant initial increase in tensile strength
D	Fluorosilicon	No significant change
E	Fluorosilicon	No significant change
F	Fluorosilicon	No significant change
G	Fluorosilicon	No significant change
H	Fluorosilicon	No significant change
I	Fluorosilicon	No significant change
J	Fluorosilicon	No significant change
A	Polyurethane	No significant change
B	Polyurethane	No significant change
C	Polyurethane	No significant change
D	Polyurethane	No significant change
E	Polyurethane	No significant change
F	Polyurethane	No significant change
G	Polyurethane	No significant change
H	Polyurethane	No significant change
I	Polyurethane	No significant change
J	Polyurethane	No significant change
A	Polypropylene	No significant change
B	Polypropylene	No significant change
C	Polypropylene	No significant change
D	Polypropylene	No significant change
E	Polypropylene	No significant change
F	Polypropylene	No significant change
G	Polypropylene	No significant change
H	Polypropylene	No significant change
I	Polypropylene	No significant change
J	Polypropylene	No significant change

TABLE 10. Changes in Elongation

<u>Fuel Blend</u>	<u>Material</u>	<u>Comments</u>
A	Teflon	No significant change
B	Teflon	No significant change
C	Teflon	No significant change
D	Teflon	No significant change
E	Teflon	No significant change
F	Teflon	No significant change
G	Teflon	Slight decrease in elasticity
H	Teflon	Slight decrease in elasticity
I	Teflon	No significant change
J	Teflon	No significant change
A	Nitrile	No significant change
B	Nitrile	Slight reduction in elasticity
C	Nitrile	No significant change
D	Nitrile	No significant change
E	Nitrile	No significant change
F	Nitrile	Moderate reduction in elasticity
G	Nitrile	No significant change
H	Nitrile	No significant change
I	Nitrile	No significant change
J	Nitrile	No significant change
A	Nylon 6/6	Significant reduction in elasticity
B	Nylon 6/6	Moderate reduction in elasticity
C	Nylon 6/6	No significant change
D	Nylon 6/6	No significant change
E	Nylon 6/6	No significant change
F	Nylon 6/6	No significant change
G	Nylon 6/6	No significant change
H	Nylon 6/6	No significant change
I	Nylon 6/6	No significant change
J	Nylon 6/6	No significant change
A	Viton A401-C	No significant change
B	Viton A401-C	No significant change
C	Viton A401-C	No significant change
D	Viton A401-C	No significant change
E	Viton A401-C	No significant change
F	Viton A401-C	No significant change
G	Viton A401-C	No significant change
H	Viton A401-C	No significant change
I	Viton A401-C	No significant change
J	Viton A401-C	No significant change

TABLE 10. Changes in Elongation, cont'd

Fuel Blend	Material	Comments
A	Viton GFLT	No significant change
B	Viton GFLT	No significant change
C	Viton GFLT	No significant change
D	Viton GFLT	No significant change
E	Viton GFLT	No significant change
F	Viton GFLT	No significant change
G	Viton GFLT	No significant change
H	Viton GFLT	No significant change
I	Viton GFLT	No significant change
J	Viton GFLT	No significant change
A	Fluorosilicon	No significant change
B	Fluorosilicon	No significant change
C	Fluorosilicon	No significant change
D	Fluorosilicon	No significant change
E	Fluorosilicon	Slight reduction in elongation
F	Fluorosilicon	Slight reduction in elongation
G	Fluorosilicon	No significant change
H	Fluorosilicon	No significant change
I	Fluorosilicon	Slight reduction in elongation
J	Fluorosilicon	No significant change
A	Polyurethane	No significant change
B	Polyurethane	No significant change
C	Polyurethane	No significant change
D	Polyurethane	No significant change
E	Polyurethane	No significant change
F	Polyurethane	No significant change
G	Polyurethane	No significant change
H	Polyurethane	No significant change
I	Polyurethane	No significant change
J	Polyurethane	Moderate increase in elongation
A	Polypropylene	No significant change
B	Polypropylene	No significant change
C	Polypropylene	No significant change
D	Polypropylene	No significant change
E	olypropylene	No significant change
F	Polypropylene	No significant change
G	Polypropylene	No significant change
H	Polypropylene	No significant change
I	Polypropylene	No significant change
J	Polypropylene	No significant change

TABLE 11. Summary of Hardness and Swell Characteristics

<u>Material</u>	<u>Comments</u>
Teflon	Relatively no changes in hardness or swell
Nylon 6/6	Relatively no changes in hardness or swell
Nitrile	Hardness was reduced approximately 20 percent; swell increased approx. 17 to 18 percent
Viton A401-C	Relatively no changes in hardness or swell
Viton GFLT	Relatively no changes in hardness or swell
Fluorosilicon	Hardness is relatively unchanged; swell increased approximately 7 percent
Polyurethane	Hardness is relatively unchanged; swell increased approximately 6 percent
Polypropylene	Hardness was reduced approximately 10 percent; swell increased from 8 to 15 percent

The swell of a material is a major factor in the design process. It was noted that for materials that exhibit measurable swell, the 100% biodiesel caused less swell than the other base fuels and blends.

B. Metal Compatibility

1. Literature Search

The literature search used for metal compatibility was employed for the elastomer search as well. Reed (14) found no degradation of aluminum, steel, or phosphatized fuel tanks. According to Romano (16), fatty acids readily react with metals such as tin, lead, cobalt, and manganese when exposed to elevated temperatures. He also stated that modern diesel engines operate at temperatures that could promote reactions with these metals (which are commonly used in diesel engines).

2. Storage Tests

The materials studied in previous literature searches and materials used in standard ASTM evaluations were considered. The materials selected for this study included C110 copper, SAE 1010 steel, C260 brass, 6061 aluminum, A319 cast aluminum, and C510 bronze.

Each material was stored in a fuel from the matrix previously described. Glass containers were used to reduce any interaction between the containers, metal coupons, and the fuel. The samples were stored at 51.6°C (125°F) for six months. Periodic visual inspections were performed.

a. Test Procedure and Results

The first visual inspection (at eight weeks) revealed fuel debris and discolored fuel in some of the fuels containing copper and its alloy, i.e., copper, brass, and bronze. After 12 weeks, the fuel degradation process had progressed and included most fuels containing these materials. The degradation included fuel debris, sediment, and discolored fuel. In addition, cast aluminum and steel had traces of fuel debris and sediment. After 16 weeks, it was determined that further investigation was required. Total acid number was determined for all samples. The TAN's ranged from <0.01 (JP-8 with various metals) to 8.33 (20% biodiesel + 80% JP-8). The TAN's after six months at 51.6°C (125°F) are presented in TABLE 12.

As shown in TABLE 12, the 100 percent biodiesel and any fuel blend containing biodiesel had a significant increase in TAN as compared to the other base fuels (A, C, and D). TAN of each fuel as a function of time is plotted in Appendix D.

The corresponding visual ratings for the metallic coupons are shown in TABLE 13. For the copper-containing materials, the ASTM D 130 (27) copper corrosion rating system was used.

TABLE 12. TAN Results, Six Months, at 51.6°C

Fuel Blend	Copper	Brass	Bronze	Steel	Cast Aluminum	Aluminum
A	0.33	0.05	0.05	0.05	0.02	0.01
B	1.07	0.85	0.48	9.75	8.89	10.55
C	0.43	0.58	0.54	0.20	0.06	0.05
D	0.49	0.38	0.23	0.05	0.05	0.05
E	4.10	3.80	3.44	5.25	1.98	5.74
F	3.99	3.03	3.12	5.90	5.88	7.79
G	3.40	1.59	3.73	0.16	0.07	0.16
H	3.91	2.67	5.14	0.32	2.30	0.44
I	2.62	2.98	10.40	10.00	4.35	9.72
J	4.12	7.29	11.06	16.62	8.87	13.83

TABLE 13. Visual Ratings, Metal Coupons, Six Months

Fuel Blend	Copper	Brass	Bronze	Steel	Cast Aluminum	Aluminum
A	1b	1a	Light Peacock	Light film	Clean	Light film
B	1b w/peacock	1a	1b w/light film	Light pitting	Light film	Clean
C	1b	Light peacock	1b w/brown film	Brown liquid film	Light film	Clean
D	HC*	HGC†	Peacock w/brown powder film	Brown film	Light film	Clean
E	2c w/deposits	1b w/yellow liquid dep.	2b w/crimson streaks	Light brown film	Yellow liquid deposit	Clean
F	HGC	2e w/deposits	1a w/brown gum	Clean	Light film	Clean
G	HGC	HGC	3a w/brown film	Brown film	Clean	Clean
H	HGC	HGC	1a w/green deposit	Brown film	Clean	Clean
I	HGC	HGC	1a w/green deposit	Brown film & brown liq.	Yellow liquid film	Clean
J	HGC	HGC	1a w/green deposit	Heavy brown liquid	Yellow liquid film	Clean

* Heavy corrosion

† Heavy gum contamination

The fuels and coupons after six-month storage at 51.6°C are presented in Figs. 11 through 16. For all applications, storage stability is questionable at best. However, blending JP-8 and biodiesel for military applications, with the military's extended idle periods, is expected to cause severe problems.

b. Analysis of Sediment/Deposits

A brief investigation was conducted to analyze the sediment and panel deposits found during storage with metal panels. Figures 17 through 20 show the FTIR traces for neat biodiesel, LSRD-4, Reference DF-2, and JP-8, respectively. Characteristic ester absorption bands are evident in the biodiesel (Fig. 17). Figure 21 shows the FTIR trace for the solid material recovered from the 20% biodiesel in JP-8 stored in the presence of brass. It reveals an -OH band at approximately 3,500 cm⁻¹, with most other absorption peaks resembling the neat biodiesel. FTIR analyses of sediment and deposits from other biodiesel blends were characteristic of neat biodiesel. Figure 22 shows the trace from 30% BD + 70% JP-8 blend stored with steel. Based on FTIR analysis, the sediment and deposits observed appeared to be mostly biodiesel related.

(This page intentionally left blank.)

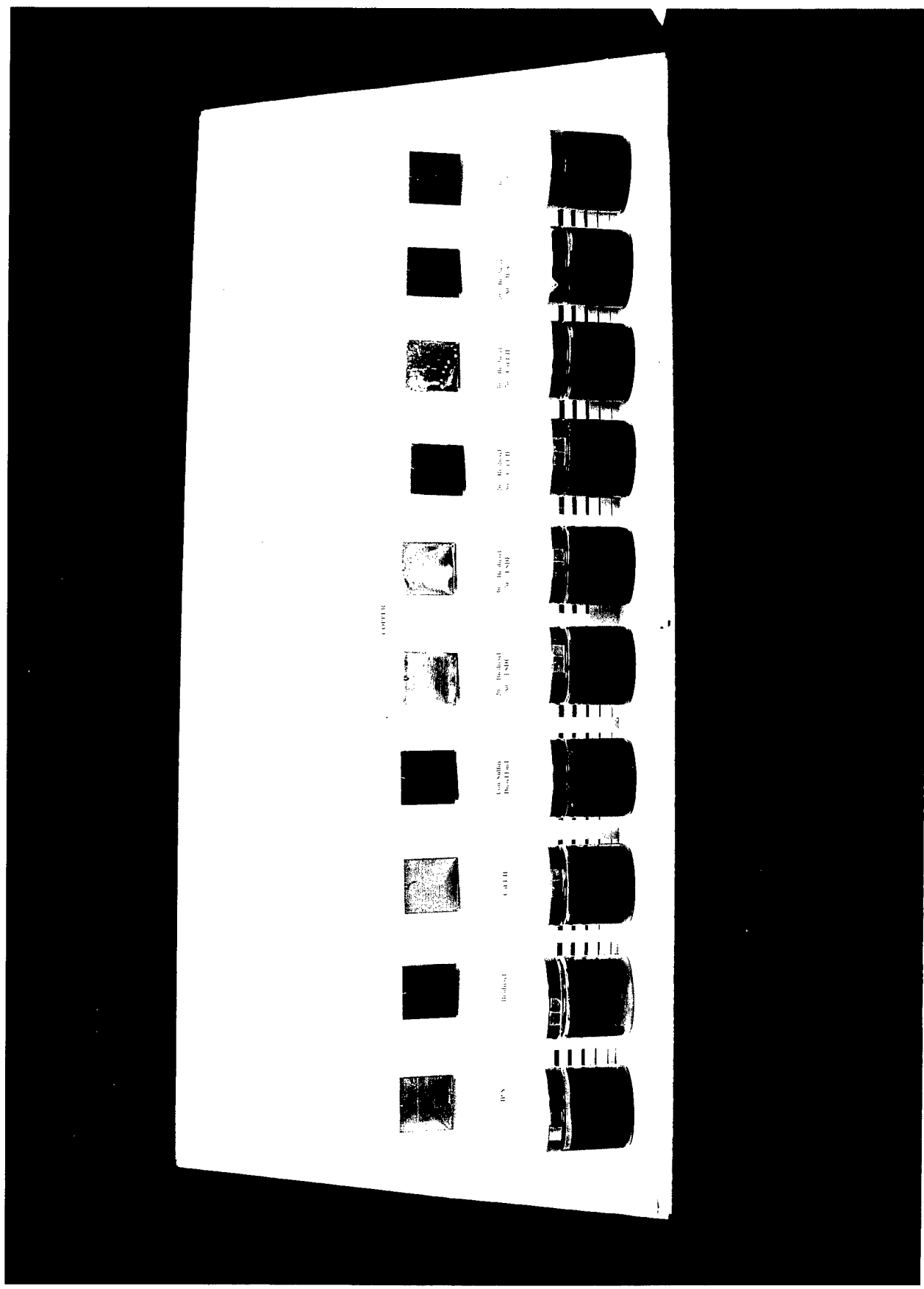


Figure 11. Fuels and copper coupons after six-month storage at 51.6°C

(This page intentionally left blank.)

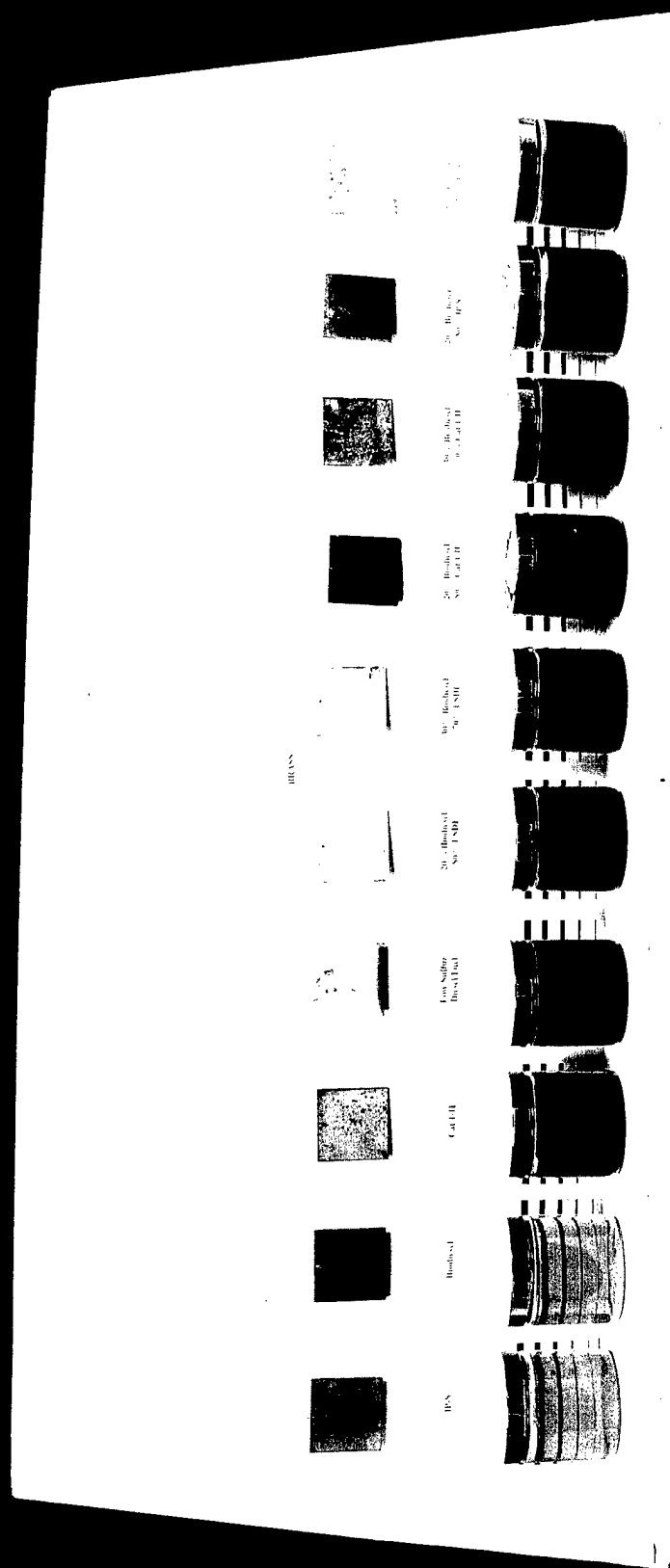


Figure 12. Fuels and brass coupons after six-month storage at 51.6°C

(This page intentionally left blank.)

(This page intentionally left blank.)

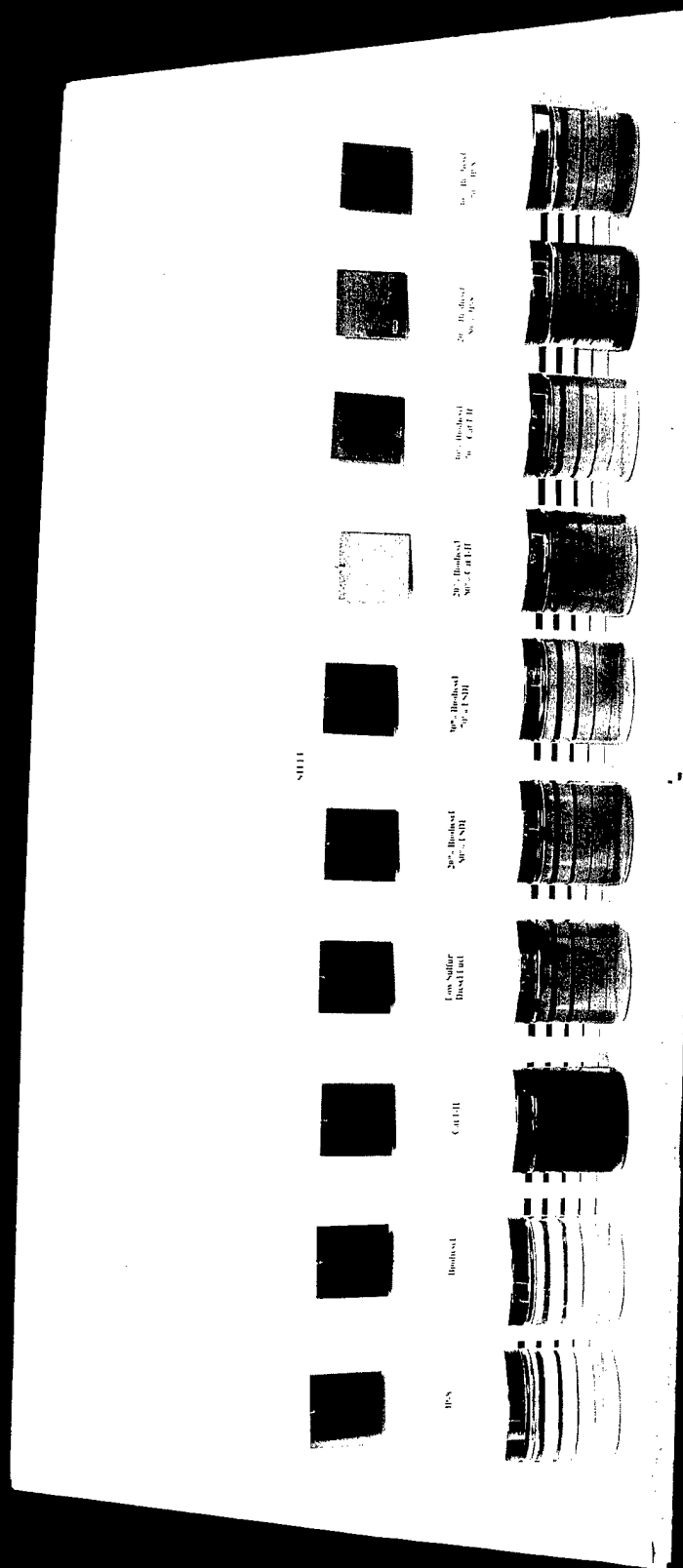


Figure 14. Fuels and steel coupons after six-month storage at 51.6°C

(This page intentionally left blank.)

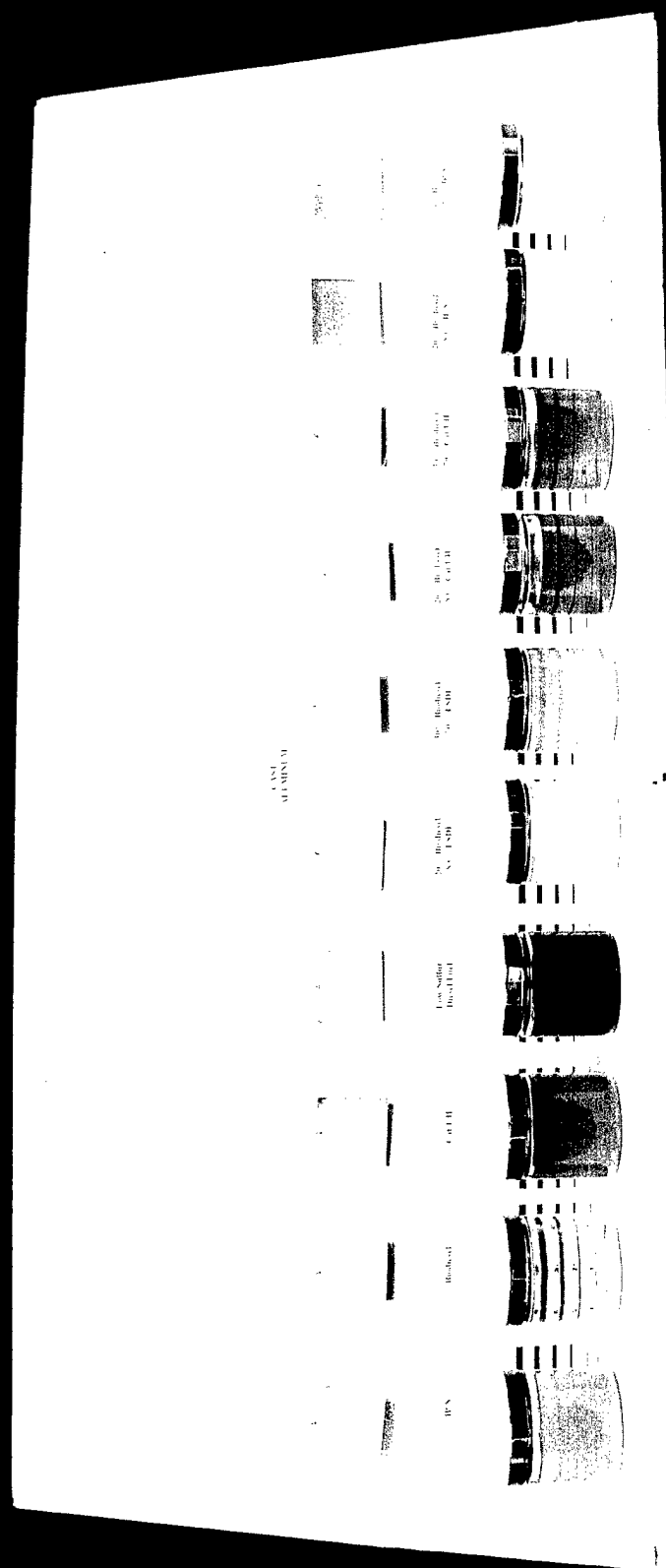


Figure 15. Fuels and cast aluminum coupons after six-month storage at 51.6°C

(This page intentionally left blank.)

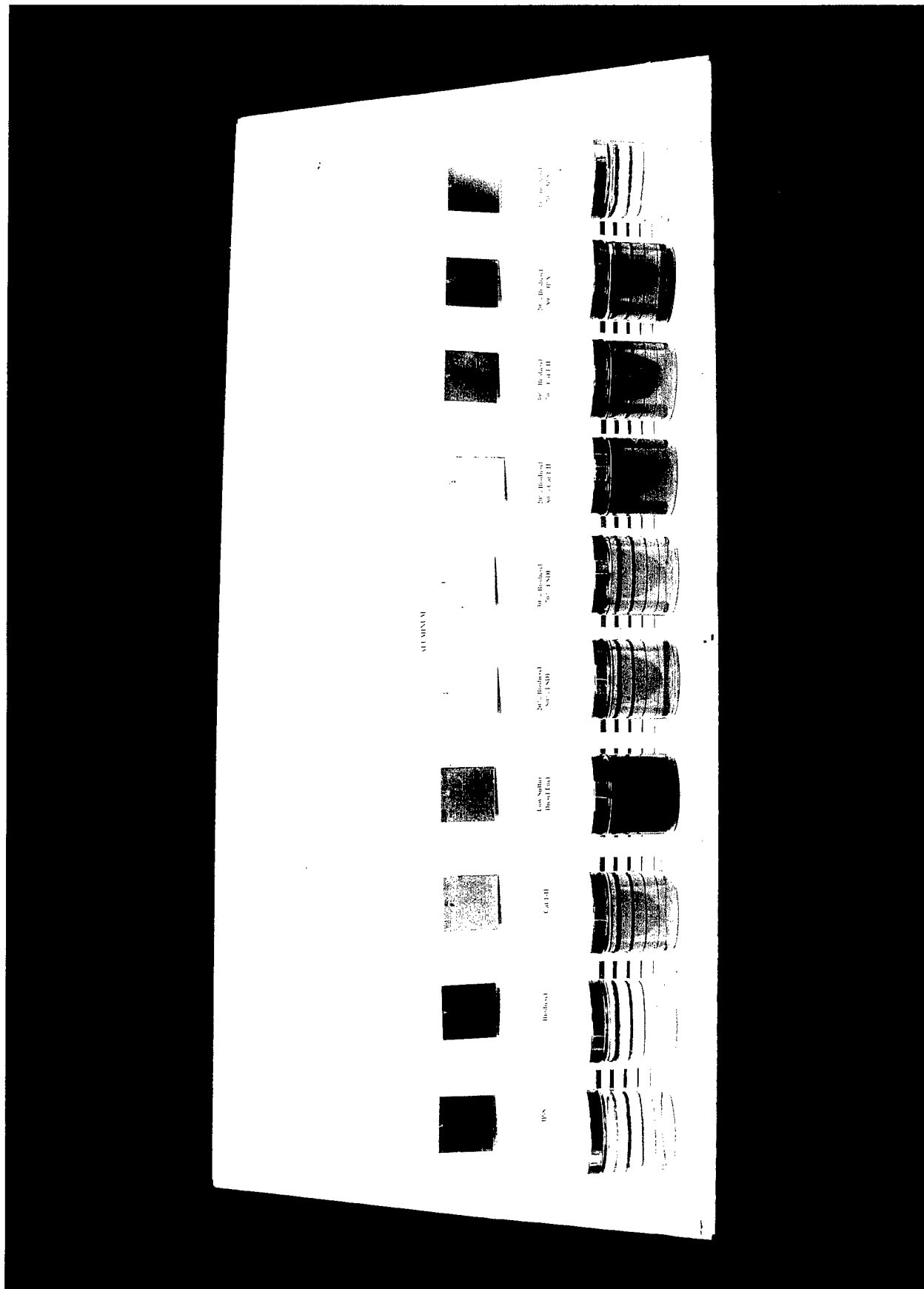


Figure 16. Fuels and aluminum coupons after six-month storage at 51.6°C

(This page intentionally left blank.)

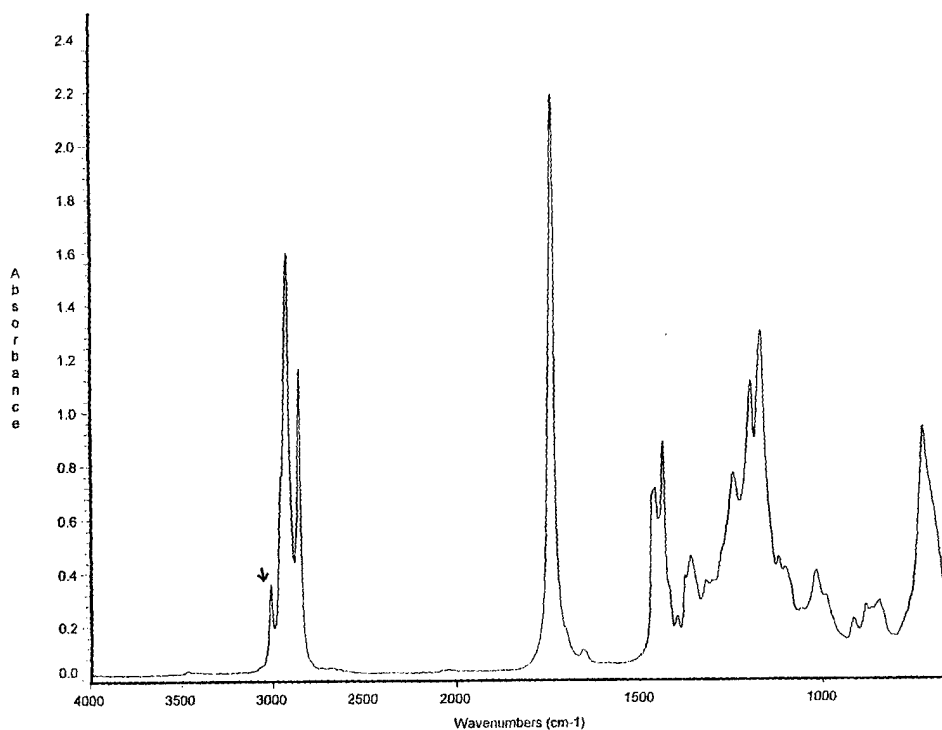


Figure 17. FTIR analysis of neat biodiesel

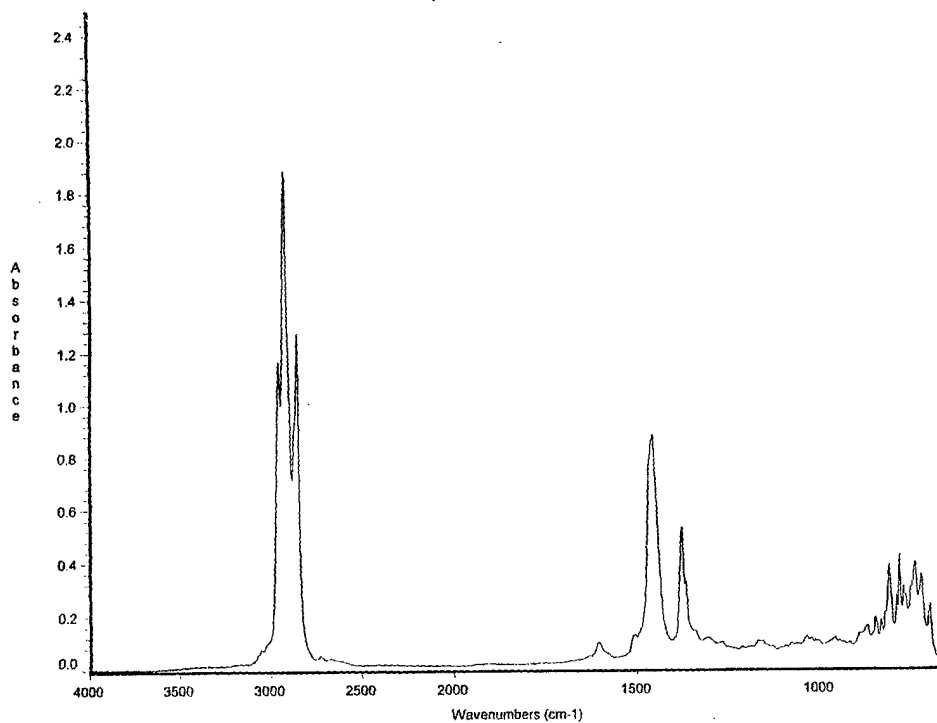


Figure 18. FTIR analysis of LSRD-4

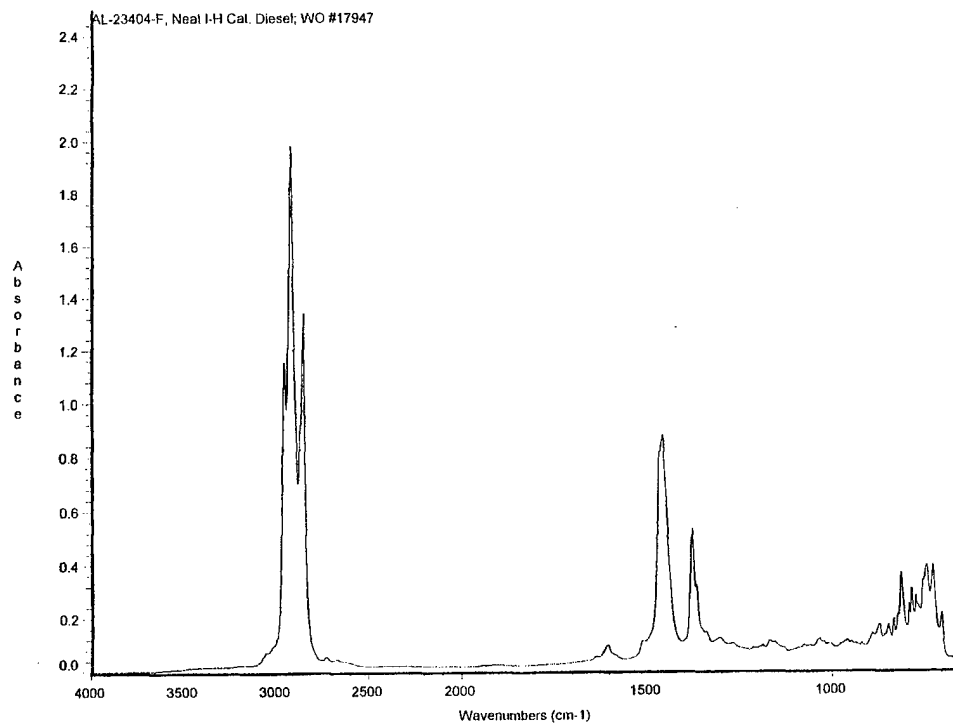


Figure 19. FTIR analysis of Reference DF-2

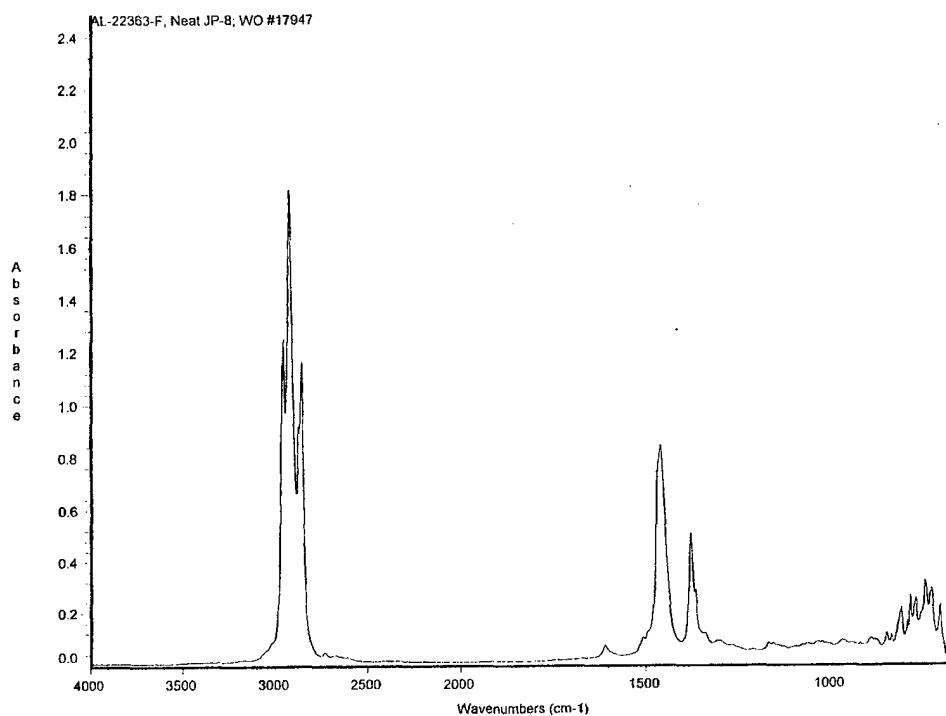
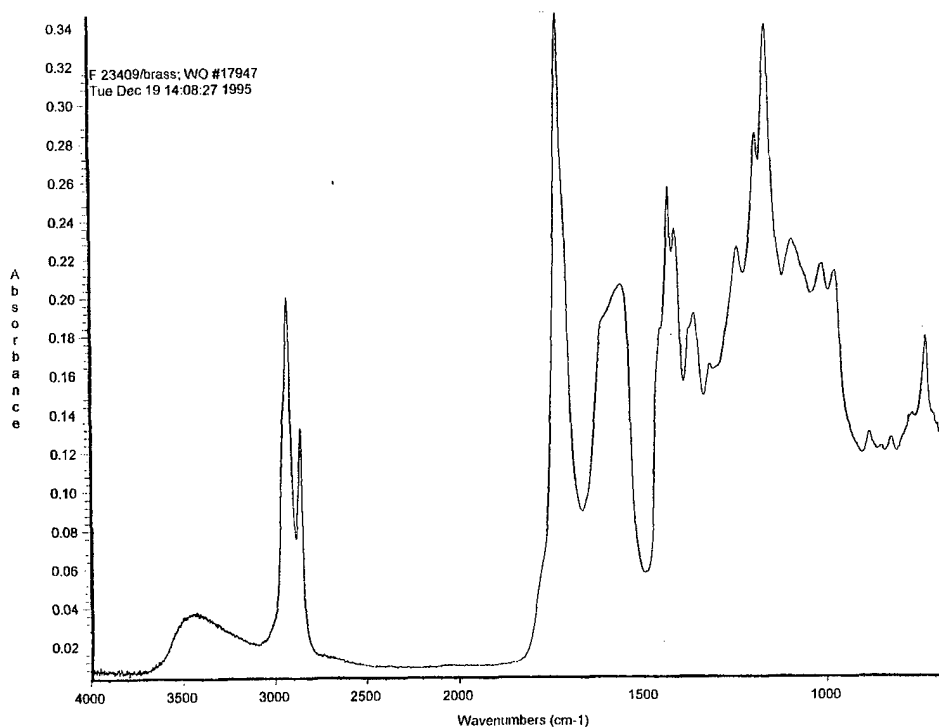


Figure 20. FTIR analysis of JP-8



**Figure 21. FTIR analysis of solid material recovered from
20% BD + 80% JP-8 blend stored in the presence of brass**

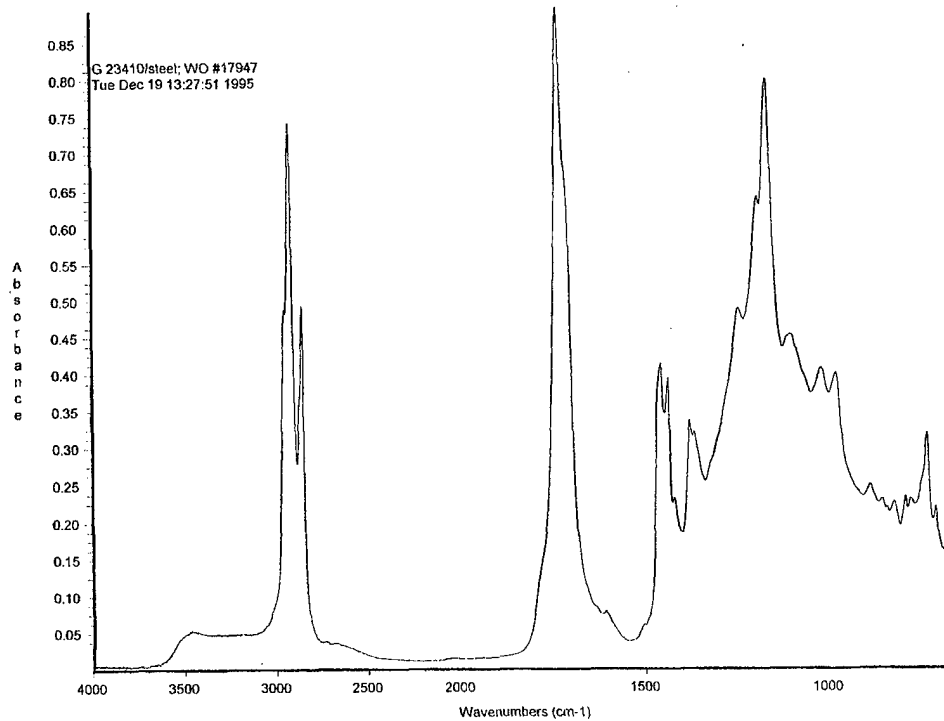


Figure 22. FTIR analysis of 30% BD + 70% JP-8 blend stored in the presence of steel

C. Fuel Filters

1. Literature Search

Two sources (17, 28) discussed problems with fuel filter plugging due to the "solvency" of the biodiesel blend. This "solvency" is claimed to dissolve varnish and polymer formation from the fuel system, thereby plugging the fuel filter. Frequent filter changes are recommended after conversion to biodiesel and RME fuel blends.(17, 28) As a result of this polymer formation, it is claimed that the fuel cannot be stored for extended periods of time.(17)

2. Test Procedure and Results

Different types of fuel filters utilized by the military were used for this compatibility evaluation. The filters selected were as follows:

- Pleated paper primary filter used on 6.2L GM engines.
- Pleated paper filter used on the High Mobility Multipurpose Wheeled Vehicle (HMMWV).
- Coalescer element used in the M-60 and M1A1 main combat tanks.
- Separator element used in the M-60 and M1A1 main combat tanks.

The filters were stored in glass containers for zero, one, three, and six months at 51.6°C. The pleated paper filters were evaluated for particle removal efficiency using a single-pass test procedure. The coalescer and separator elements were evaluated together for water removal using SAE J 1839 Coarse Droplet Water/Fuel Separation Test procedure.(29)

The pleated paper elements were evaluated in their respective housing and flow rates. The filters were challenged with approximately 5 mg/L AC Fine Test Dust on a single-pass test stand. In

addition to the particulate removal efficiency, media migration was determined. This identified if the fuel blends were degrading the filter media with time. Most filters will have some media migration at the beginning of the test. However, the fuel should wash away most within a few minutes of operation.

The 6.2L fuel filters were rated by the manufacturer as 10 μm . This rating will be defined as the filtration ratio equals 75 at 10 μm for these evaluations. Three 6.2L GM filters were evaluated to establish a baseline. The media migration was determined for particles 5 μm and larger. The media migration for the three filters was approximately 65,000, 10,000, and 10,000 counts per milliliter, respectively. The efficiencies ranged from 90 to 99 percent at 10 μm , respectively. After five minutes, the media migration was below 500 counts per milliliter, which was a general guideline for addition of the AC Fine Test Dust.

These results indicate a poorer quality filter with poor repeatability in the manufacturing process. It is noted that these filters are older technology as compared to the HMMWV and M1A1 filter elements. Therefore, these results may not be as poor as they appear when compared to new filtration technology.

The 100% biodiesel had an increase in media migration over the six-month storage period. Media migration increased from less than 500 counts/mL after one month to almost 40,000 counts/mL after six months. It is also noted that the baseline filters had a large discrepancy in media migration. The efficiency ranged from 97 to 99 percent.

The six-month filter in low-sulfur diesel fuel had an efficiency of less than 30 percent. This is most likely a defective filter. Another probable defective filter is the six-month element stored in Blend G. The efficiency fluctuated between 65 and 85 percent.

Blend H (30% biodiesel + 70% No. 2 Reference fuel) had a substantial increase in media migration. After one month, the media migration was 25,000 counts/mL; after three months,

approximately 100,000 counts/mL; and after six months, almost 200,000 counts/mL. The efficiencies for elements ranged from 96 to 98 percent.

Blend I (20% biodiesel + 80% JP-8) had the worse media migration. After one month, it was less than 5,000 counts/mL; three months increased it to more than 20,000 counts/mL; and after six months, the media migration increased to almost 350,000 counts/mL. Again, the efficiencies remained at approximately 98 percent.

Blend J (30% biodiesel + 70% JP-8) showed a trend of increasing media migration after three months. Unfortunately, due to computer problems, the six-month media migration data were lost.

All unmentioned elements had normal media migration, and the particulate efficiencies were approximately 98 percent at 10 μ m. The media migration and particulate efficiencies for the 6.2L GM filters are shown in Appendix E.

The HMMWV pleated paper element was rated by the manufacturer at 5 μ m. The same rating system was used as described above.

The media migration with 100% biodiesel was normal for all storage periods. However, the six-month low-sulfur diesel fuel element had a media migration of more than 100,000 counts/mL.

Blend F had an increase in media migration after three months to 90,000 counts/mL, which is similar to the neat low-sulfur diesel fuel sample. It would appear that this increase in media migration is not due to the biodiesel portion of the blend.

Blend H had an increase on media migration after one month of storage with a poor initial efficiency, i.e., less than 93 percent at 5 μ m. However, the three- and six-month samples did not demonstrate this increased media migration.

The other elements appeared to have normal media migration and particulate efficiencies of 98 percent at 5 μm . The media migrations and particulate efficiencies for the HMMWV filters are given in Appendix F.

The coalescers and separator elements for the M-60 and M1A1 were evaluated together since they operate together in the fuel system. The coalescer elements combine small water droplets into large droplets, which are forced through the coalescer media and separated by gravity and the separator element.

SAE J1839 Coarse Droplet Fuel/Water test procedure was used for these evaluations. A known quantity of water, approximately 2,500 ppm, is injected into the fluid stream before the filter. Fuel/water samples are obtained before and after the filtration system to determine the water removal efficiency. The evaluation was only performed for 30 minutes, with samples obtained at 10, 20, and 30 minutes.

Two new coalescer/separator systems were evaluated as a baseline. The baseline water removal efficiency was 95 percent, with excellent repeatability.

Fuels A, B, C, and D all had repeatable efficiencies greater than 90 percent water removal for the entire six-month storage period, which would be accepted by most engine manufacturers. The 30-minute evaluation from the six-month sample in Blend E (20% biodiesel + 80% LSDF) deteriorated to 80 percent water removal efficiency. The water removal efficiency for Blend F had a wide range, but the overall water removal was significantly less than the baseline or the neat fuels. The average efficiency was approximately 75 percent water removal. Water removal efficiency for Blend G was more consistent but was only approximately 85 percent. This is slightly lower than engine manufacturers would approve. Blend H water removal efficiency was better than its 20% biodiesel counterpart. The water removal efficiency was approximately 90 percent. The three-month, ten-minute fuel-water sample may be an outlier. Blends I and J had excellent water removal efficiencies, approximately 95 percent.

It was noted that although the water removal efficiencies were overall very good, the coalescer element did not function for biodiesel and fuel blends containing biodiesel as it did with Fuels A, C, and D. As previously mentioned, the coalescer allows small water droplets to combine on the fiberglass media until the fuel flow removes the water droplet, passing it through the coalescer element. Once it passes through the coalescer element, the water droplet is separated by the separator element or falls to the bottom of the filter housing due to gravity. With fuels containing biodiesel, the water remained in the coalescer element and did not pass through to the separator. This could create significant problems once the element fills with water; large slugs of water could pass through the coalescer and separator and into the fuel system, creating corrosion or other problems. This may also create an additional problem. It was noted that the differential pressure across the separation system was 3 to 5 psid higher than with the base fuels.

The water removal efficiencies for the coalescer/separator systems are presented in Appendix G.

D. Conclusions

Biodiesel reduces the swell characteristics of elastomeric materials, which depend upon swell to seal. The reduced swelling causes leakage from seals and o-rings similar to the problems found with the change to low-sulfur diesel fuel.(1) The elastomer needs to be engineered properly to perform the desired operation.

Biodiesel and biodiesel blends exhibited severe corrosion with copper-containing metals and high TAN's with all metals evaluated. Heavy gum formation occurred, which will create severe operational problems in the field, in particular, military operations which may have long storage periods. Although some materials showed no visual signs of corrosion, e.g., steel, aluminum, and cast aluminum, they generated higher total acid number than the other samples.

Biodiesel and biodiesel blend particle removal efficiency remained relatively constant for the materials evaluated. However, it appears that these fuel blends may degrade some filter media,

resulting in high media migration and short filter life. Although most water removal efficiencies were acceptable, the coalescing process was altered. Further research is required to better understand the fuel/water interactions and determine the consequences if the element fills with water.

VII. ADDITIVE COMPATIBILITY

Since this extensive corrosion had not been previously documented, an additional material compatibility evaluation was performed with JP-8, biodiesel, copper, brass, and bronze. Also, a new sample of JP-8 was obtained from a local U.S. Air Force base. The objective of this second evaluation was to determine the validity of this reaction and identify the additive components in JP-8 that may be causing these problems.

The new JP-8 was clay-treated to remove any additives, thus creating a Jet A sample. The additives were replaced, as shown in TABLE 14. The following additions were reblended into the Jet A (with 20 percent biodiesel) in a stepwise manner to determine their individual and combined effects with biodiesel on copper-containing materials.

- DCI4A corrosion inhibitor
- di-EGME fuel system icing inhibitor
- STADIS 450 static dissipator additive

The TAN's for all blends after eight weeks and six months of storage at 51.6°C are shown in TABLE 15.

TABLE 14. Additized Jet A Fuel Blends

<u>Blend</u>	<u>Components</u>
1	Jet A with 20 ppm DCI 4A
2	Jet A with 0.15 vol% di-EGME
3	Jet A with Stadis 450 (Note: Conductivity 300 to 400 pS/m)
4	Jet A with 20 ppm DCI 4A and 0.15 vol% di-EGME
5	Jet A with 20 ppm DCI 4A and Stadis 450
6	Jet A with 0.15 vol% di-EGME and Stadis 450
7*	Jet A with 20 ppm DCI 4A, 0.15 vol% di-EGME, and Stadis 450

* Blend 7 is a laboratory-produced JP-8.

TABLE 15. TAN's for New JP-8 Blends

<u>Blend</u>	<u>Copper</u>		<u>Brass</u>		<u>Bronze</u>	
	<u>8 wks</u>	<u>6 mos.</u>	<u>8 wks</u>	<u>6 mos.</u>	<u>8 wks</u>	<u>6 mos</u>
New JP-8	0.01	0.21	<0.01	0.05	<0.01	0.16
Biodiesel	*	0.34	*	0.06	*	0.63
Original JP-8	<0.01	0.06	*	0.02	<0.01	<0.01
20% Biodiesel + 80% Original JP-8	*	1.80	0.60	4.24	1.11	8.16

The TAN's for all seven blends began at <0.01 and remained at that level after six months. Photographs of the fuels and coupons after six months were presented as Figs. 11 through 16.

This evaluation confirmed that the original degradation does occur. Since no degradation occurred in the blended JP-8, it appears that the degradation is a function of the particular base stock used to produce JP-8.

VIII. FUEL LUBRICITY EVALUATIONS WITH BIODIESEL

The U.S. Army/Department of Defense has a large quantity of diesel-powered vehicles and equipment that utilizes rotary-type fuel injection pumps sensitive to fuel lubricity. The potential for accelerated wear in these pumps when using fuels with inadequate lubricity properties has been documented (29-34). The objective of the current investigation was to determine and document the effect of biodiesel on fuel lubricity. The methodology included bench-scale lubricity evaluations and pump stand durability tests.

A. Laboratory Wear Tests

Lubricity properties were determined for each fuel in the ten-fuel matrix (TABLE 16) by the test methods that follow.

TABLE 16. Ten-Fuel Matrix

<u>Fuel No.</u>	<u>Code</u>	<u>Description</u>
1	AL-23395-F	Biodiesel (methyl soyate)
2	AL-23403-F	Low-Sulfur Diesel Fuel, LSRD-4
3	AL-23404-F	Reference DF-2
4	AL-22363-F	JP-8
5	AL-23405-F	20% Biodiesel + 80% Low-Sulfur Diesel Fuel
6	AL-23406-F	30% Biodiesel + 70% Low-Sulfur Diesel Fuel
7	AL-23407-F	20% Biodiesel + 80% Ref. DF-2
8	AL-23408-F	30% Biodiesel + 70% Ref. DF-2
9	AL-23409-F	20% Biodiesel + 80% JP-8
10	AL-23410-F	30% Biodiesel + 70% JP-8

1. U.S. Army Scuffing Load Wear Test

This method uses a non-rotating steel ball held in a vertically mounted chuck and forced against an axially mounted steel ring with an applied load. The test ring/cylinder is rotated at a fixed

speed while being partially immersed in a test fluid. The applied load is systematically increased from 500 to 7,000 g until a distinct variation in both friction and wear is observed. (6, 35-37)

The neat biodiesel and all the blends performed better than the neat LSDF and Ref. No. 2 and JP-8 fuels. It appears to act as a lubricity agent.

2. High-Frequency Reciprocating Rig (HFRR) Tests

This test uses an electromagnetic vibrator to oscillate a moving specimen over a small amplitude while pressing against a fixed specimen. The fixed specimen is held in a small bath containing the test fuel. The produced scar is measured in both directions, averaged, and reported in millimeters. (7, 38). An illustration of the HFRR is given in Fig. 23.

The four blends with biodiesel using Ref. No. 2 and JP-8 and neat Ref. No. 2 and neat JP-8 produced results better than neat biodiesel, biodiesel blends with LSDF, and JP-8.

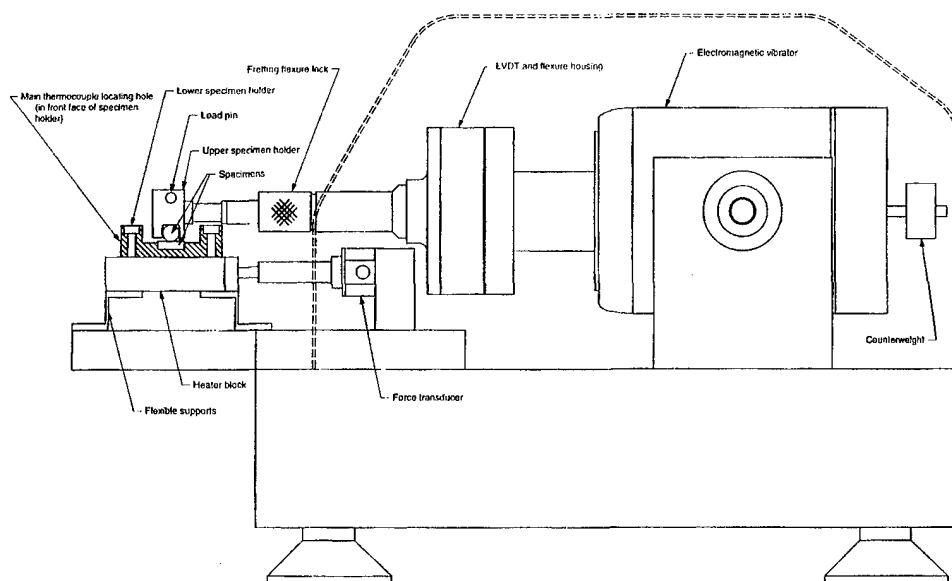


Figure 23. High-frequency reciprocating rig

B. Results

Figure 24 presents the results of the U.S. Army SLWT expressed in scuff load (grams) for the ten-fuel matrix. The results of the HFRR tests (i.e., wear scar in mm) conducted at 25°C are presented in Fig. 25. The descriptions of Fuels 1 through 10 are repeated in TABLE 16. The addition of biodiesel to low-sulfur diesel fuel (LSRD-4), reference DF-2, and JP-8 resulted in an increase in SLWT load and a decrease in HFRR wear scar. The improvement in fuel lubricity was evident in the JP-8 fuel with 20 and 30% biodiesel, as summarized in Figs. 26 and 27.

Because the 20 and 30% biodiesel blends showed such great lubricity improvement, the investigation of biodiesel lubricity effects was extended to include low level blends using a Jet A-1 fuel that had poor lubricity properties. Figure 28 illustrates the decrease in HFRR wear scar observed with blends containing 1 to 8% biodiesel in Jet A-1. Based on these HFRR results, the blend consisting of 8% biodiesel in Jet A-1 was selected for evaluation in a 200-hour rotary fuel injection pump test.

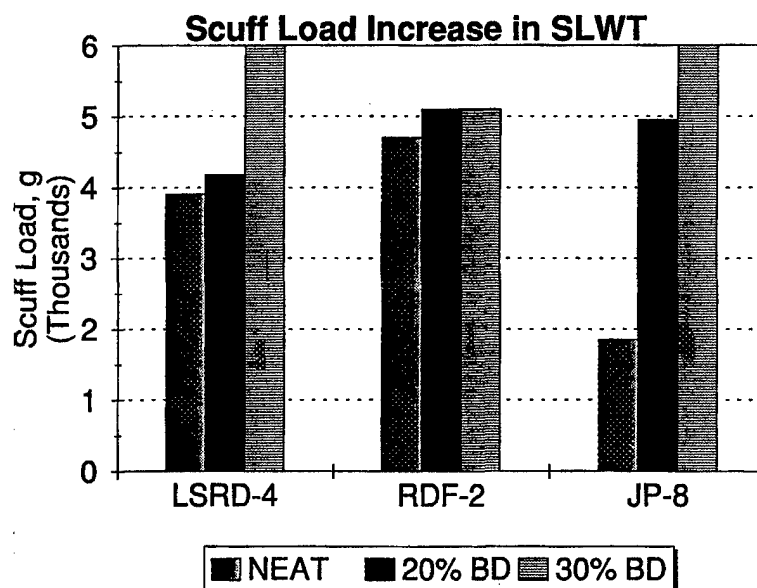


Figure 24. Scuffing load increase in SLWT

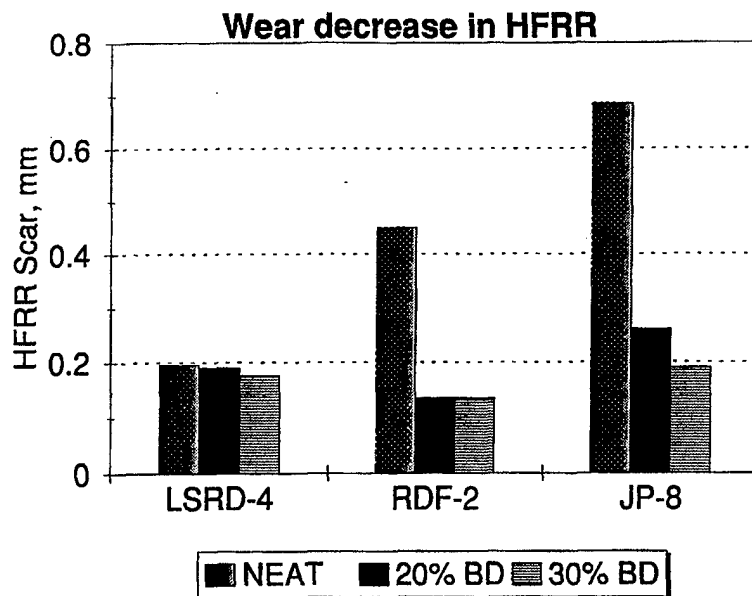


Figure 25. Wear decrease in HFRR

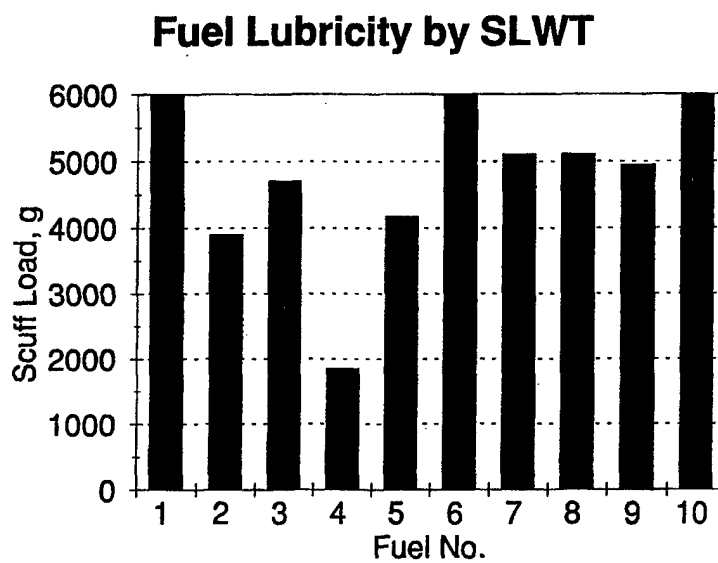


Figure 26. Fuel lubricity by SLWT

Fuel Lubricity by HFRR

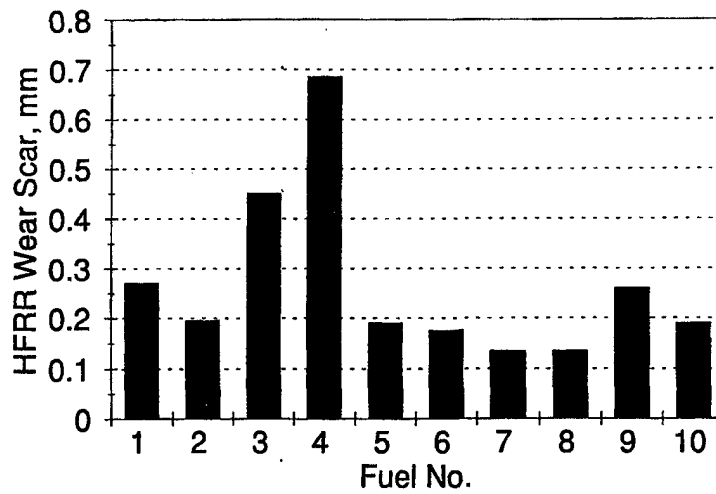


Figure 27. Fuel lubricity by HFRR

Lubricity Improvement With Biodiesel

HFRR Wear Scar, mm

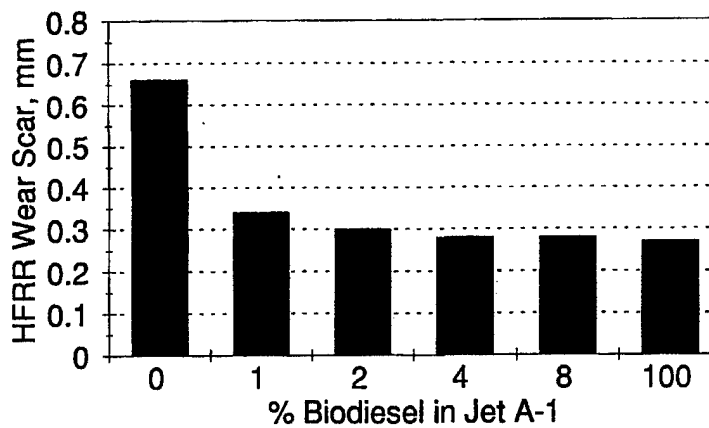


Figure 28. Lubricity improvement with biodiesel

C. Lubricity Effects With Storage Time

Lubricity properties of the ten-fuel matrix were determined after 0, 8, 12, and 18 weeks of storage. The storage conditions were described in Section IV. The results of the U.S. Army SLWT are presented in TABLE 17. The scuffing load of the neat biodiesel (Fuel No. 1) increased with storage time. The petrofuels (Fuels Nos. 2 through 4) had mixed lubricity results with storage time. Overall storage time did not appear to have a substantial effect on scuffing load of the petrofuels. The blends of biodiesel and petrofuel experienced increased scuffing load with storage duration.

TABLE 17. U.S. Army Scuffing Load Wear Test Data

Fuel No.	Fuel Code	Scuffing Load. g			
		0 wk	8 wk	12 wk	18 wk
1	AL-23395-F	6,000	>7,000	>7,000	6,250
2	AL-23403-F	3,900	3,400	3,700	4,200
3	AL-23404-F	4,700	5,500	5,000	4,650
4	AL-22363-F	1,850	3,200	1,800	1,900
5	AL-23405-F	4,175	5,400	6,900	>7,000
6	AL-23406-F	6,000	>7,000	>7,000	>7,000
7	AL-23407-F	5,100	5,200	5,000	5,800
8	AL-23408-F	5,100	>7,000	7,000	>7,000
9	AL-23409-F	4,950	>7,000	>7,000	>7,000
10	AL-23410-F	6,000	>7,000	>7,000	>7,000

The results of HFRR lubricity tests conducted on biodiesel, petrofuels, and blends after storage are presented in TABLE 18.

TABLE 18. High-Frequency Reciprocating Rig Data

Fuel No.	Fuel Code	Scar, mm			
		0 wk	8 wk	12 wk	18 wk
1	AL-23395-F	0.270	0.290	0.295	0.310
2	AL-23403-F	0.195	0.205	0.210	0.155
3	AL-23404-F	0.450	0.185	0.270	0.195
4	AL-22363-F	0.685	0.220	0.660	0.675
5	AL-23405-F	0.190	0.205	0.255	0.370
6	AL-23406-F	0.175	0.215	0.280	0.385
7	AL-23407-F	0.135	0.160	0.165	0.130
8	AL-23408-F	0.135	0.150	0.155	0.170
9	AL-23409-F	0.260	0.220	0.250	0.225
10	AL-23410-F	0.190	0.200	0.300	0.200

The HFRR wear scar increased slightly with storage time for the neat biodiesel. The reference DF-2 had decreased wear scar with storage time. The remaining fuels and blends did not exhibit any strong wear scar effect with prolonged storage.

D. Pump Stand Evaluations

Two pump stand evaluations were conducted using low-level biodiesel blends in a low lubricity fuel (Jet A-1). The rationale for investigating low-level biodiesel blends was to define a minimum level that provided acceptable improvement in fuel lubricity in a low lubricity fuel. Based on the bench tests, the 20 and 30% biodiesel blends would be expected to perform exceptionally well in the 200-hour pump stand tests. A listing of the 200-hour pump stand tests is presented in TABLE 19. Data from previous baseline pump stand tests that used Jet A-1 and DF-2 (34) are included for comparison with the biodiesel blend fuels. Brief properties of the 8 and 1 vol% blends of biodiesel in Jet A-1 are presented in TABLE 20. Complete fuel properties for Jet A-1 and Reference DF-2 (37) are presented in Appendix H.

TABLE 19. Description of 200-hr Pump Stand Tests

<u>Pump No.</u>	<u>Type</u>	<u>Pump Serial No.</u>	<u>Fuel Description</u>
1	S	6627504	Jet A-1
2	A	6624985	Jet A-1
3	S	8239195	Jet A-1 + 8% Biodiesel
4	A	8164638	Jet A-1 + 8% Biodiesel
5	S	8239196	Jet A-1 + 1% Biodiesel
6	A	8164639	Jet A-1 + 1% Biodiesel
7	S	6627507	DF-2
8	A	6624981	DF-2

S = Standard

A = Arctic

TABLE 20. Biodiesel Blend Properties

<u>Property</u>	<u>8% Biodiesel AL-24252</u>	<u>1% Biodiesel AL-24322</u>
Kinematic Viscosity, 40°C, cSt, D 445	1.14	1.04
Water, ppm, Karl Fischer	180	114
HFRR at 25°C, wear, mm	0.28	0.34

E. Procedure

The 200-hour pump stand evaluation procedure is described in Reference 33. The test uses two Stanadyne rotary injection pumps from a GM 6.2L diesel engine. One pump is standard configuration while the other pump is an arctic configuration that contains hardened parts. The pumps were not disassembled prior to testing, and no dimensional measurements were made on pump components. Before testing, all pumps were precisely calibrated to Stanadyne specifications

for fuel delivery and injection timing by a local diesel injection service company. A schematic of the pump test rig is presented in Fig. 29, with additional description of the pump stand details available in Reference 33. Each 200-hour pump stand test was conducted at 77°C fuel-in temperature and 1,800 pump rpm. Fuel flow, transfer pump pressure, and pump housing pressure were recorded during the test. After the 200-hour test, each pump was retested by the local diesel injection service company to determine any changes in calibration parameters. The pumps were then disassembled and visually rated for wear in 17 areas. Previous work by Lacey (39, 40) indicated that accurate post-test wear measurements can be made using surface profilometry. Seven internal pump components were measured for wear volume by the surface profilometry method.

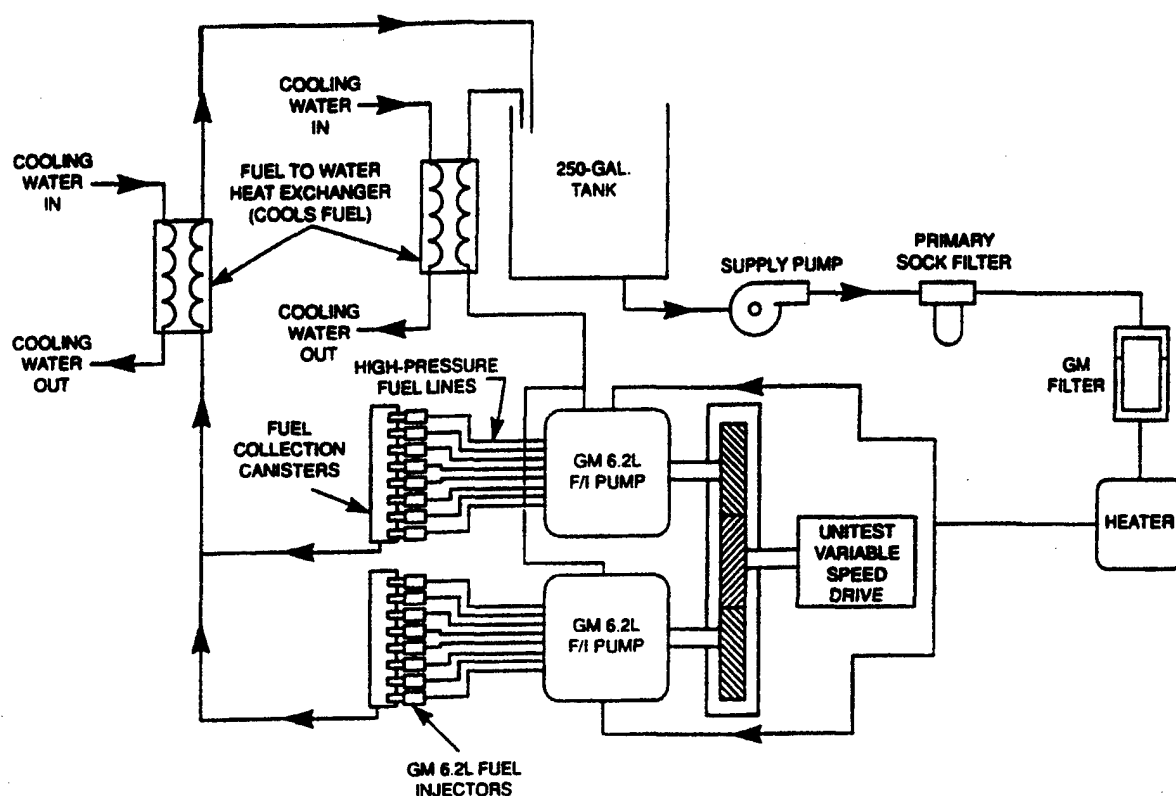


Figure 29. Fuel system schematic

F. Results of Pump Stand Evaluations

Complete test reports for the two pump stand evaluations that used biodiesel blend fuel are presented in Appendices I and J. Key aspects of each pump condition after test are discussed and compared with results for Jet A-1 and reference DF-2 in the section that follows.

Results of the pretest calibration of all eight pumps (TABLE 19) are presented in TABLES 21 through 24 for pump delivery, transfer pump pressure, injection advance, and miscellaneous measurements, respectively. The post-test calibration results are presented in TABLES 25 through 28. Key changes in calibration performance parameters are indicative of pump condition at end of test. Note that because the head, rotor assembly, and drive tang were replaced during the 200-hour test of the 1 vol% biodiesel blend (Pumps 5 and 6), the post-test calibration data are for information only. The parts replacement occurred because both Pumps 5 and 6 seized at 46 hours upon start-up due to improper start-up procedure.

TABLE 21. Pre-Test Pump Delivery

Pump No.	Delivery, mm ³ /St* at rpm				
	75	200	1,000	1,800	1,950
Spec.	>29	>47	51 to 55	>46	>44
1	38.1	50.7	53.4	53.6	51.1
2	42.8	51.0	53.3	52.0	49.1
3	38.5	48.5	54.5	53.5	51.0
4	38.5	49.5	54.0	52.5	50.5
5	37.5	48.5	55.0	54.5	51.5
6	37.5	49.5	54.0	55.5	53.0
7	39.9	50.2	54.1	54.1	51.1
8	42.1	51.5	53.1	51.7	49.8

Note: Readings at wide open throttle

* St = Stroke

TABLE 22. Pre-Test Transfer Pump Pressure

Pump No.	Pressure, psi at rpm			
	75	1,000	1,800	2,100
Spec.	>12	70 to 76	70 to 76	<135
1	--	75	--	130
2	27	73	--	130
3	24	75	--	132
4	19	74	--	140
5	30	75	--	136
6	22	75	--	138
7	25	75	--	135
8	25	73	--	130

Note: Readings at wide open throttle.

TABLE 23. Pre-Test Injection Advance Measurement

Pump No.	Advance, degrees on pump			
	325	1,000	1,600	1,600
Speed	LI*	WOT†	WOT	LI
Throttle				
Spec.	>1.5	0.5 to 2.5	4.2 to 6.7	<10
1	3.0	1.5	6.0	10
2	3.5	1.5	5.5	10
3	4.0	1.5	--	--
4	3.0	1.5	--	--
5	5.0	1.5	--	--
6	3.5	1.5	--	--
7	3.0	1.5	6.0	10
8	2.5	1.5	5.5	10

* LI = Low Idle

† WOT = Wide Open Throttle

TABLE 24. Pre-Test Sundry Measurements

Pump No.	RF*	SO†	BA‡
	cc/min	mm ³ /St	mm ³ /St
Units	225 to 375	<4	<8
Spec.			
1	350	0	0
2	200	0	0
3	300	0	0
4	375	0	0
5	300	0	0
6	325	0	0
7	350	0	0.7
8	200	0	2.8

* RF = Return Fuel From Housing to Tank

† SO = Shut Off Fuel Flow

‡ BA = Fuel Flow at Break-Away Speed
(2,100 pump rpm)

TABLE 25. Post-Test Pump Delivery

Pump No.	Delivery, mm ³ /St* at rpm				
	75	200	1,000	1,800	1,950
Spec.	>29	>47	51 to 55	>46	>44
1	35.4	49.5	51.6	51.1	51.3
2	39.9	50.5	51.9	51.5	50.0
3	38.5	48.5	53.5	54.0	52.0
4	37.0	48.5	53.0	52.5	50.5
5	35.0	46.0	51.0	52.0	52.0
6	44.0	50.0	54.0	54.0	55.0
7	35.7	50.0	52.8	52.5	50.2
8	37.9	49.1	52.4	51.0	48.7

Note: Readings at wide open throttle

* St = Stroke

TABLE 26. Post-Test Transfer Pump Pressure

Pump No.	Pressure, psi at rpm			
	75	1,000	1,800	2,100
Spec.	>12	70 to 76	70 to 76	<135
1	18	68	96	115
2	18	66	95	123
3	26	75	--	140
4	18	72	--	140
5	24	72	--	122
6	22	74	--	126
7	24	76	107	129
8	24	73	103	129

Note: Readings at wide open throttle.

TABLE 27. Post-Test Injection Advance Measurement

Pump No.	Advance, degrees on pump			
	325	1,000	1,600	1,600
Speed	LI*	WOT†	WOT	LI
Throttle				
Spec.	>1.5	0.5 to 2.5	4.2 to 6.7	<10
1	2.5	0.5	4.5	10
2	2.2	0.5	4.5	10
3	3.5	1.5	--	--
4	3.0	1.25	--	--
5	4.0	0.75	--	--
6	2.5	1.5	--	--
7	2.7	2.0	5.5	9.7
8	2.5	1.5	5.5	10

* LI = Low Idle

† WOT = Wide Open Throttle

TABLE 28. Post-Test Sundry Measurements

Pump No.	RF*	SO†	BA‡
Units	cc/min	mm ³ /St	mm ³ /St
Spec.	225 to 375	<4	<8
1	325	0	1.6
2	200	0	47
3	300	0	0
4	400	0	0
5	300	0	0
6	300	0	0
7	375	0	0
8	220	0	47

* RF = Return Fuel From Housing to Tank

† SO = Shut Off Fuel Flow

‡ BA = Fuel Flow at Break-Away Speed
(2,100 pump rpm)

Transfer pump pressure decrease has been related to the use of low lubricity fuels.(39-41) The percent decrease in transfer pump pressure at 1,000 rpm is shown for each pump in Fig. 30. The presence of biodiesel at either 8 vol% (Pumps 3 and 4) or 1 vol% (Pumps 5 and 6) helped control the decrease in transfer pump pressure observed with Jet A-1 fuel (Pumps 1 and 2) at 1,000 rpm. The percent transfer pump pressure decrease at 2,100 rpm is presented in Fig. 31. At this speed, Pumps 2 and 3, operated on 8 vol% biodiesel blend, did not experience transfer pump pressure decrease as observed for Pumps 1 and 2, which were operated on Jet A-1 fuel. At 1 vol%, biodiesel was not effective in preventing transfer pump pressure decrease (Pumps 5 and 6) at 2,100 rpm. The effect on transfer pump pressure of replacing the parts at 46 hours appears to be minimal, based on the transfer pump pressure data collected during the test.

A decrease in pump injection advance was observed after a 200-hour pump stand test when using Jet A-1 fuel (Pumps 1 and 2).(33) Retarded fuel injection results in poor engine performance. The decrease in fuel injection advance at 1,000 rpm is presented in Fig. 32. In the current work,

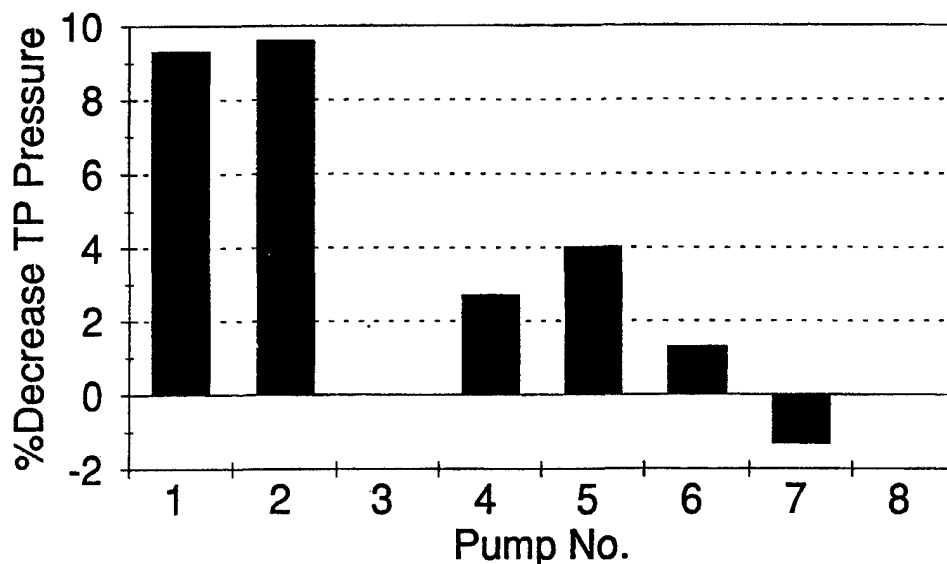


Figure 30. Transfer pump pressure percent decrease at 1,000 rpm

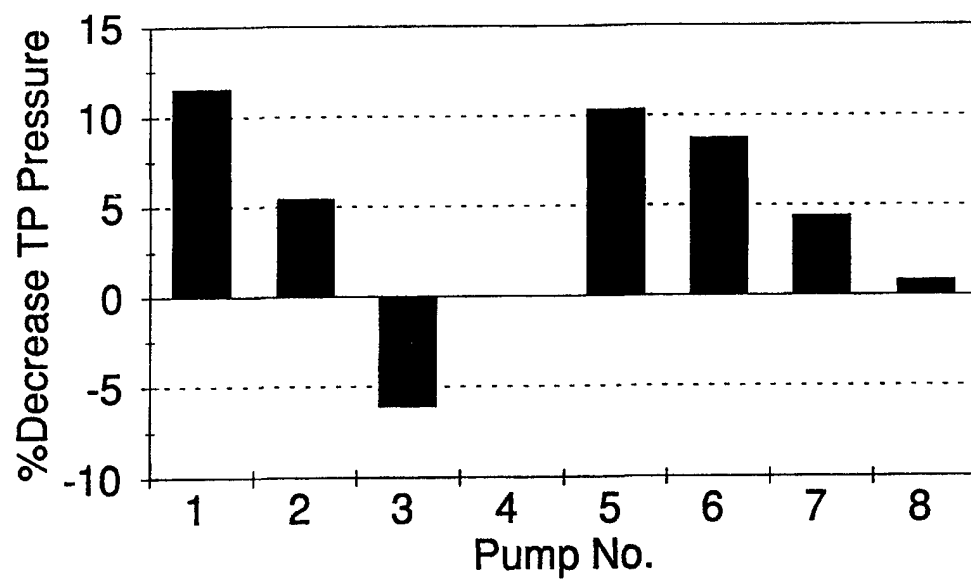


Figure 31. Transfer pump pressure percent decrease at 2,100 rpm

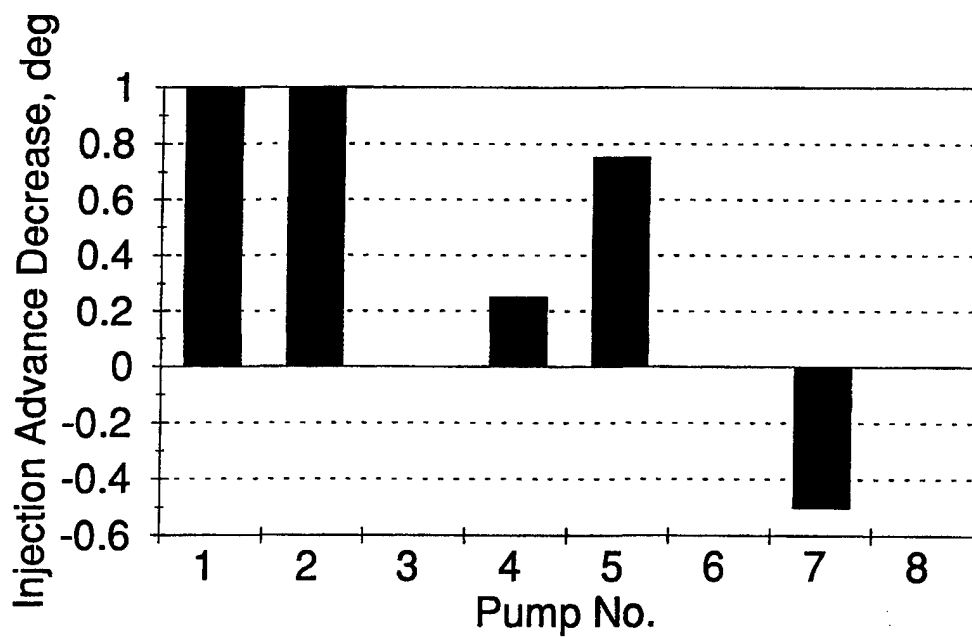


Figure 32. Injection advance decrease degrees at 1,000 rpm

use of the 8 vol% biodiesel blend (Pumps 3 and 4) resulted in minimal to no fuel injection retardation. The use of 1 vol% biodiesel blend resulted in nearly the same decrease in injection timing as Jet A-1 for the standard pump (No. 5) and no decrease for the arctic pump. Overall, the use of 8% biodiesel blend resulted in an acceptable level of decreased injection timing.

A visual wear level rating was made for seventeen critical pump components, as shown in TABLE 29. This subjective rating scale ranged from 0 = no wear to 5 = failure. A plot of the average visual wear rating is shown in Fig. 33. The 8 vol% biodiesel blend was effective in reducing the visual wear rating to near Reference DF-2 levels. The 1 vol% biodiesel blend also was effective in reducing visual wear levels compared to neat Jet A-1; however, it did not reduce the wear rating to the Reference DF-2 level.

Wear of internal pump components was measured using surface profilometry. Details and assumptions used in calculating the wear are presented in each test report (Appendices I and J). TABLE 30 presents a summary of the calculated wear volume for seven internal pump components. The pump blades, drive tang, drive slot, and thrust washer are hardened parts in the arctic pump; all other components are the same in both standard and arctic pumps.

The Archard's wear coefficients calculated for each component are presented in TABLE 31. In examining the wear volume and wear coefficient data, several effects were noted.

- In standard pumps, the use of biodiesel (1 or 8%) in Jet A-1 resulted in the following:
 - Measured wear in drive tang and drive slot was reduced from Jet A-1 level. Wear was essentially equivalent to DF-2.
 - Pump blade wear was reduced from Jet A-1 levels to DF-2 level.
 - Thrust washer wear was reduced from Jet A-1 levels to near DF-2 level.

TABLE 29. Visual Wear Level on Critical Pump Components

Component	Std. Jet A-1	Arctic Jet A-1	Std. 8% Biodiesel	Arctic 8% Biodiesel	Std. 1% Biodiesel	Arctic 1% Biodiesel	Std. Diesel	Arctic Diesel
Hydraulic Head and Rotor								
Distributor Rotor	1	1	1	0	1*	1*	1	0
Delivery Valve	2	2	1	1	1	1	1	1
Pumping Plungers	4	3	4	4	4*	2*	1	1
Cam Rollers and Shoes	3	4	2	2	2	2	1	1
Leaf Spring	1	1	1	1	1	1	1	1
Drive Shaft Tang	5	1	2	1	1*	1*	2	1
Cam	1	1	1	1	1	1	1	1
Governor Weights	4	3	1	1	1	2	1	1
Governor Thrust Washer	4	3	1	1	1	2	1	1
Governor Thrust Sleeve	4	2	1	1	1	1	1	1
Transfer Pump								
Pressure Regulator	3	3	1	2	1	2	1	2
Pressure Regulator Piston	2	2	2	2	3	2	2	2
Transfer Pump Blades	3	1	1	1	2	1	2	1
Liner	3	3	1	1	2	2	1	2
Rotor Retainers	3	3	1	1	2	2	1	1
Governor								
Metering Valve	3	2	1	1	2	2		
Advance								
Advance Piston	4	3	2	2	3	3	2	2
Average	2.76	2.06	1.35	1.29	1.70	1.64	1.23	1.17

0 = No wear

5 = Failure

* Part changed during test

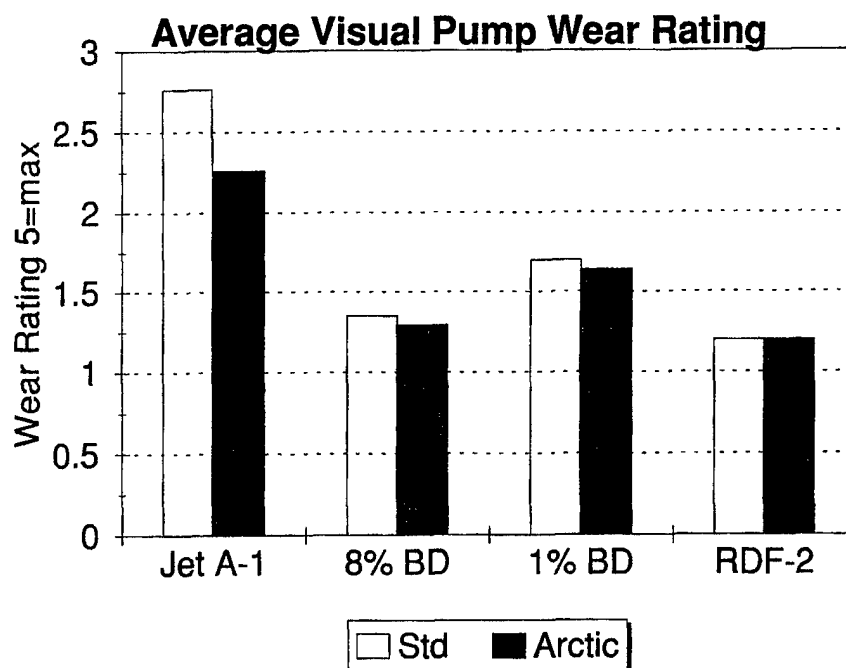


Figure 33. Average visual pump wear rating

TABLE 30. Wear Volume on Selected Pump Components ($\text{mm}^3 \times 10^{-3}$)

Pump	Fuel*	Pump	Drive	Drive	Thrust	Governor Weights	Roller	Rotor
		Blades	Tang	Slot	Washer		Shoe	Retainers
Std. (No. 1)	J	26	11000	14000	372	408	470	2112
Arctic (No. 2)	J	1.7	43	48	274	264	1160	3300
Std. (No. 3)	J + 8 BD	6.0	144	124	90	28	10	71
Arctic (No. 4)	J + 8 BD	8.8	46	22	195	37	10	726
Std. (No. 5)	J + 1 BD	0	90†	72†	117	18	6	1745
Arctic (No. 6)	J + 1 BD	7.7	226†	283†	30	50	16	693
Std. (No. 7)	DF-2	7.1	101	31	--	36	38	99
Arctic (No. 8)	DF-2	2.4	5	36	135	36	24	132

* Fuel Identities:

J = Jet A-1

J + 8 BD = Jet A-1 + 8% Biodiesel

J + 1 BD = Jet A-1 + 1% Biodiesel

DF-2 = Diesel Fuel

† Replacement parts at 46 test hours

TABLE 31. Archard's Wear Coefficient

		Pump	Drive	Drive	Thrust	Governor	Roller	Rotor
<u>Pump</u>	<u>Fuel*</u>	<u>Blades</u>	<u>Tang</u>	<u>Slot</u>	<u>Washer</u>	<u>Weights</u>	<u>Shoe</u>	<u>Retainers</u>
Std. (No. 1)	J	67	503	705	107	15	236	69
Arctic (No. 2)	J	7	2	2	79	10	582	107
Std. (No. 3)	J + 8 BD	11	6	5	26	1	5	2
Arctic (No. 4)	J + 8 BD	38	1	1	56	1	5	23
Std. (No. 5)	J + 1 BD	0	4†	3†	33	1	3	56
Arctic (No. 6)	J + 1 BD	33	6†	11†	9	2	8	22
Std. (No. 7)	DF-2	17	5	2	0	1	19	3
Arctic (No. 8)	DF-2	10	8	2	39	1	12	4

* Fuel Identities:

J = Jet A-1

J + 8 BD = Jet A-1 + 8% Biodiesel

J + 1 BD = Jet A-1 + 1% Biodiesel

DF-2 = Diesel Fuel

† Replacement parts at 46 test hours

- In both standard and arctic pumps, the use of biodiesel (1 or 8%) in Jet A-1 resulted in the following:
 - Governor weight wear was reduced from Jet A-1 levels to DF-2 level.
 - Roller shoe wear was reduced from Jet A-1 levels to slightly less than DF-2 level.
 - Rotor retainer wear was reduced from Jet A-1 levels but did not approach DF-2 level.

Overall, with respect to measured wear, biodiesel in Jet A-1 at 1 and 8% resulted in substantial wear reductions compared to neat Jet A-1.

IX. CONCLUSIONS

Specific, detailed conclusions are presented in each section of this report. The following summarized, general conclusions are offered.

A. Properties of Ten-Fuel Matrix

Compared to the petrofuels, neat biodiesel has higher flash, cloud, freeze, and pour points; higher viscosity; lower heat of combustion; narrow distillation range; and increased water content.

In the blended fuels, these property differences were approximately in proportion to the biodiesel concentration of the blend.

B. Storage Stability

Relatively poor fuel storage stability was observed for neat biodiesel and petrofuel/biodiesel blends. Increased insolubles, total acid number, and water content were observed.

C. Material Compatibility

1. Elastomers

- Biodiesel increased the swell characteristics of nitrile, fluorosilicon, polyurethane and polypropylene materials.
- Biodiesel reduced the hardness of nitrile and polypropylene.
- Neat biodiesel caused a significant initial decrease in nylon 6/6 tensile strength.

2. Metals

- Neat biodiesel and biodiesel blends exhibited severe corrosion with copper-containing metals.
- High total acid numbers were observed with all metals during storage, which is related to the poor storage stability of biodiesel.

3. Filters

- Particle removal efficiency remained relatively constant for the filters evaluated in neat biodiesel and biodiesel blends.
- Biodiesel blends may degrade some filter media, resulting in media migration.
- Most water removal efficiencies were acceptable; however, the coalescing process was altered.

D. Additive Compatibility (JP-8 Additives)

JP-8 additives (i.e., corrosion inhibitor, fuel system icing inhibitor, anti-static agent) were compatible with biodiesel stored in the presence of copper-containing materials.

E. Fuel Lubricity

- Neat biodiesel has excellent bench-scale lubricity performance as demonstrated in the U.S. Army SLWT and the HFRR.
- Biodiesel improves the bench lubricity performance of poor lubricity fuels such as Jet A-1.
- An 8 vol% blend of biodiesel in low lubricity Jet A-1 had acceptable performance in a 200-hr rotary injection pump stand test.
- A 1 vol% blend of biodiesel in low lubricity Jet A-1 had overall performance that approached the performance of Reference DF-2 in the 200-hr pump stand test.

- The effect of storage time on lubricity properties of neat biodiesel and petrofuel blends was determined. SLWT had increased scuffing load with storage time for the biodiesel/petrofuel blends. No strong effects of storage time on HFRR wear scar were observed.

X. RECOMMENDATIONS

Based on the results of this program, the following recommendations for additional investigations are made:

- Evaluation of additives to improve the storage stability of biodiesel and biodiesel blends should be conducted.
- The effects of trace manufacturing contaminants on biodiesel storage stability should be determined.
- The effects and mechanisms of biodiesel fuel interaction with water and filter/coalescer performance need to be investigated.
- Fuel injector cleanliness, diesel engine endurance (including wear and deposits under Army operating conditions) need to be defined.
- Once the above issues are resolved, a well-controlled field demonstration program using a biodiesel blend should be conducted at an Army installation.

XI. LIST OF REFERENCES

1. McDonald, J.F., Purcell, D.L., McClure, B.T., and Kittleson, D.B., "Emissions Characteristics of Soy Methyl Ester Fuels in an IDI Compression Ignition Engine," SAE Technical Paper No. 950400, February 27-March 2, 1995.
2. Scholl, Kyle W. and Sorenson, Spencer C., "Combustion of Soybean Oil Methyl Ester in a Direct Injection Diesel Engine," SAE Paper No. 930934, 1993.

3. Holmberg, William C. and Peeples, James E., "Biodiesel: A Technology, Performance, and Regulatory Overview," prepared for the National Soy Diesel Development Board by American Biofuels Association and Information Resources, Inc., February 1994.
4. Draft American Society of Agricultural Engineers (ASAE) Engineering Practice: ASAE EP $\times 552$, June 28, 1993.
5. American Society for Testing and Materials Method D 3948, "Standard Test Method for Determining Water Separation Characteristics of Aviation Turbine Fuels by Portable Separometer," ASTM, 1916 Race Street, Philadelphia, PA, 1993.
6. American Society for Testing and Materials Method D 4625, "Standard Test Method for Distillate Fuel Storage Stability at 43°C (110°F)," ASTM, 1916 Race Street, Philadelphia, PA, 1992.
7. Lacey, P.I., "Development of a Lubricity Test Based on the Transition From Boundary Lubrication to Severe Adhesive Wear in Fuels," Society of Tribologists and Lubrication Engineers, Preprint No. 94AM5J1, 1994.
8. American Society for Testing and Materials Method D 664, "Standard Test Method for Acid Number of Petroleum Products by Potentiometric Titration," ASTM, 1916 Race Street, Philadelphia, PA, 1989.
9. American Society for Testing and Materials Method D 1500, "Standard Test Method for ASTM Color of Petroleum Products (ASTM Color Scale)," ASTM, 1916 Race Street, Philadelphia, PA, 1991.
10. American Society for Testing and Materials Method D 381, "Standard Test Method for Existent Gum in Fuels by Jet Evaporation," ASTM, 1916 Race Street, Philadelphia, PA, 1994.
11. American Society for Testing and Materials Method D 3241, "Standard Test Method for Thermal Oxidation Stability of Aviation Turbine Fuels (JFTOT Procedure)," ASTM, 1916 Race Street, Philadelphia, PA, 1994.
12. American Society for Testing and Materials Method D 4928, "Standard Test Method for Water in Crude Oils by Coulometric Karl Fischer Titration," ASTM, 1916 Race Street, Philadelphia, PA, 1989.
13. Cusano, C.M., Stafford, R.J., and Lucas, J.M., "Changes in Elastomer Swell with Diesel Fuel Composition," Society of Automotive Engineers (SAE) Paper No. 942017, presented at the 1994 Fuels and Lubricants Meeting and Exposition, Baltimore, MD.

14. Reed, Thomas B., "An Overview of the Current Status of Biodiesel," Department of Chemical Engineering, Colorado School of Mines, Golden, CO.
15. Holmberg, William C., Gavett, Earle E., Merrill, Peter N., and Peebles, James E., "National Soydiesel Development Board Standards for Biodiesel," June 1993.
16. Schumaker, Leon G., Hires, William G., and Borgelt, Steven C., "Fueling a Diesel Engine With Methyl-Ester Soybean Oil," Agricultural Engineering, University of Missouri-Columbia, Columbia, MO.
17. "Final Report of GE Demonstration Program With Rape Seed Methyl Ester as Diesel Engine Fuel," Project No. EB 160 M 5337, AC 112/WG 4/Ground Fuels Working Party, Non-Fossil Fuels, 17 December 1993.
18. Hawkins, C.S., Fuls, J., and Hugo, F.J.C., "Sunflower Oil Esters: An Alternative Fuel for Direct Injection Diesel Engines," Society of Automotive Engineers (SAE) Paper No. 831356, presented at the 1983 International Off-Highway Meeting and Exposition, Milwaukee, WI.
19. Goldsberry, D. Roy, "Fuel Hose Permeation of Fluoropolymers," Society of Automotive Engineers (SAE) Paper No. 930992, presented at the 1993 International Congress and Exposition, Detroit, MI.
20. Kusher, Kurt S., "Alternate Materials for Alternative Fuels," Society of Automotive Engineers (SAE) Paper No. 920165, presented at the 1992 International Congress and Exposition, Detroit, MI.
21. Carpenter, Mary S., Chillous, Sandra E., and Will, Rod R., "High Temperature Resistance of Fluoropolymers in Automotive Fuels," Society of Automotive Engineers (SAE) Paper No. 910103, presented at the 1991 International Congress and Exposition, Detroit, MI.
22. Stahl, W.M. and Stevens, R.D., "Fuel-Alcohol Permeation Rates of Fluoroelastomers, Fluoroplastics, and Other Fuel Resistant Materials," Society of Automotive Engineers (SAE) Paper No. 920163, presented at the 1992 International Congress and Exposition, Detroit, MI.
23. Abu-Isa, Ismat A., "Effects of Mixtures of Gasoline with Methanol and With Ethanol on Automotive Elastomers," Society of Automotive Engineers (SAE) Paper No. 800786, presented at the 1980 Passenger Car Meeting, Dearborn, MI.
24. Goldsberry, D. Roy, Chillous, Sandra E., and Will, Rod R., "Fluoropolymer Resins: Permeation of Automotive Fuels," Society of Automotive Engineers (SAE) Paper No. 910104, presented at the 1991 International Congress and Exposition, Detroit, MI.

25. American Society for Testing and Materials Method D 471, "Standard Test Method for Rubber Property—Effect of Liquids," ASTM, 1916 Race Street, Philadelphia, PA, 1991.
26. American Society for Testing and Materials Method D 412, "Standard Test Method for Rubber Properties in Tension," ASTM, 1916 Race Street, Philadelphia, PA, 1992.
27. American Society for Testing and Materials Method D 130, "Standard Test Method for Detection of Copper Corrosion from Petroleum Products by the Copper Strip Tarnish Test," ASTM, 1916 Race Street, Philadelphia, PA, 1994.
28. Lucas, Wayne, "Summary Test Report for the Biodiesel Fuel Evaluation for the U.S. Army Tactical Wheeled Vehicles - Volume I of Series," Material Test Directorate, U.S. Army Yuma Proving Ground, Yuma, AZ, May 1995.
29. Society of Automotive Engineers Information Report J1839, "Coarse Droplet Water/Fuel Separation Test Procedure," 1995 SAE Handbook, Vol. 2, SAE, 400 Commonwealth Drive, Warrendale, PA 15096-0001, May 1990.
30. Lacey, P.I. and Westbrook, S.R., "The Effect of Increased Refining on the Lubricity of Diesel Fuel," Proceedings of the Fifth International Conference on Stability and Handling of Liquid Fuels, October 1994.
31. Lacey, P.I. and Lestz, S.J., "Fuel Lubricity Requirements for Diesel Injection Systems," Interim Report BFLRF No. 270, AD A235972, prepared by the U.S. Army Belvoir Fuels and Lubricants Research Facility (SwRI), Southwest Research Institute, San Antonio, TX, February 1991.
32. Lacey, P.I., "Wear Mechanism Evaluation and Measurement in Fuel-Lubricated Components," Interim Report BFLRF No. 286, AD A284870, prepared by the U.S. Army Belvoir Fuels and Lubricants Research Facility (SwRI), Southwest Research Institute, San Antonio, TX, September 1994.
33. Lacey, P.I. and Lestz, S.J., "Effect of Low-Lubricity Fuels on Diesel Injection Pumps—Part I: Field Performance," SAE Technical Paper No. 920823, February 24-28, 1992.
34. Lacey, P.I., "The Relationship Between Fuel Lubricity and Diesel Injection System Wear," Interim Report BFLRF No. 275, AD A247927, prepared by the U.S. Army Belvoir Fuels and Lubricants Research Facility (SwRI), Southwest Research Institute, San Antonio, TX, January 1992.
35. Lacey, P.I. and Westbrook, S.R., "Diesel Fuel Lubricity," SAE Technical Paper No. 950248, February 27-March 2, 1995.

36. Lacey, P.I., "Development of a Lubricity Test Based on the Transition From Boundary Lubrication to Severe Adhesive Wear in Fuels," *Lubrication Engineering*, **50**, No. 10, October 1994.
37. Lacey, P.I. and Lestz, S.J., "Effect of Low-Lubricity Fuels on Diesel Injection Pumps-Part II: Laboratory Evaluation," SAE Technical Paper No. 920824, February 24-28, 1992.
38. Westbrook, S.R., Lacey, P.I., McInnis, L.A., Lestz, S.J., and LePera, M.E., "Survey of Low Sulfur Diesel Fuels and Aviation Kerosenes From U.S. Military Installations," SAE Technical Paper No. 952369, October 16-19, 1995.
39. Meeting Minutes, International Standards Organization (ISO), Technical Committee 22, Subcommittee 7, Working Group 6, (TC22, SC7, WG6), 17 October 1994, Baltimore, MD, Document N-88.
40. Lacey, P.I. and Lestz, S.J., "Failure Analysis of Fuel Injection Pumps From Generator Sets Fueled With Jet A-1," Interim Report BFLRF No. 268, AD A234930, prepared by the U.S. Army Belvoir Fuels and Lubricants Research Facility (SwRI), Southwest Research Institute, San Antonio, TX, January 1991.
41. Lacey, P.I. and Lestz, S.J., "Wear Analysis of Diesel Engine Fuel Injection Pumps From Military Ground Equipment Fueled With Jet A-1," Interim Report BFLRF No. 272, AD A239022, prepared by the U.S. Army Belvoir Fuels and Lubricants Research Facility (SwRI), Southwest Research Institute, San Antonio, TX, May 1991.

APPENDIX A

Statement of Work for Biodiesel Fuel Evaluation

Preceding Page Blank

Belvoir RDE Center/BFLRF (SwRI)
STATEMENT OF WORK
for
Biodiesel Fuel Evaluation

Introduction

The purpose of the proposed program is to determine the acceptability of biodiesel fuel as an alternative fuel for use in military ground equipment/systems. The proposed program consists of the following five phases:

- Phase 1 - Biofuel/Materials Compatibility
- Phase 2 - Fuel Blend Characteristics
- Phase 3 - Engine Dynamometer Evaluations
- Phase 4 - Pilot Field Demonstrations
- Phase 5 - User Impact/Acceptance-Full Field Demonstration

Discussion of each phase will be presented separately.

Phase 1 - Biofuel/Materials Compatibility

Objective

The objective of this phase of the program is to determine the short-term compatibility of biodiesel fuel blends with fuel system materials.

Description of Work

The short-term compatibility of diesel engine fuel system materials will be determined in the following manner:

- a. Identify engine fuel system components from the following diesel engines: DDC 6V-92, Cummins L10, and Navistar 7.3L.
- b. Identify the materials present in these fuel system components. This will include elastomer types, plastics, and metallic materials. In a previous program*, the following materials were investigated for compatibility with a fuel additive:

* Frame, E.A., "Evaluations of Preservative Engine Oil Containing Vapor-Phase Corrosion Inhibitor and a Simplified Engine Preservation Technique," Interim Report BFLRF No. 269 (AD A240100), prepared by Belvoir Fuels and Lubricants Research Facility (SwRI), San Antonio, Texas, December 1990.

Metals
Copper, Electrolytic (QQ-C-576)
Aluminum (QQ-A-250/4E)
Steel (ASTM A 366, Class 1) = 1018 Low C. Mild Steel
Zinc (QQ-Z-301C)
Cadmium (QQ-A-671)
Magnesium (QQ-M-44B, AZ31B)
Lead (QQ-L-201F(2), Grade B)
Brass (QQ-B-613D, Composition 342)
Bronze (QQ-B-728, Class A)
Tin (MIL-T-12076A, Grade B)
Babbitt
Silver
Nickel

Elastomers
Medium Nitrile
Low Nitrile
High Nitrile
Polyester Polyurethane
Polyether Polyurethane
Fluorosilicone
Teflon®
Viton®

- c. Identify or design material compatibility procedure. We will investigate the material compatibility tests used by DDC, Cummins, Navistar, and other diesel engine manufacturers. A single static storage/exposure test procedure will be conducted with representative fuel system materials with and without moisture being added. Temperature and test duration are important variables that will be held constant. The following seven-fuel matrix will be investigated:

Fuel Component	Fuel Designation						
	<u>A</u>	<u>B</u>	<u>C</u>	<u>D</u>	<u>E</u>	<u>F</u>	<u>G</u>
Low-sulfur fuel (0.05 % S)	100	0	0	80	70	0	0
Off-highway fuel (> 0.05 % S)	0	100	0	0	0	80	70
Methyl soyate	0	0	100	20	30	20	30

After exposure, the metallic panels will be inspected and rated for corrosion and tarnish while the elastomeric materials will be evaluated for standard properties such as swell, hardness, and tensile strength.

- d. Determine biodiesel fuel compatibility with typical fuel filters such as the following:
- Pleated paper
 - Wound cotton string
 - Cotton sock
 - Phenolic resin.

After exposure to the test fuel, filter performance parameters will be determined, such as:

- Time to a standard 15-psi pressure drop
 - Media migration
 - Solids removal (test dust).
- e. Results will be evaluated and a report prepared.

Phase 2 - Fuel Blend Characteristics (Partial)

Objective

The objectives of this phase are to determine fuel blend characteristics relative to military fuel requirements. The estimates are based on using the seven-fuel matrix from Phase 1.

Description of Work

- a. Fuel filter compatibility evaluations will be completed using representative fuel filters from military equipment. These evaluations will be conducted with and without moisture present.
- b. Water bottoms are a frequent occurrence in military fuel tanks. Therefore, the fuel emulsification potential of biodiesel fuel blends will be determined using the microsep procedure.
- c. Military fuel generally has a longer turnover time than commercial fuel, which makes storage stability an important concern for the military. Storage/thermal stability properties will be determined in a six-month storage test, by assessing the increase in total acid number (TAN), and by running JFTOT evaluations.
- d. A large number of vehicles within the DOD inventory are powered by the GM 6.2L diesel engine that has a well-known fuel lubricity requirement. Lubricity characteristics of the biodiesel fuel blends will be determined using bench-test procedures.
- e. We have identified the need for assessing the ability for field blending that may occur at differing ambient temperatures, as this was a requirement with previous fuels such as gasohol. In addition, additive compatibility and effectiveness will be determined. Three different biocide types and possibly other additive systems will be evaluated for compatibility with the biodiesel fuel blends by blending them in biofuel and determining biocide and other additive effectiveness.

- f. Fuel flammability characteristics will be determined to investigate if the presence of methyl soyate, which contains oxygen, alters the flammability of the base fuel. This will be accomplished using bench tests developed by BFLRF.
- g. The remaining fuel inspection properties (e.g., gravity, viscosity, cloud point, TAN, particulates, filter blocking tendency, distillation, pour point, cetane number, etc.) will be determined on the seven-fuel matrix from Phase 1.

Phase 3 - Engine Dynamometer Evaluations

Objective

The objectives of this phase will be to determine engine performance when using biodiesel fuels and determine compatibility with military engine oils.

Description of Work

- a. Diesel engine starting under low ambient temperatures is of concern to the military. As a minimum, it is recommended that the low-temperature starting properties of base and biodiesel fuels (A, B, D, E, F, G) be mapped using the 6.2L engine. If low-temperature starting characteristics are not equal to reference base fuel, then additional low-temperature starting determinations would be recommended for other engine types to establish the extent of low-temperature starting capability degradation.
- b. Turbine engine acceptability is of concern to us because the Abrams Main Battle Tank is turbine powered. The proposed effort will include evaluations in the BFLRF Combustor Lab. One combustor can configuration will be examined in a cyclic procedure with a minimum of six test fuels.
- c. Thermal stability and deposition properties of the biodiesel fuels will be determined using an Injector Fouling Procedure, which is run in a Cummins L10 engine. A minimum of six fuels (A, B, D, E, F, G) should be examined.
- d. Compatibility of biodiesel fuel with PC-6 type engine lubricants should be examined in the GM 6.2L Soot-Wear Test (50 hr). As a minimum, a biodiesel fuel blend should be evaluated in this procedure with both high- and low-wear reference oils. If wear performance is degraded, additional tests would be recommended to completely define the effects.
- e. Performance of biodiesel fuel in a fuel sensitive two-cycle diesel engine needs to be determined. As a minimum, we propose to conduct a 240-hour Fuel-Engine-Lubricant Compatibility evaluation in a military two-cycle diesel engine using a biodiesel fuel

blend and reference engine oil. This procedure has been correlated to 4,000 miles of proving ground operation. A 240-hour compatibility evaluation should be performed for each biofuel blend to be used in the field. The biodiesel fuel evaluations will be compared to reference oil and fuel performance.

- f. The effect of biodiesel fuel on four-cycle diesel engine piston deposits should be determined using a standard Caterpillar single-cylinder engine test. Each biofuel blend to be used in the field should be evaluated. Results will be compared to reference oil and fuel performance.

Phase 4 - Pilot Field Demonstrations

Objective

The objective of Phase 4 is to determine field performance of biodiesel fuel blends using a small number of vehicles, under fairly well controlled operating conditions.

Description of Work

- a. Fleet A will be operated at YPG in conjunction with other TACOM evaluations and will include relatively quick fuel turnover and fast accumulation of mileage for durability in 1 year. BFLRF will monitor the fleet performance. The proposed pilot fleet will consist of a maximum of 10 tactical-wheeled vehicles, including both test and control vehicles. The biofuel component of the fuel blend will be supplied by the field test sponsor. Quarterly used oil analyses will be conducted, and a driver performance survey will be conducted. A minimum of one biofuel vehicle will be shipped to Southwest Research Institute (SwRI) in San Antonio, Texas, for exhaust emissions determinations at the start of the field evaluation and be retested at the end of 1 year of biodiesel fuel use.
- b. Fleet B will be operated at Fort McCoy, Wisconsin, and will provide operational durability data under conditions of slow-mileage accumulation and fuel turnover for a 1-year period. BFLRF will monitor the fleet performance. The proposed pilot fleet will consist of 5 to 10 tactical-wheeled vehicles, including both test and control vehicles. The biofuel component will be supplied by the evaluation sponsor. Quarterly used oil analyses and driver surveys will be conducted. A minimum of one biofuel vehicle will be tested for exhaust emissions before and after the field evaluation.

Phase 5 - User Impact/Acceptance-Full Field Demonstration

Objective

The objectives of this phase are to demonstrate the acceptability of using biodiesel fuel in a wide variety of military vehicles and equipment designed to consume diesel fuel.

Description of Work

A portion of a single Army installation will be converted to biodiesel fuel. The biofuel component will be supplied by the test sponsor. It is anticipated that this will include 100+ vehicles and equipment for a period of 1 year. BFLRF will facilitate the implementation of the demonstration program and monitor the fleet operation. Data acquisition for a biodiesel fuel demonstration will be conducted on a noninterference basis with the cooperating installation unit, such as was done in the JP-8 Demonstration at Fort Bliss, Texas. In a previous Army field demonstration program for a new fuel, the following information was collected:

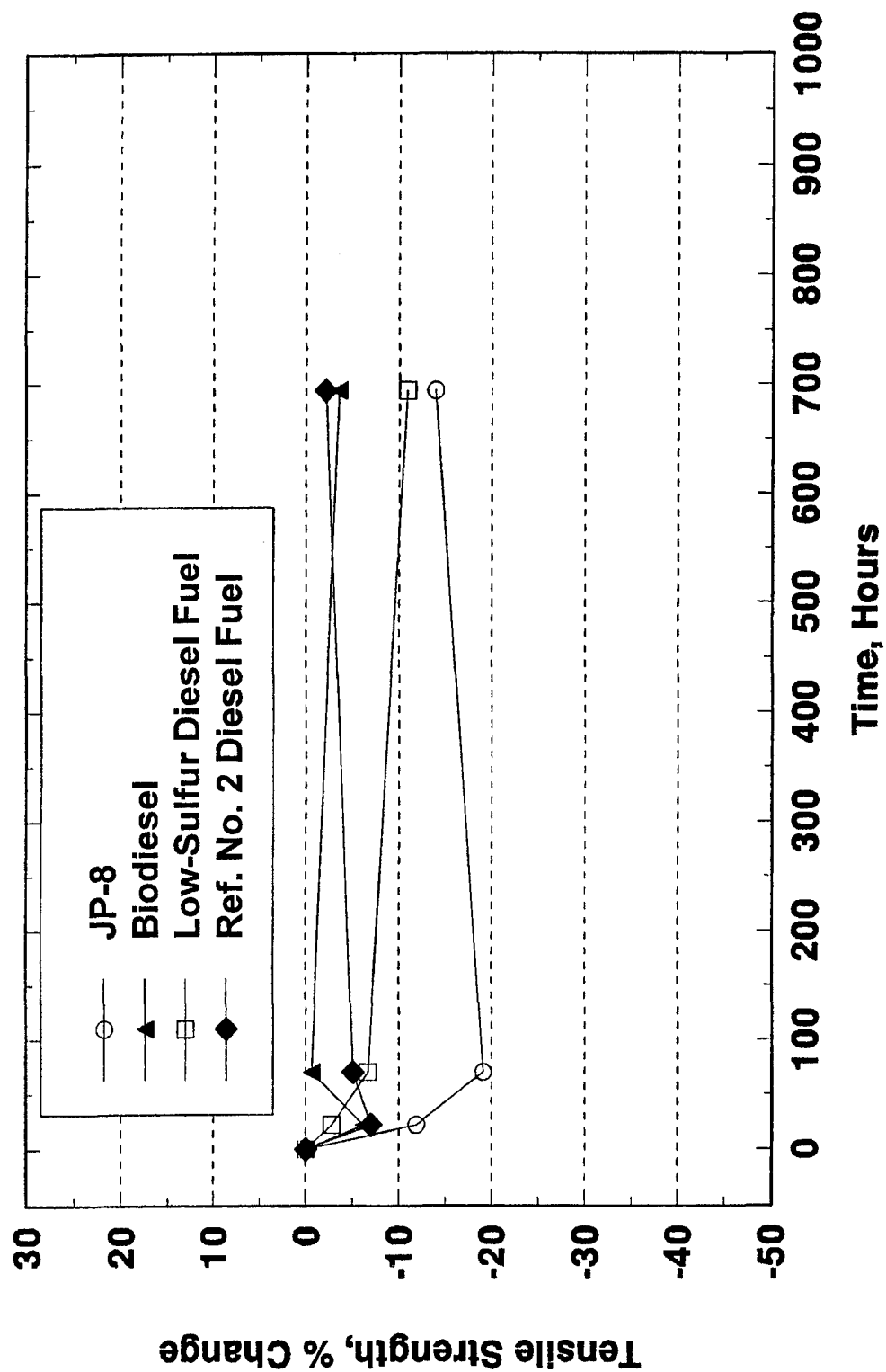
<u>Item No.</u>	<u>Information Collected</u>	<u>Data Source</u>
1	Ambient Temperature History	National Climatic Data Center
2	Bulk Fuel Dispensings	Directorate of Installation Support (DIS)
3	Fuel Samples; Analyses	On-site monitors: BFLRF, USA, GMPA
4	Fuel Transition Periods	DIS; sample analysis
5	Fuel Wetted Components Usage	Army Maintenance Form 2407
6	Mileage (km)/Hours of Operation	The Army Maintenance Management System (TAMMS)
7	Fuel Consumption Data	Merger of vehicle fuel dispensing from Army Form 3643 with AOAP mileage (km) data
8	Engine Oil Degradation	AOAP: Oil change interval, wear metal levels
9	Resolution of User/Maintenance Concerns	On-site monitors investigation; back-to-back fuel-related comparisons
10	Major Field Exercises	Unit command personnel

A similar data collection system will be designed for this field demonstration program. This program will determine the overall acceptability for biodiesel fuel in Army equipment.

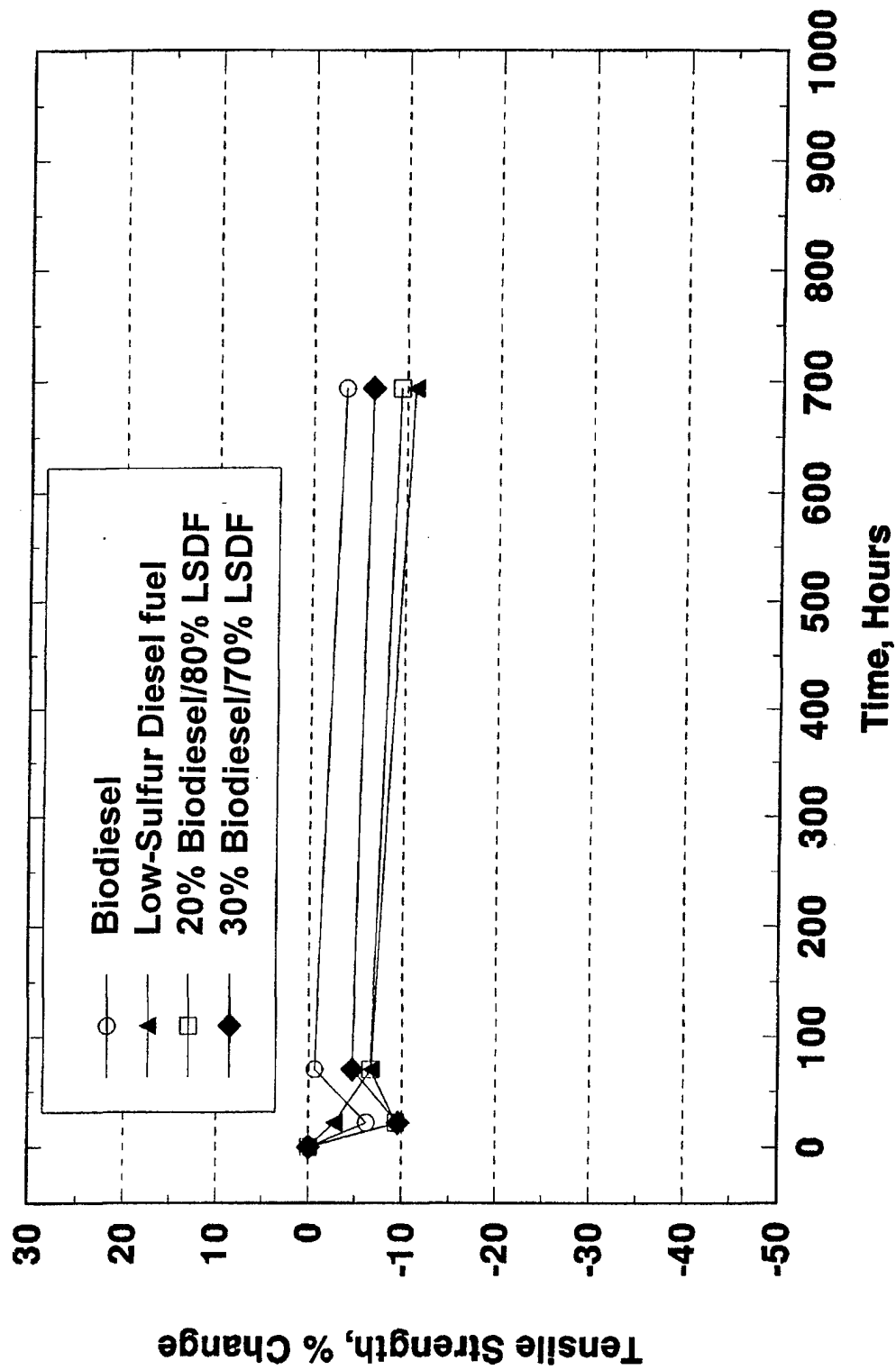
APPENDIX B

Elastomer Tensile Strength

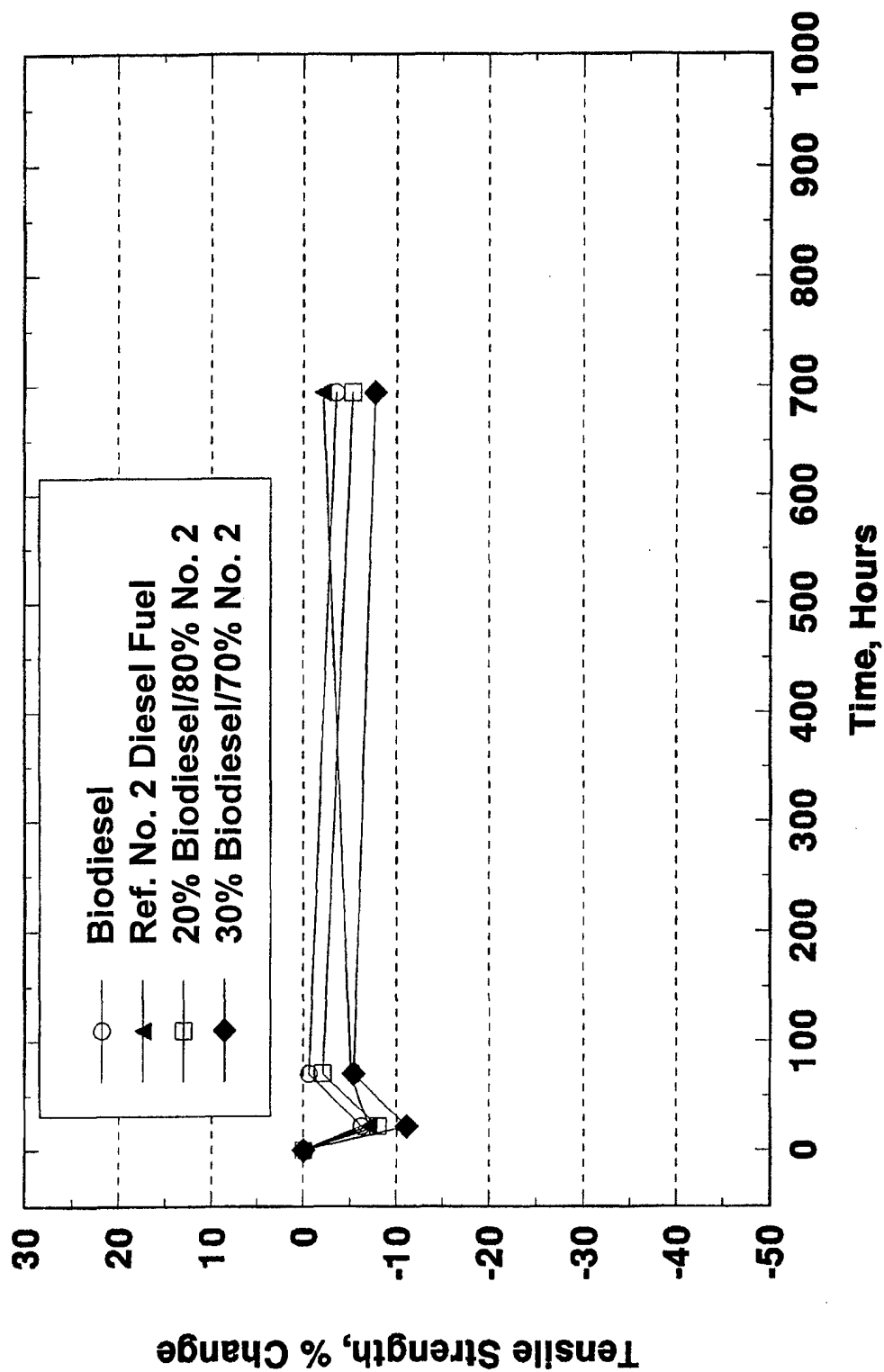
Tensile Strength Teflon



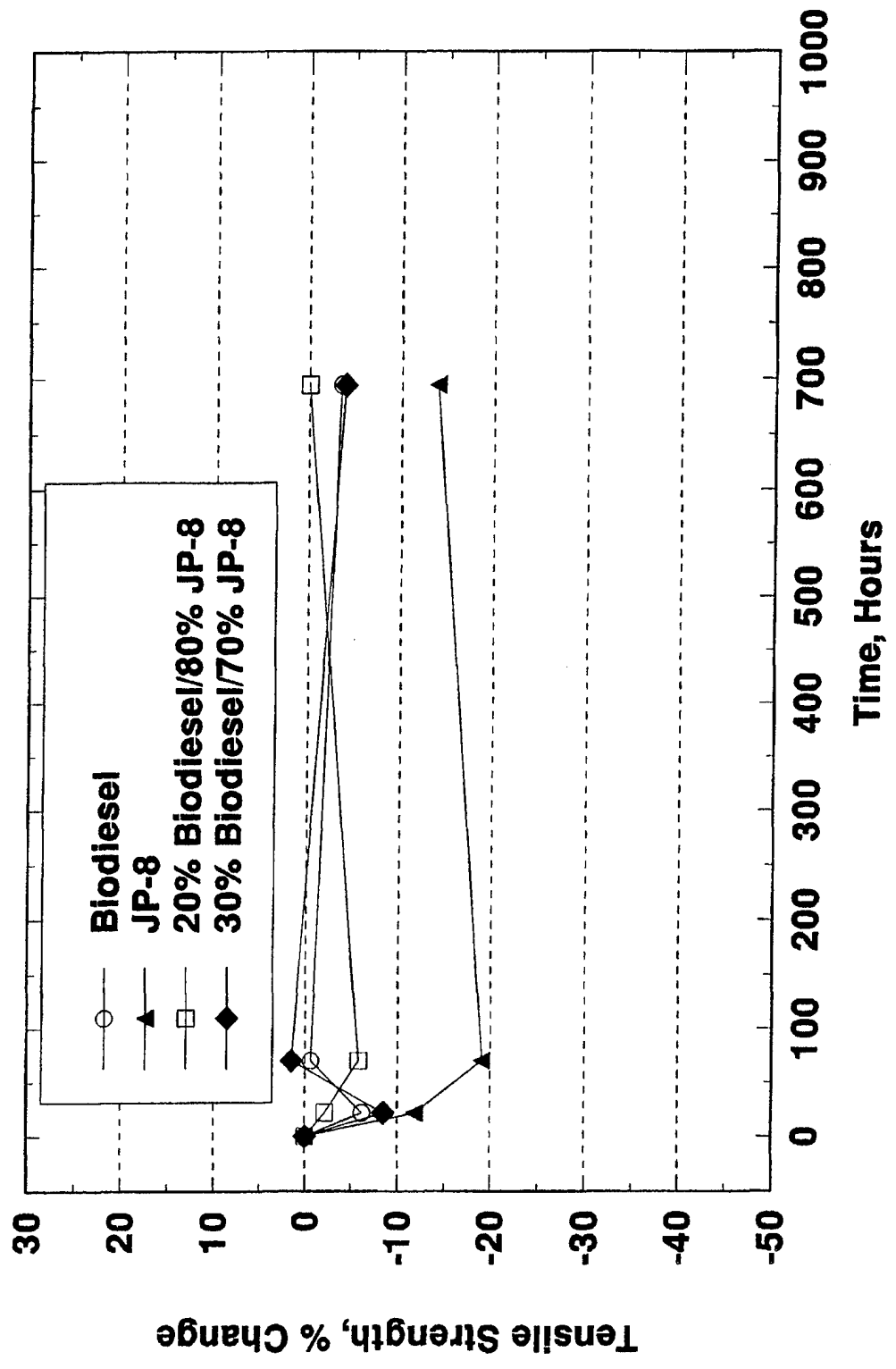
Tensile Strength Teflon



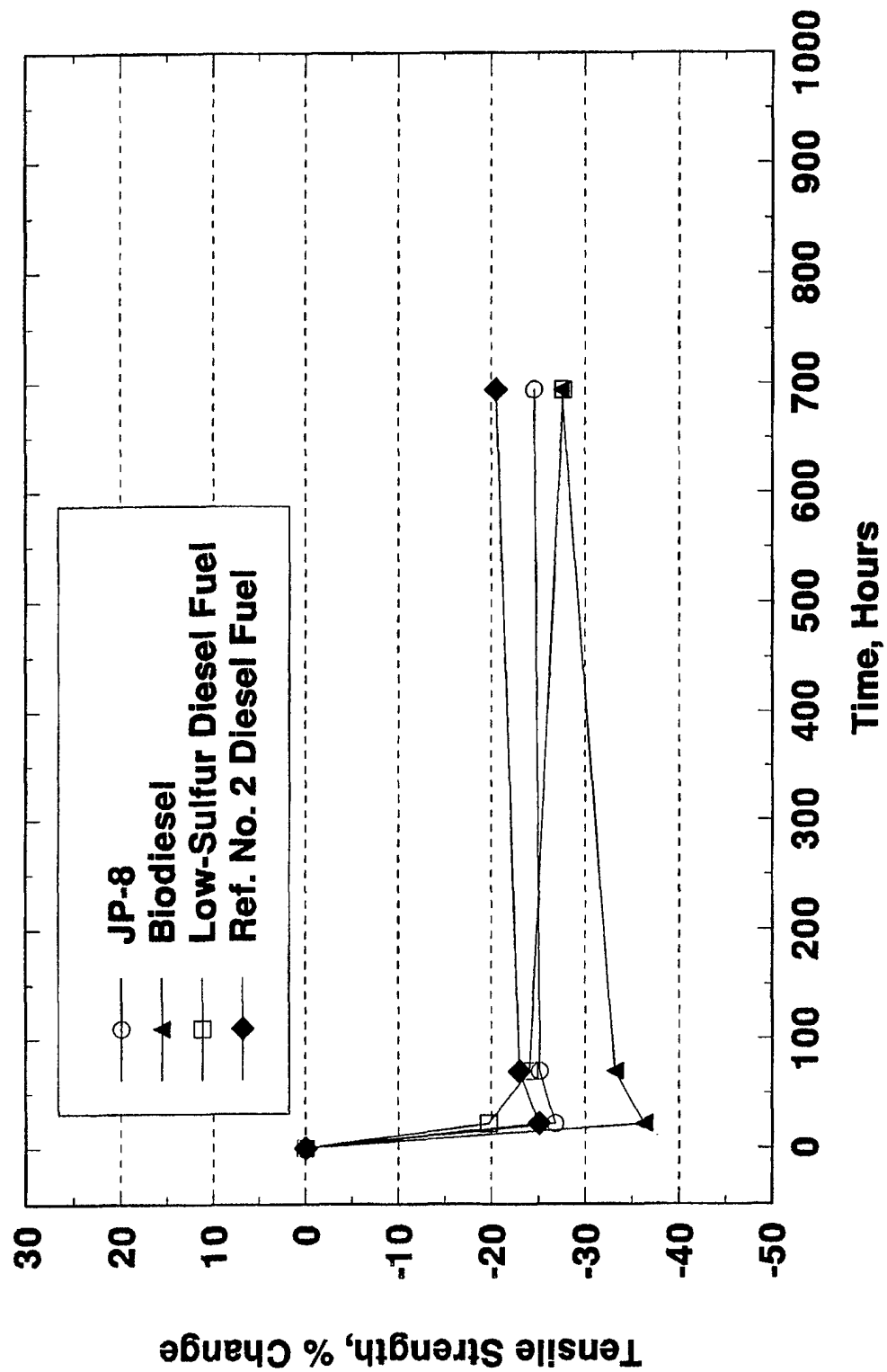
Tensile Strength Teflon



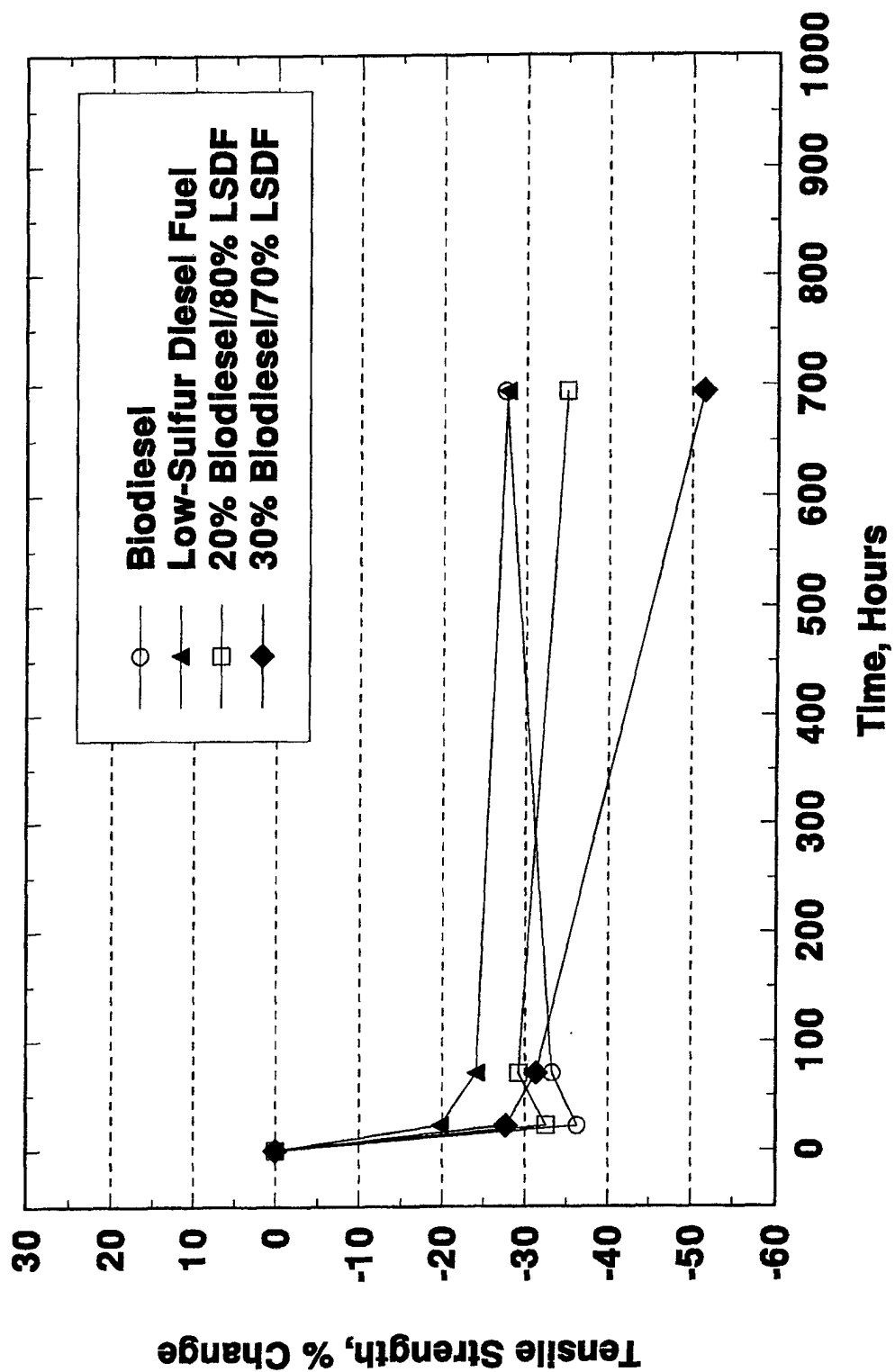
Tensile Strength Teflon



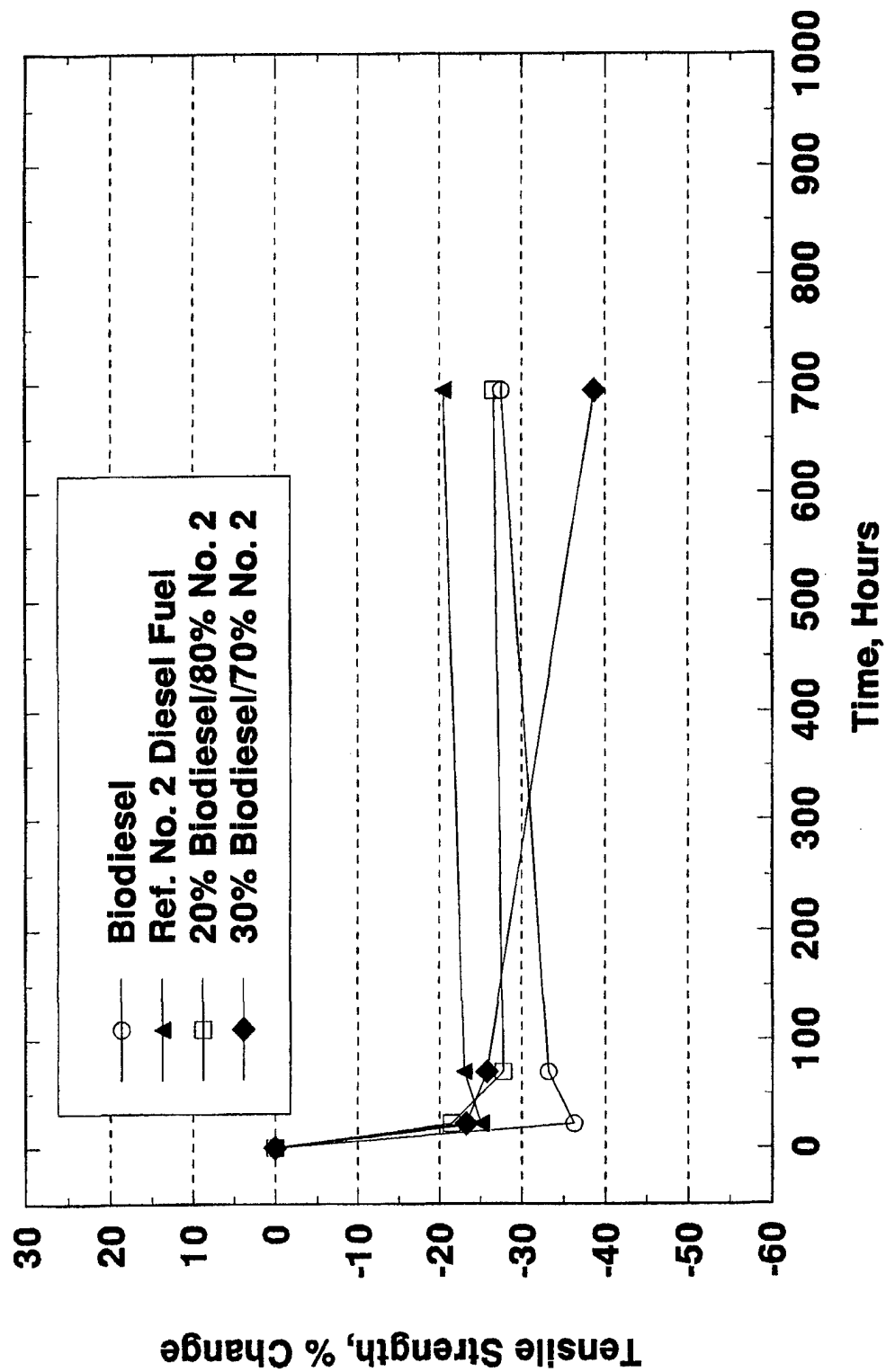
Tensile Strength Nitrile Rubber



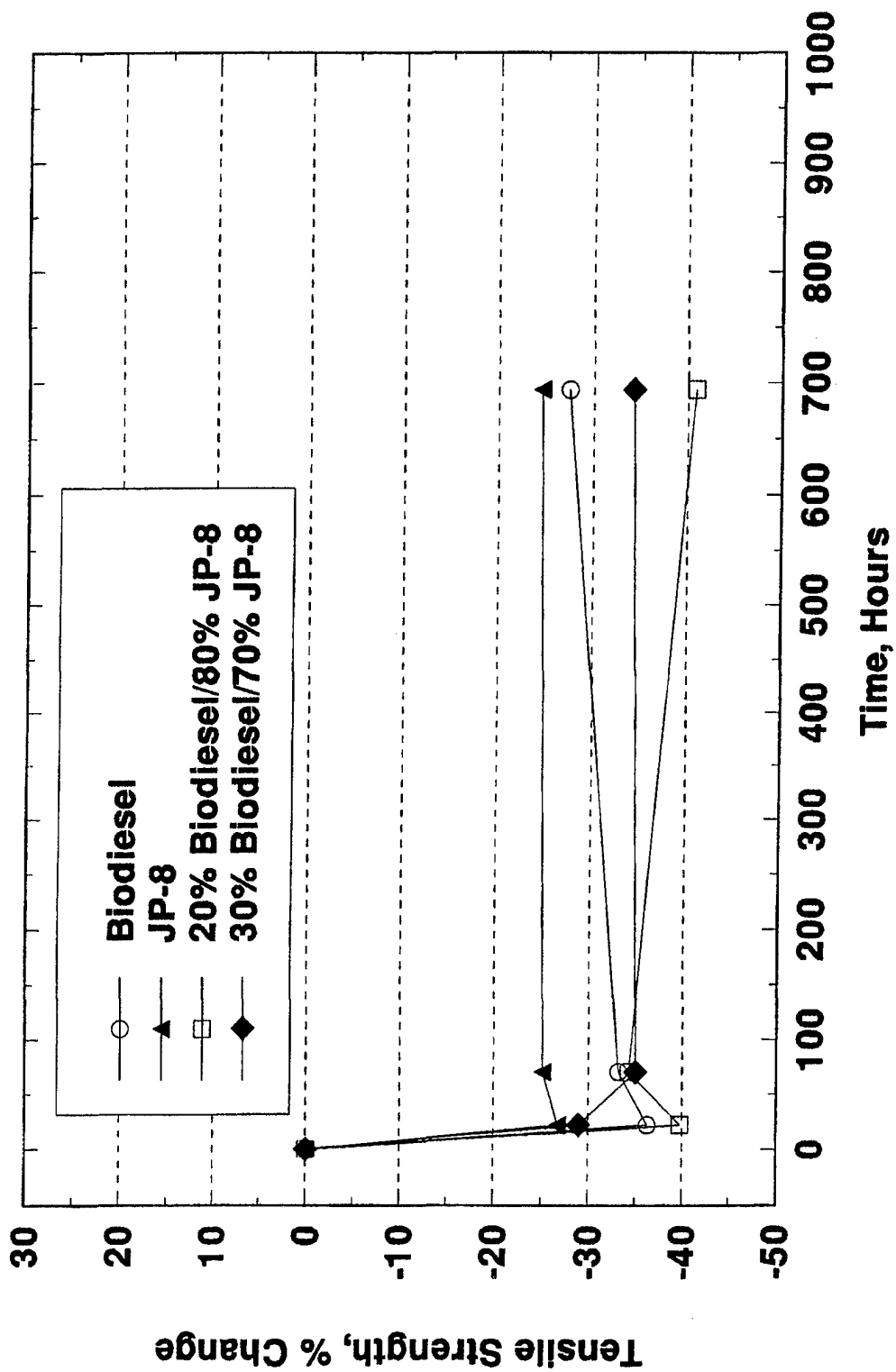
Tensile Strength Nitrile Rubber



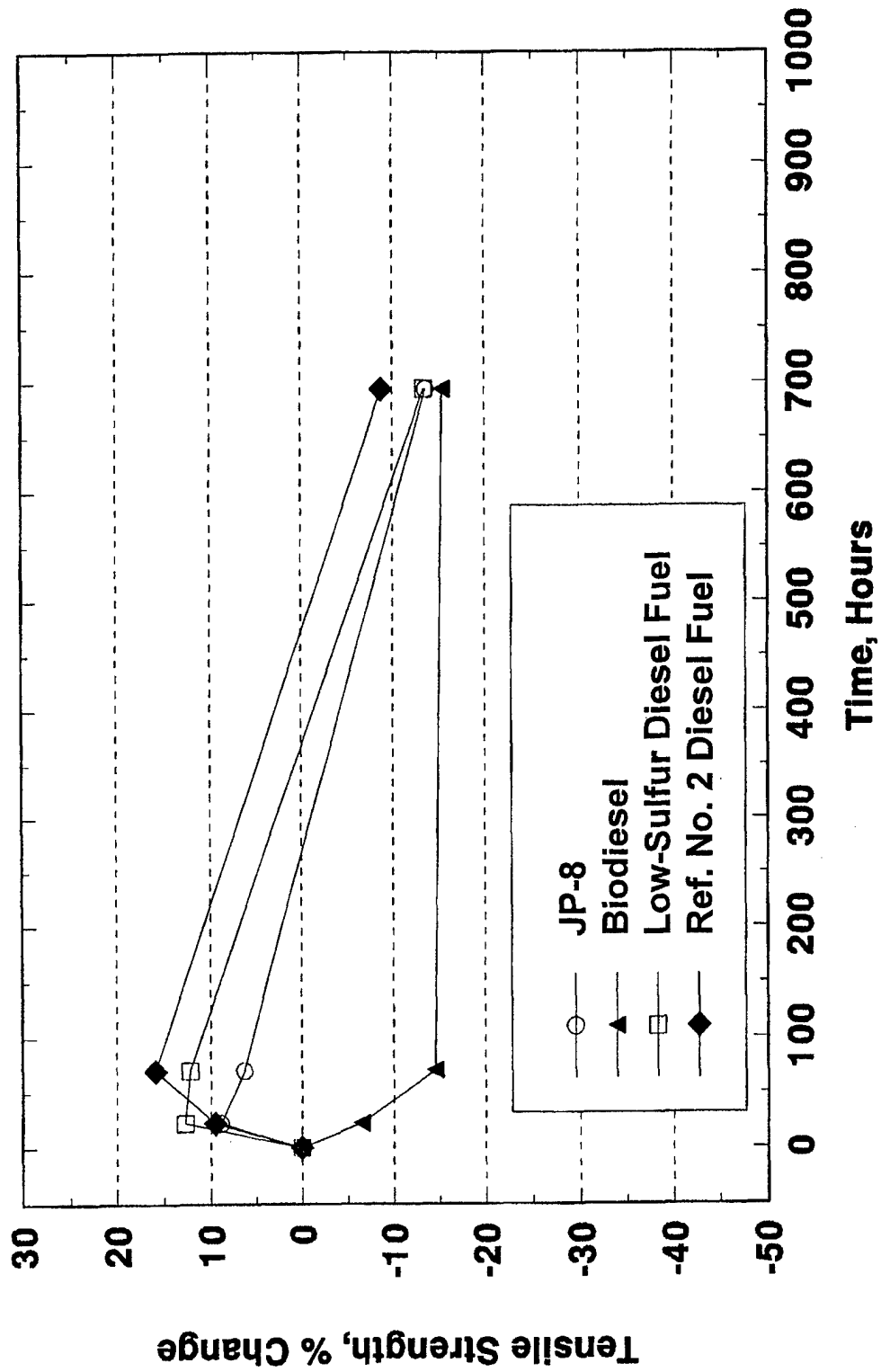
Tensile Strength Nitrile Rubber



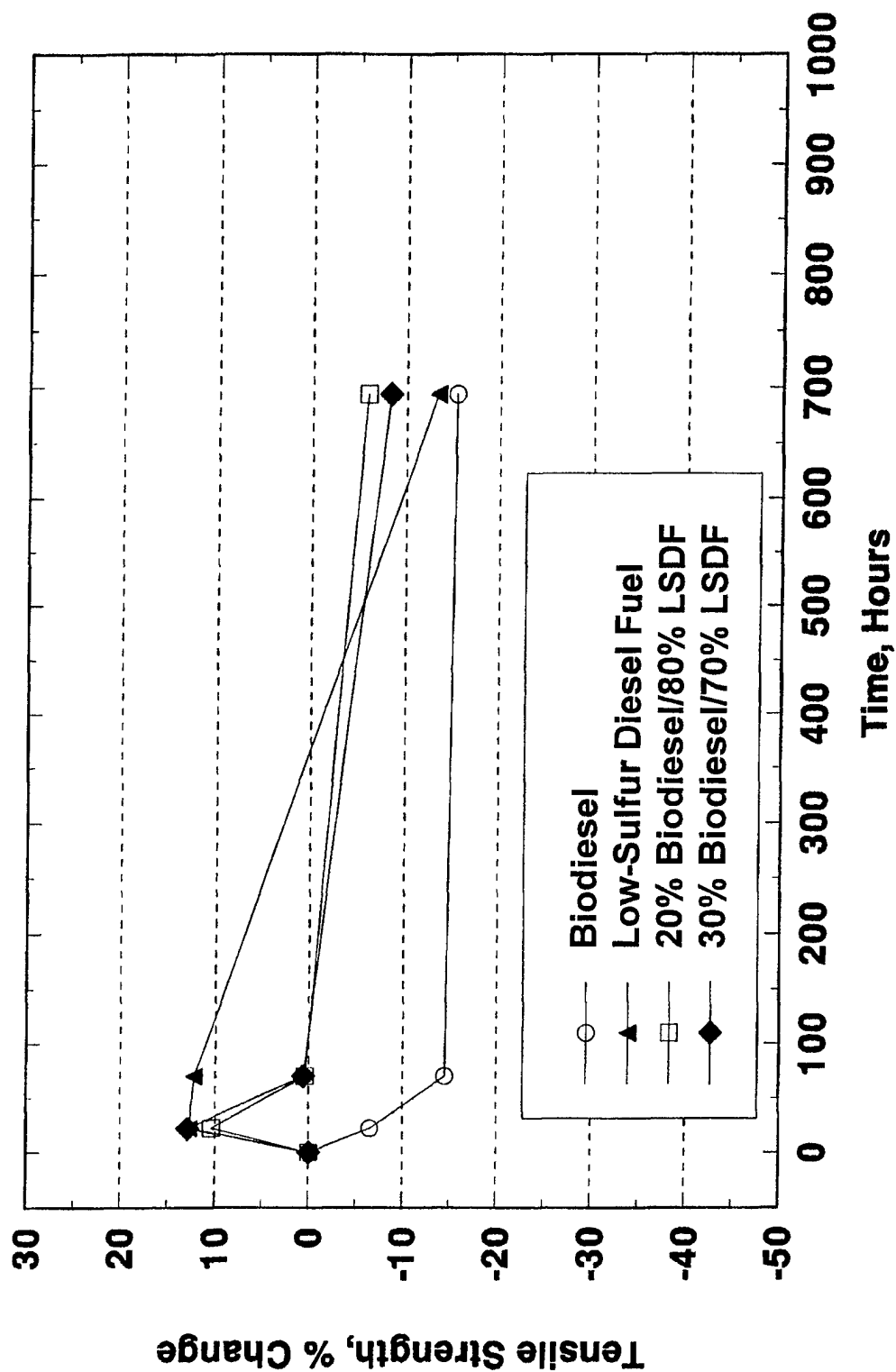
Tensile Strength Nitrile Rubber



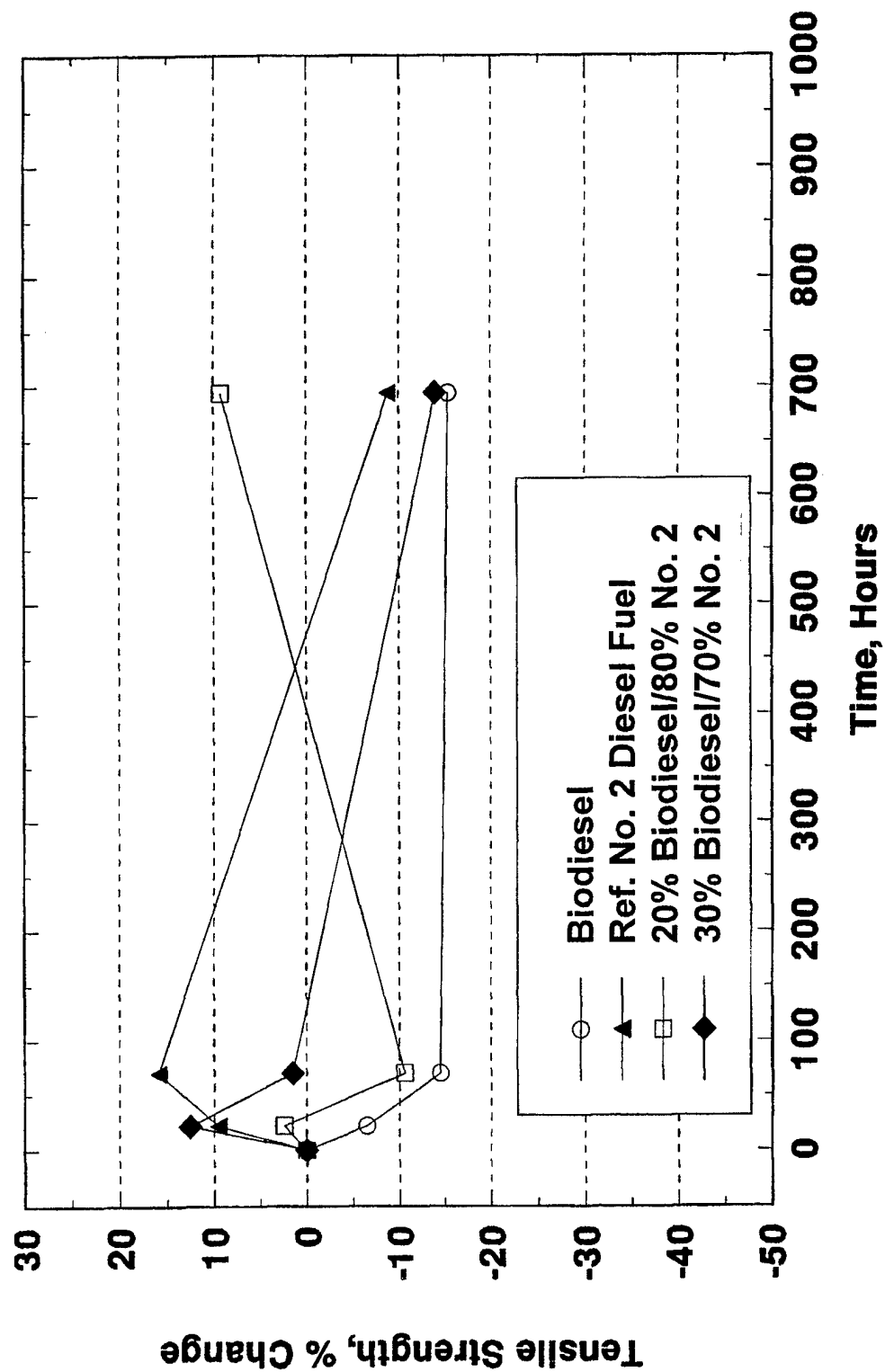
Tensile Strength Nylon 6/6



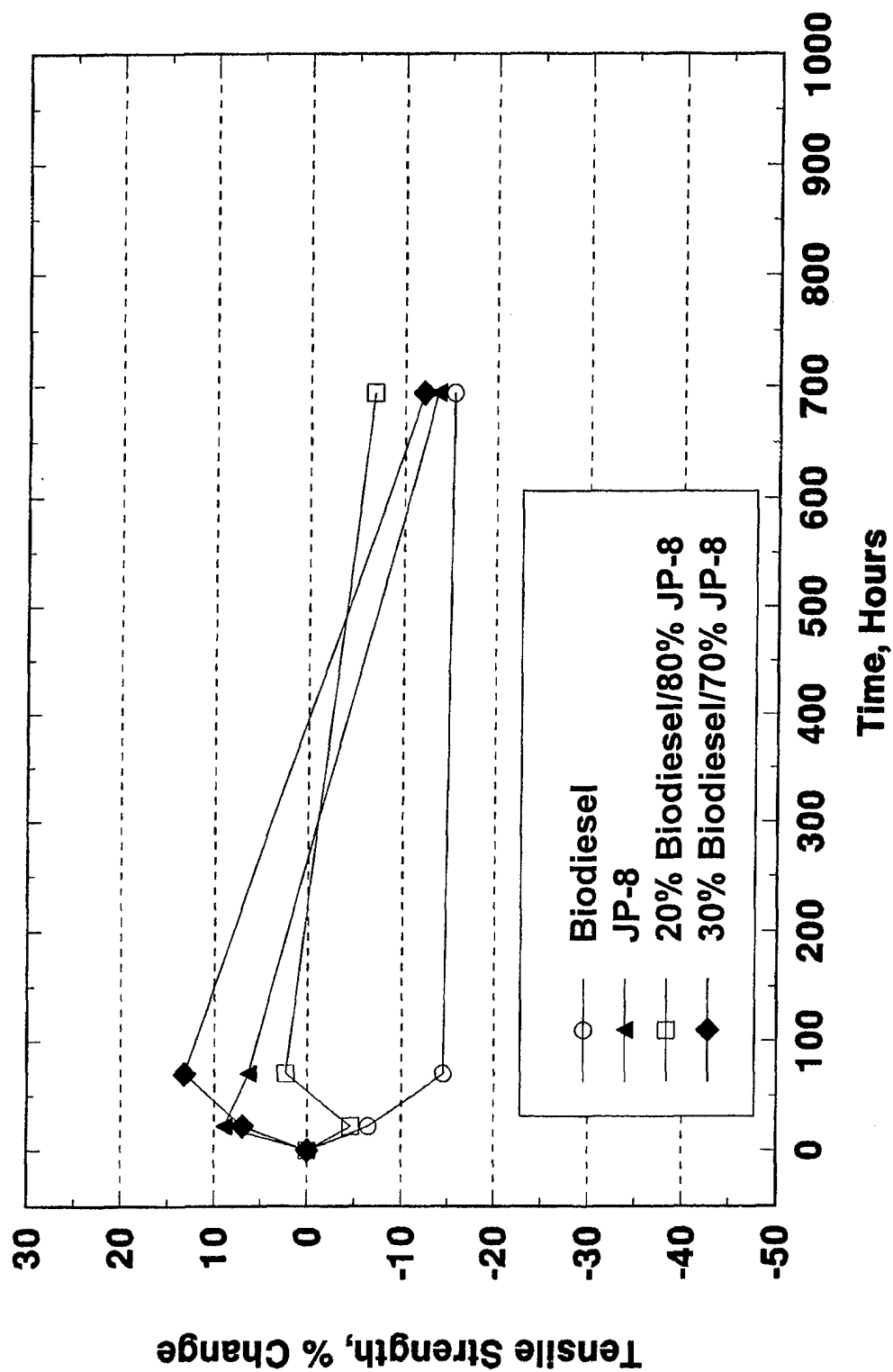
Tensile Strength Nylon 6/6



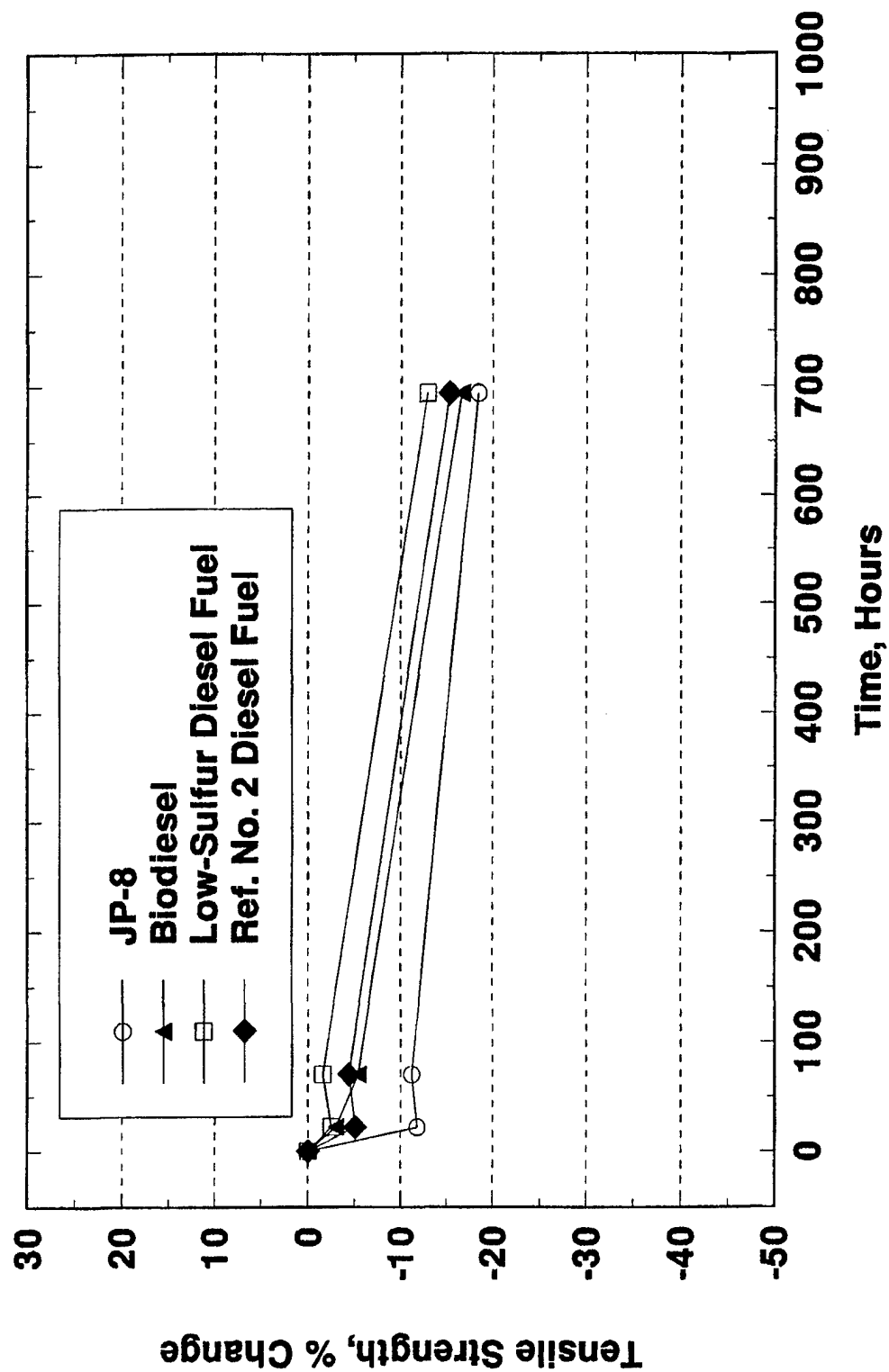
Tensile Strength Nylon 6/6



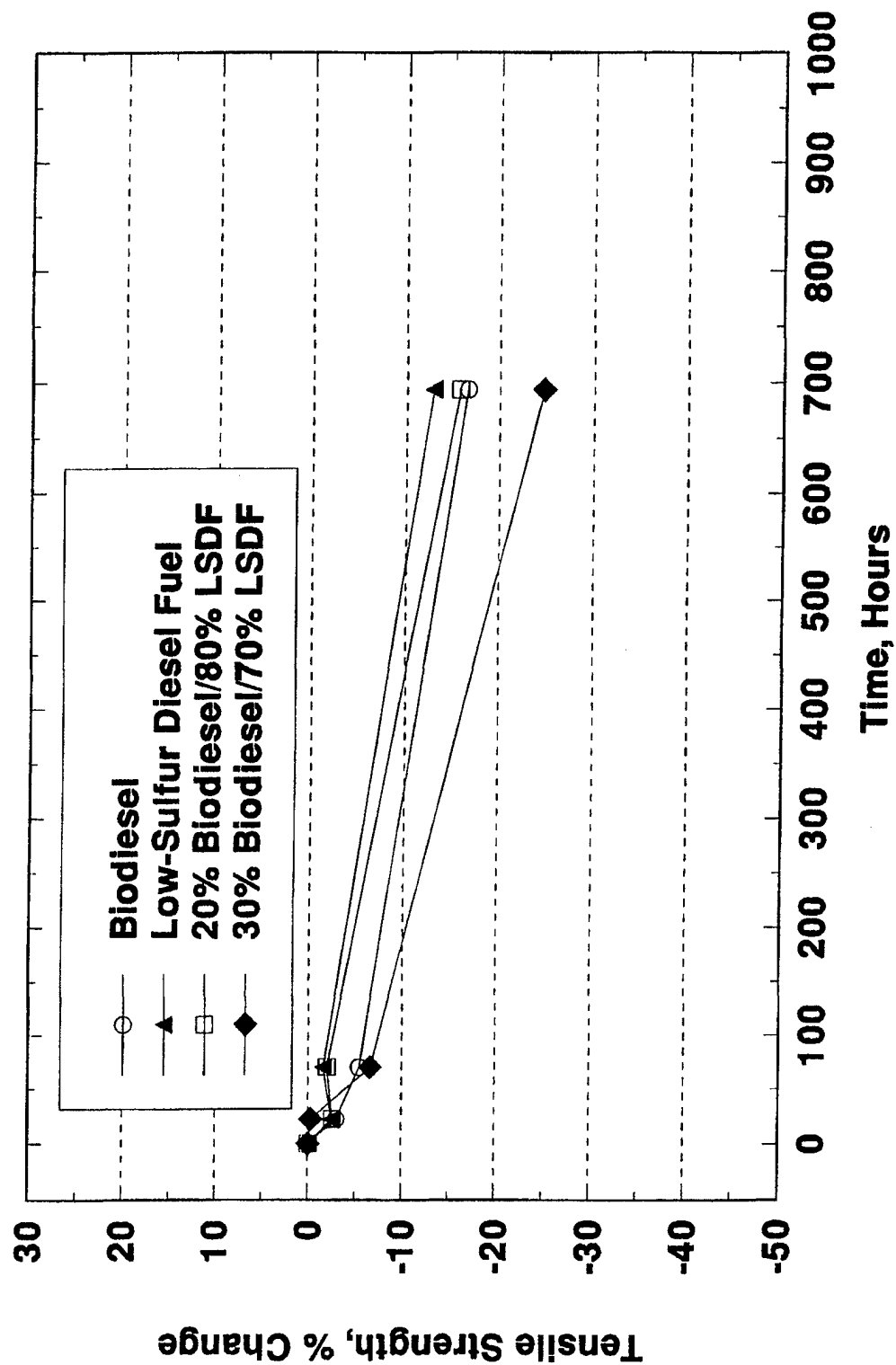
Tensile Strength Nylon 6/6



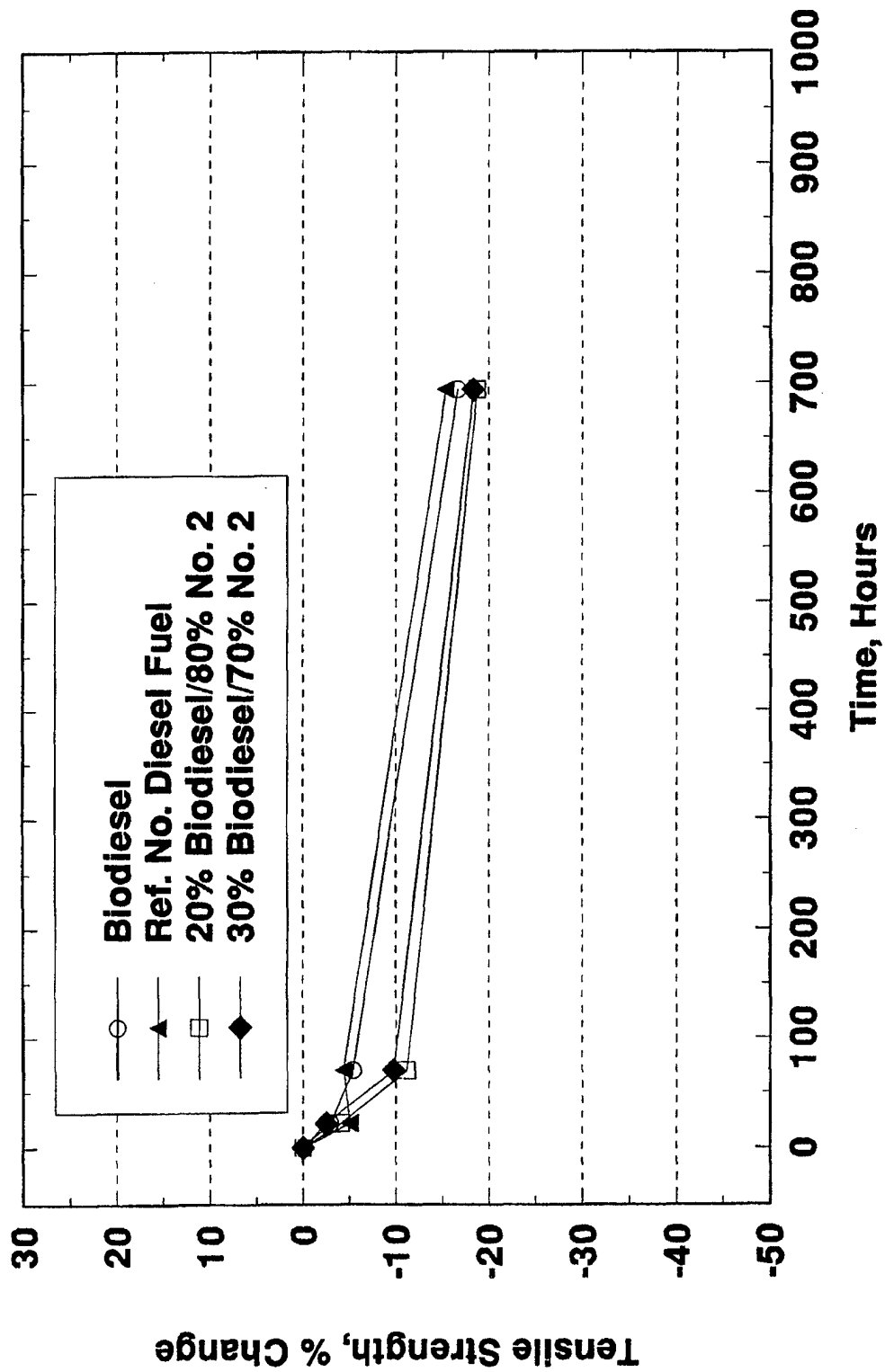
Tensile Strength Viton 401-C



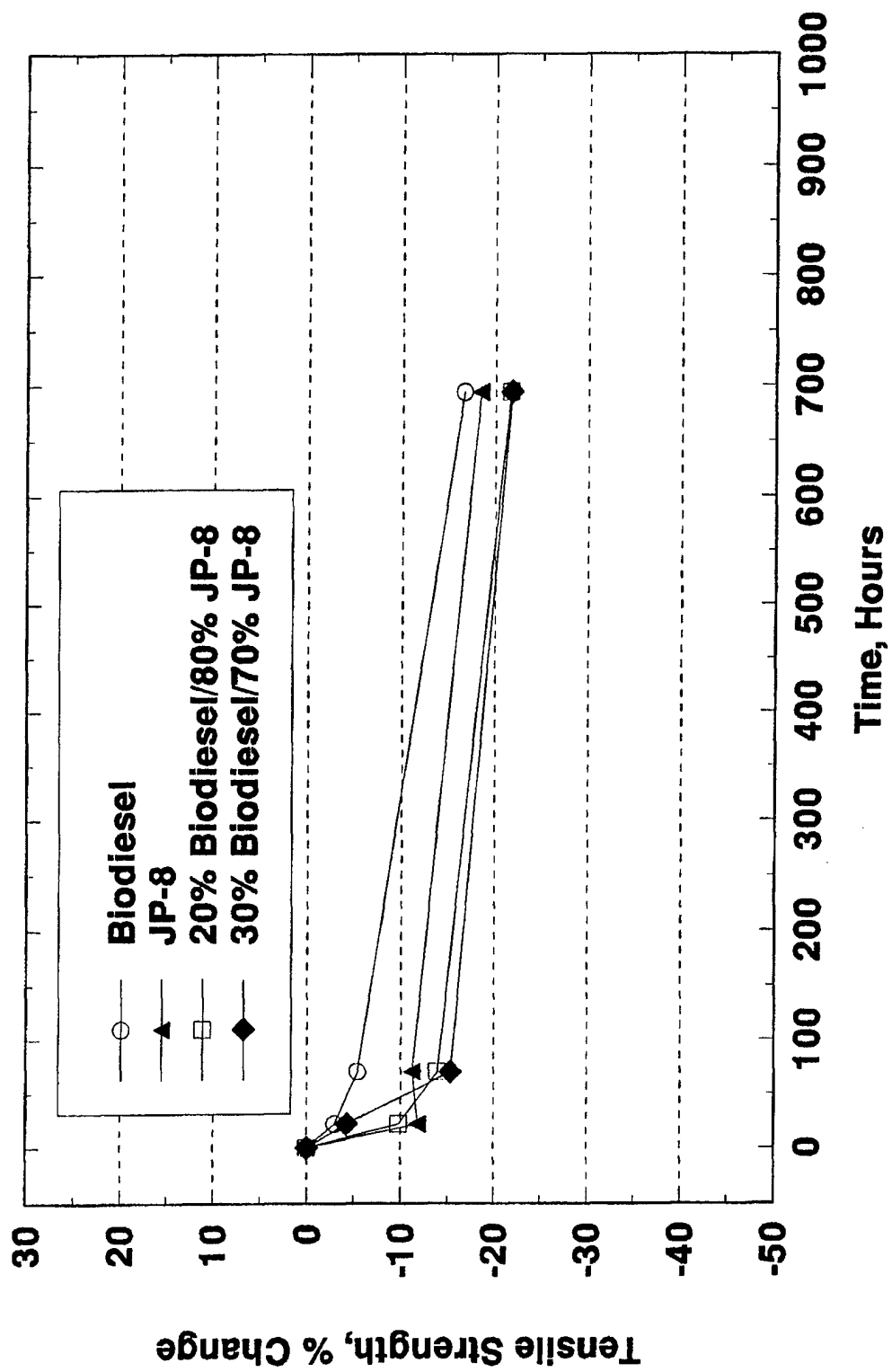
Tensile Strength Viton 401-C



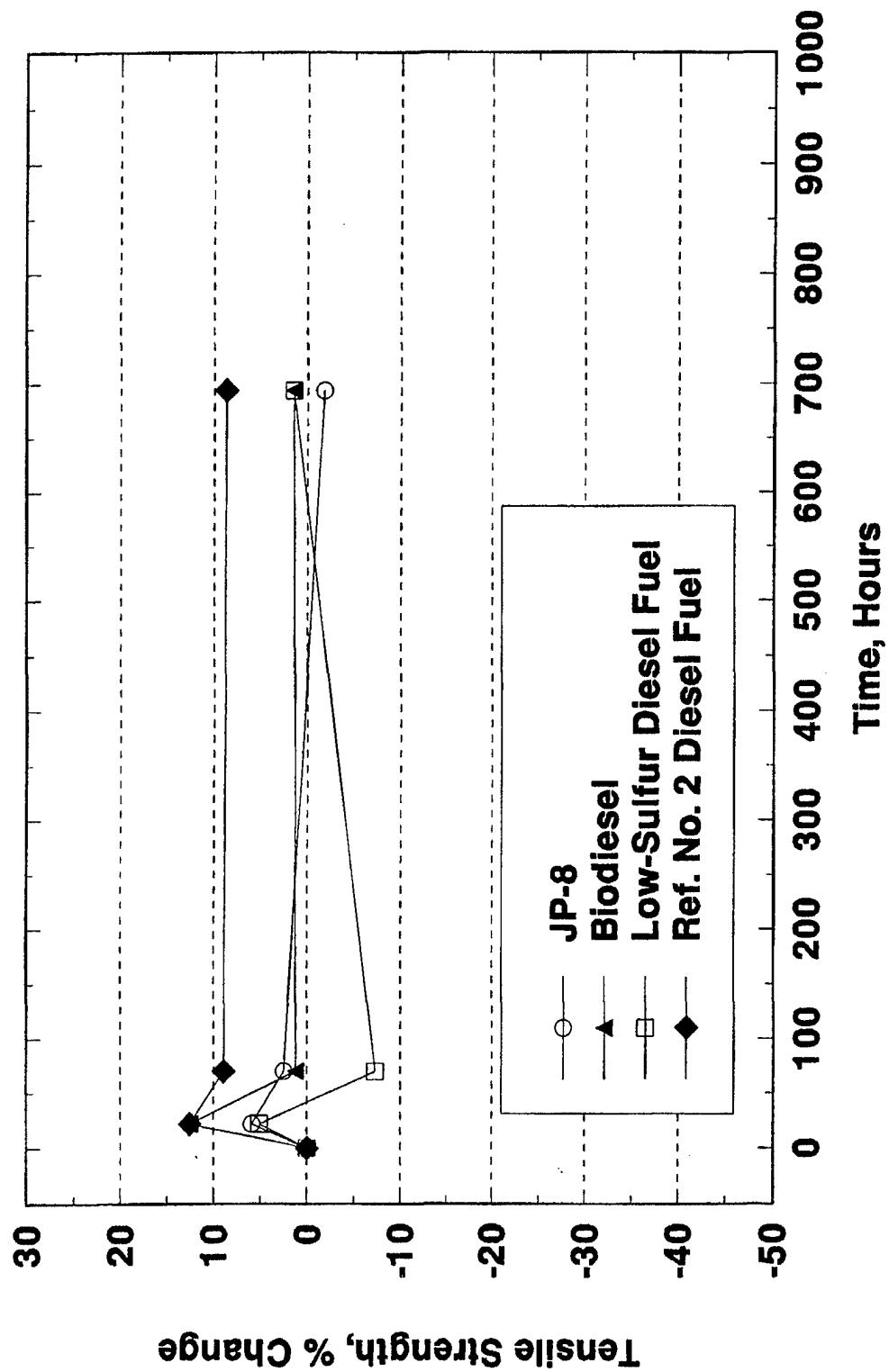
Tensile Strength Viton 401-C



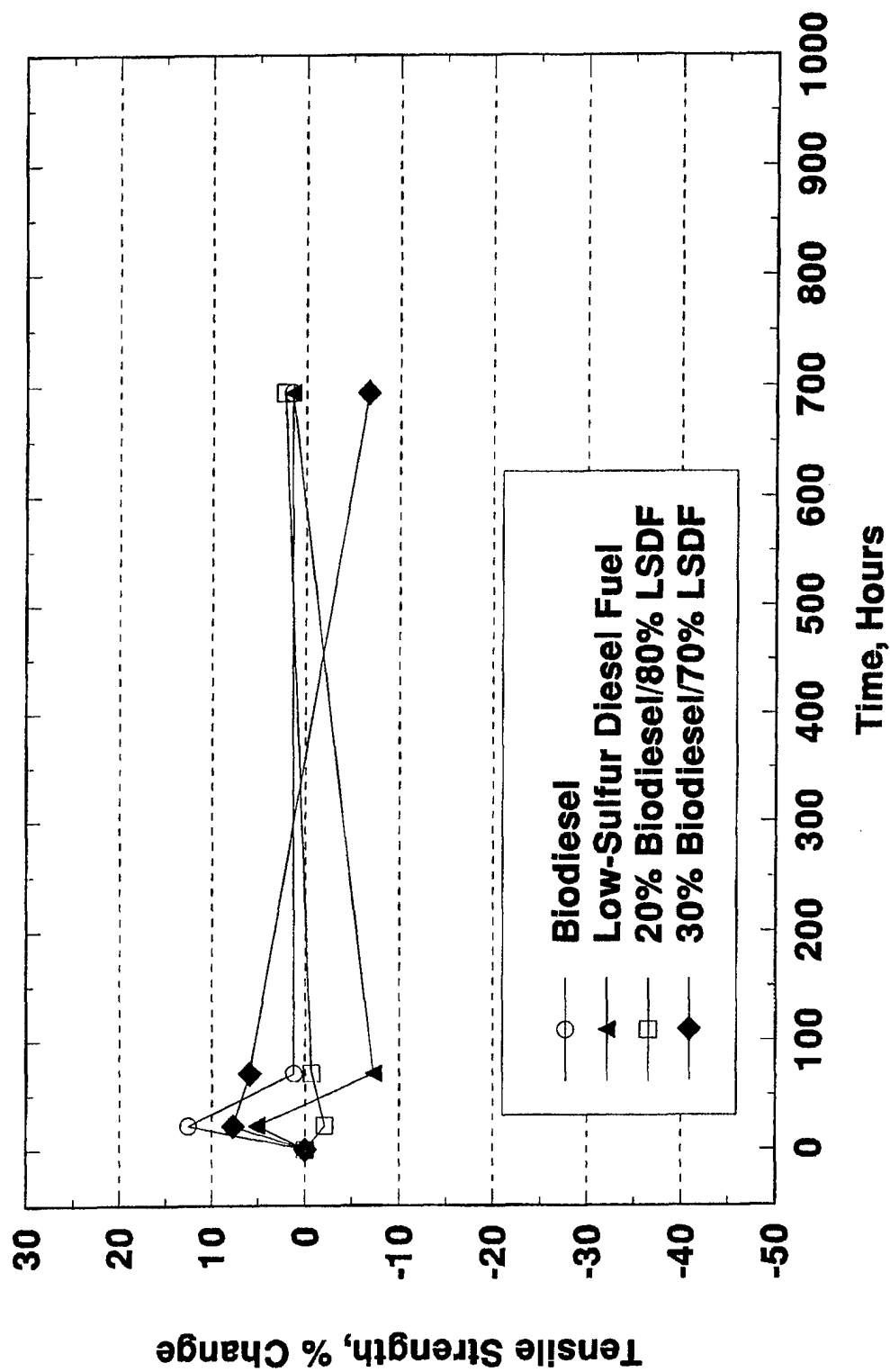
Tensile Strength Viton 401-C



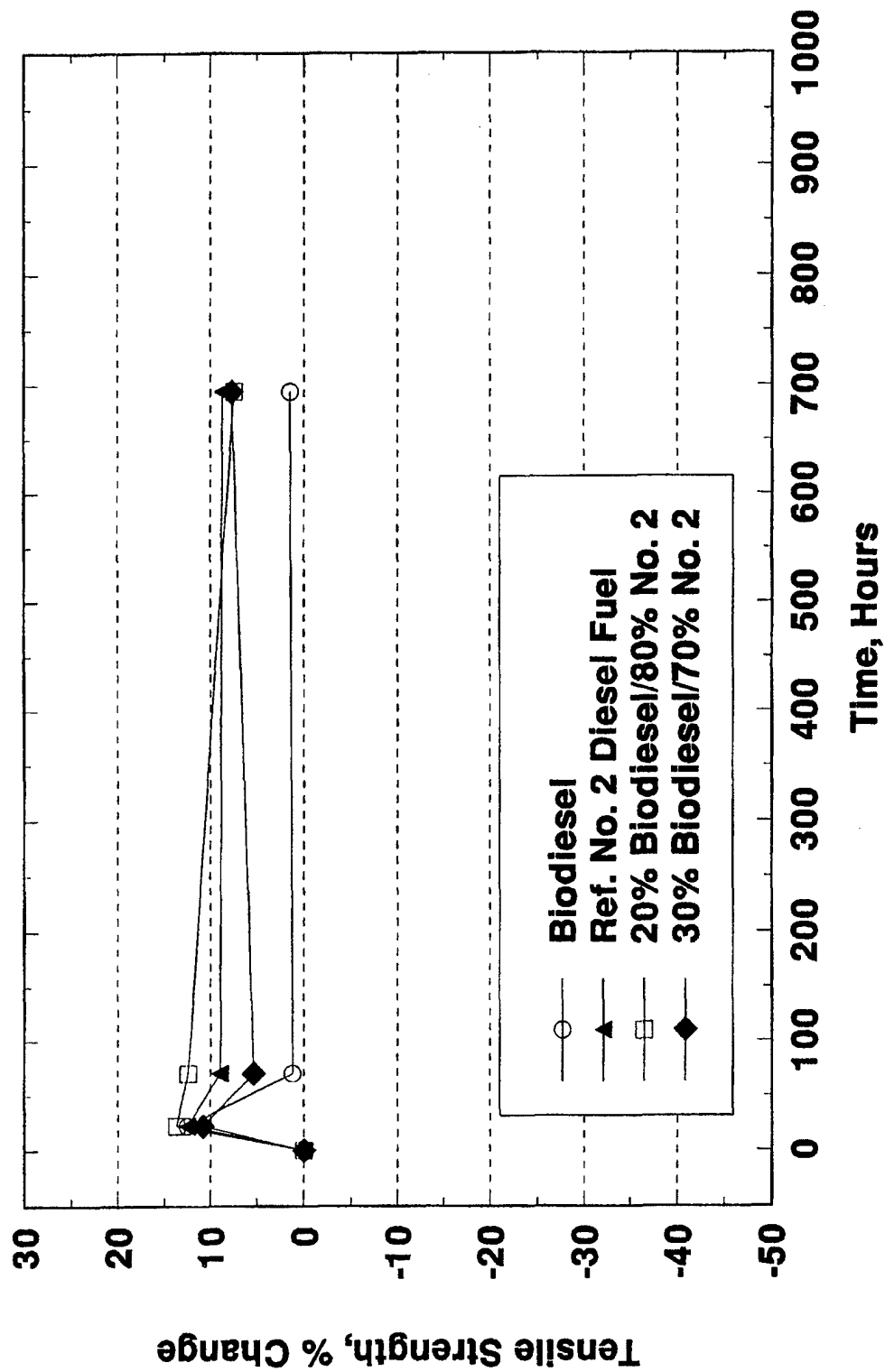
Tensile Strength Viton GFLT



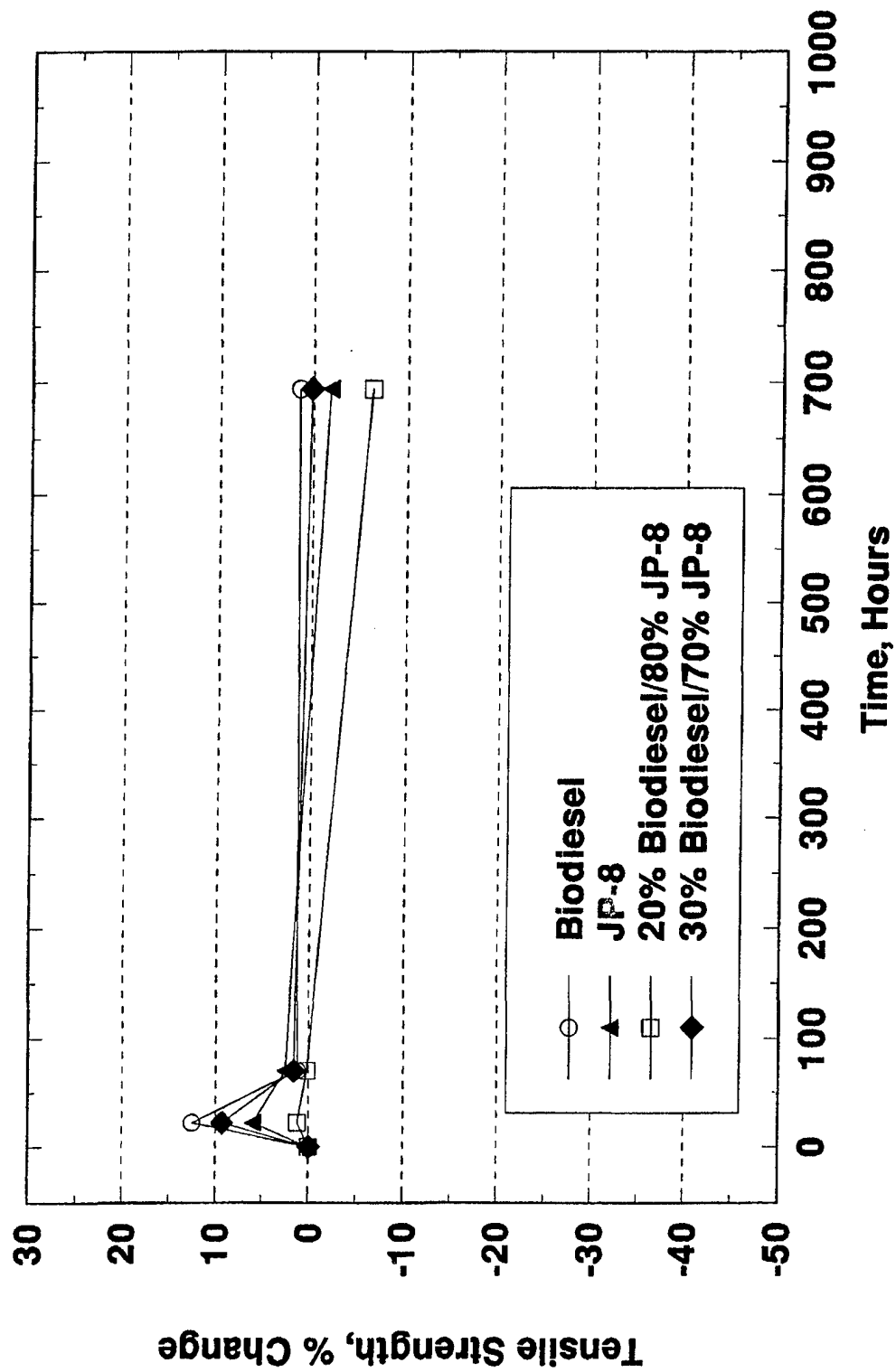
Tensile Strength Viton GFLT



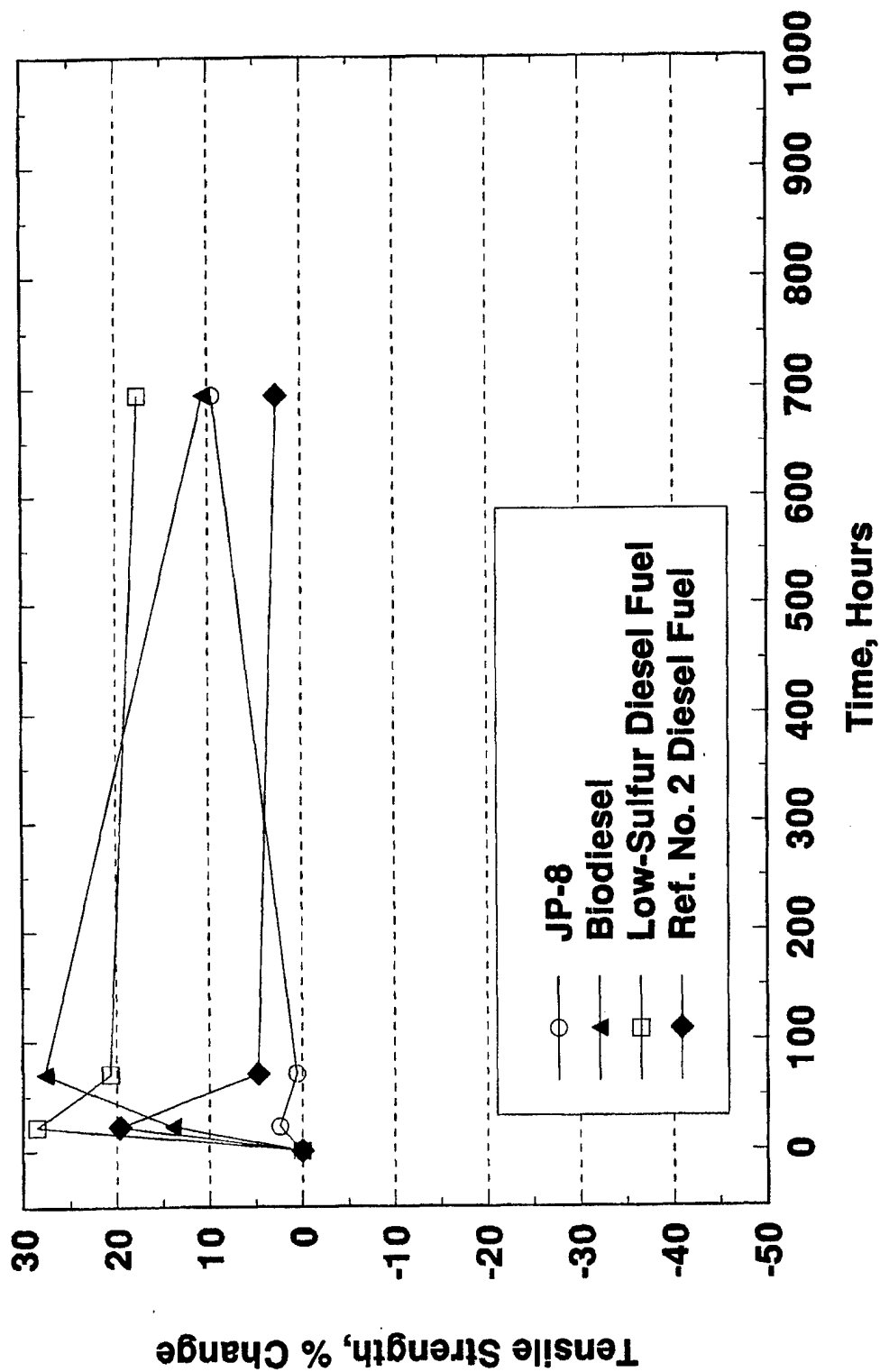
Tensile Strength Viton GFLT



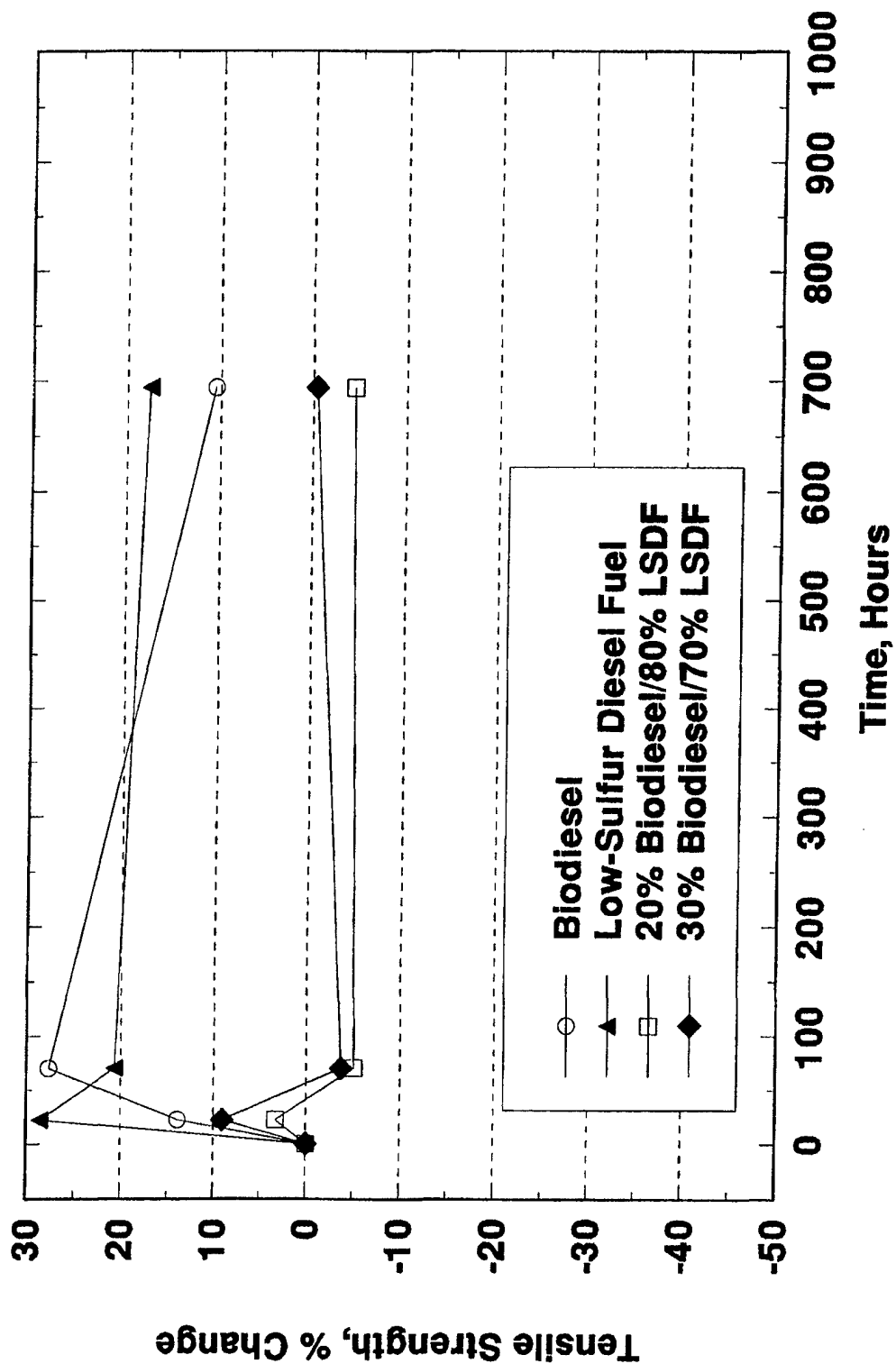
Tensile Strength Viton GFLT



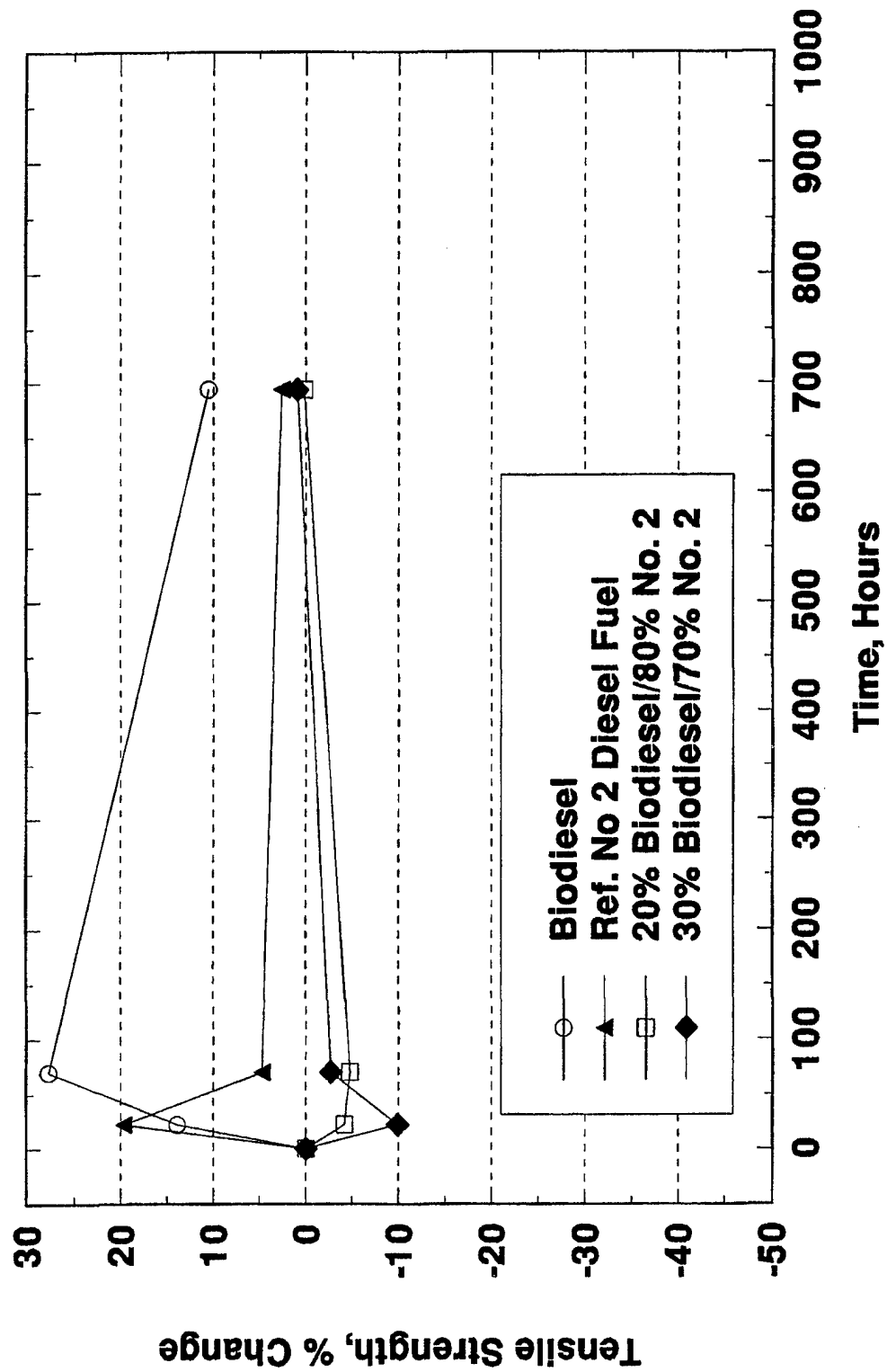
Tensile Strength Fluorosilicon



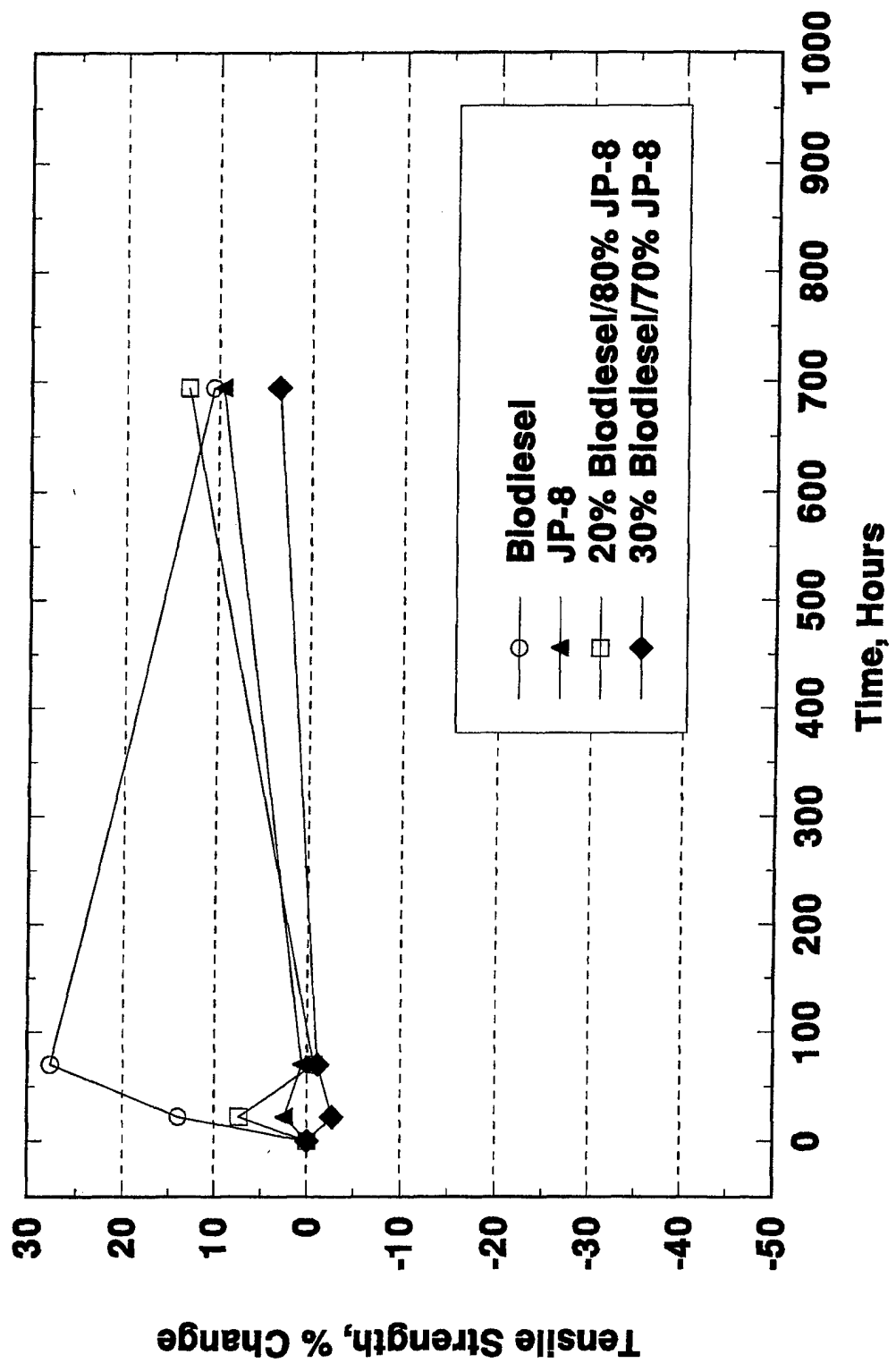
Tensile Strength Fluorosilicon



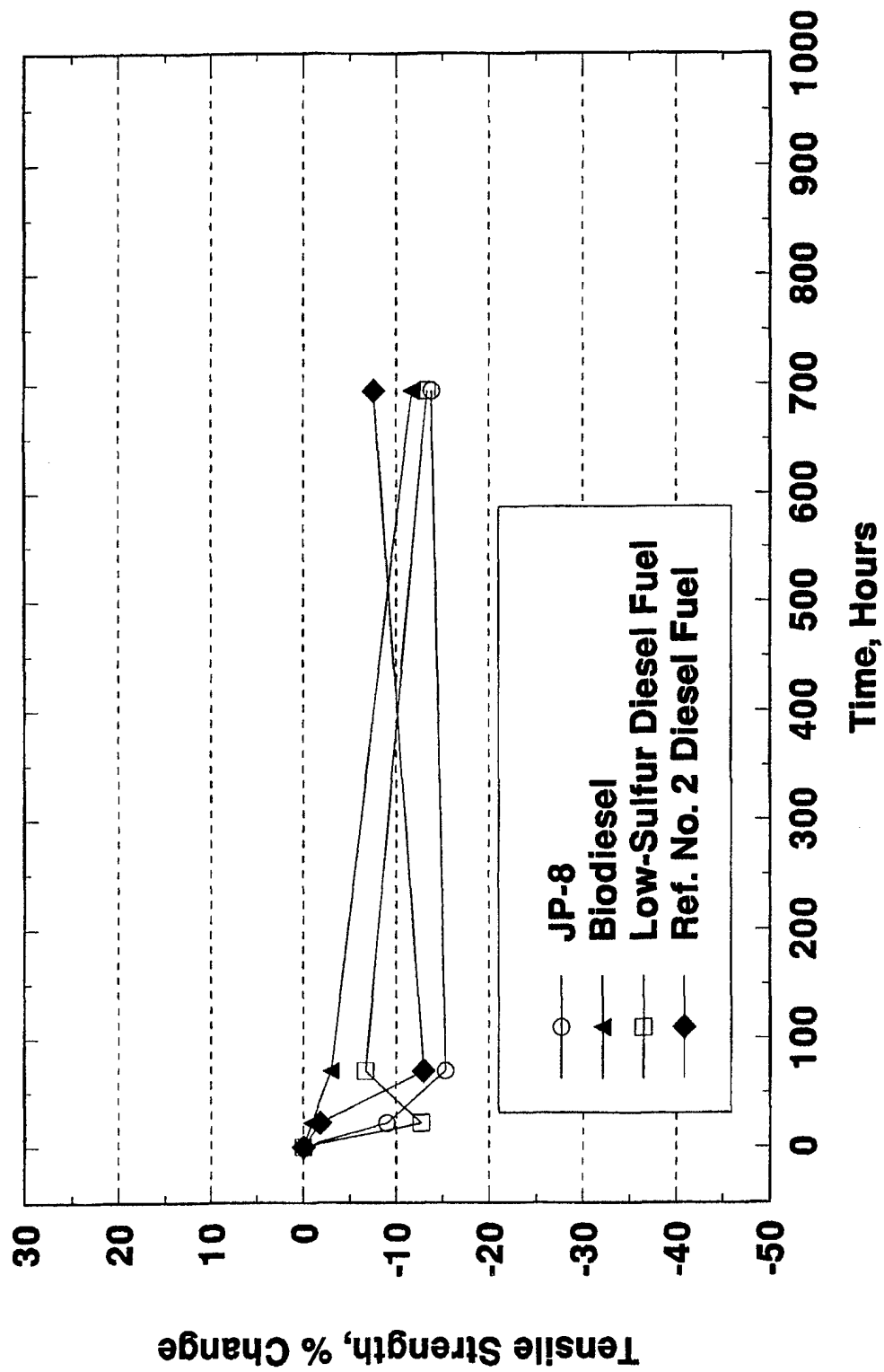
Tensile Strength Fluorosilicon



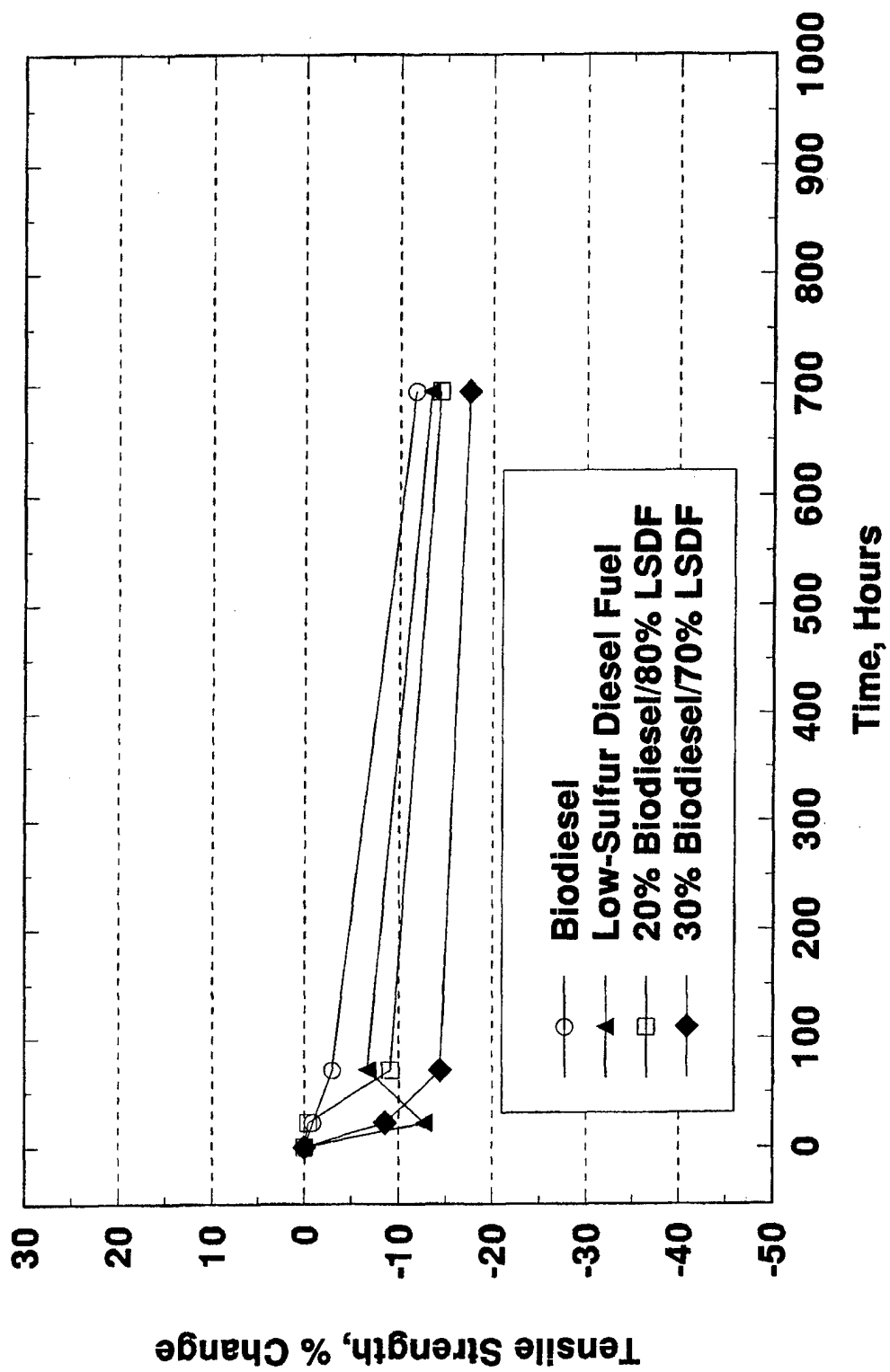
Tensile Strength Fluorosilicon



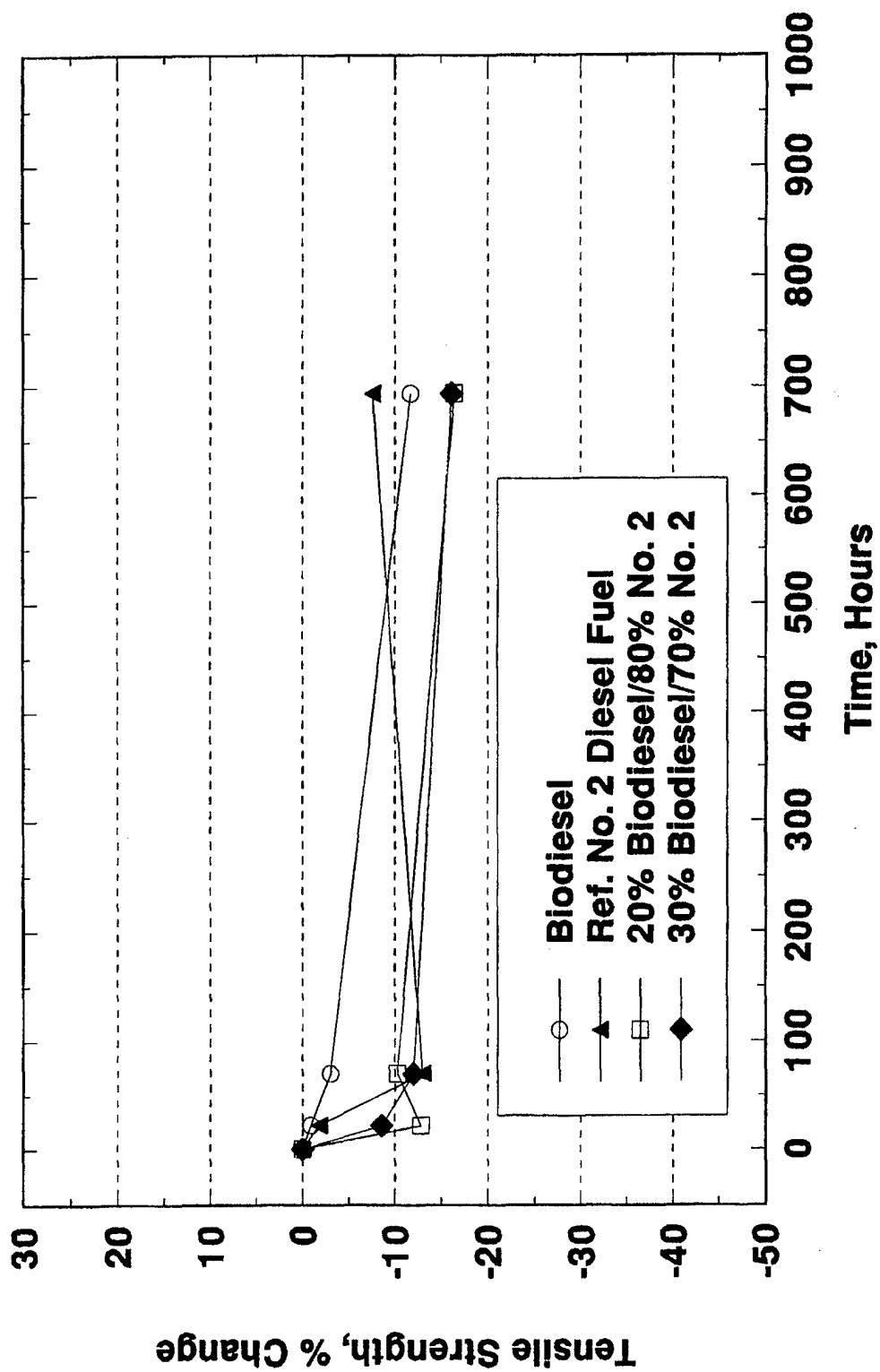
Tensile Strength Polyurethane



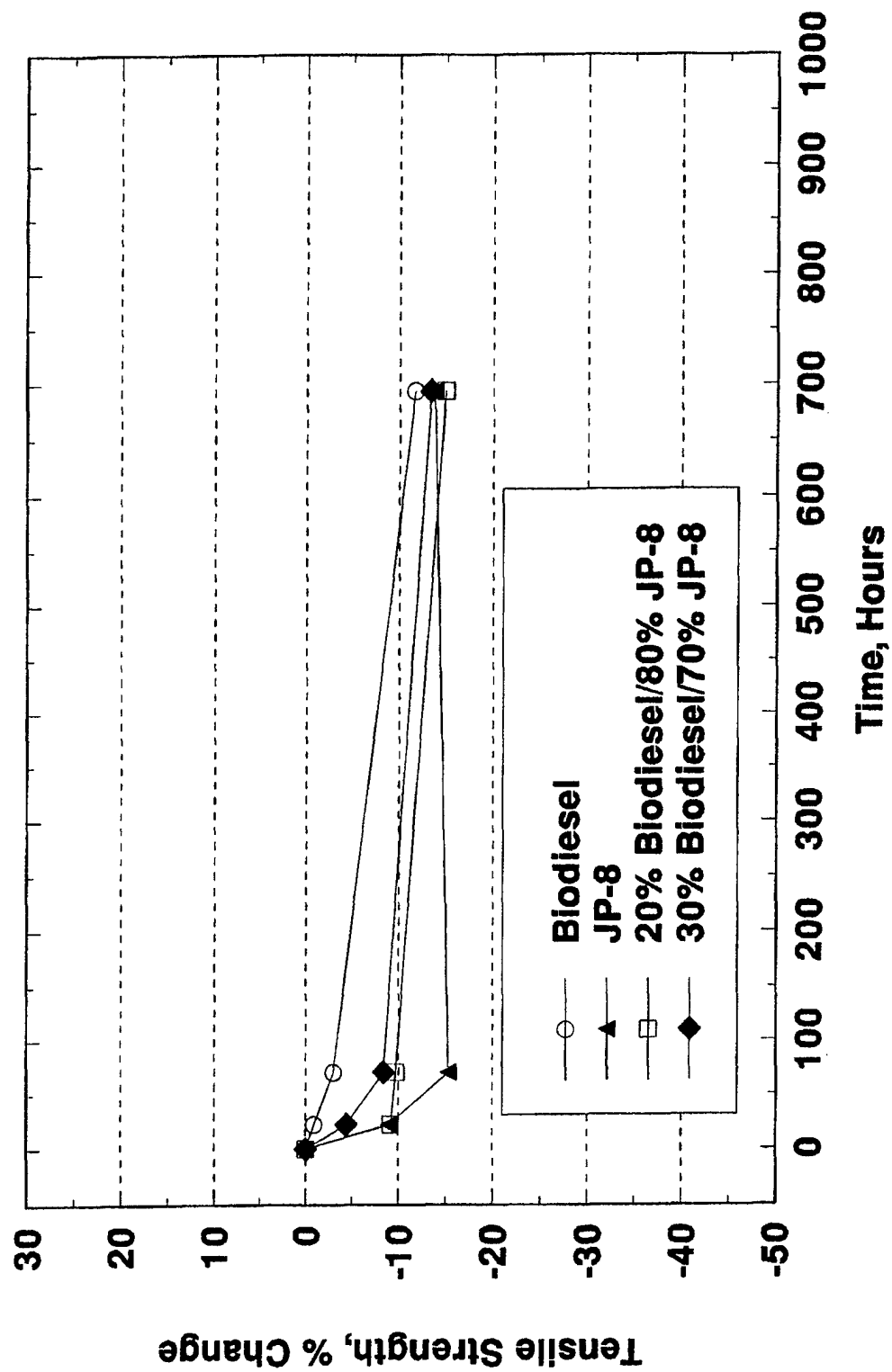
Tensile Strength Polyurethane



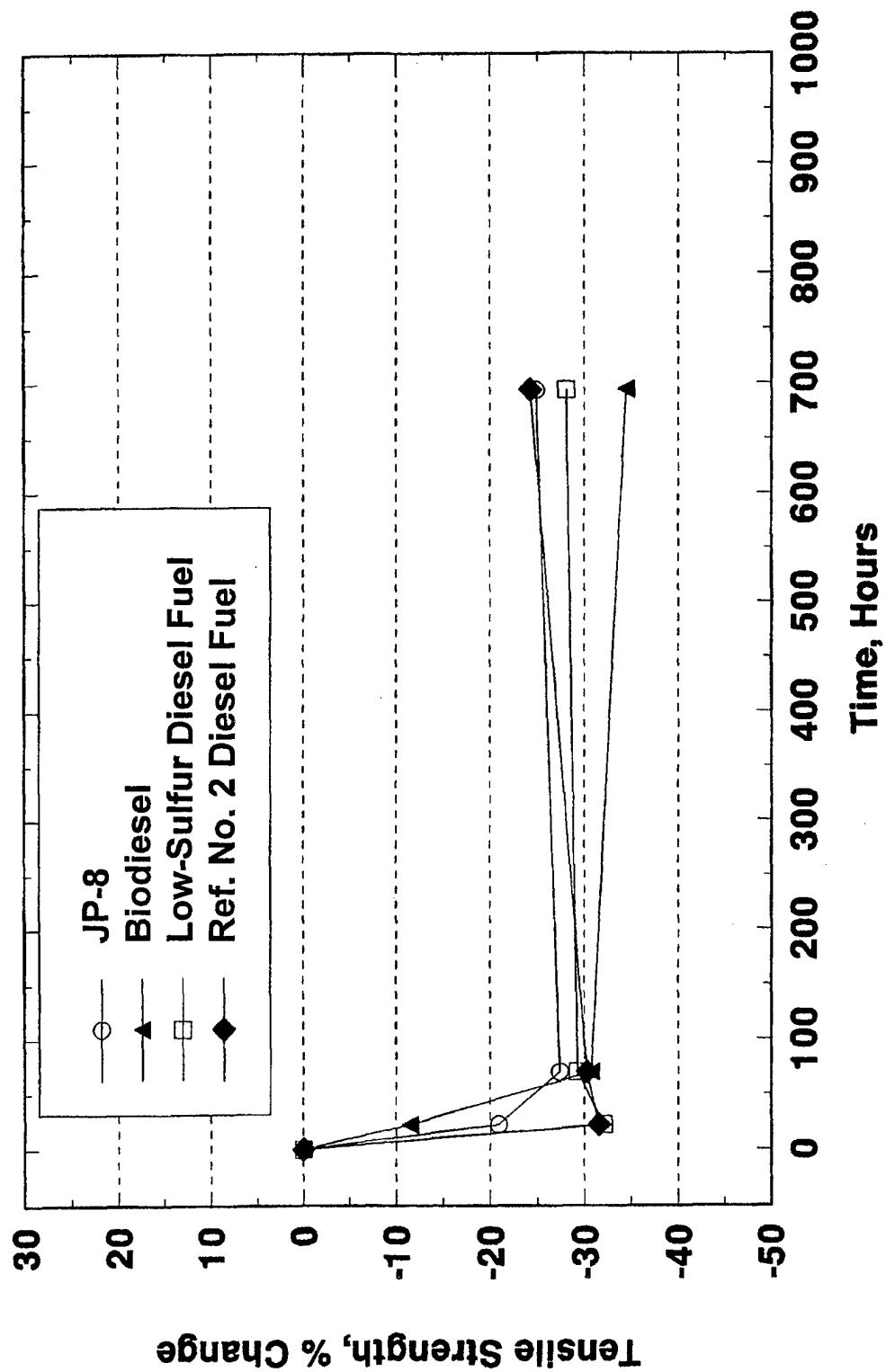
Tensile Strength Polyurethane



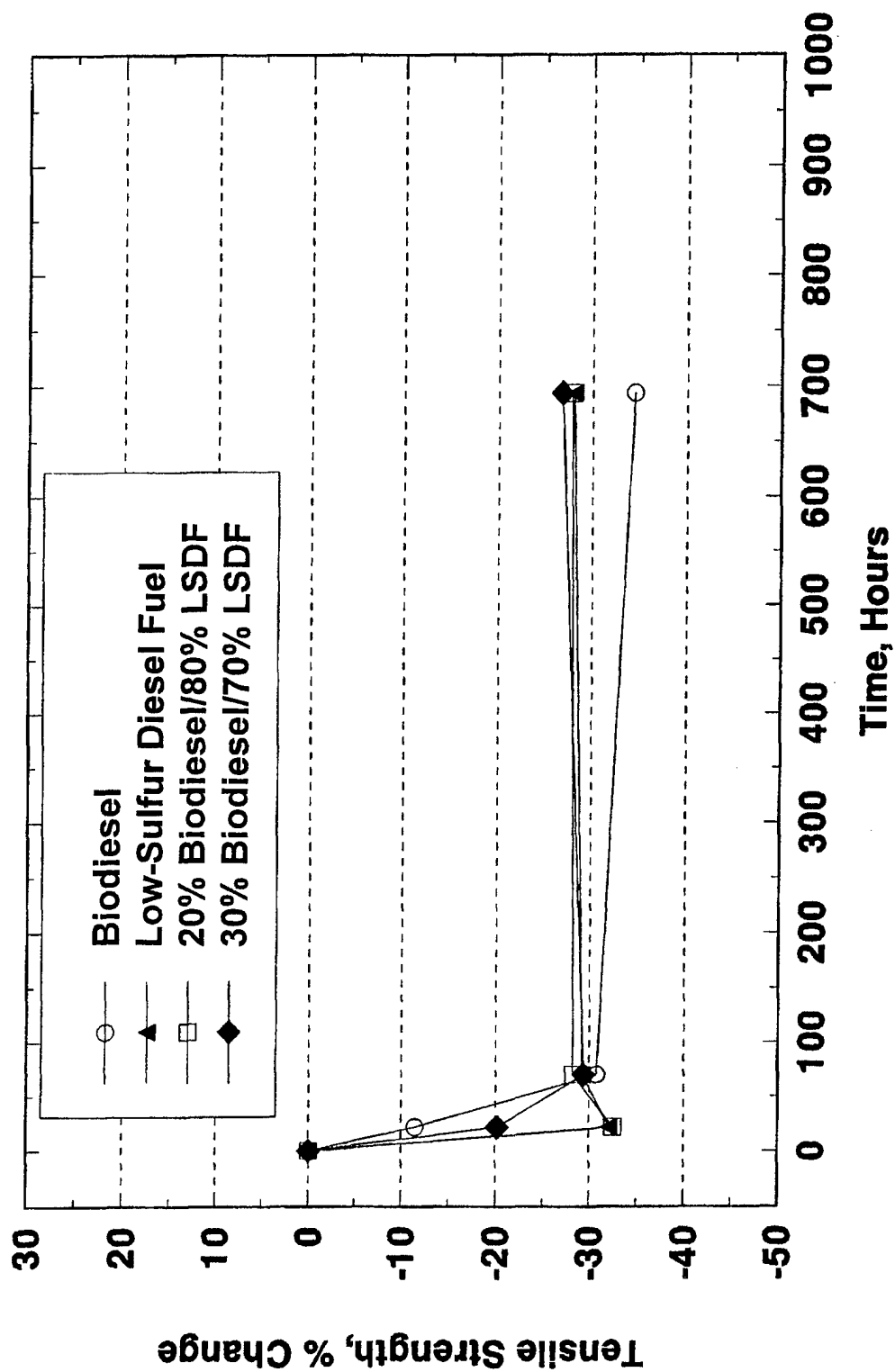
Tensile Strength Polyurethane



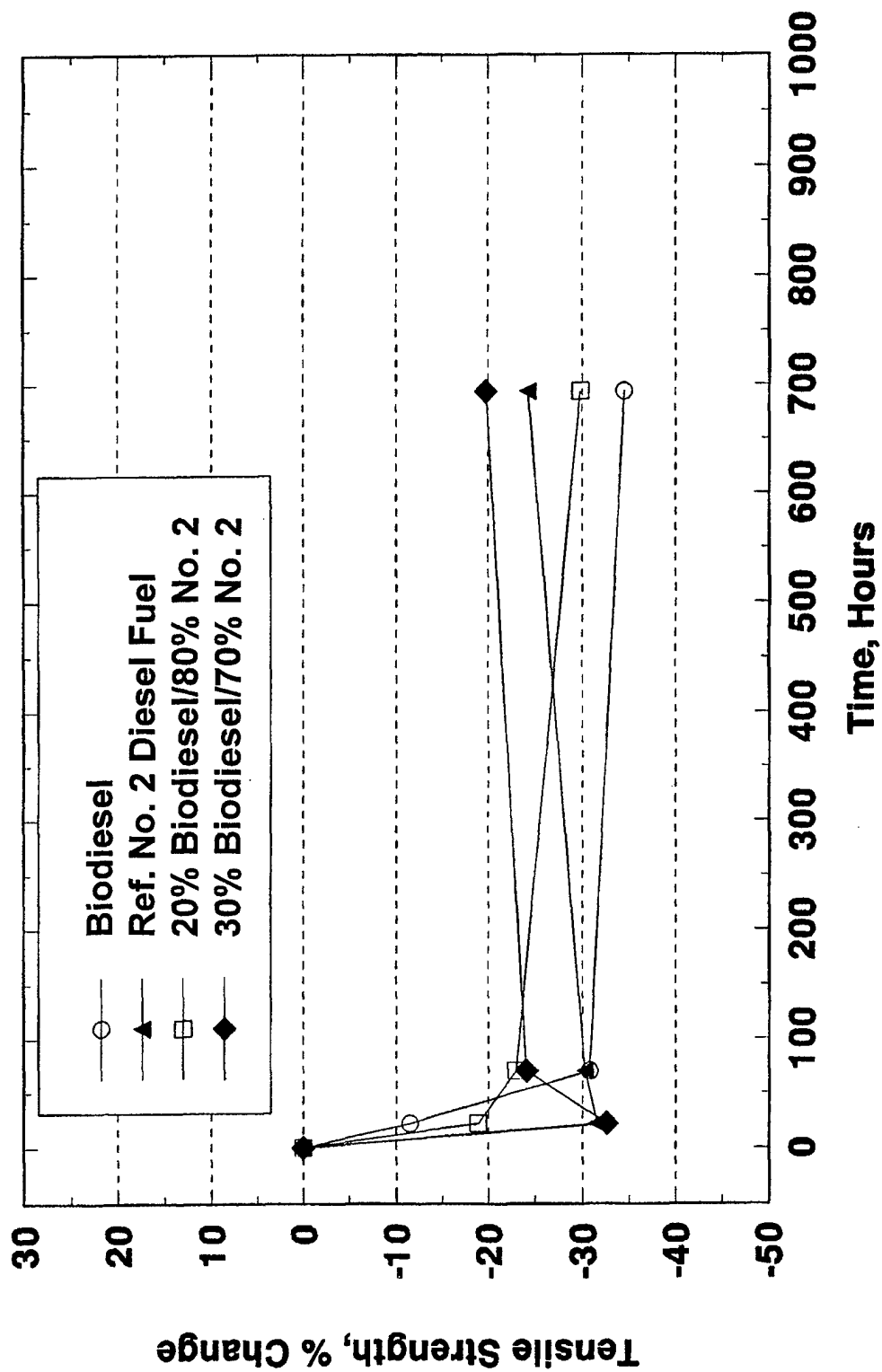
Tensile Strength High Density Polypropylene



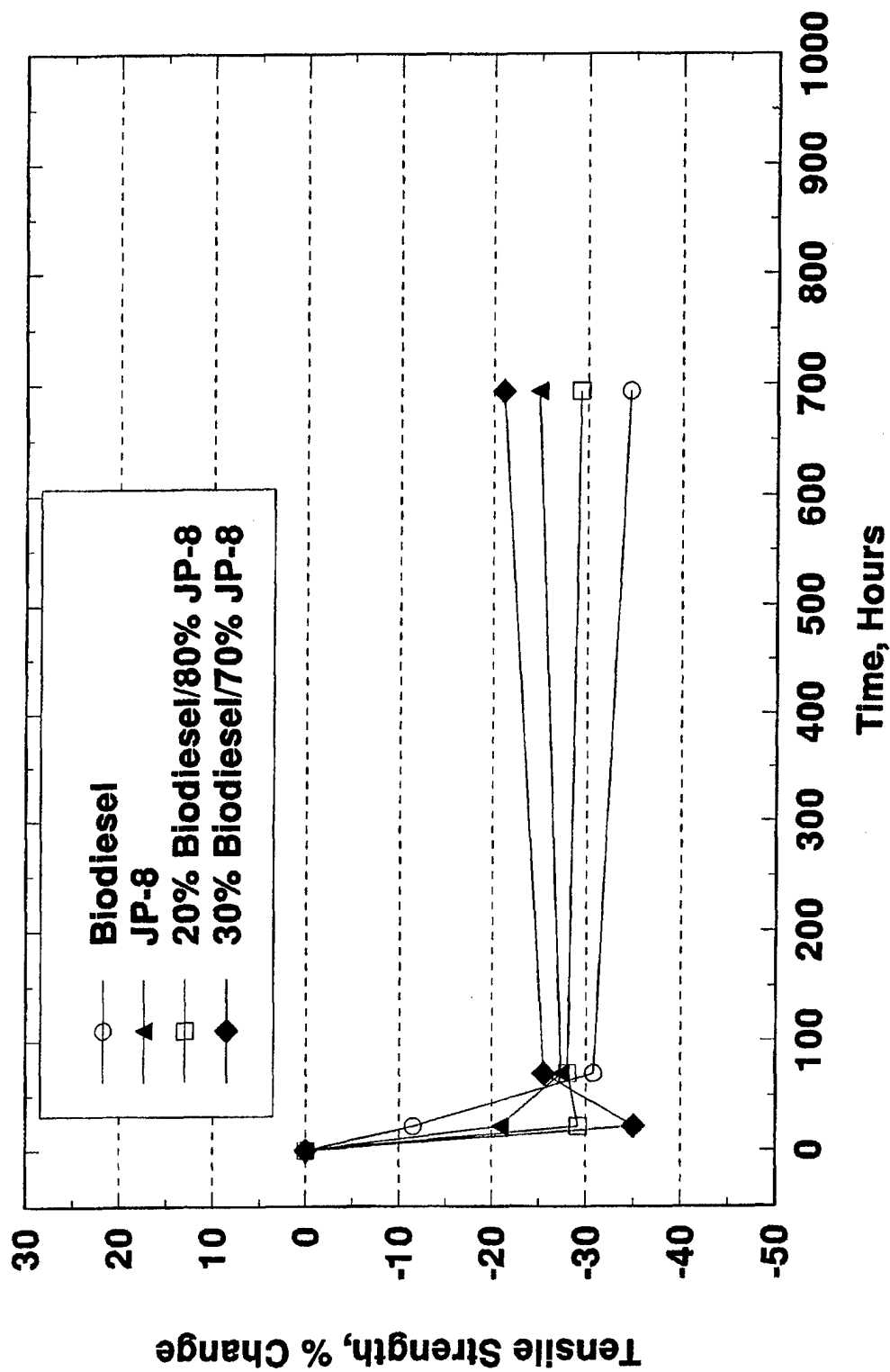
Tensile Strength High Density Polypropylene



Tensile Strength High Density Polypropylene

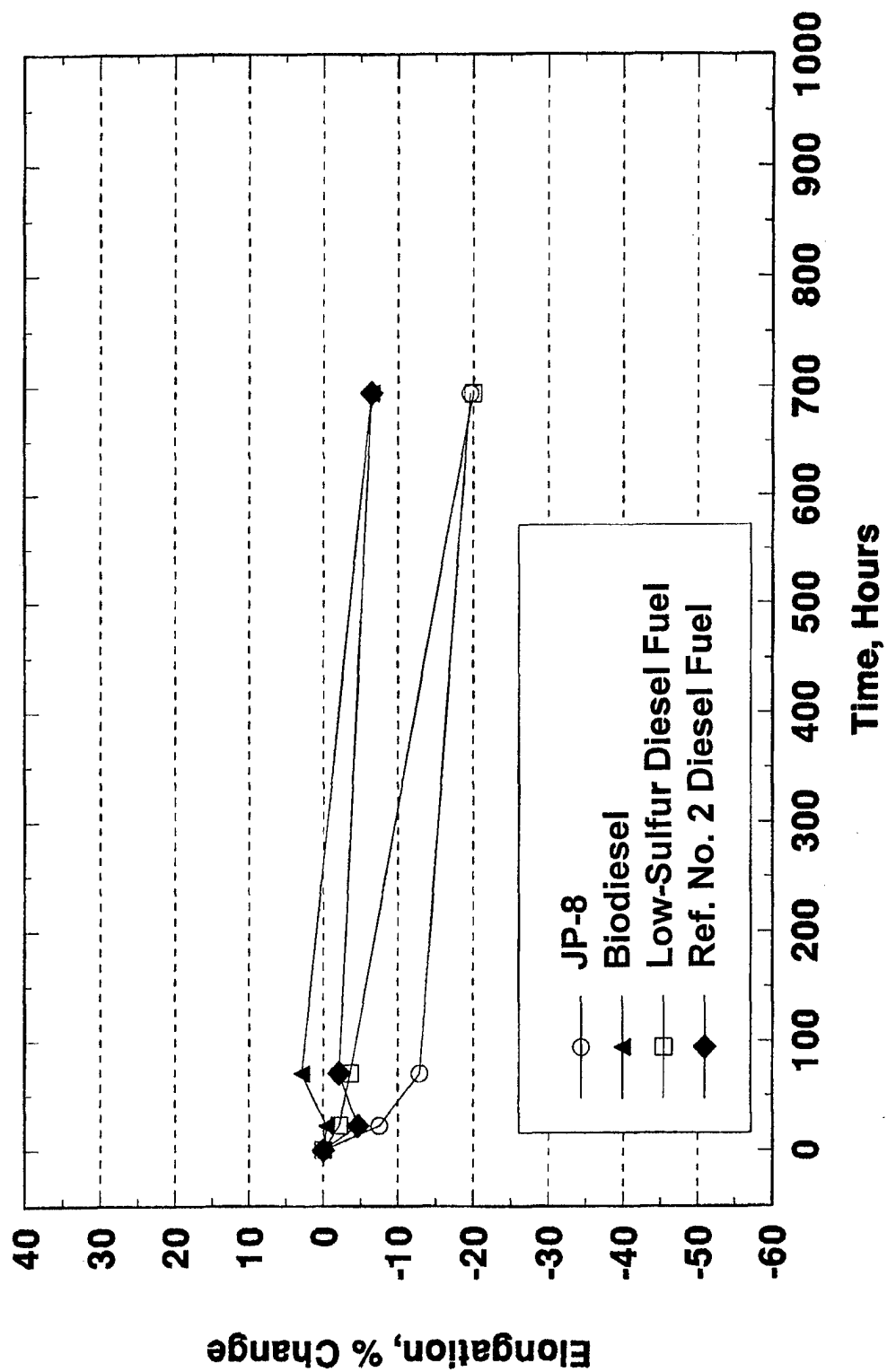


Tensile Strength High Density Polypropylene

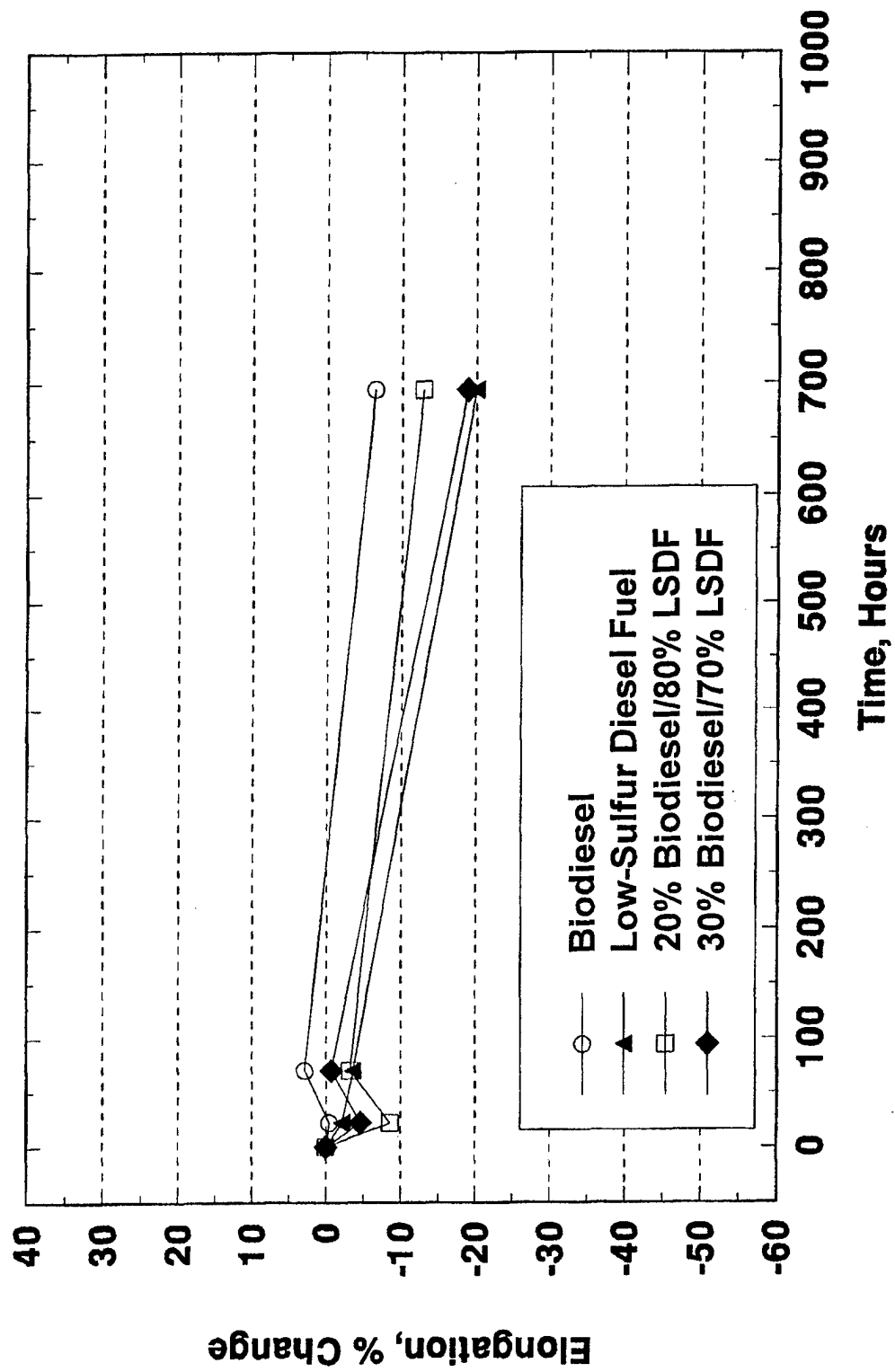


APPENDIX C
Elastomer Elongation

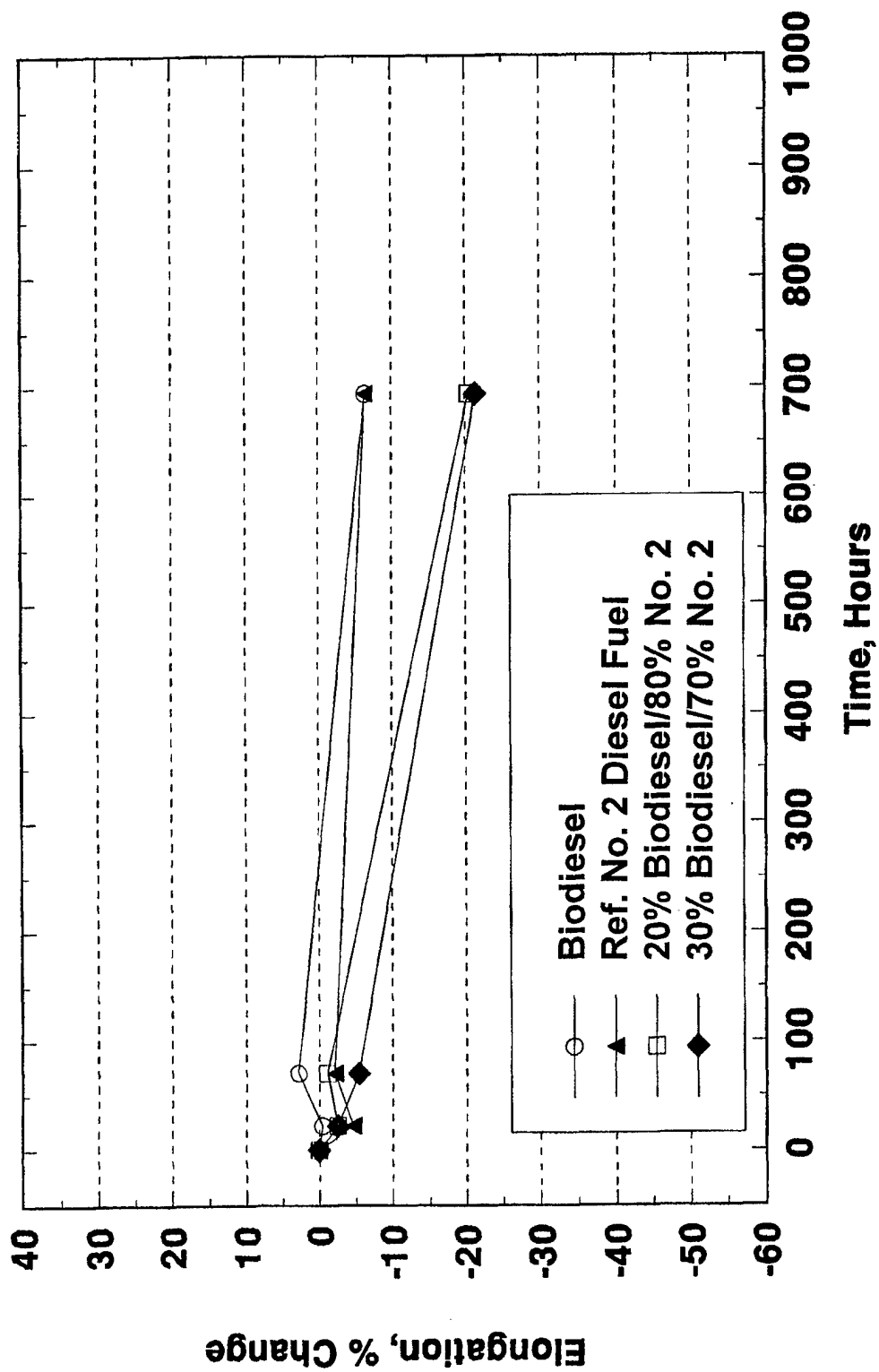
Elongation Teflon



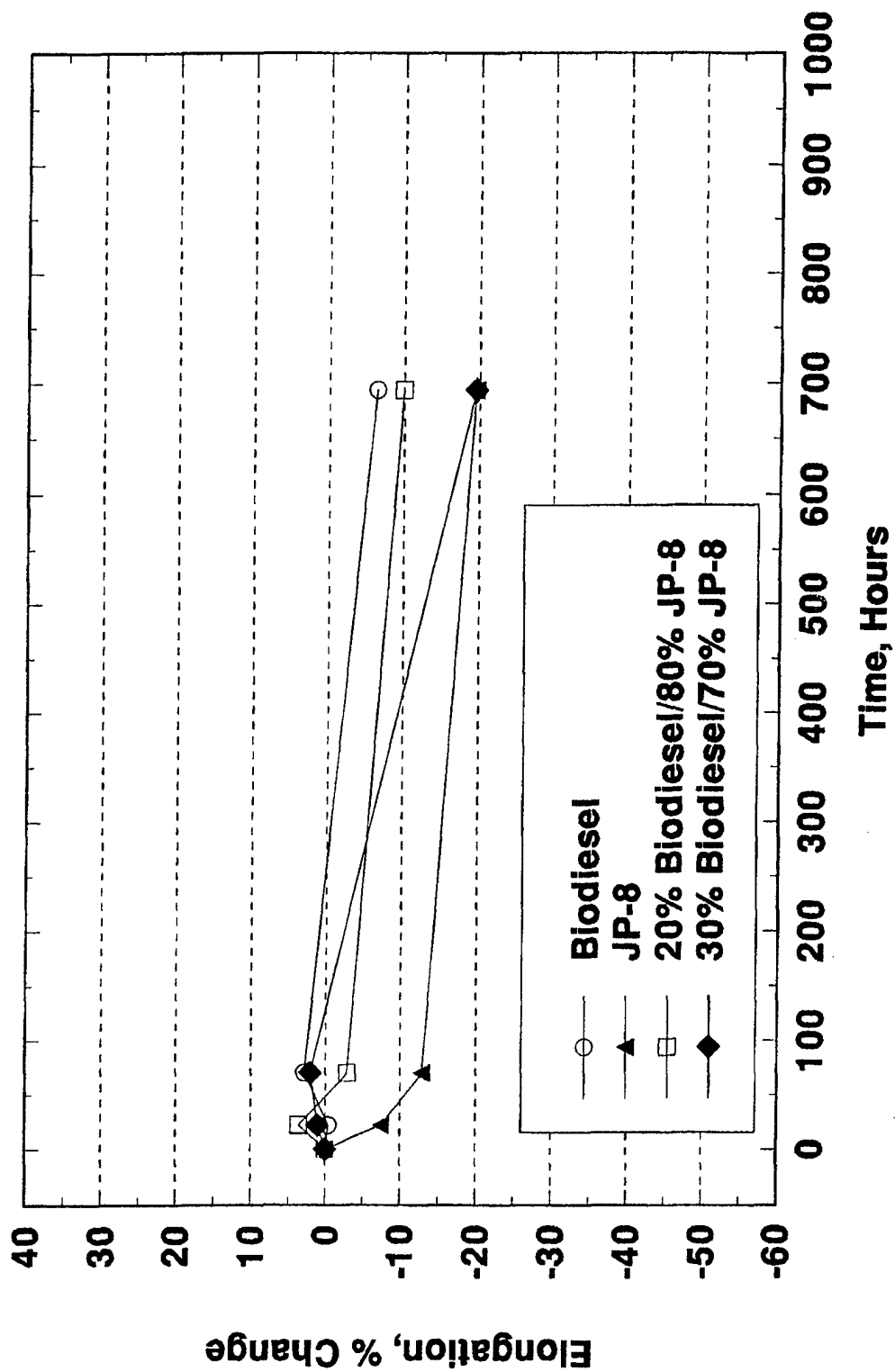
Elongation Teflon



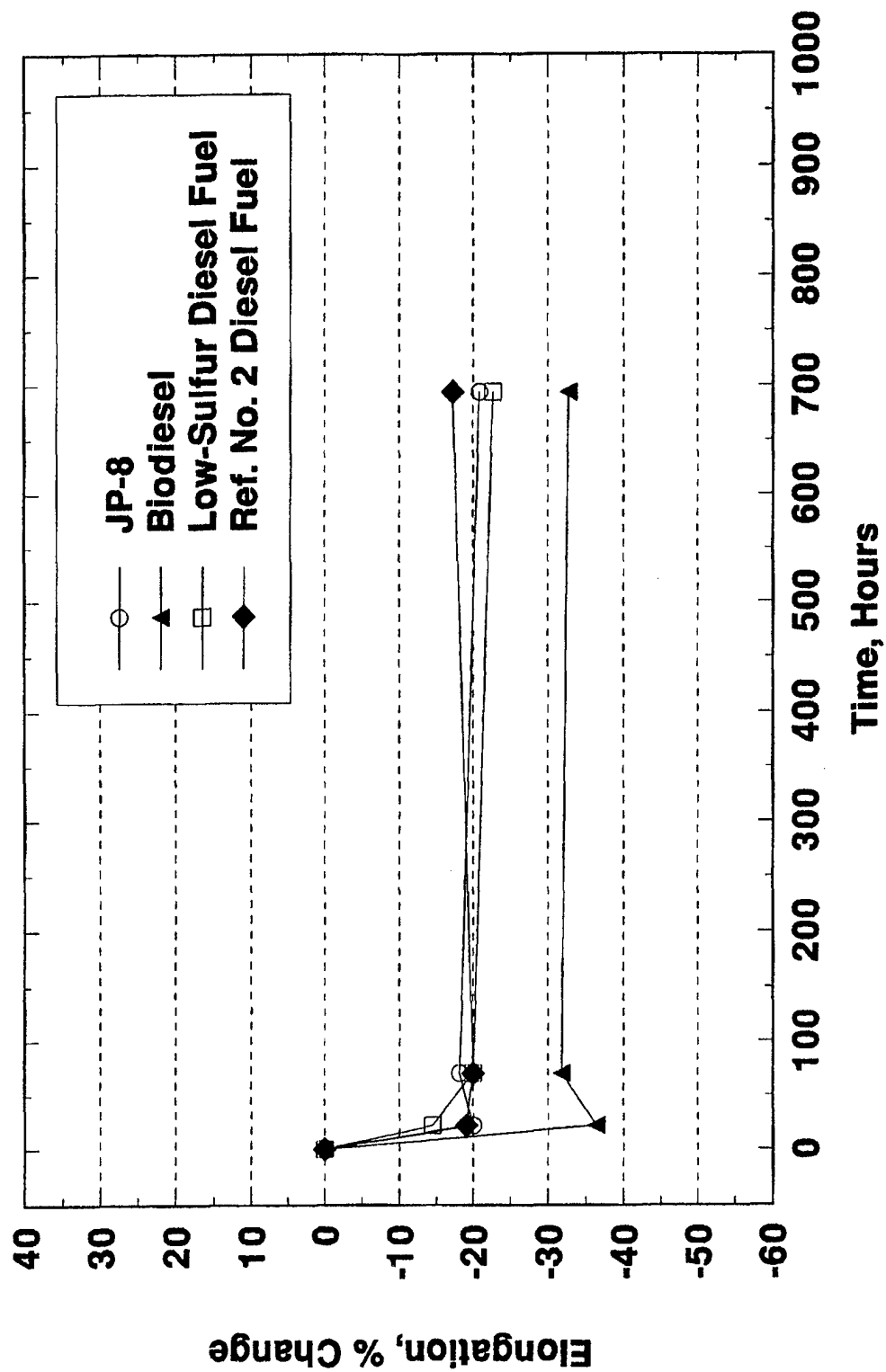
Elongation Teflon



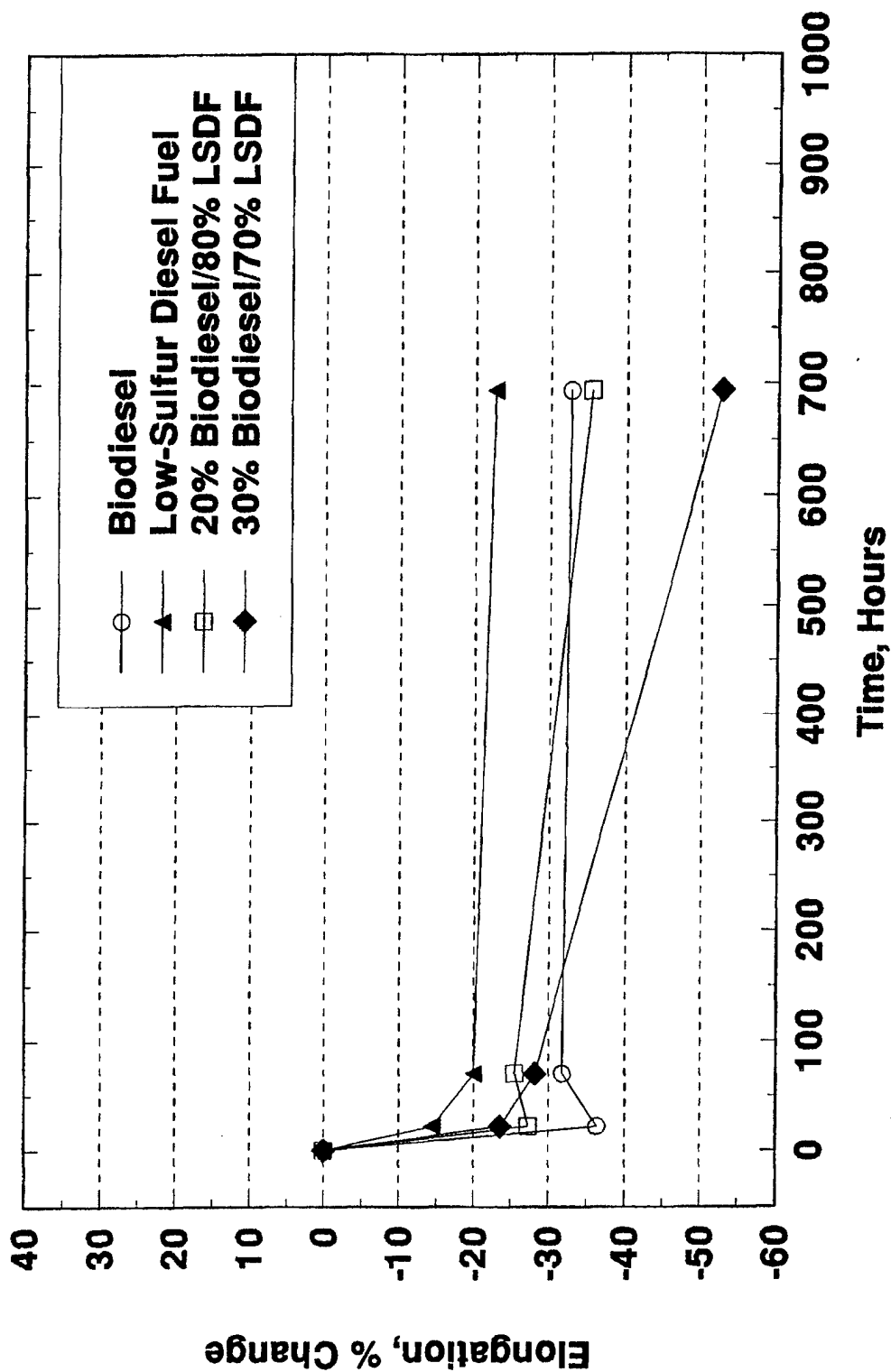
Elongation Teflon



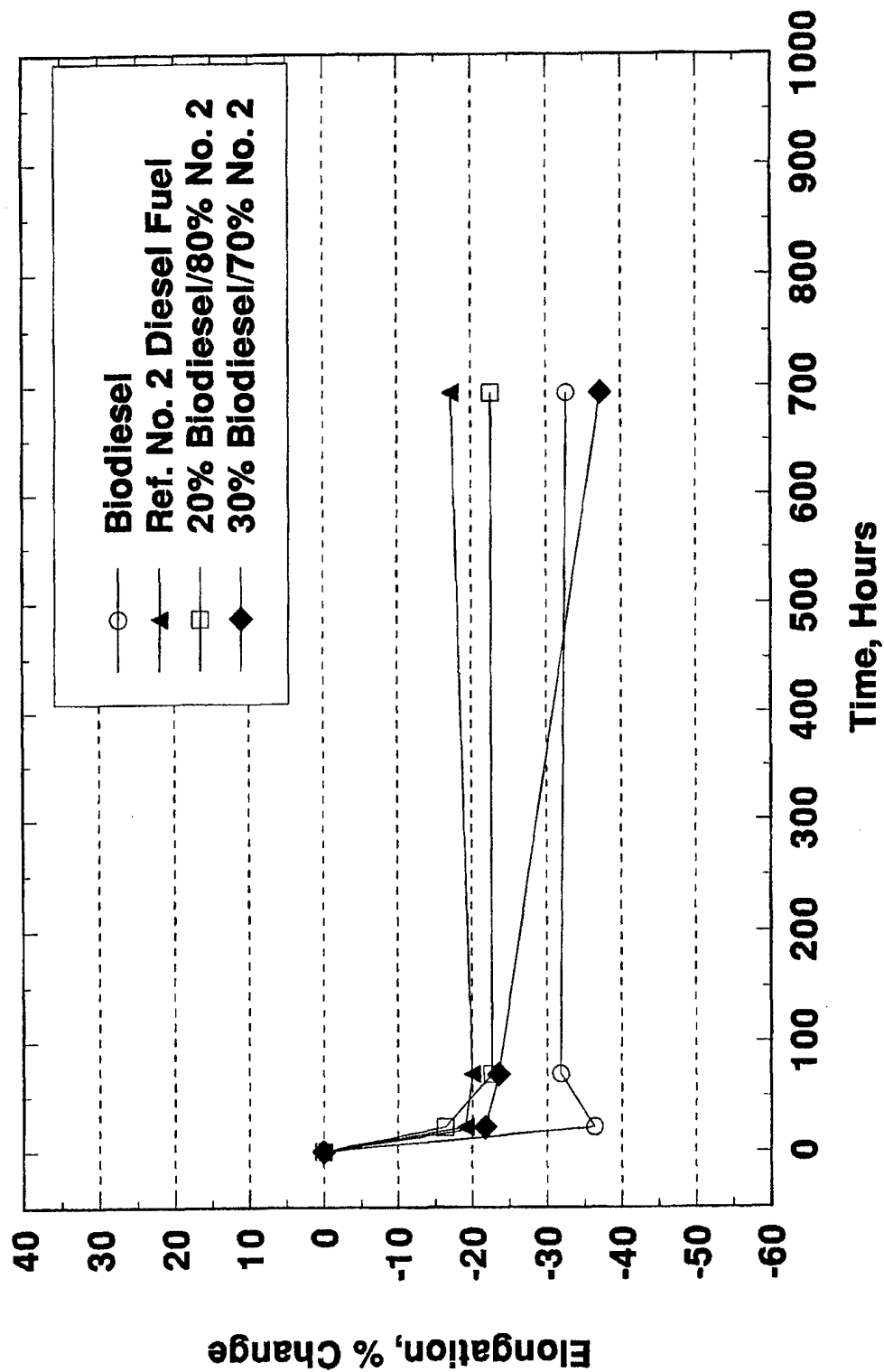
Elongation Nitrile Rubber



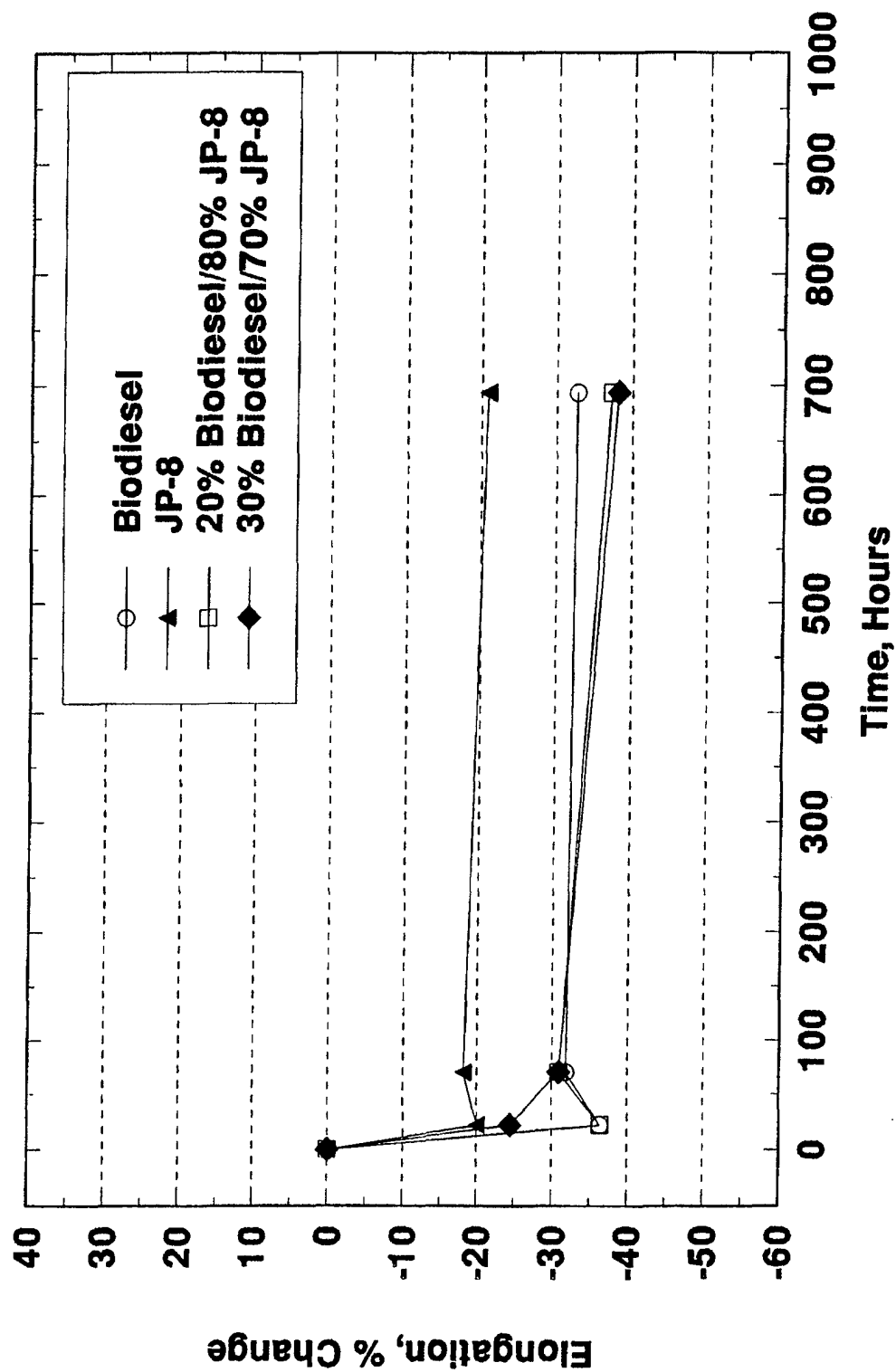
Elongation Nitrile Rubber



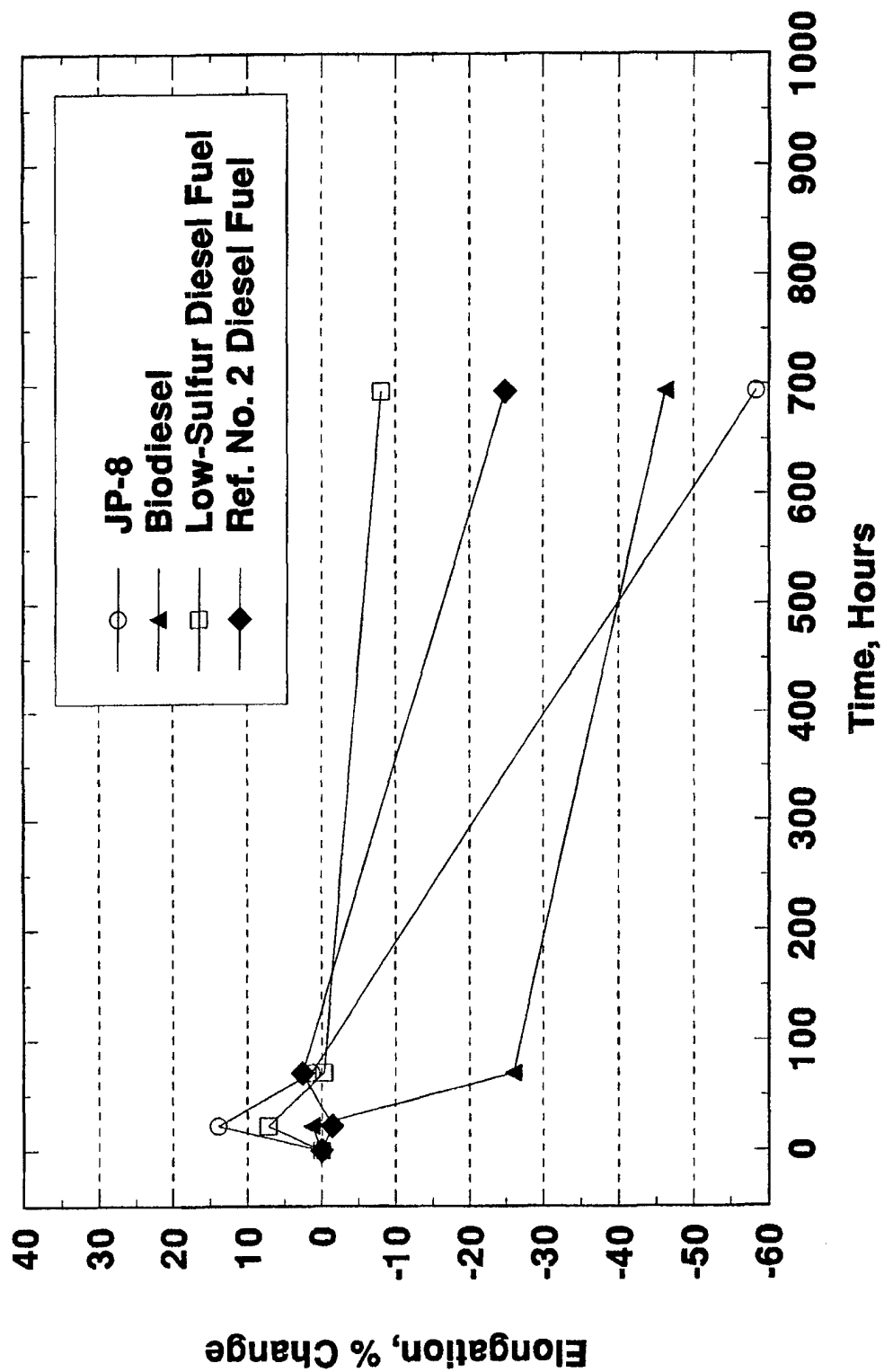
Elongation Nitrile Rubber



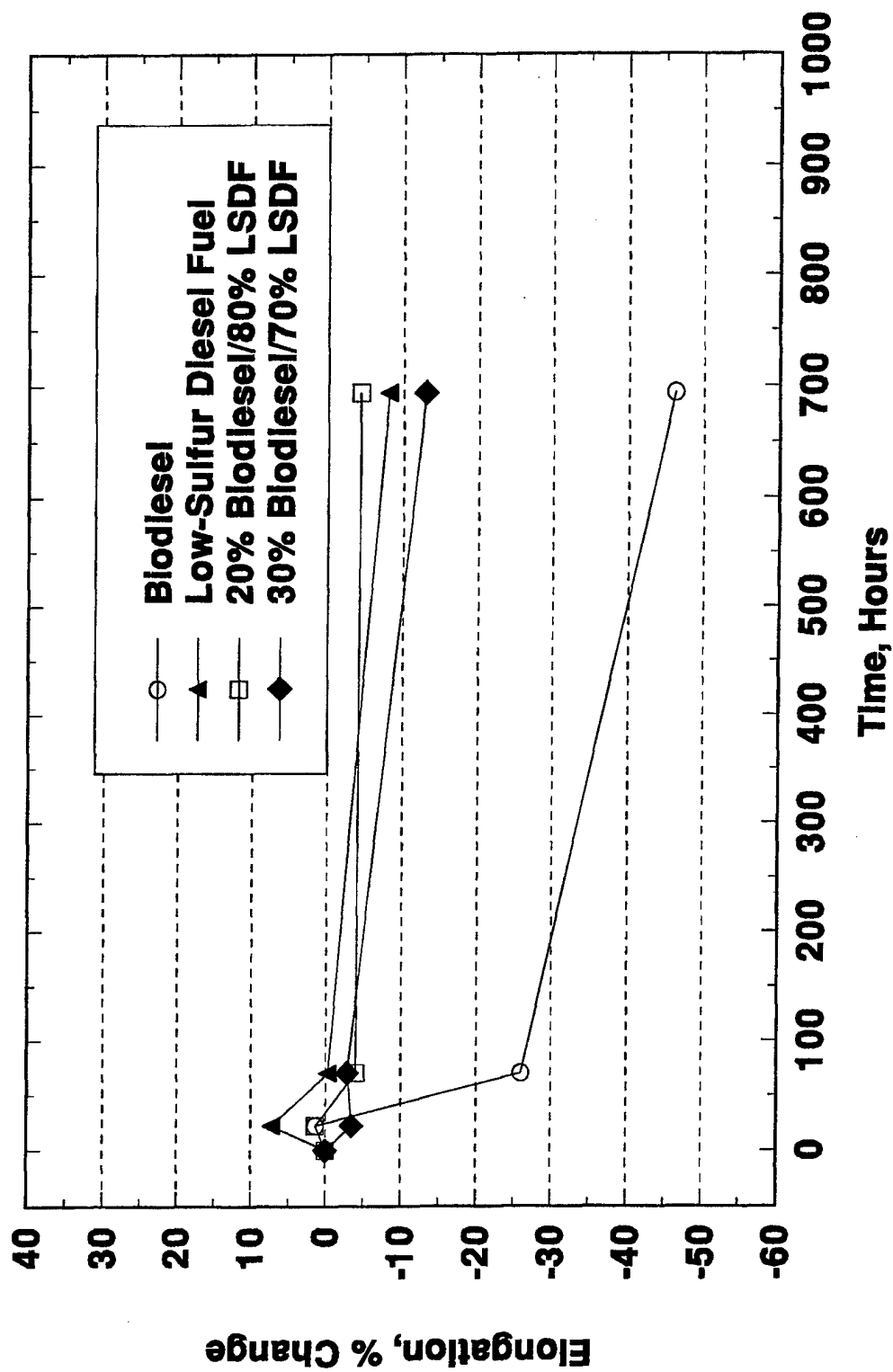
Elongation Nitrile Rubber



Elongation Nylon 6/6

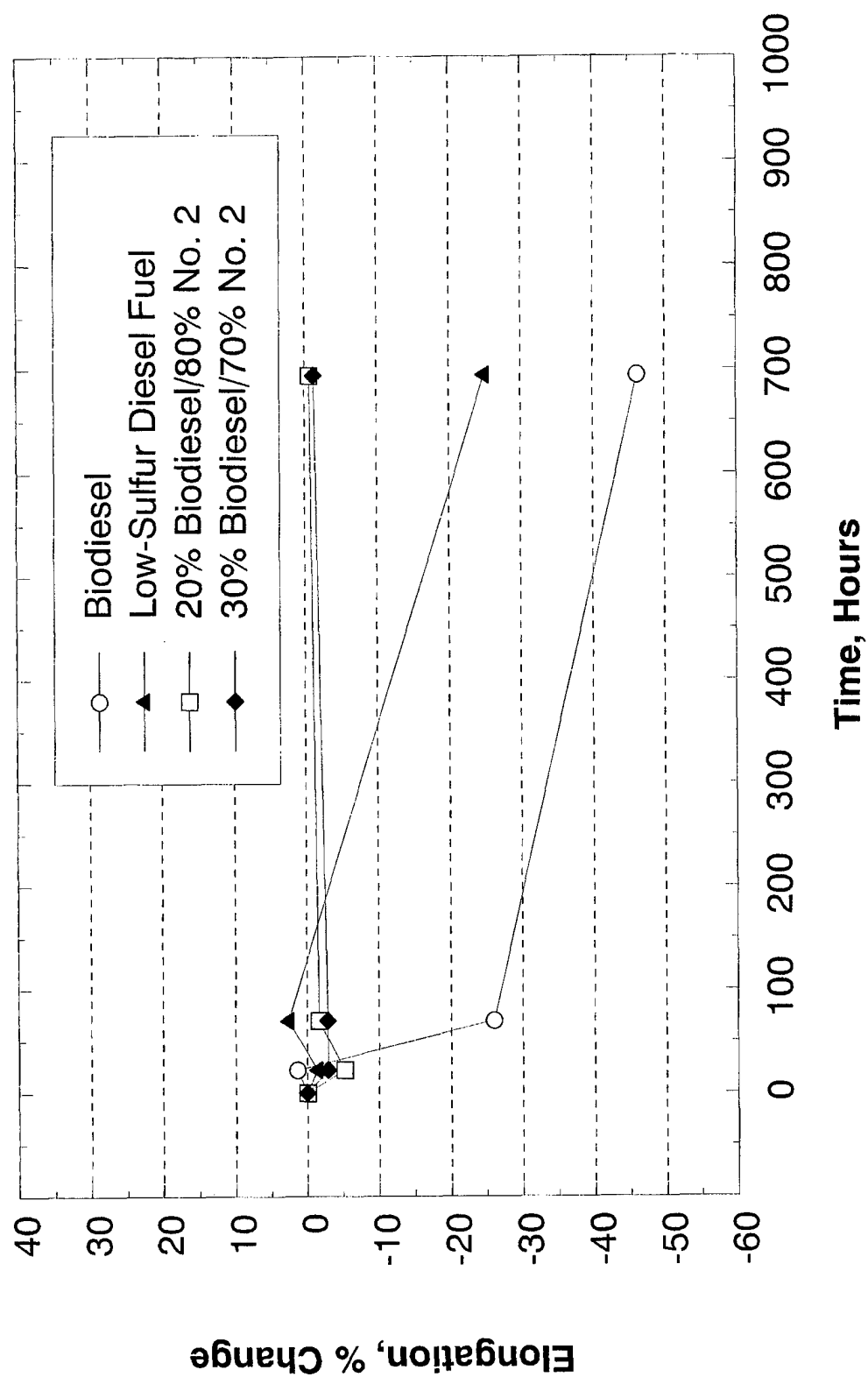


Elongation Nylon 6/6

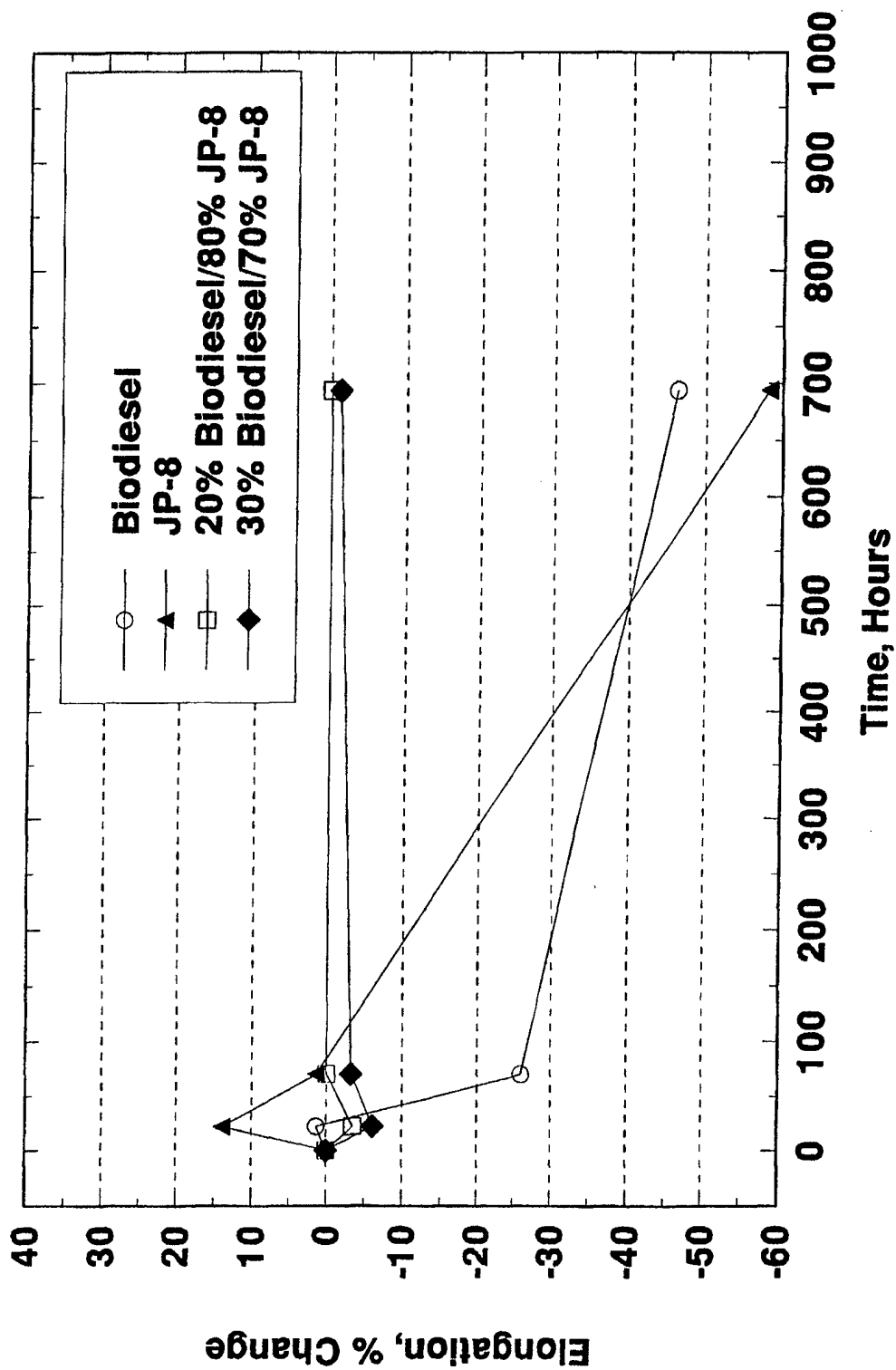


Elongation

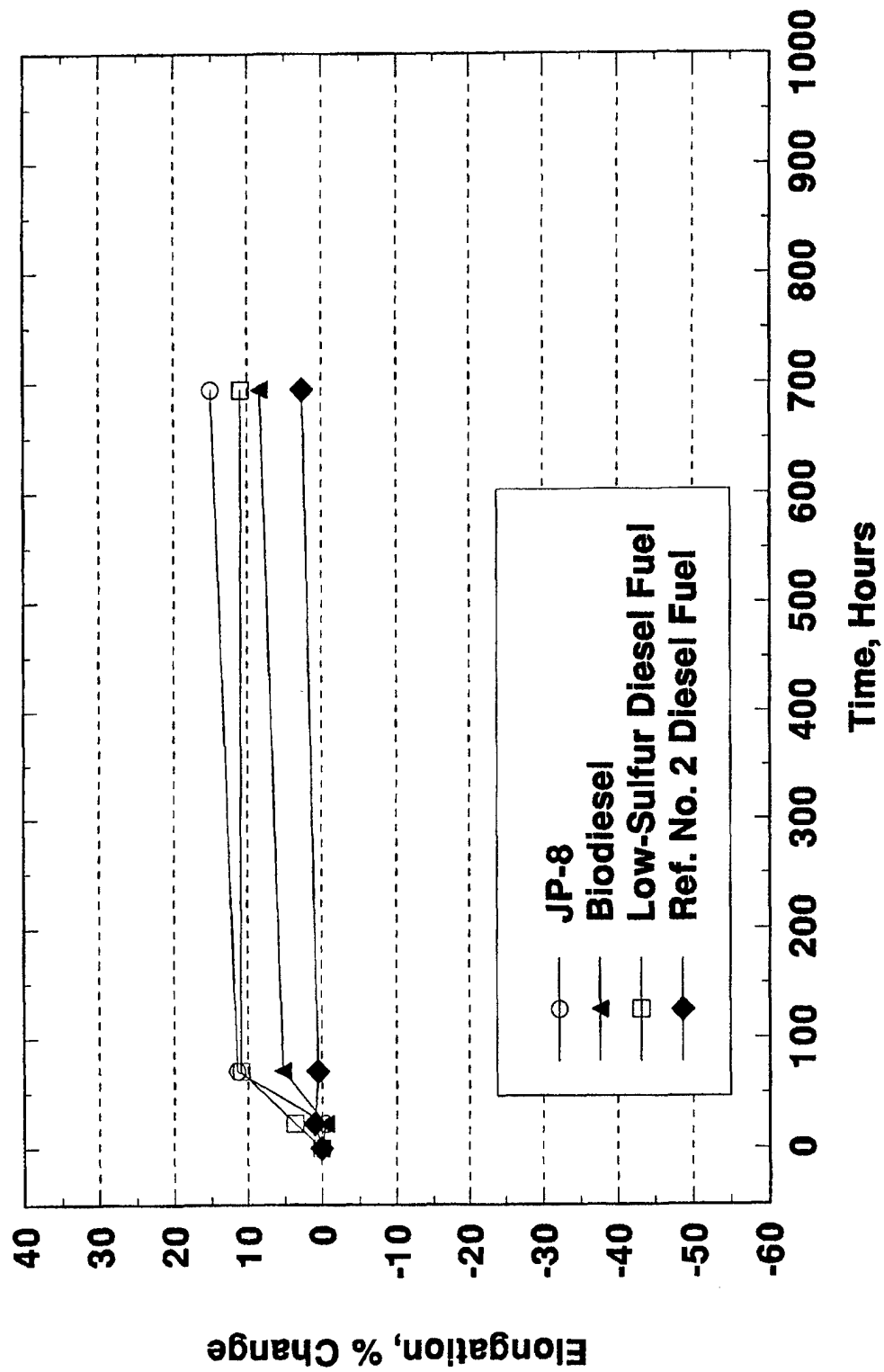
Nylon 6/6



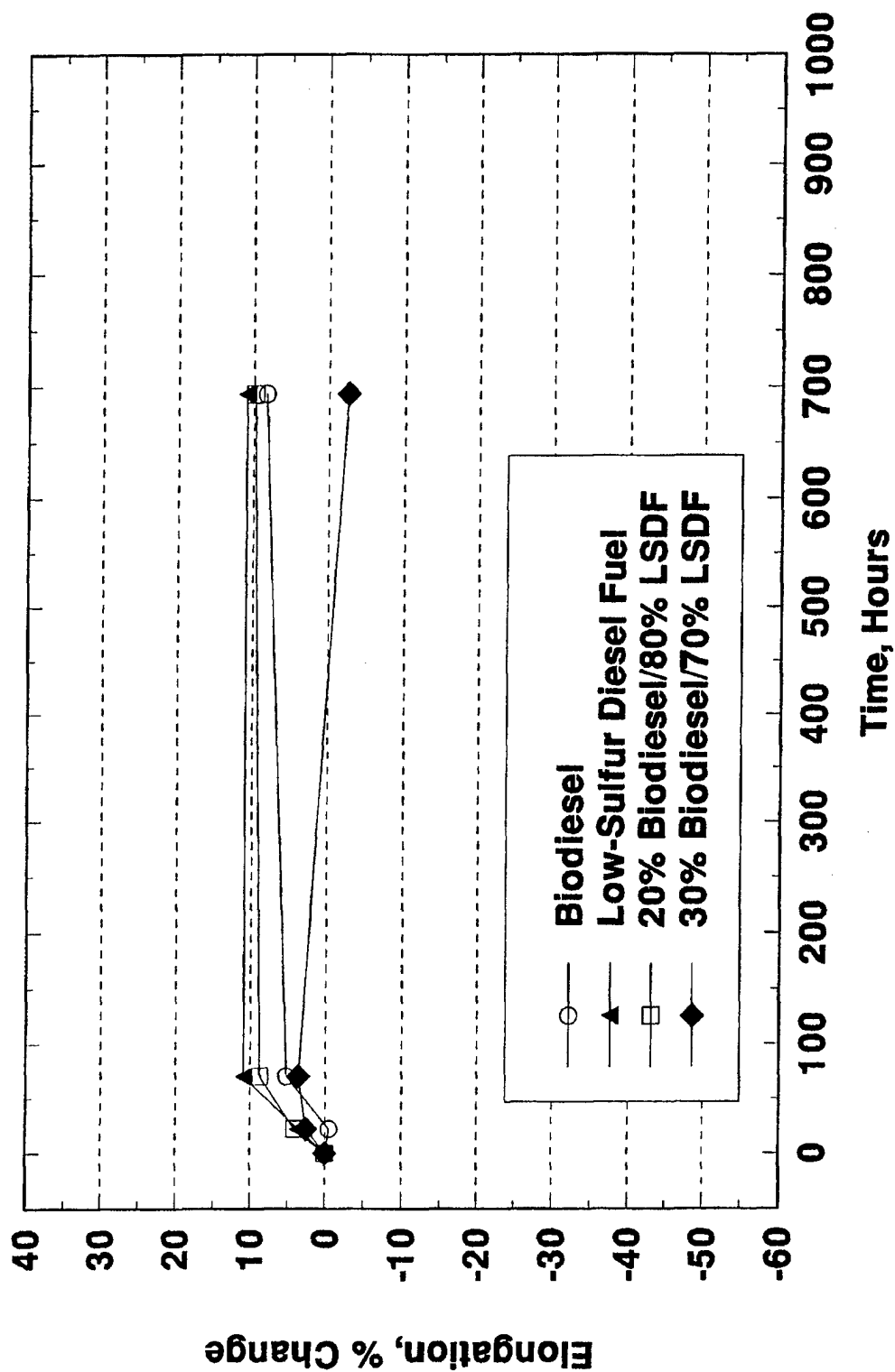
Elongation Nylon 6/6



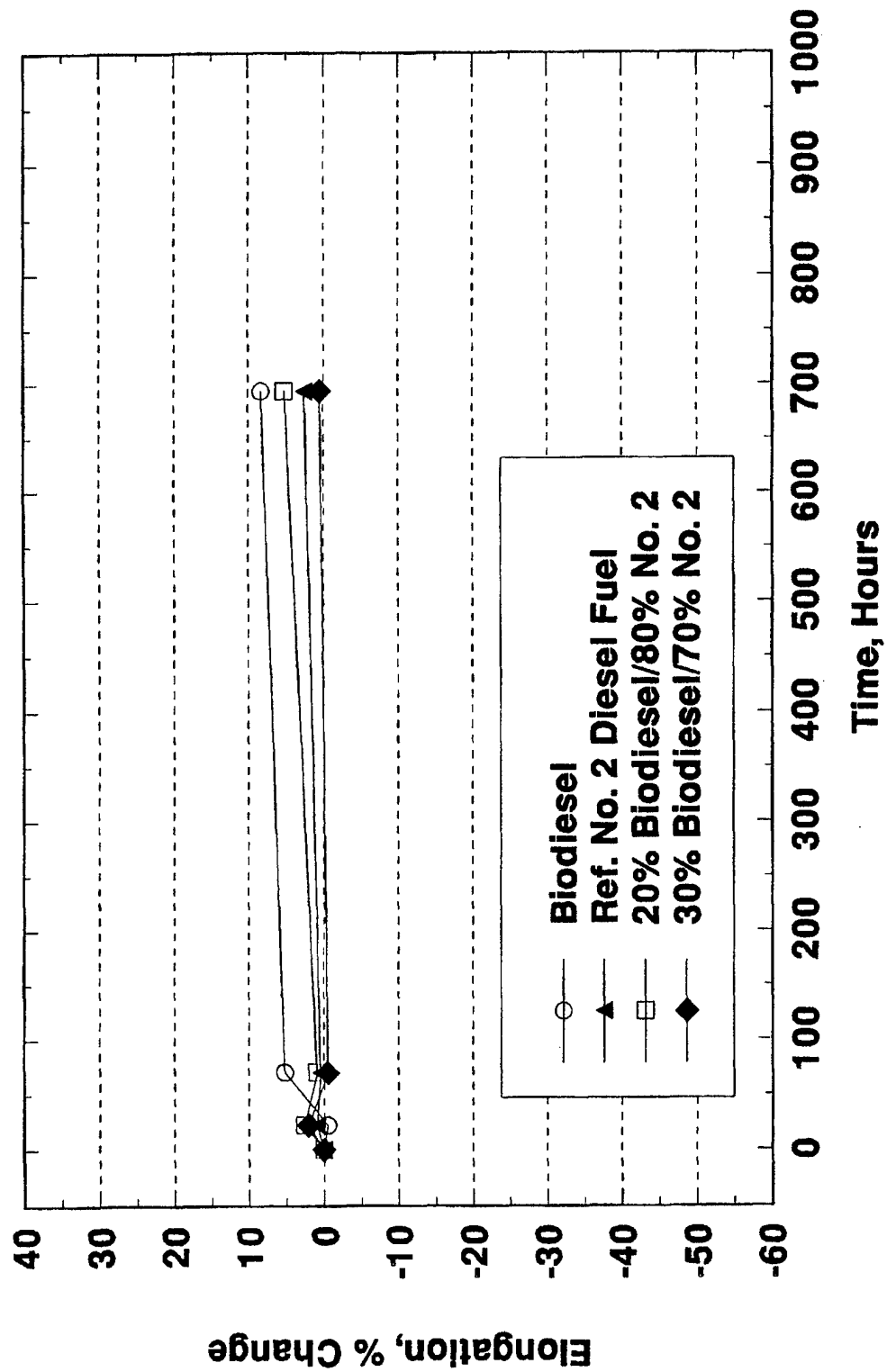
**Elongation
Viton 401-C**



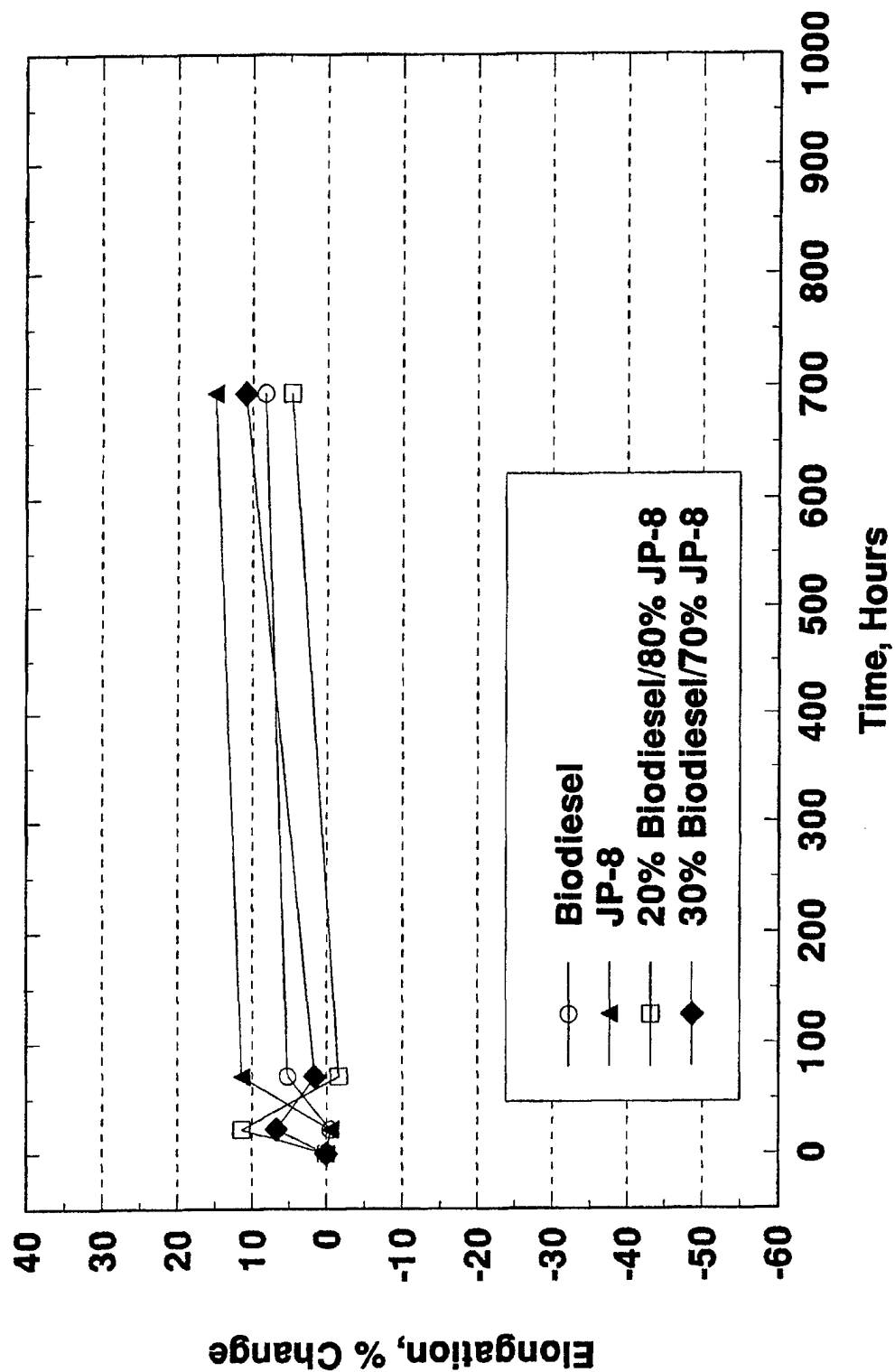
**Elongation
Viton 401-C**



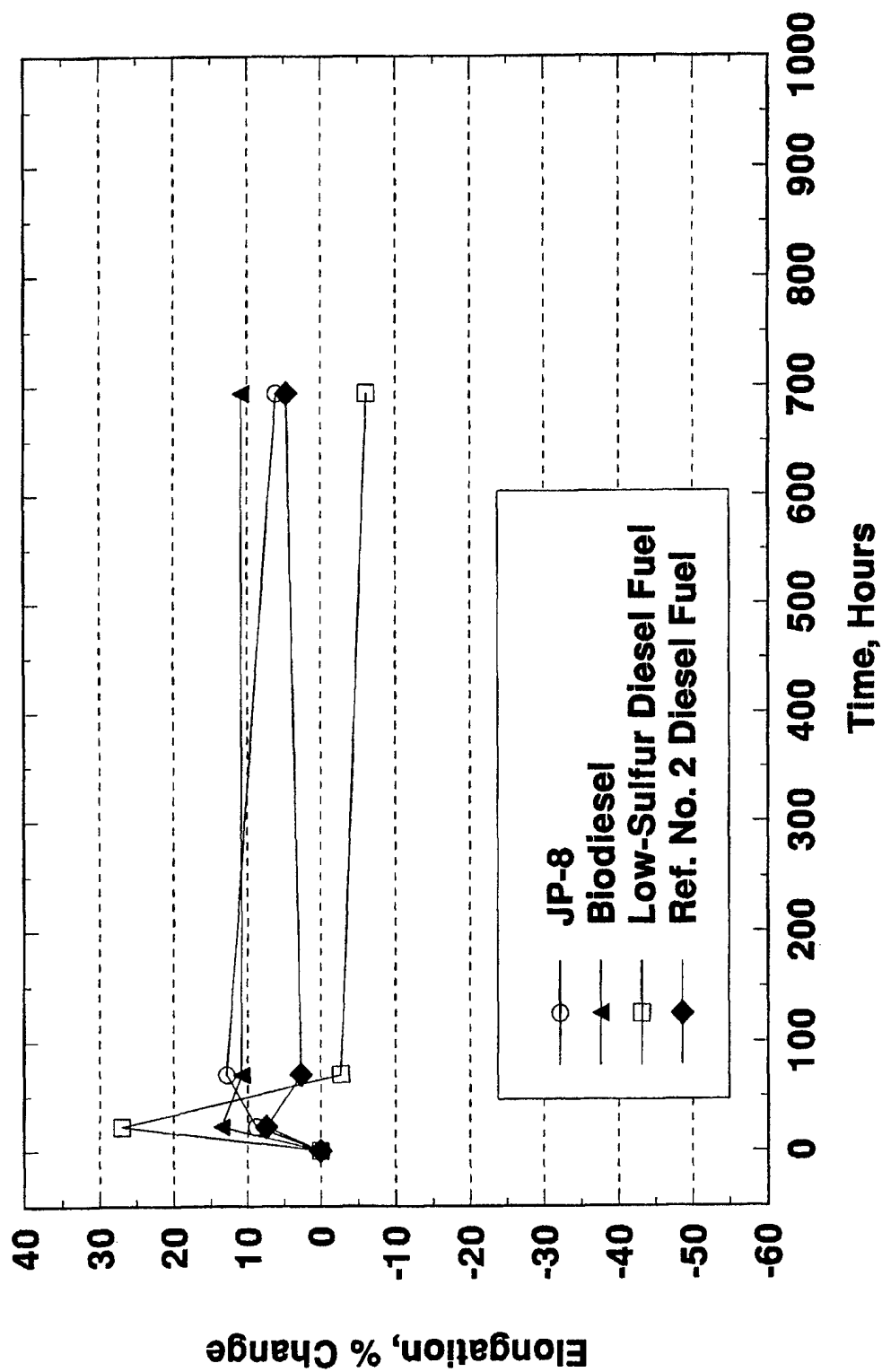
Elongation Viton 401-C



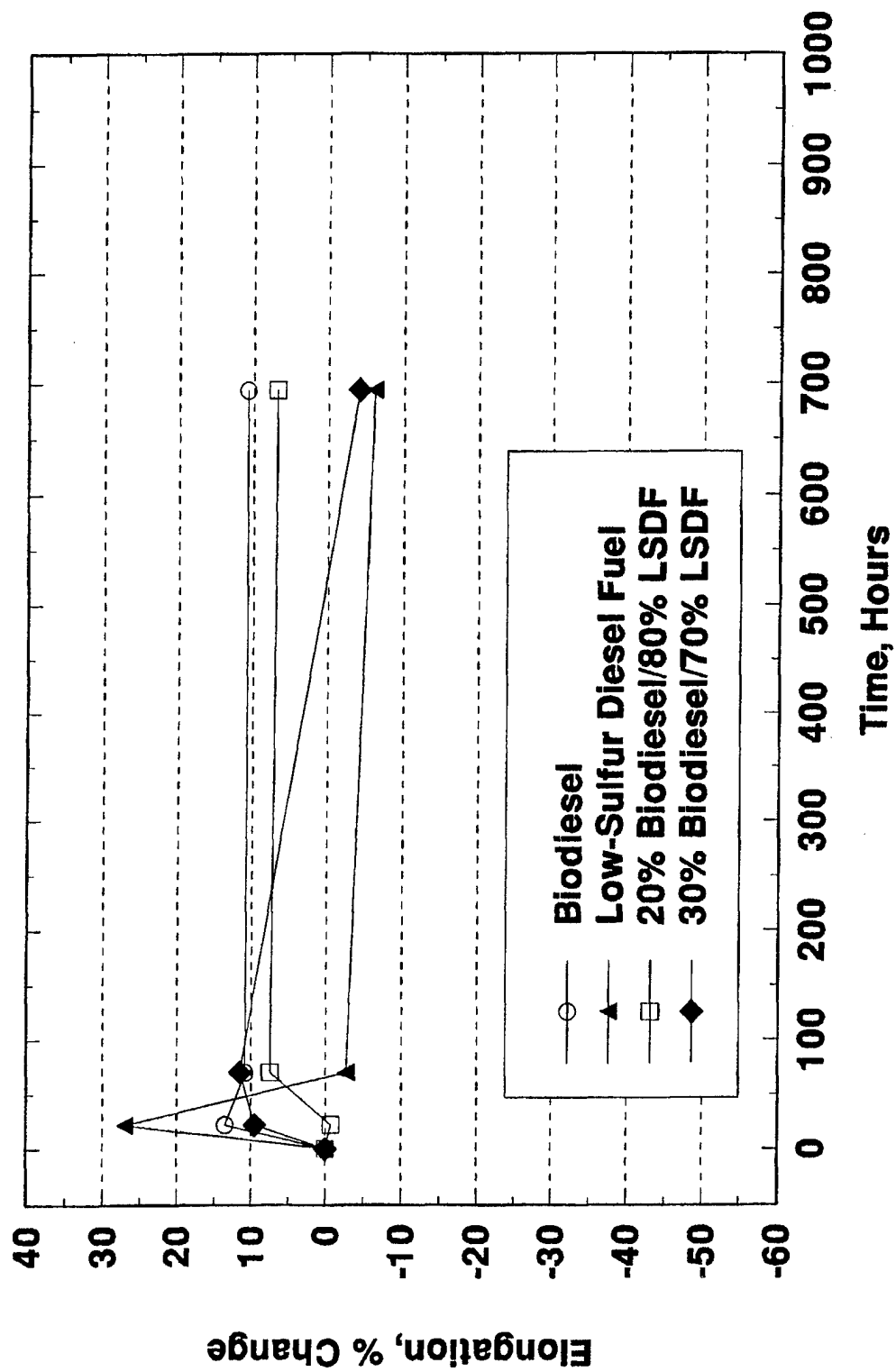
Elongation Viton 401-C



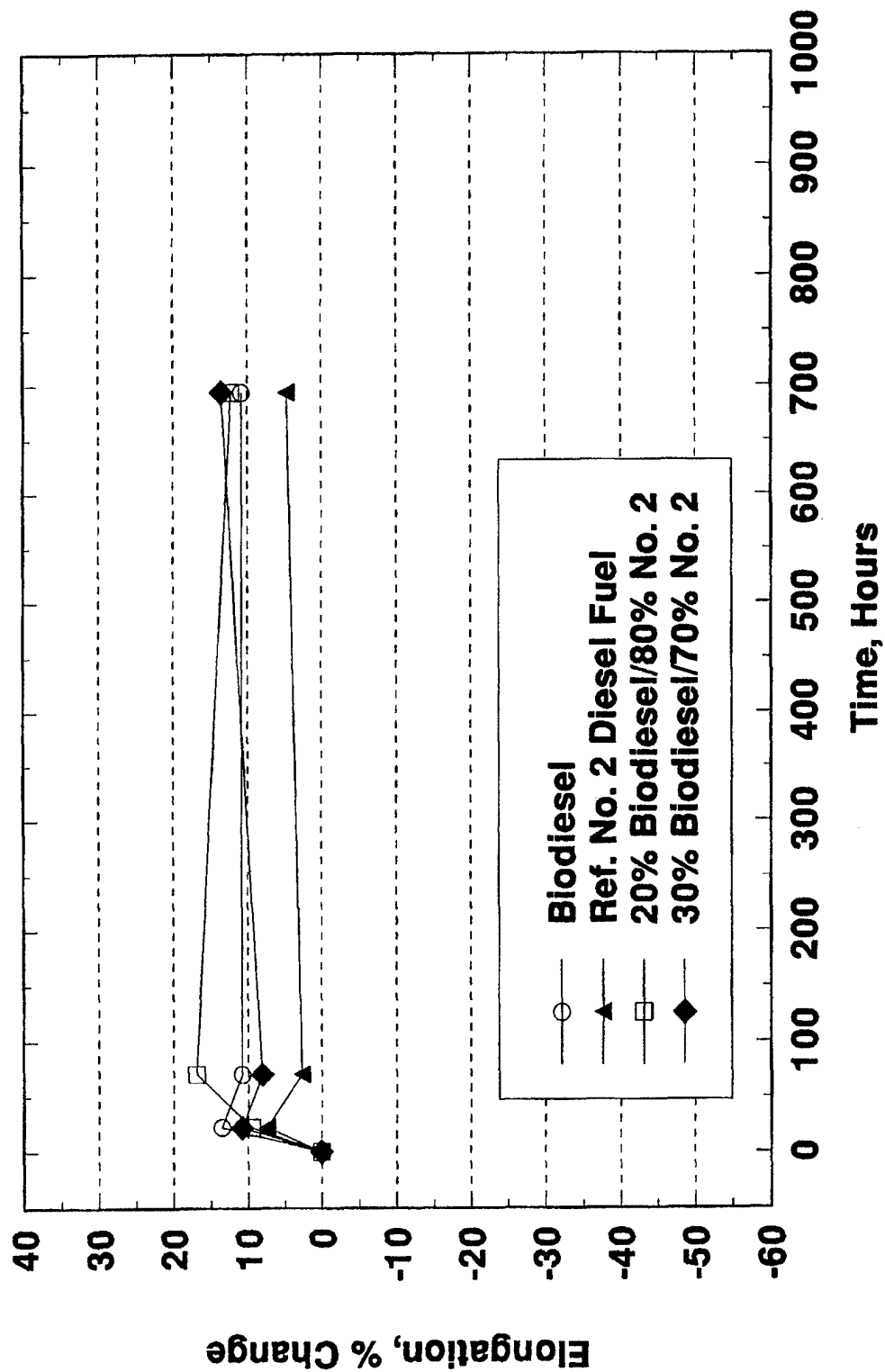
Elongation Viton GFLT



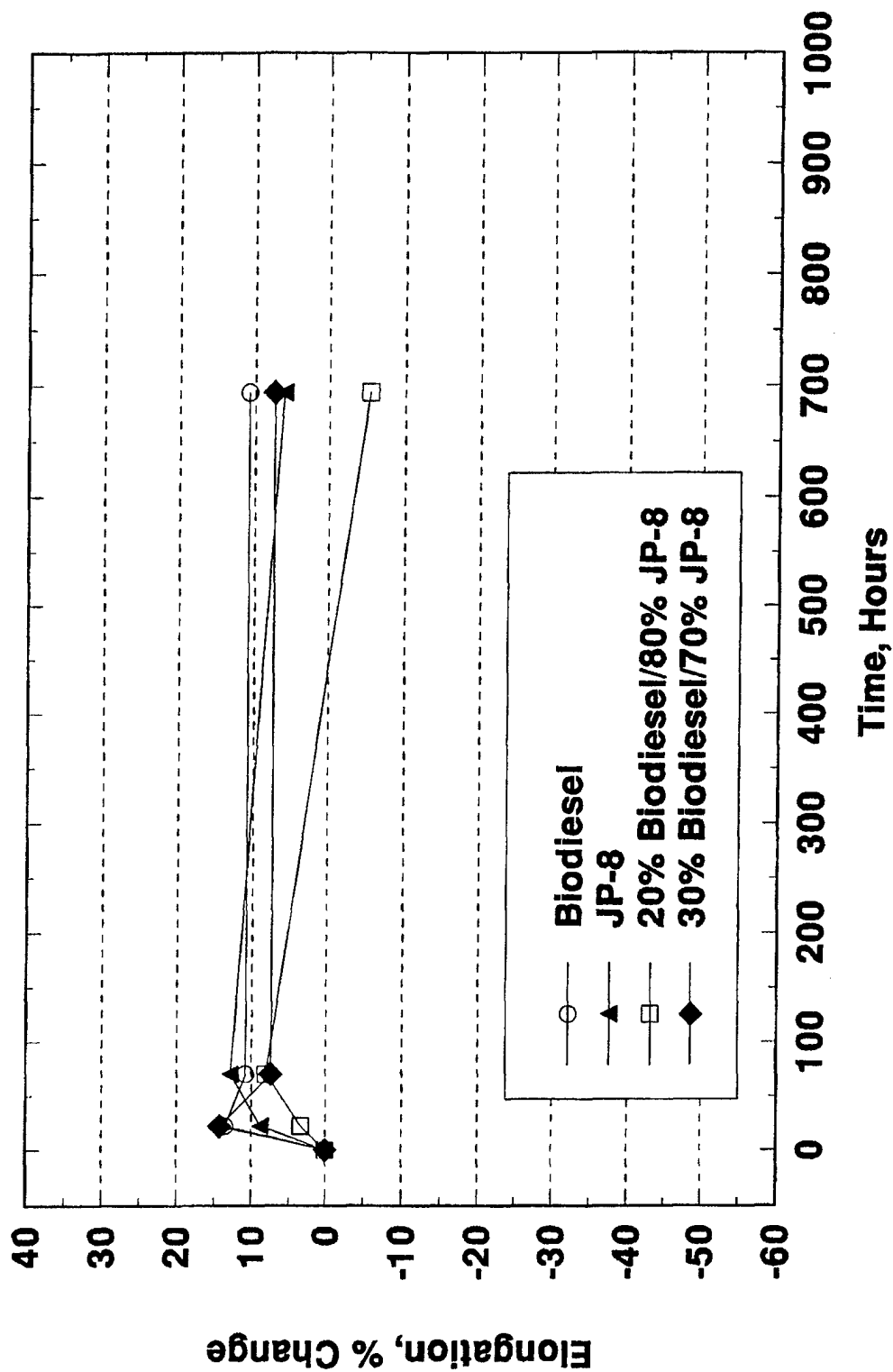
Elongation Viton GFLT



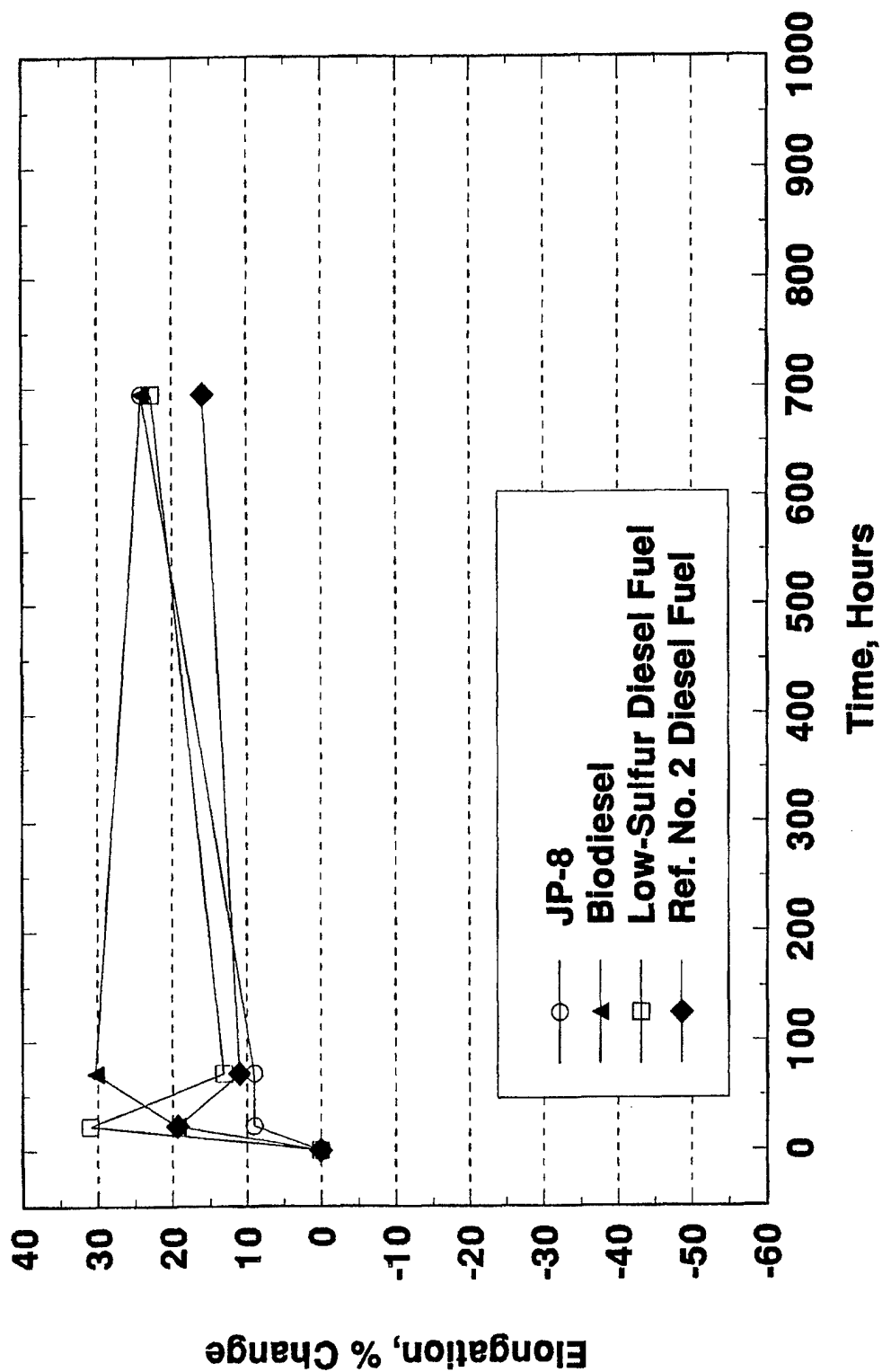
Elongation Viton GFLT



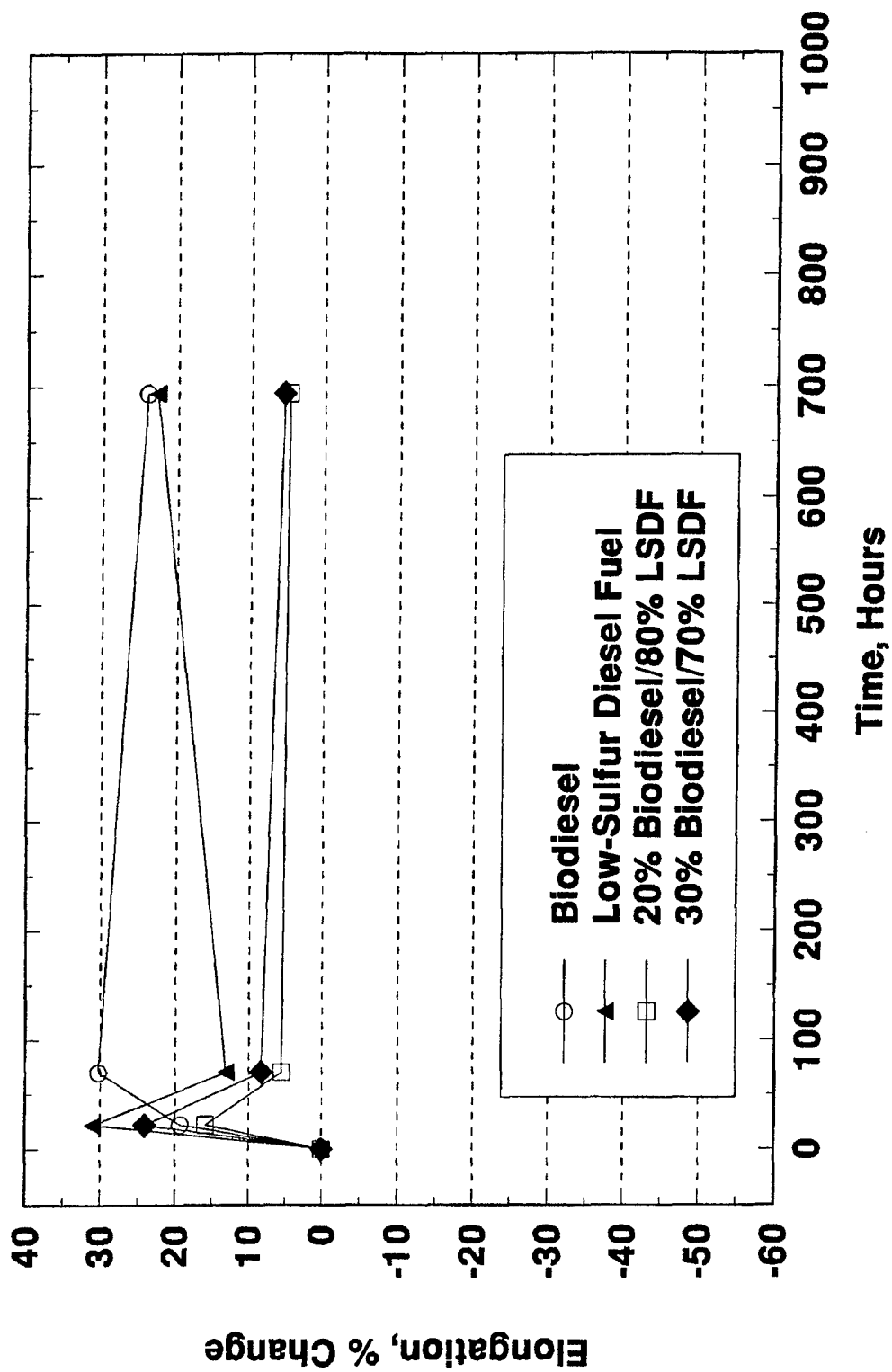
Elongation Viton GFLT



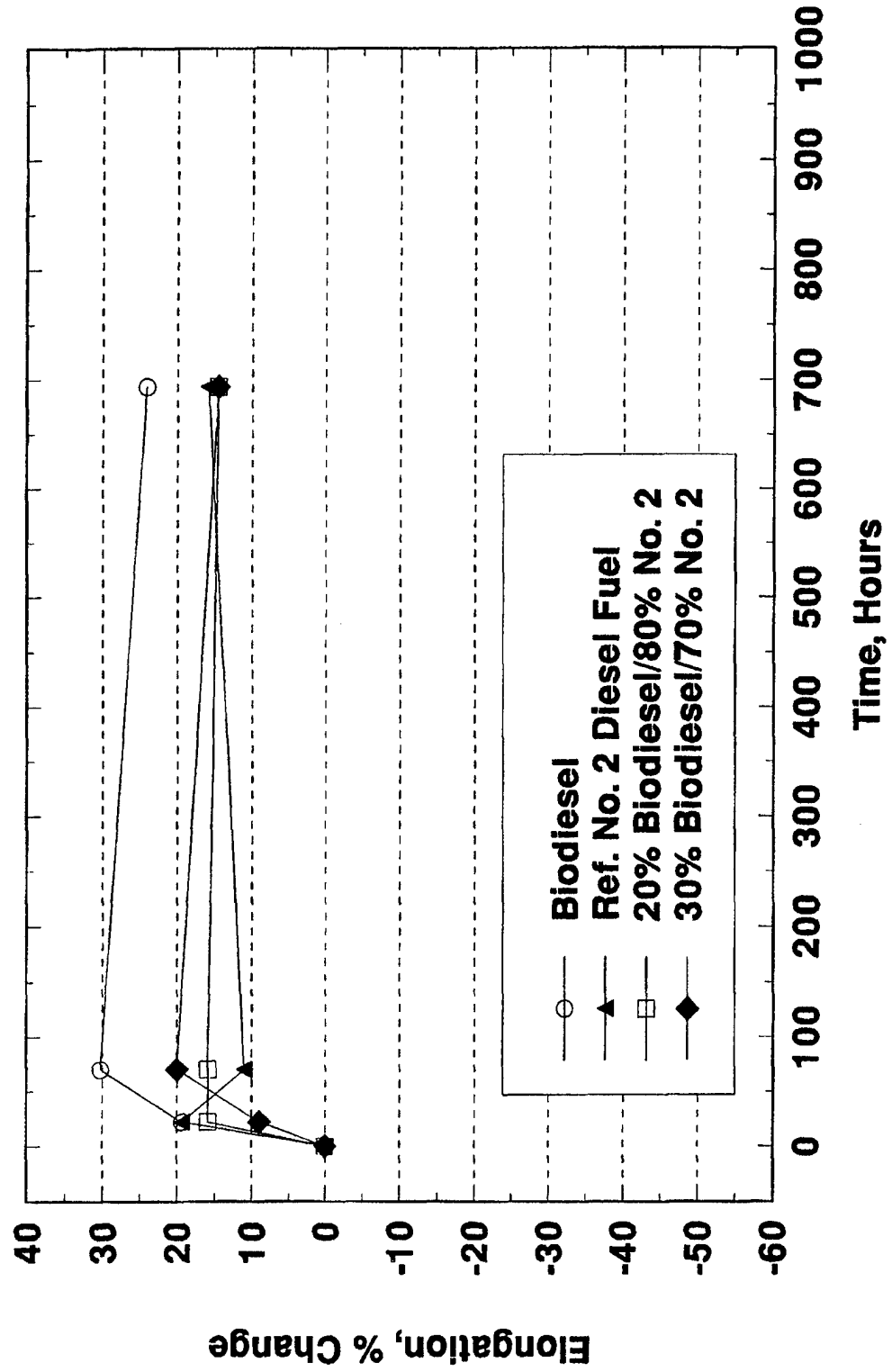
Elongation Fluorosilicon



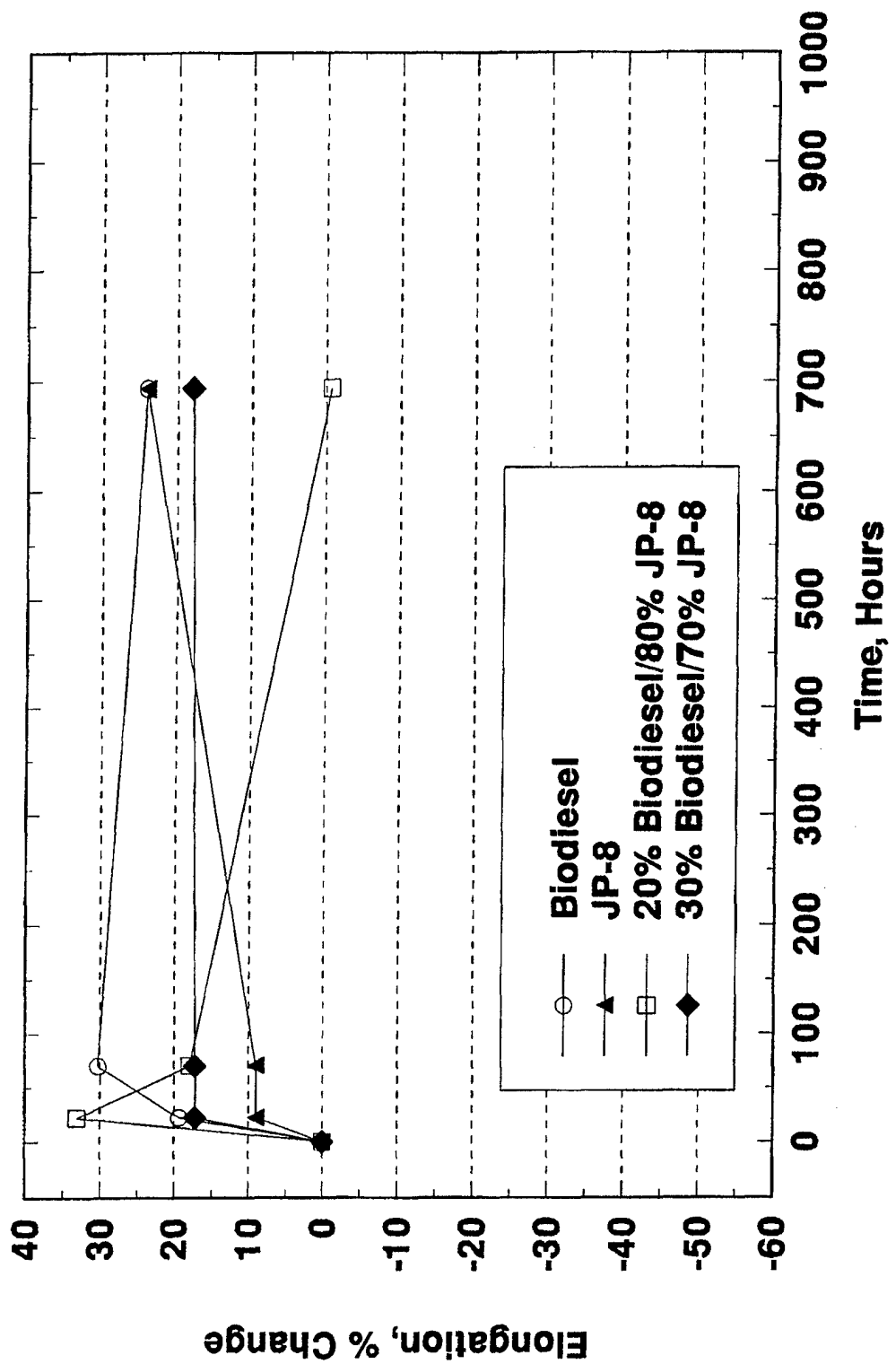
Elongation Fluorosilicon



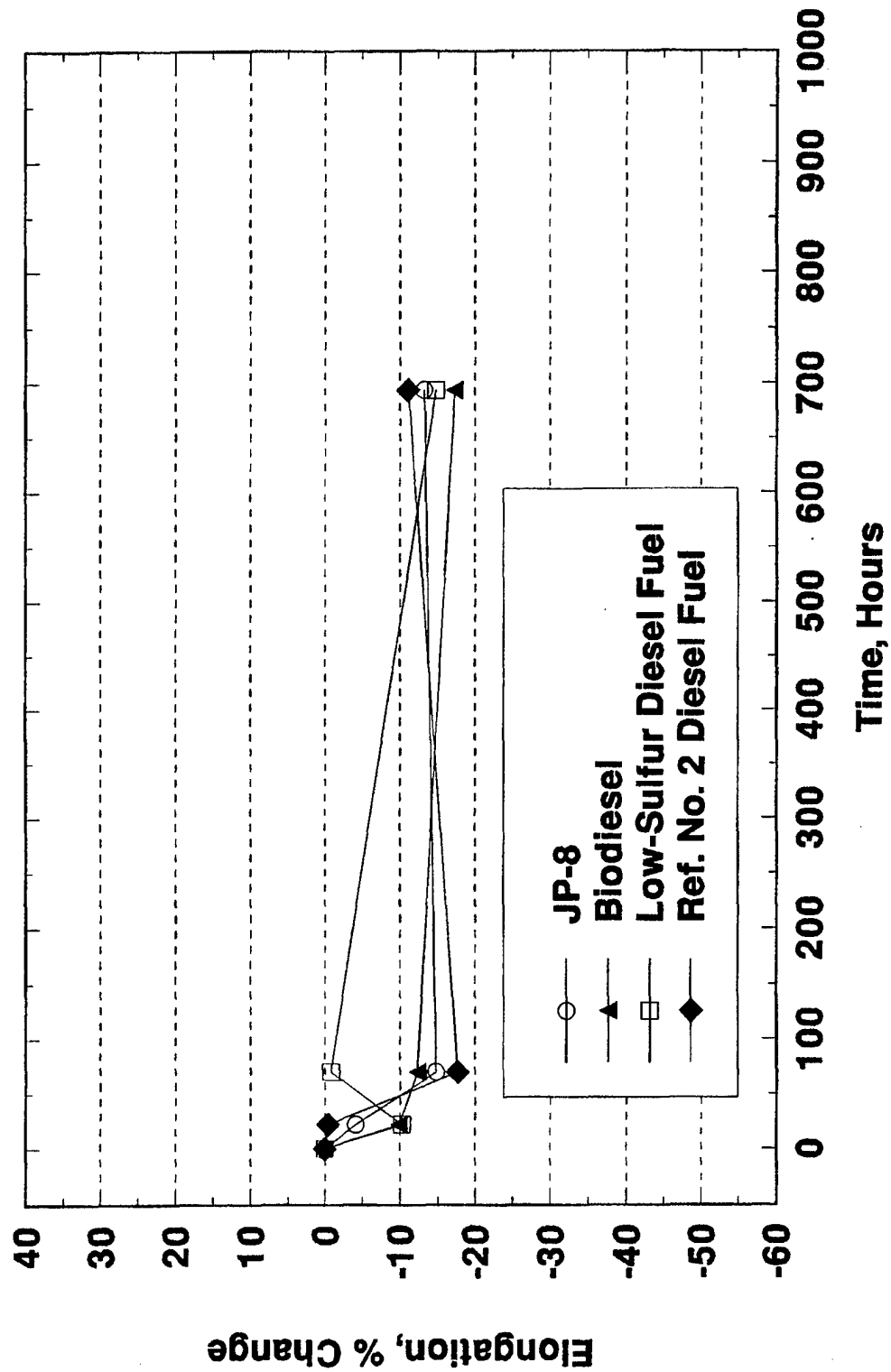
Elongation Fluorosilicon



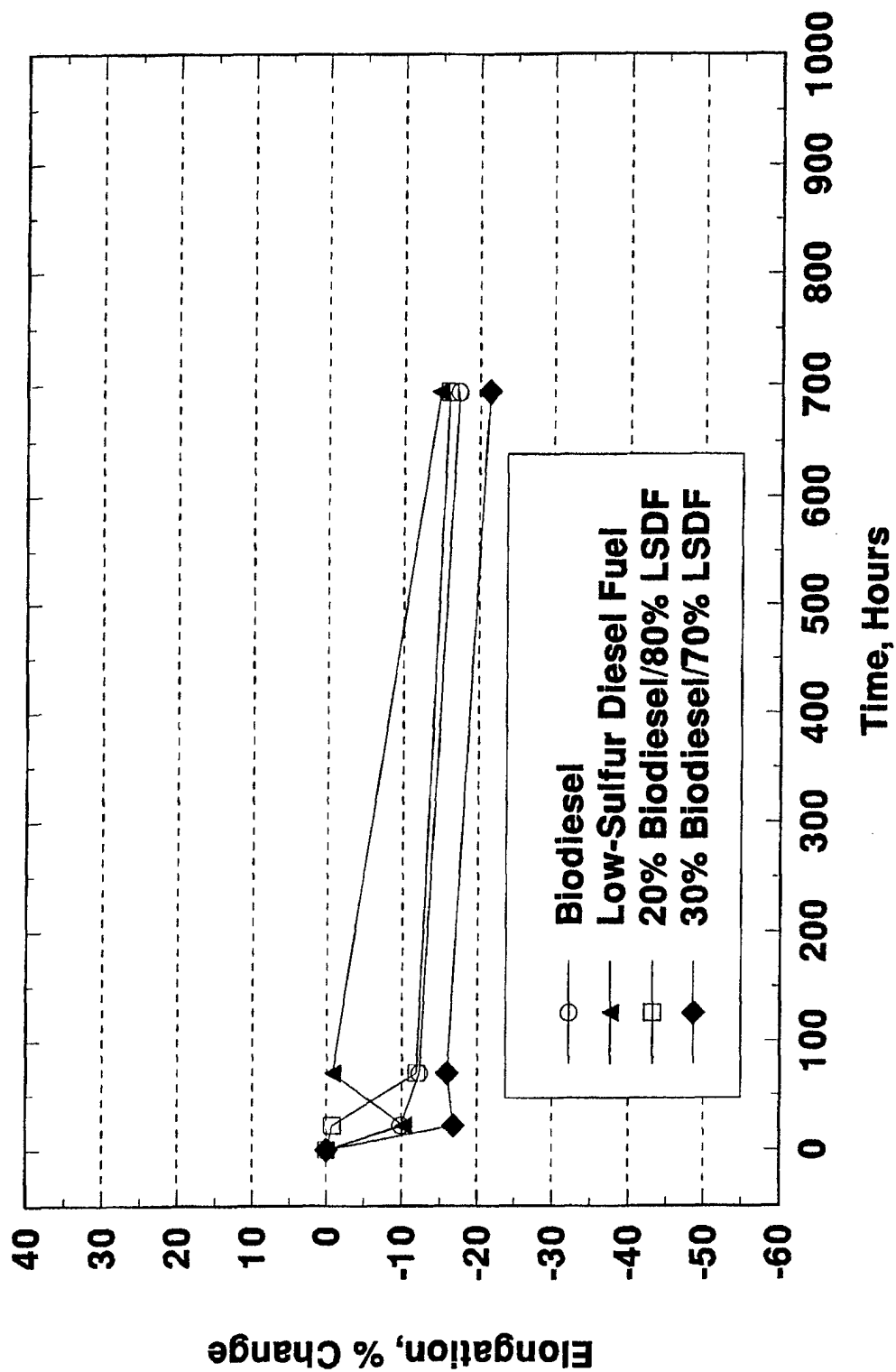
Elongation Fluorosilicon



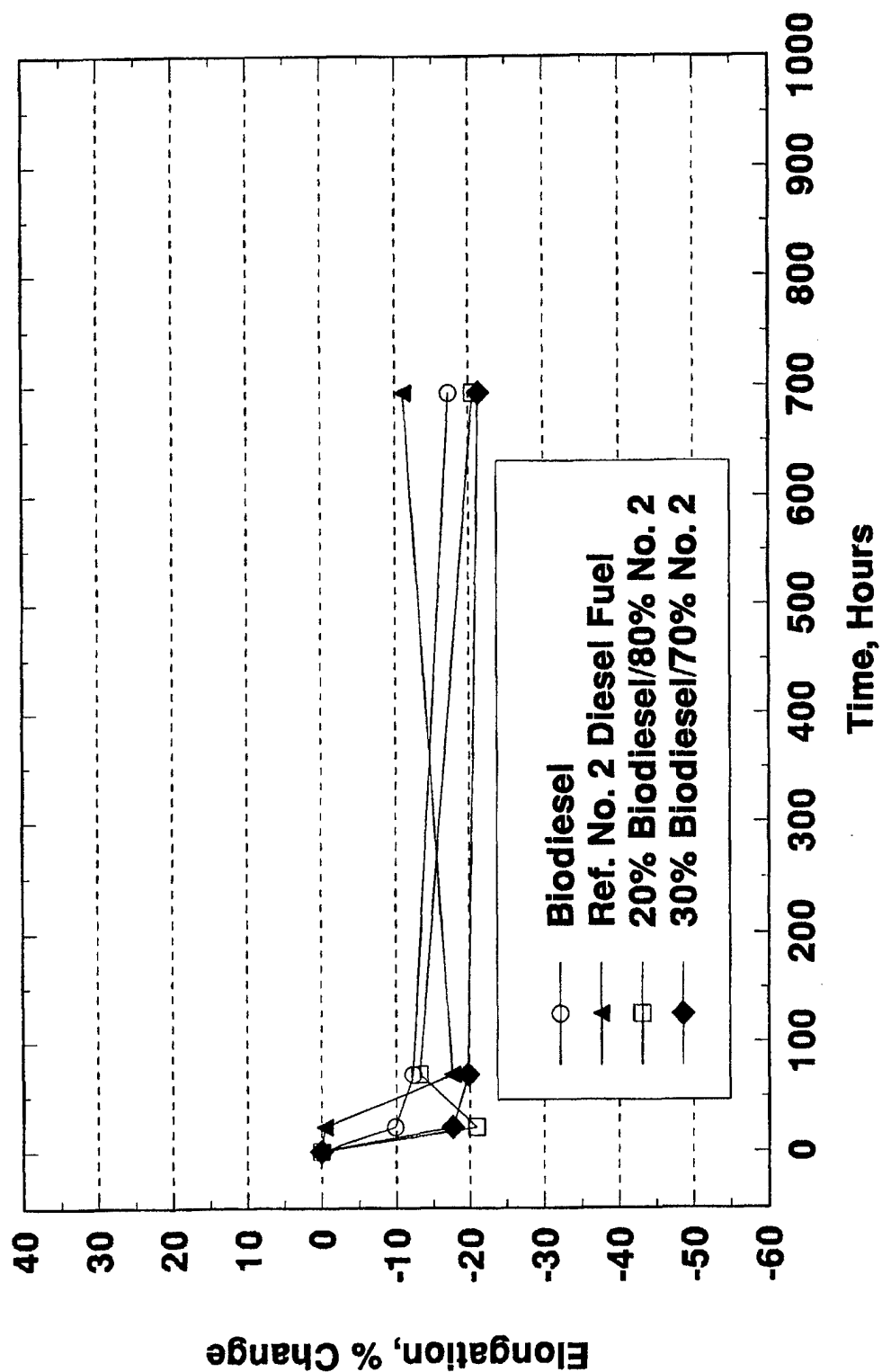
Elongation Polyurethane



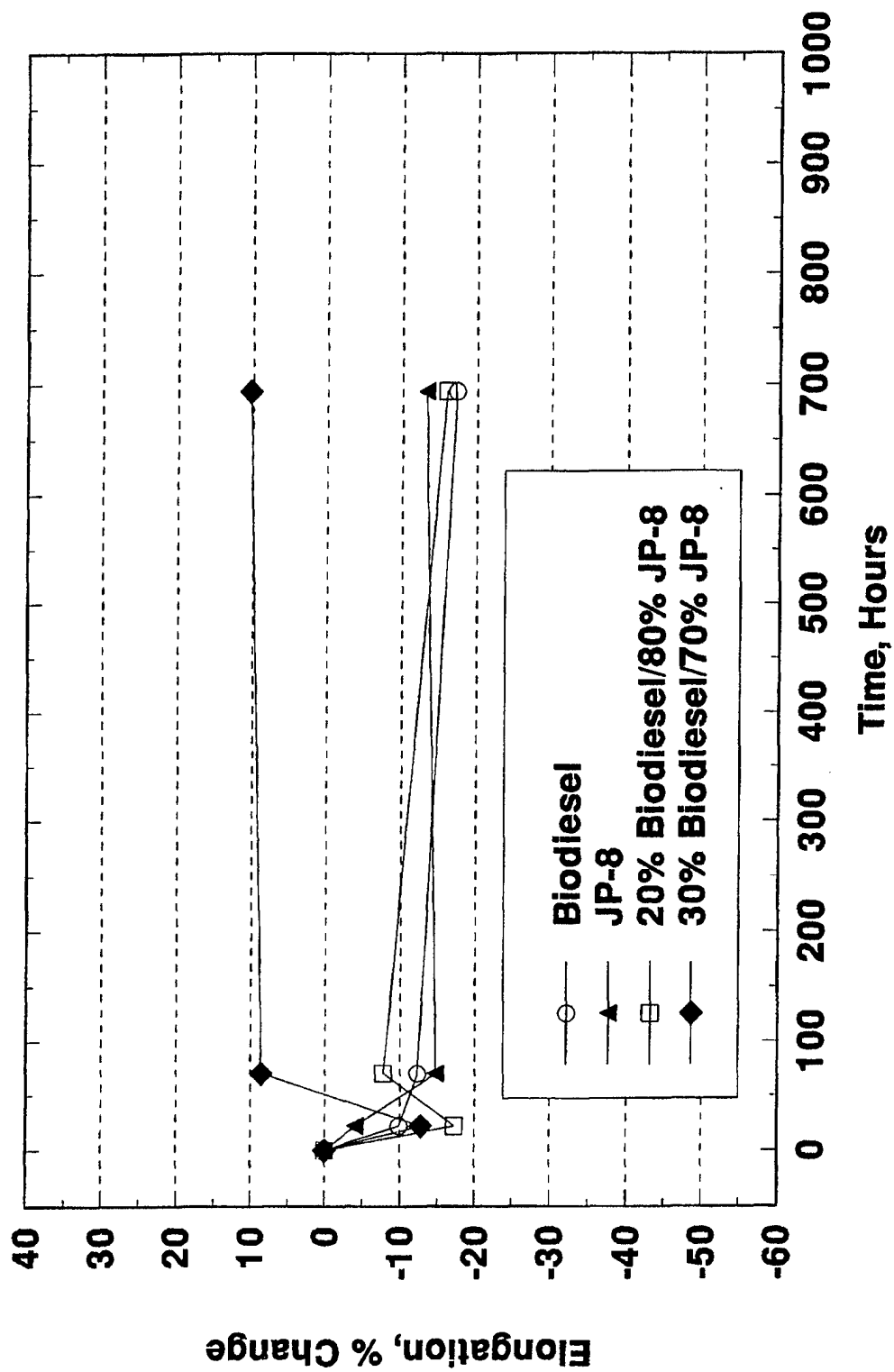
Elongation Polyurethane



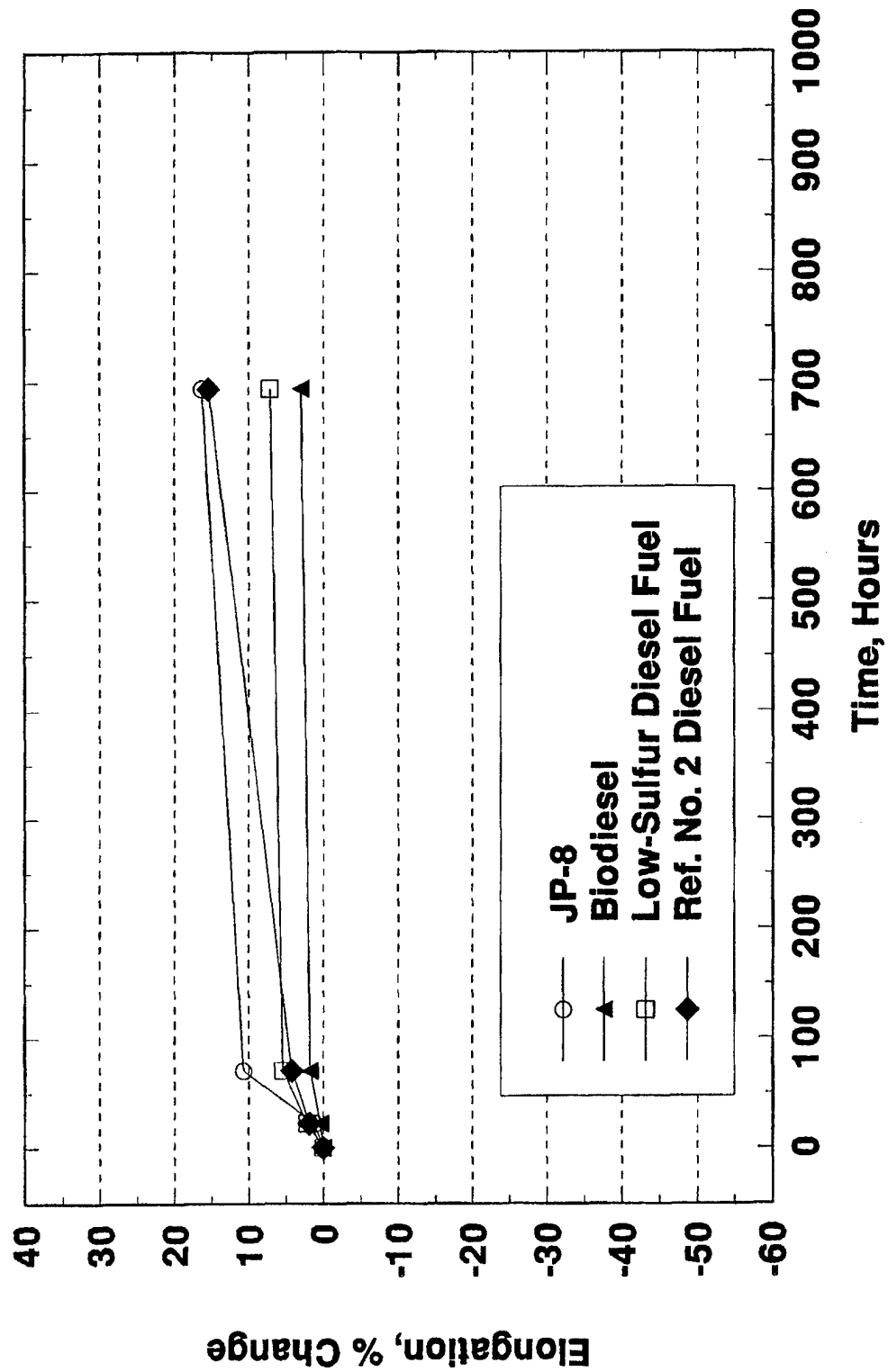
Elongation Polyurethane



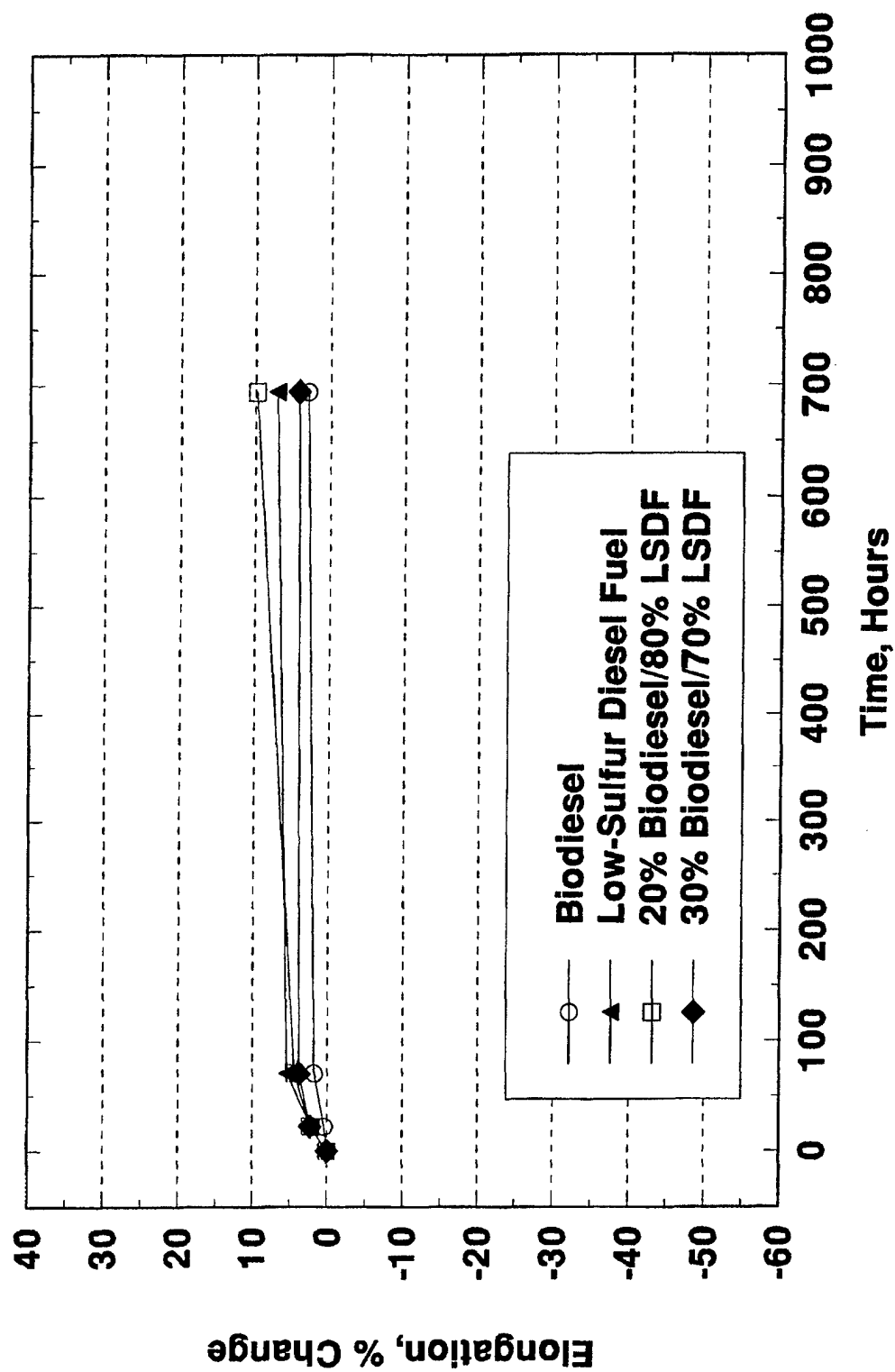
Elongation Polyurethane



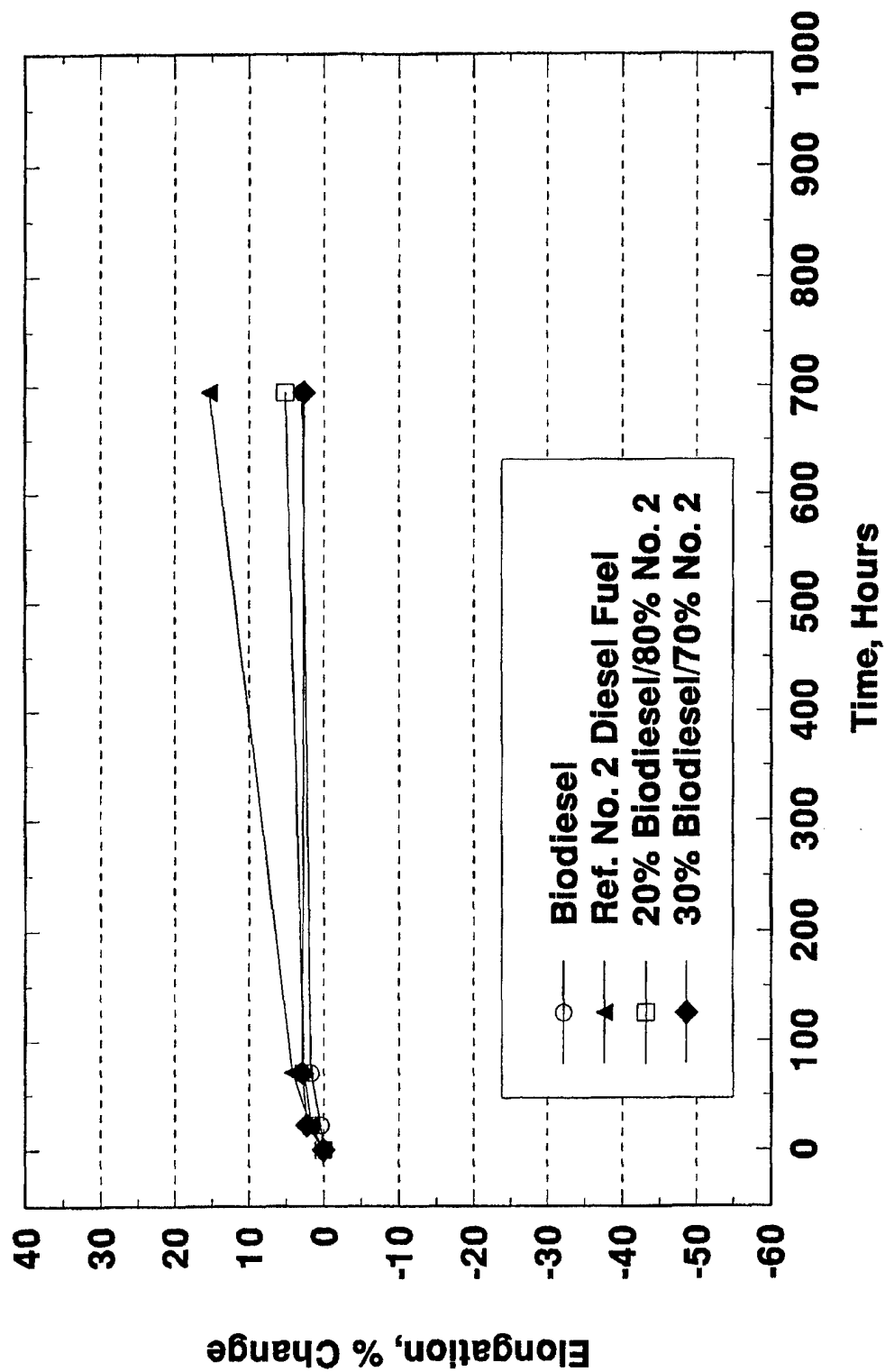
Elongation High Density Polypropylene



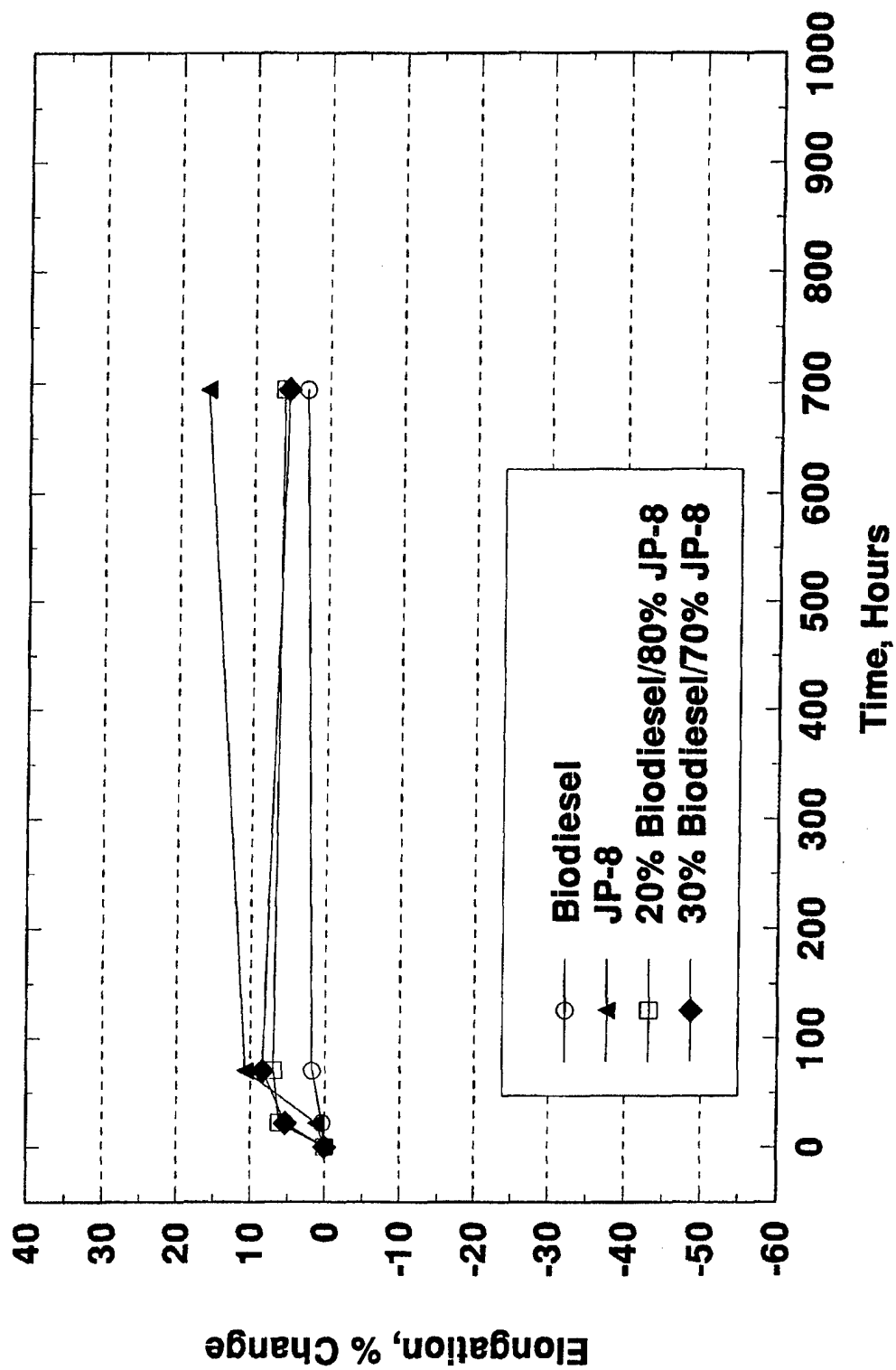
Elongation High Density Polypropylene



Elongation High Density Polypropylene



Elongation High Density Polypropylene



APPENDIX D

Shore A Hardness and Swell of Evaluated Materials

TABLE D-1. Shore A Hardness and Swell of Evaluated Materials

<u>Fuel/Time,</u> <u>hr</u>	<u>Material</u>	<u>Durometer</u>	<u>% Swell</u>
A/0	Teflon	59	0
A/22	Teflon	61	-0.17
A/70	Teflon	53	-0.18
A/694	Teflon	60	-0.77
B/0	Teflon	59	0
B/22	Teflon	60	-0.37
B/70	Teflon	56	0
B/694	Teflon	59	0
C/0	Teflon	59	0
C/22	Teflon	60	0
C/70	Teflon	56	-3.03
C/694	Teflon	60	0
D/0	Teflon	59	0
D/22	Teflon	59	1.48
D/70	Teflon	56	4.34
D/694	Teflon	55	-0.73
E/0	Teflon	59	0
E/22	Teflon	60	0.87
E/70	Teflon	56	-0.18
E/694	Teflon	60	0
F/0	Teflon	59	0
F/22	Teflon	57	-0.18
F/70	Teflon	59	0
F/694	Teflon	60	0.32
G/0	Teflon	59	0
G/22	Teflon	57	-0.82
G/70	Teflon	59	-0.18
G/694	Teflon	60	0
H/0	Teflon	59	0
H/22	Teflon	56	0.15
H/70	Teflon	58	0.81
H/694	Teflon	60	0.50
I/0	Teflon	59	0
I/22	Teflon	57	0.18
I/70	Teflon	58	-0.51
I/694	Teflon	60	0

TABLE D-1. Shore A Hardness and Swell of Evaluated Materials, cont'd

<u>Fuel/Time,</u> <u>hr</u>	<u>Material</u>	<u>Durometer</u>	<u>% Swell</u>
J/0	Teflon	59	0
J/22	Teflon	57	-0.53
J/70	Teflon		
J/694	Teflon		
A/0	Nylon 6/6	81	0
A/22	Nylon 6/6	84	1.04
A/70	Nylon 6/6	84	-0.17
A/694	Nylon 6/6	81	0
B/0	Nylon 6/6	81	0
B/22	Nylon 6/6	82	1.02
B/70	Nylon 6/6	82	-0.35
B/694	Nylon 6/6	84	0
C/0	Nylon 6/6	81	0
C/22	Nylon 6/6	80	0.51
C/70	Nylon 6/6	81	1.56
C/694	Nylon 6/6	82	0
D/0	Nylon 6/6	81	0
D/22	Nylon 6/6	81	0.51
D/70	Nylon 6/6	81	0.34
D/694	Nylon 6/6	83	0
E/0	Nylon 6/6	81	0
E/22	Nylon 6/6	84	0.69
E/70	Nylon 6/6	81	0
E/694	Nylon 6/6	84	0.17
F/0	Nylon 6/6	81	0
F/22	Nylon 6/6	83	-1.03
F/70	Nylon 6/6	83	-1.02
F/694	Nylon 6/6	84	-0.85
G/0	Nylon 6/6	81	0
G/22	Nylon 6/6	83	-0.51
G/70	Nylon 6/6	80	-0.51
G/694	Nylon 6/6	80	-1.19
H/0	Nylon 6/6	81	0
H/22	Nylon 6/6	82	-0.52
H/70	Nylon 6/6	83	-0.34
H/694	Nylon 6/6	83	-0.84

TABLE D-1. Shore A Hardness and Swell of Evaluated Materials, cont'd

<u>Fuel/Time,</u> <u>hr</u>	<u>Material</u>	<u>Durometer</u>	<u>% Swell</u>
I/0	Nylon 6/6	81	0
I/22	Nylon 6/6	82	0.17
I/70	Nylon 6/6	83	-1.03
I/694	Nylon 6/6	83	-0.33
J/0	Nylon 6/6	81	0
J/22	Nylon 6/6	82	0
J/70	Nylon 6/6	78	-0.87
J/694	Nylon 6/6	83	-0.33
A/0	Nitrile	52	0
A/22	Nitrile	47	9.80
A/70	Nitrile	46	12.97
A/694	Nitrile	45	14.13
B/0	Nitrile	52	0
B/22	Nitrile	43	14.77
B/70	Nitrile	39	18.67
B/694	Nitrile	39	18.64
C/0	Nitrile	52	0
C/22	Nitrile	43	11.79
C/70	Nitrile	42	16.84
C/694	Nitrile	43	17.20
D/0	Nitrile	52	0
D/22	Nitrile	43	11.94
D/70	Nitrile	43	15.56
D/694	Nitrile	42	17.20
E/0	Nitrile	52	0
E/22	Nitrile	42	12.79
E/70	Nitrile	41	16.70
E/694	Nitrile	42	17.64
F/0	Nitrile	52	0
F/22	Nitrile	45	12.23
F/70	Nitrile	43	17.94
F/694	Nitrile	42	19.50
G/0	Nitrile	52	0
G/22	Nitrile	46	11.95
G/70	Nitrile	42	19.19
G/694	Nitrile	41	19.26

TABLE D-1. Shore A Hardness and Swell of Evaluated Materials, cont'd

<u>Fuel/Time,</u> <u>hr</u>	<u>Material</u>	<u>Durometer</u>	<u>% Swell</u>
H/0	Nitrile	52	0
H/22	Nitrile	45	12.15
H/70	Nitrile	42	17.92
H/694	Nitrile	41	19.13
I/0	Nitrile	52	0
I/22	Nitrile	46	13.98
I/70	Nitrile	44	15.28
I/694	Nitrile	44	15.68
J/0	Nitrile	52	0
J/22	Nitrile	45	12.08
J/70	Nitrile	44	16.32
J/694	Nitrile	44	17.12
A/0	Viton A401-C	79	0
A/22	Viton A401-C	77	0.29
A/70	Viton A401-C	78	0.85
A/694	Viton A401-C	77	0.97
B/0	Viton A401-C	79	0
B/22	Viton A401-C	78	1.03
B/70	Viton A401-C	77	-0.54
B/694	Viton A401-C	77	1.27
C/0	Viton A401-C	79	0
C/22	Viton A401-C	78	-0.55
C/70	Viton A401-C	78	-0.81
C/694	Viton A401-C	77	0.55
D/0	Viton A401-C	79	0
D/22	Viton A401-C	77	-0.13
D/70	Viton A401-C	78	0
D/694	Viton A401-C	78	2.5
E/0	Viton A401-C	79	0
E/22	Viton A401-C	76	-0.60
E/70	Viton A401-C	78	0.42
E/694	Viton A401-C	77	-0.12
F/0	Viton A401-C	79	0
F/22	Viton A401-C	78	-0.42
F/70	Viton A401-C	78	0.28
F/694	Viton A401-C	77	0.80

TABLE D-1. Shore A Hardness and Swell of Evaluated Materials, cont'd

<u>Fuel/Time,</u> <u>hr</u>	<u>Material</u>	<u>Durometer</u>	<u>% Swell</u>
G/0	Viton A401-C	79	0
G/22	Viton A401-C	78	-2.55
G/70	Viton A401-C	79	0.27
G/694	Viton A401-C	78	1.94
H/0	Viton A401-C	79	0
H/22	Viton A401-C	78	-0.69
H/70	Viton A401-C	79	1.10
H/694	Viton A401-C	78	1.10
I/0	Viton A401-C	79	0
I/22	Viton A401-C	77	0.86
I/70	Viton A401-C	77	0.83
I/694	Viton A401-C	76	1.86
J/0	Viton A401-C	79	0
J/22	Viton A401-C	77	0.72
J/70	Viton A401-C	78	0.71
J/694	Viton A401-C	77	1.37
A/0	Viton GFLT	77	0
A/22	Viton GFLT	75	1.30
A/70	Viton GFLT	75	0.16
A/694	Viton GFLT	74	1.84
B/0	Viton GFLT	77	0
B/22	Viton GFLT	76	-3.12
B/70	Viton GFLT	76	0.14
B/694	Viton GFLT	76	1.49
C/0	Viton GFLT	77	0
C/22	Viton GFLT	77	0.42
C/70	Viton GFLT	74	0
C/694	Viton GFLT	75	0.02
D/0	Viton GFLT	77	0
D/22	Viton GFLT	75	-0.68
D/70	Viton GFLT	75	-0.41
D/694	Viton GFLT	75	0.27
E/0	Viton GFLT	77	0
E/22	Viton GFLT	75	-0.54
E/70	Viton GFLT	76	1.60
E/694	Viton GFLT	76	1.13

TABLE D-1. Shore A Hardness and Swell of Evaluated Materials, cont'd

<u>Fuel/Time,</u> <u>hr</u>	<u>Material</u>	<u>Durometer</u>	<u>% Swell</u>
F/0	Viton GFLT	77	0
F/22	Viton GFLT	73	0.39
F/70	Viton GFLT	75	-0.13
F/694	Viton GFLT	75	-0.51
G/0	Viton GFLT	77	0
G/22	Viton GFLT	73	0.15
G/70	Viton GFLT	75	-0.56
G/694	Viton GFLT	75	1.08
H/0	Viton GFLT	77	0
H/22	Viton GFLT	74	-0.92
H/70	Viton GFLT	75	0
H/694	Viton GFLT	75	0.31
I/0	Viton GFLT	75	0
I/22	Viton GFLT	77	0.80
I/70	Viton GFLT	73	0.41
I/694	Viton GFLT	76	1.87
J/0	Viton GFLT	77	0
J/22	Viton GFLT	75	-0.26
J/70	Viton GFLT	76	-0.39
J/694	Viton GFLT	75	2.08
A/0	Fluorosilicon	67	0
A/22	Fluorosilicon	62	8.36
A/70	Fluorosilicon	62	9.96
A/694	Fluorosilicon	63	9.08
B/0	Fluorosilicon	67	0
B/22	Fluorosilicon	64	2.64
B/70	Fluorosilicon	62	4.81
B/694	Fluorosilicon	63	4.39
C/0	Fluorosilicon	67	0
C/22	Fluorosilicon	63	6.15
C/70	Fluorosilicon	64	6.40
C/694	Fluorosilicon	64	8.30
D/0	Fluorosilicon	67	0
D/22	Fluorosilicon	63	4.63
D/70	Fluorosilicon	65	5.34
D/694	Fluorosilicon	65	5.80

TABLE D-1. Shore A Hardness and Swell of Evaluated Materials, cont'd

<u>Fuel/Time,</u> <u>hr</u>	<u>Material</u>	<u>Durometer</u>	<u>% Swell</u>
E/0	Fluorosilicon	67	0
E/22	Fluorosilicon	63	4.22
E/70	Fluorosilicon	63	6.44
E/694	Fluorosilicon	65	6.91
F/0	Fluorosilicon	67	0
F/22	Fluorosilicon	64	5.13
F/70	Fluorosilicon	64	5.18
F/694	Fluorosilicon	64	6.27
G/0	Fluorosilicon	67	0
G/22	Fluorosilicon	63	5.47
G/70	Fluorosilicon	64	5.82
G/694	Fluorosilicon	65	6.81
H/0	Fluorosilicon	67	0
H/22	Fluorosilicon	63	4.98
H/70	Fluorosilicon	62	6.66
H/694	Fluorosilicon	64	4.93
I/0	Fluorosilicon	67	0
I/22	Fluorosilicon	62	7.15
I/70	Fluorosilicon	62	7.65
I/694	Fluorosilicon	63	7.69
J/0	Fluorosilicon	67	0
J/22	Fluorosilicon	62	7.45
J/70	Fluorosilicon	62	7.92
J/694	Fluorosilicon	63	7.86
A/0	Polyurethane	75	0
A/22	Polyurethane	72	2.19
A/70	Polyurethane	71	4.70
A/694	Polyurethane	72	5.76
B/0	Polyurethane	75	0
B/22	Polyurethane	74	1.31
B/70	Polyurethane	74	2.99
B/694	Polyurethane	72	4.35
C/0	Polyurethane	75	0
C/22	Polyurethane	73	2.54
C/70	Polyurethane	73	4.42
C/694	Polyurethane	72	6.50

TABLE D-1. Shore A Hardness and Swell of Evaluated Materials, cont'd

<u>Fuel/Time,</u> <u>hr</u>	<u>Material</u>	<u>Durometer</u>	<u>% Swell</u>
D/0	Polyurethane	75	0
D/22	Polyurethane	74	2.17
D/70	Polyurethane	73	3.09
D/694	Polyurethane	72	5.84
E/0	Polyurethane	75	0
E/22	Polyurethane	73	2.42
E/70	Polyurethane	73	4.47
E/694	Polyurethane	72	7.47
F/0	Polyurethane	75	0
F/22	Polyurethane	73	1.94
F/70	Polyurethane	73	3.16
F/694	Polyurethane	73	7.41
G/0	Polyurethane	75	0
G/22	Polyurethane	74	2.64
G/70	Polyurethane	73	2.46
G/694	Polyurethane	71	5.65
H/0	Polyurethane	75	0
H/22	Polyurethane	73	1.23
H/70	Polyurethane	72	2.99
H/694	Polyurethane	72	7.21
I/0	Polyurethane	75	0
I/22	Polyurethane	73	1.23
I/70	Polyurethane	73	4.25
I/694	Polyurethane	72	6.06
J/0	Polyurethane	75	0
J/22	Polyurethane	73	1.59
J/70	Polyurethane	72	4.43
J/694	Polyurethane	72	6.04
A/0	Polypropylene	78	0
A/22	Polypropylene	66	13.59
A/70	Polypropylene	65	15.91
A/694	Polypropylene	65	15.09
B/0	Polypropylene	78	0
B/22	Polypropylene	75	2.24
B/70	Polypropylene	73	5.56
B/694	Polypropylene	72	8.02

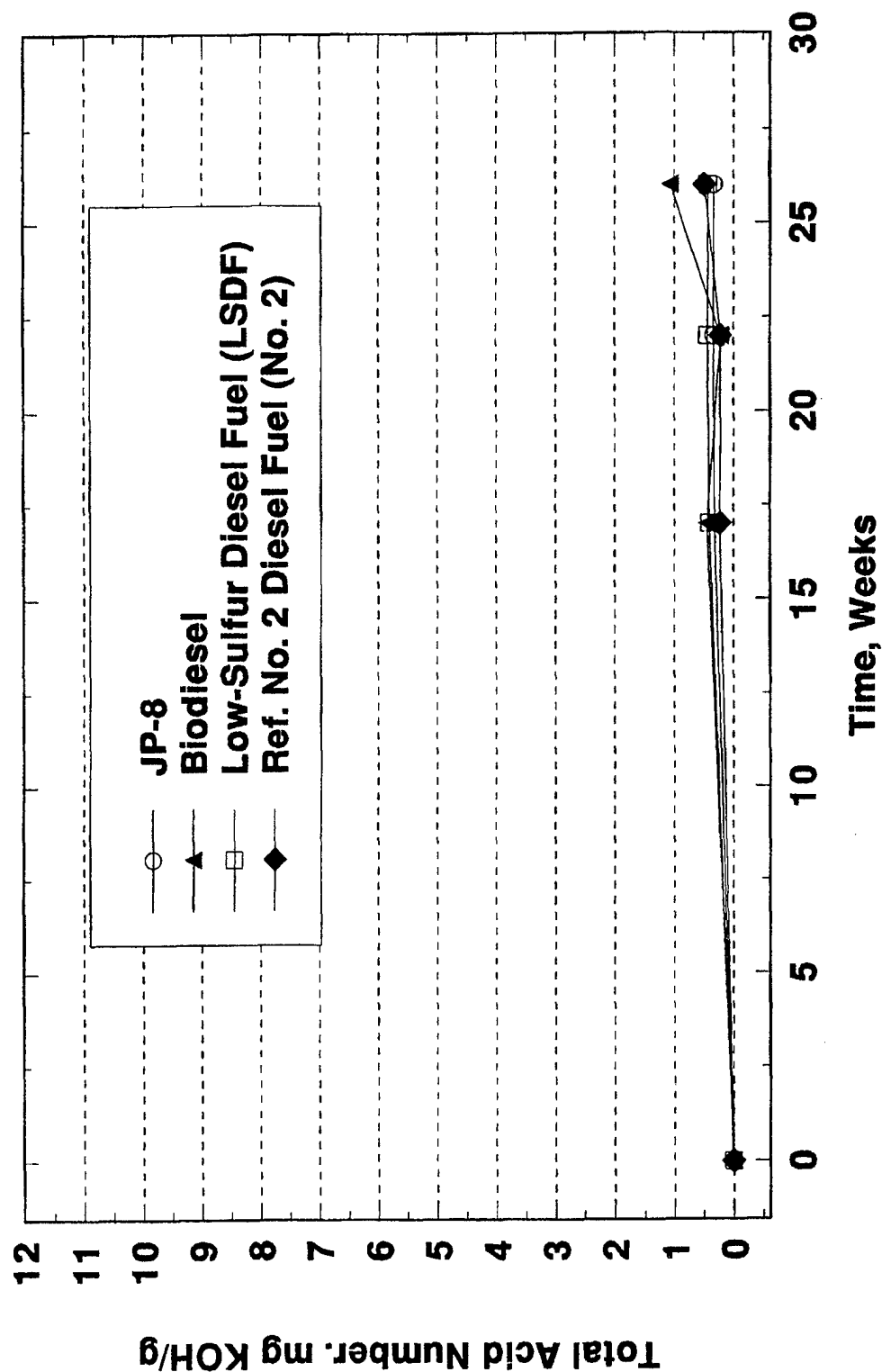
TABLE D-1. Shore A Hardness and Swell of Evaluated Materials, cont'd

<u>Fuel/Time,</u> <u>hr</u>	<u>Material</u>	<u>Durometer</u>	<u>% Swell</u>
C/0	Polypropylene	78	0
C/22	Polypropylene	73	5.97
C/70	Polypropylene	69	12.84
C/694	Polypropylene	67	12.39
D/0	Polypropylene	78	0
D/22	Polypropylene	74	4.10
D/70	Polypropylene	70	11.26
D/694	Polypropylene	68	13.82
E/0	Polypropylene	78	0
E/22	Polypropylene	73	3.48
E/70	Polypropylene	70	12.05
E/694	Polypropylene	68	10.87
F/0	Polypropylene	78	0
F/22	Polypropylene	75	4.29
F/70	Polypropylene	70	10.11
F/694	Polypropylene	70	8.18
G/0	Polypropylene	78	0
G/22	Polypropylene	75	3.33
G/70	Polypropylene	72	9.42
G/694	Polypropylene	69	11.53
H/0	Polypropylene	78	0
H/22	Polypropylene	75	3.68
H/70	Polypropylene	70	7.64
H/694	Polypropylene	68	8.82
I/0	Polypropylene	78	0
I/22	Polypropylene	70	11.93
I/70	Polypropylene	68	12.28
I/694	Polypropylene	67	10.56
J/0	Polypropylene	78	0
J/22	Polypropylene	71	7.72
J/70	Polypropylene	68	10.41
J/694	Polypropylene	64	10.50

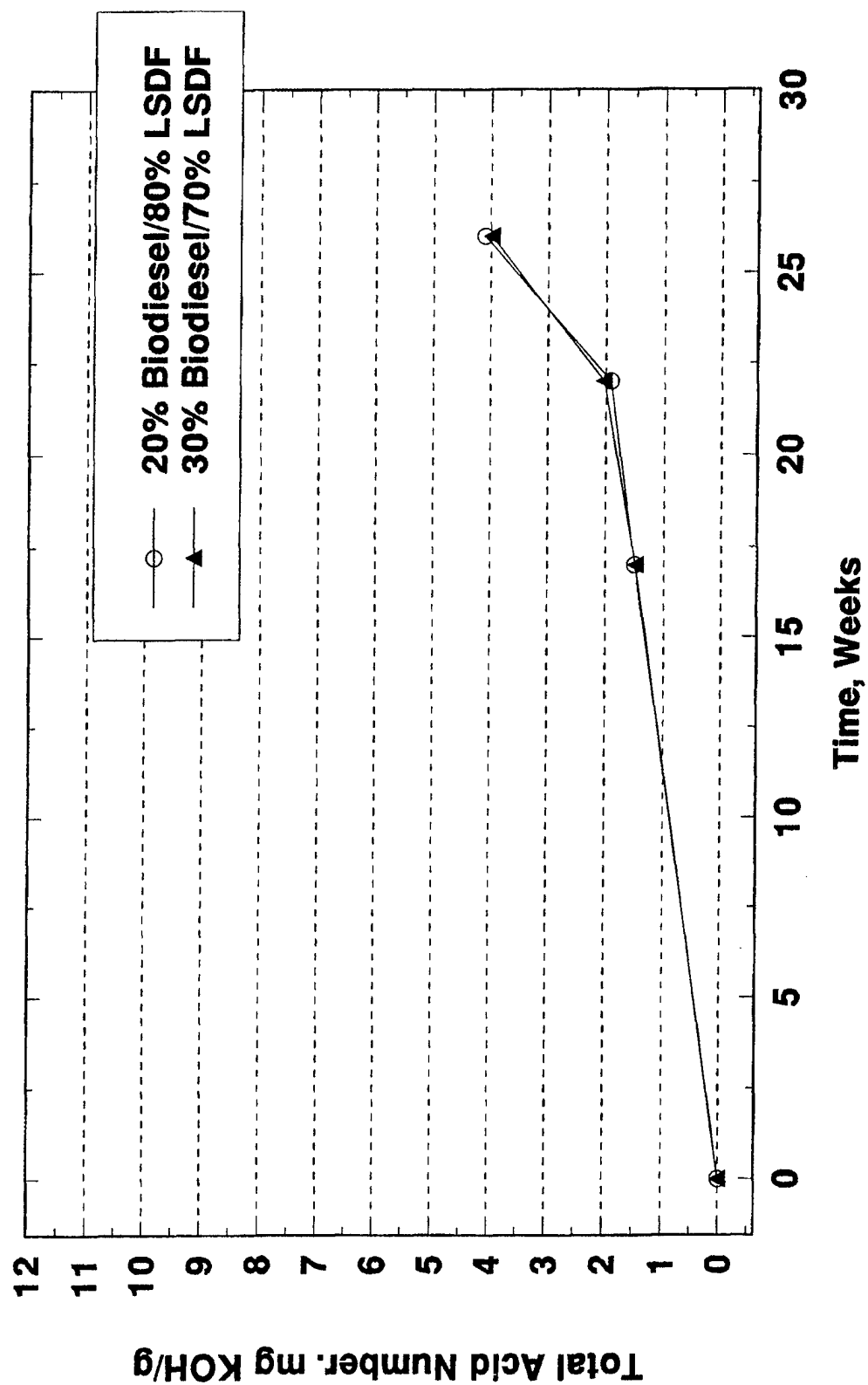
APPENDIX E
Total Acid Number (TAN)

Preceding Page Blank

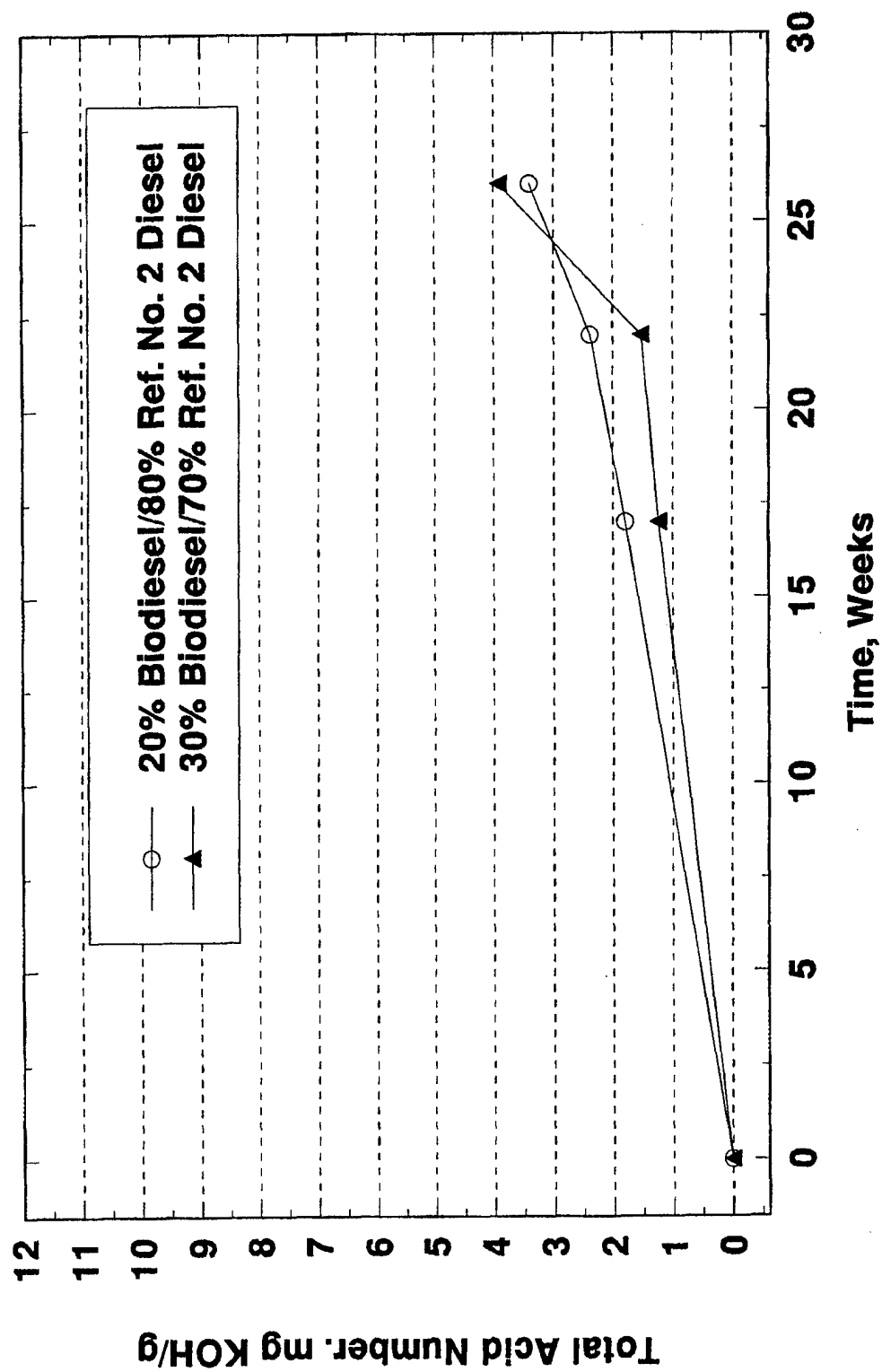
Total Acid Number (TAN) Copper



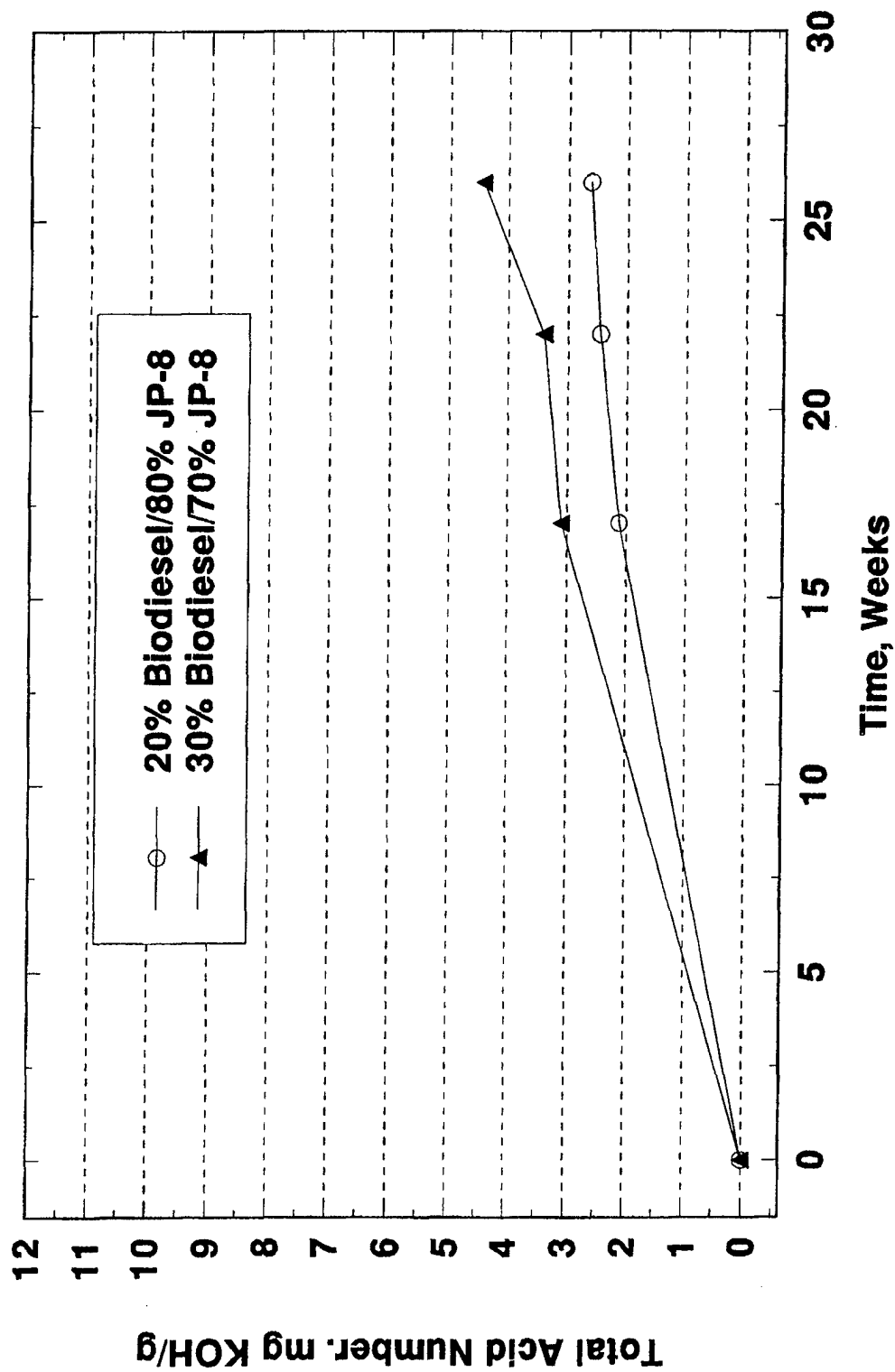
Total Acid Number (TAN) Copper



Total Acid Number (TAN) Copper

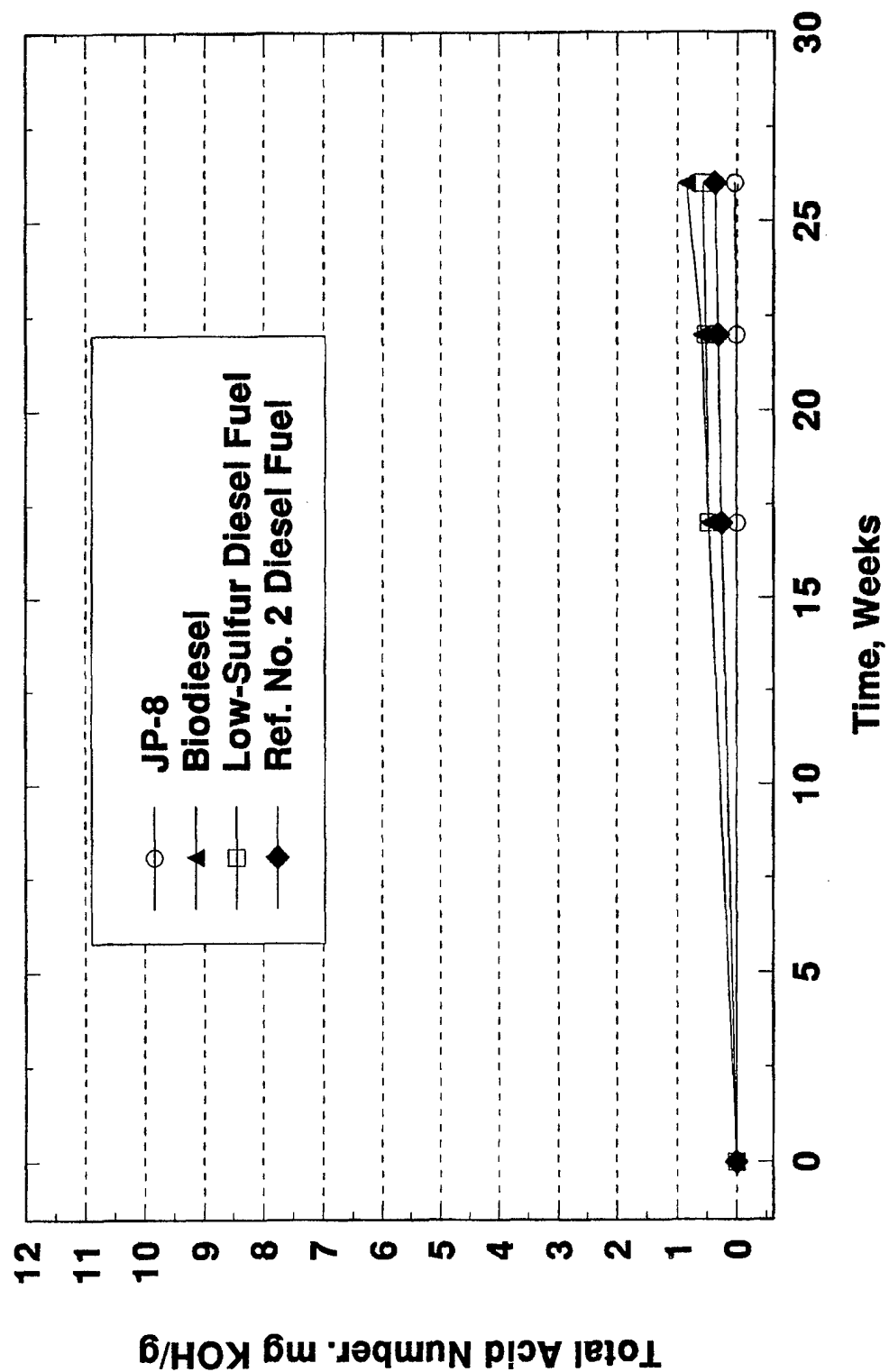


Total Acid Number (TAN) Copper

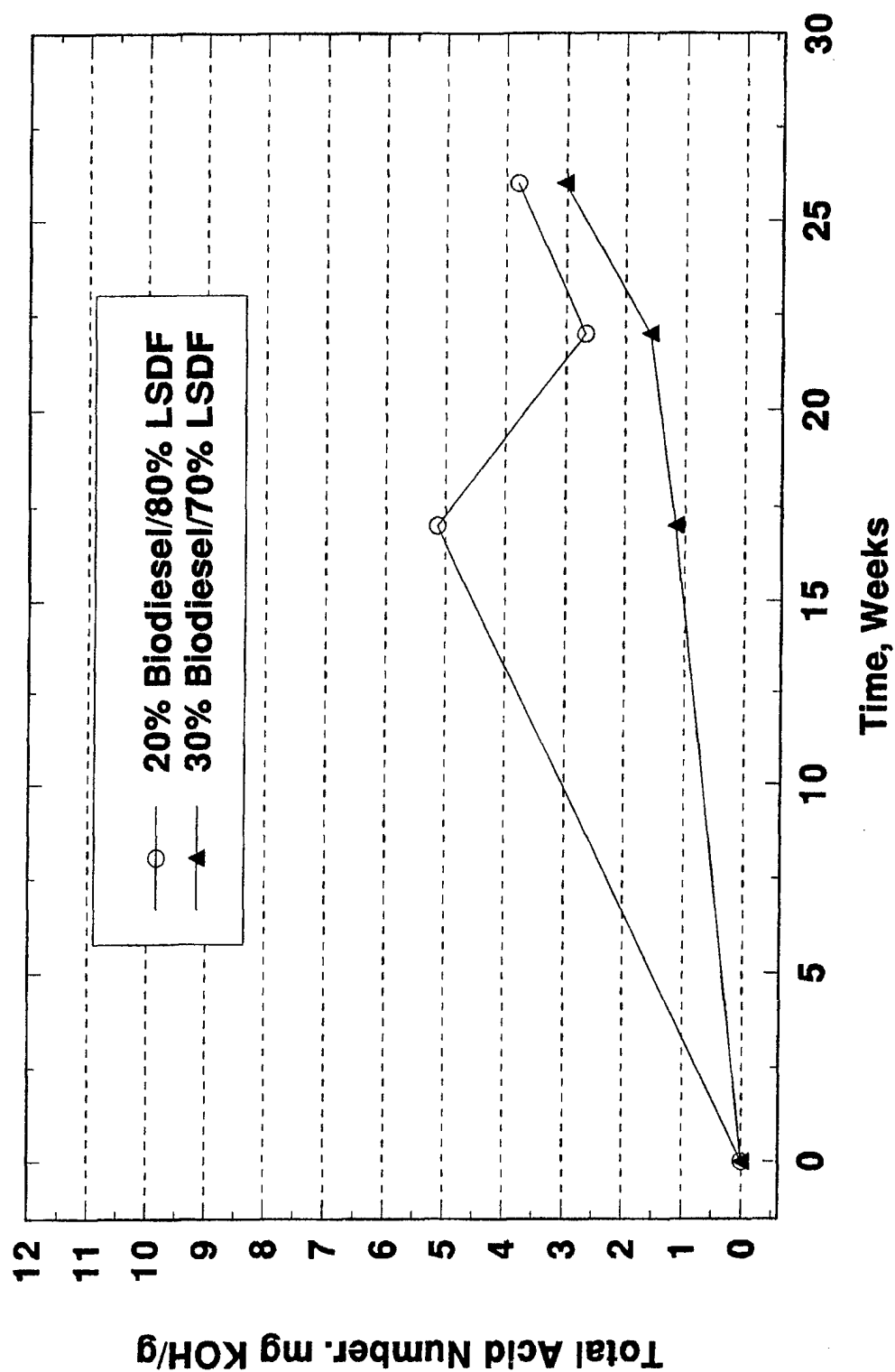


Total Acid Number (TAN)

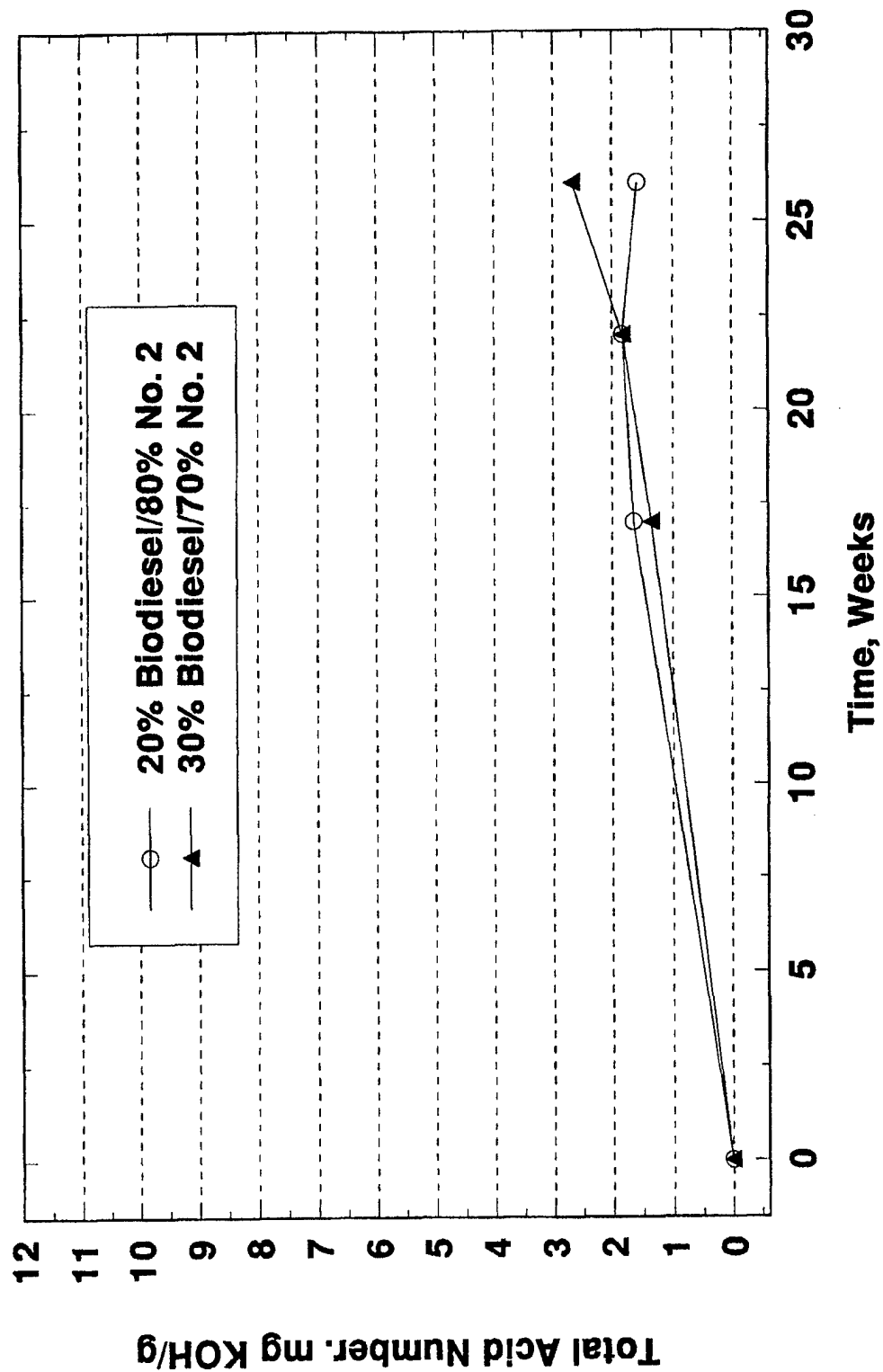
Brass



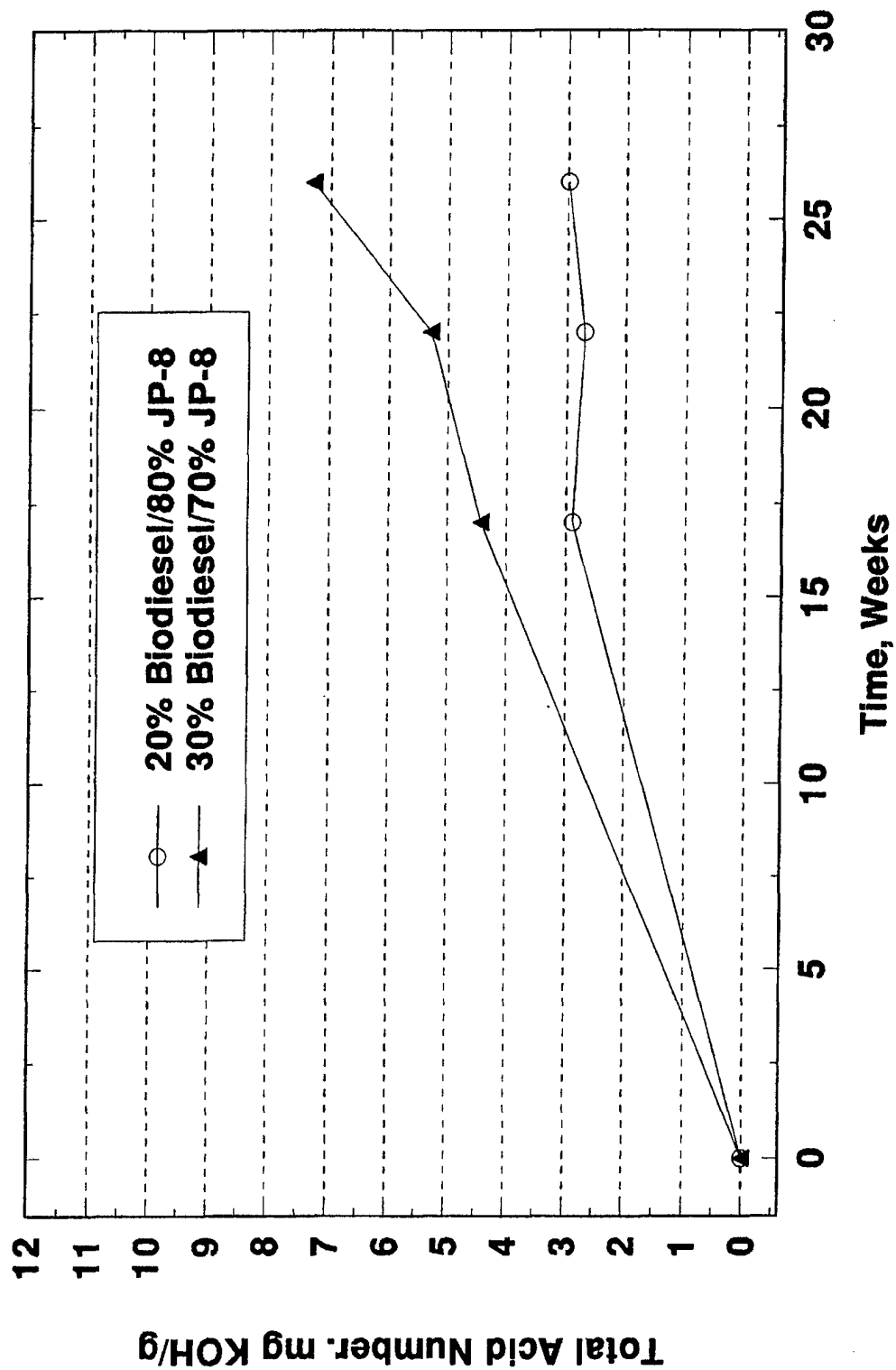
Total Acid Number (TAN) Brass



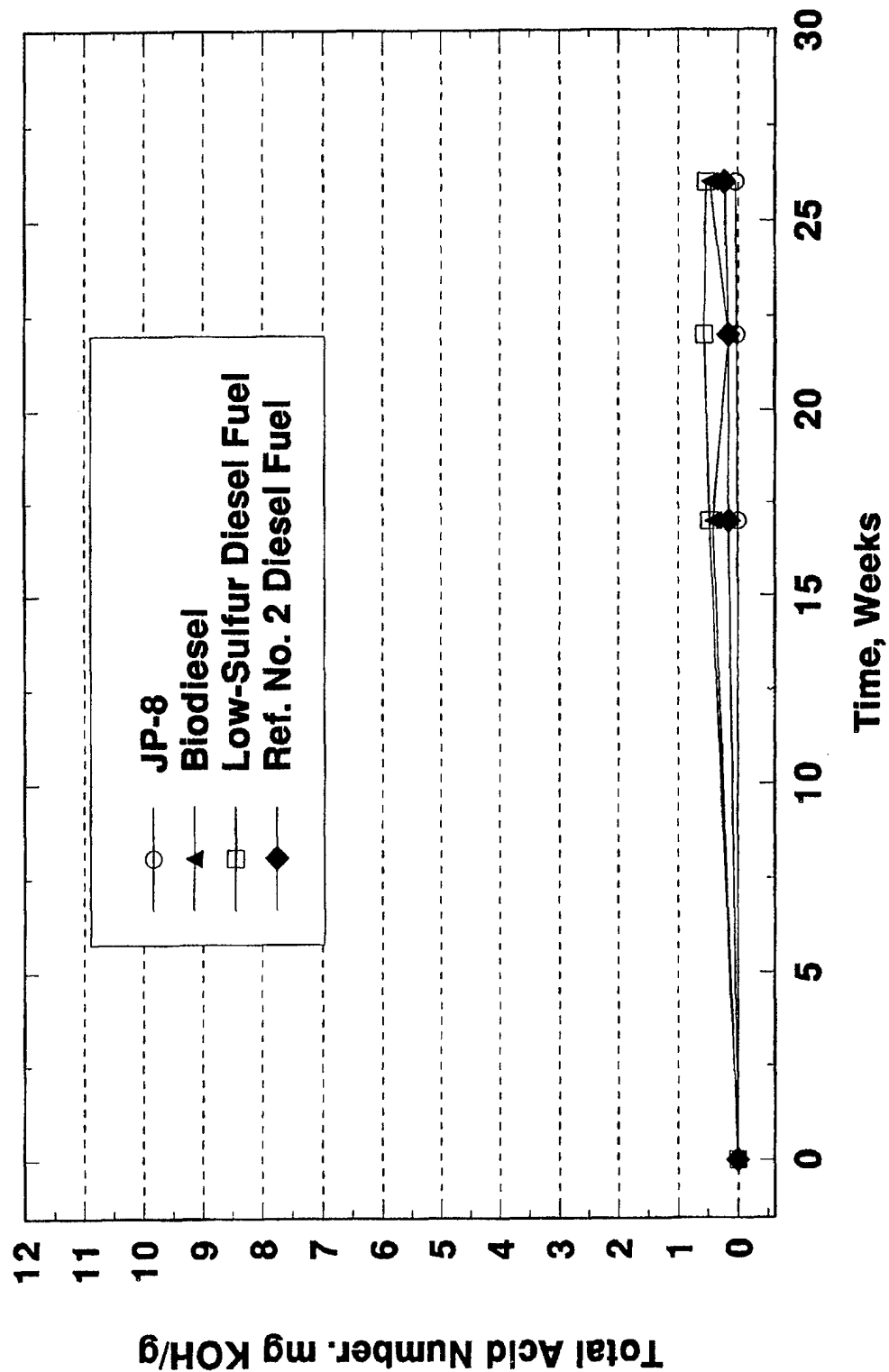
Total Acid Number (TAN) Brass



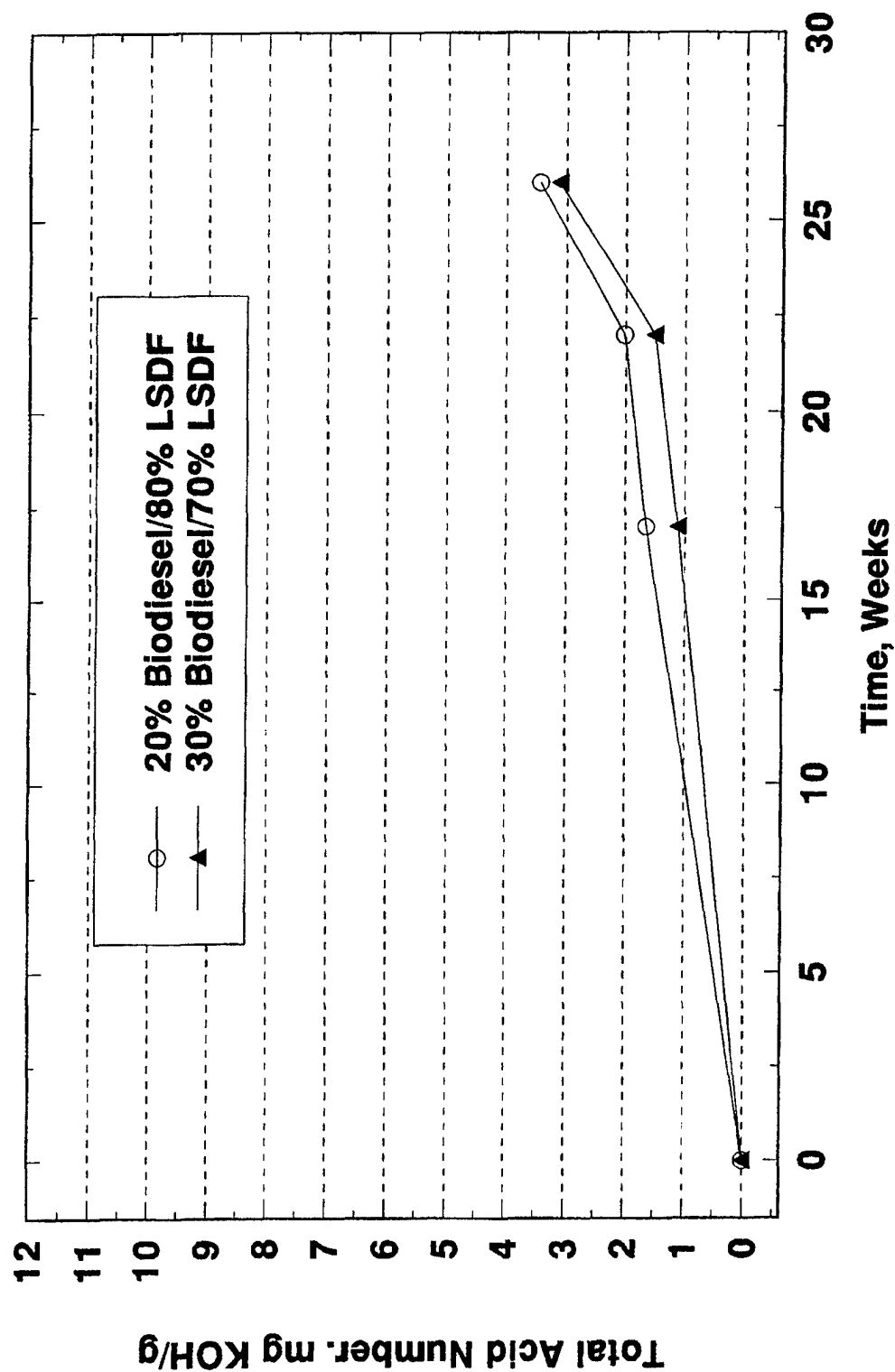
Total Acid Number (TAN) Brass



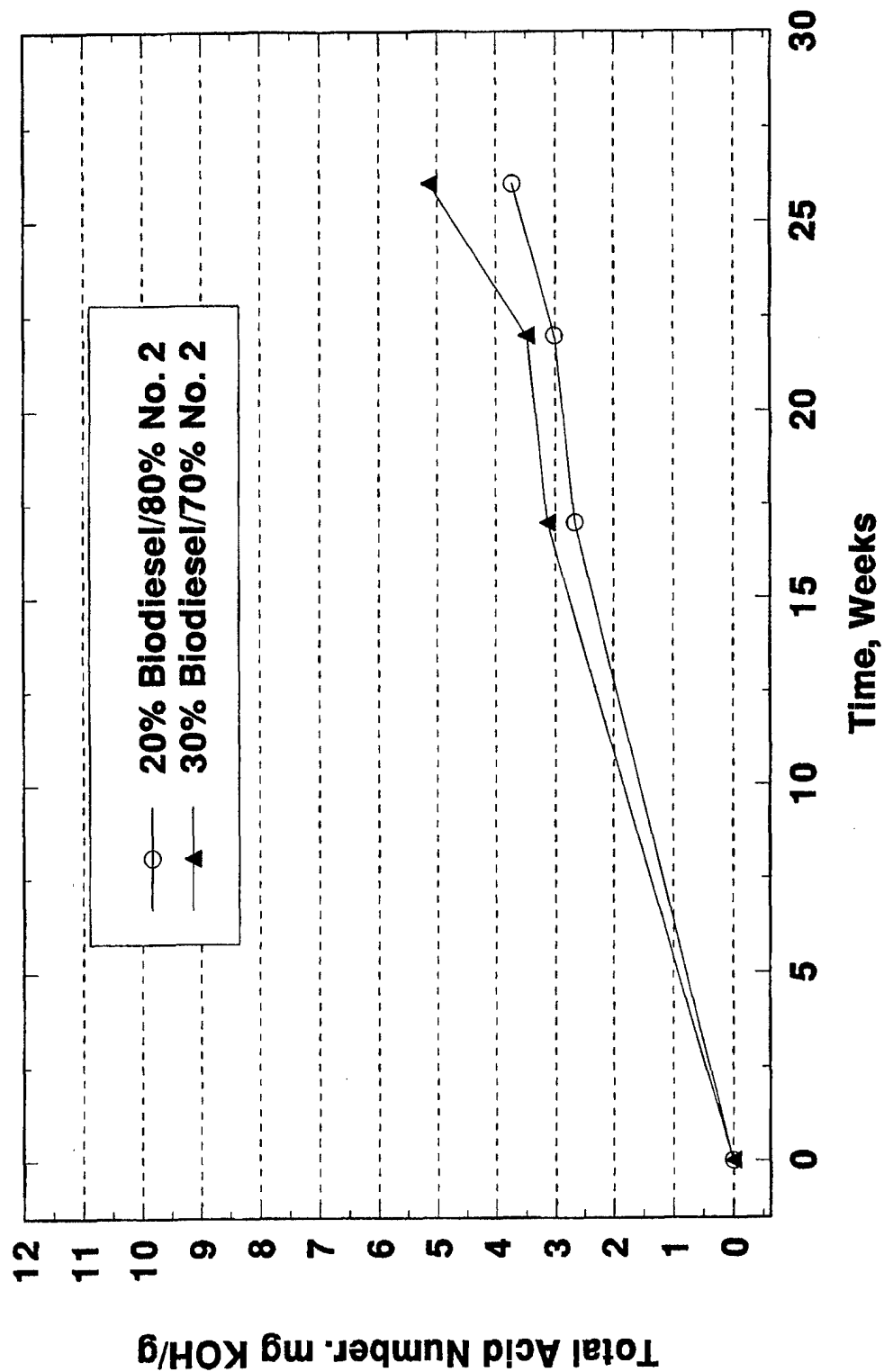
**Total Acid Number (TAN)
Bronze**



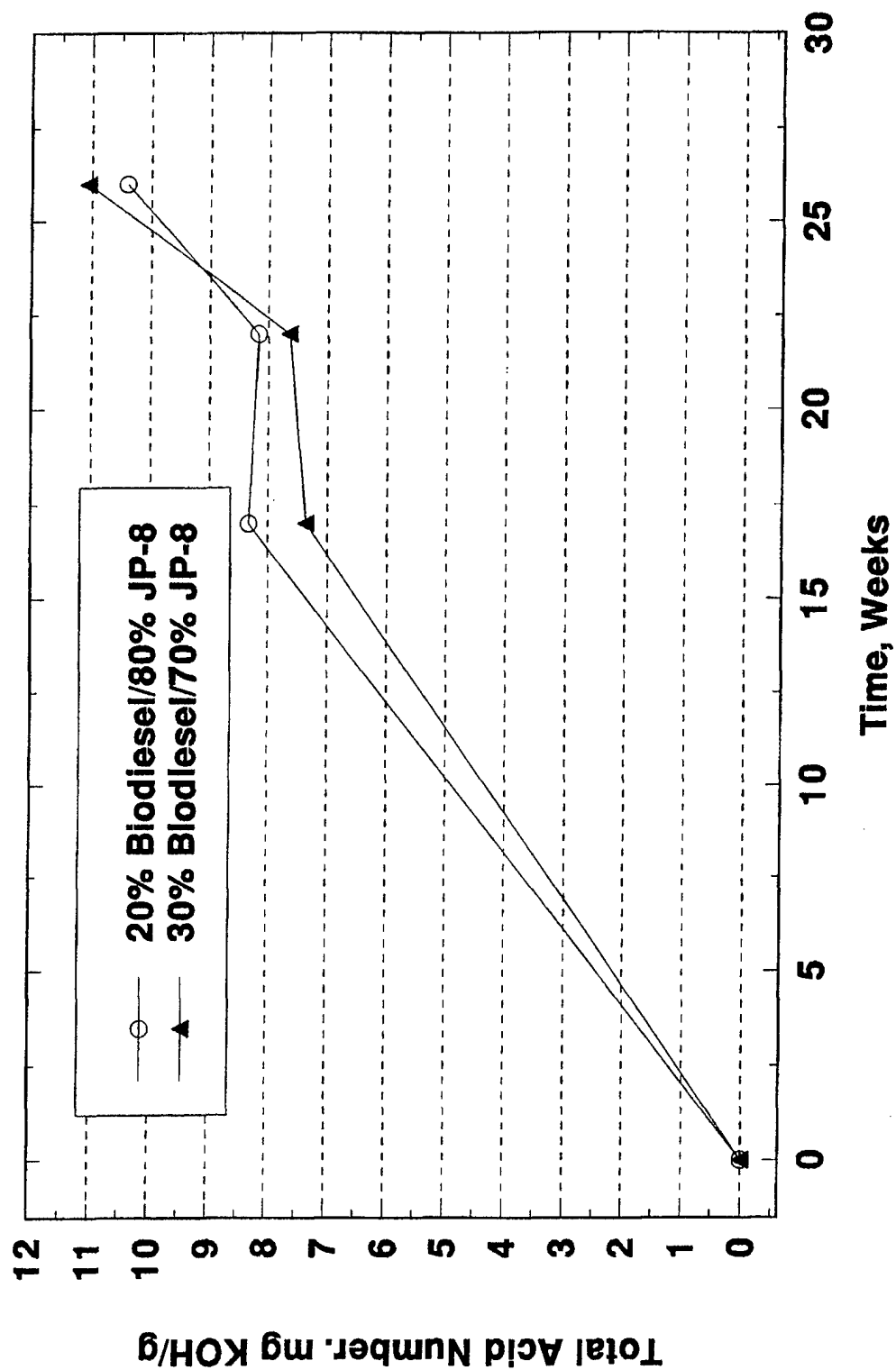
**Total Acid Number (TAN)
Bronze**



Total Acid Number (TAN) Bronze



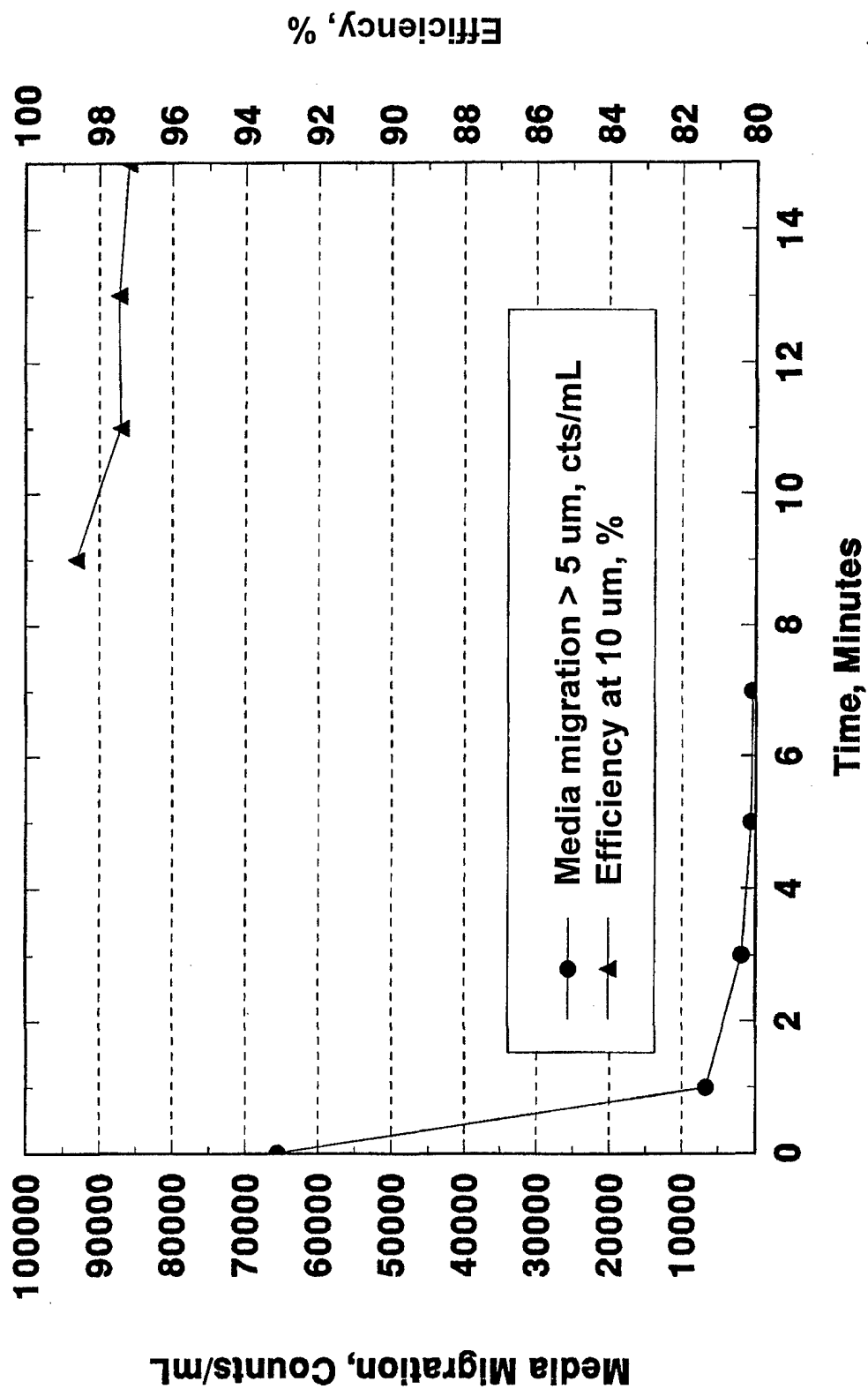
Total Acid Number (TAN) Bronze



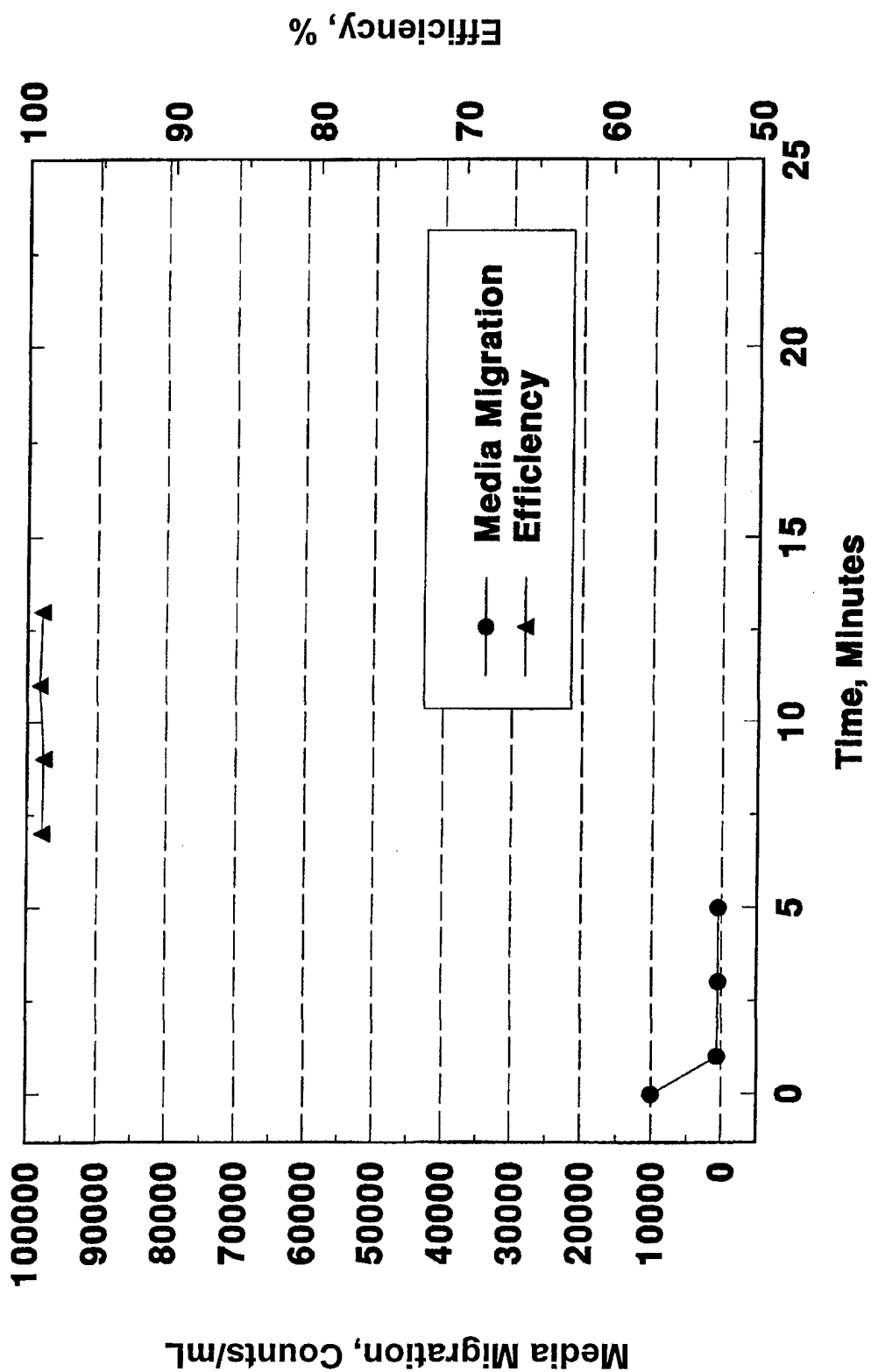
APPENDIX F

6.2L GM Single-Pass Filter Evaluation

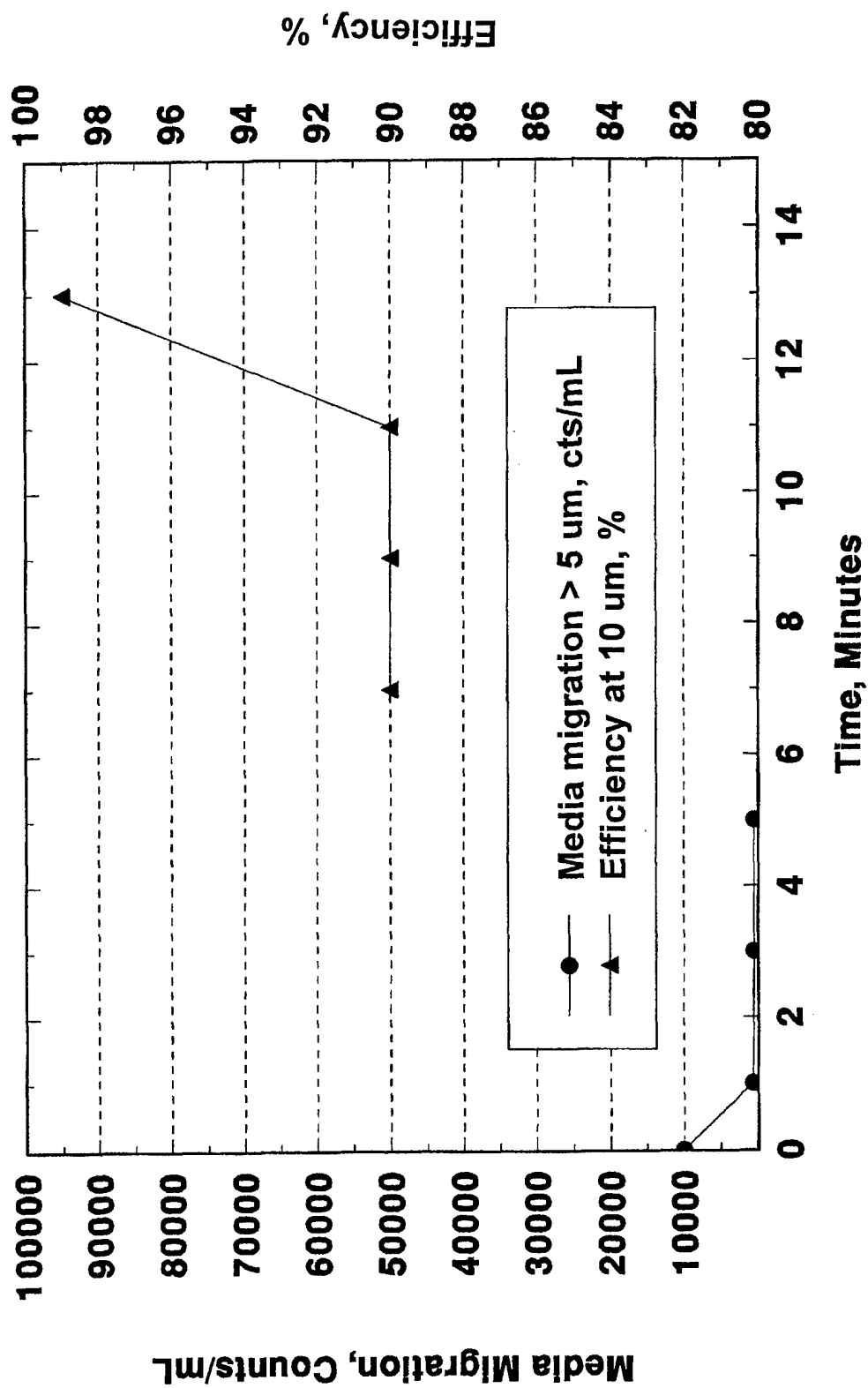
AC Fuel Filter Evaluation Baseline



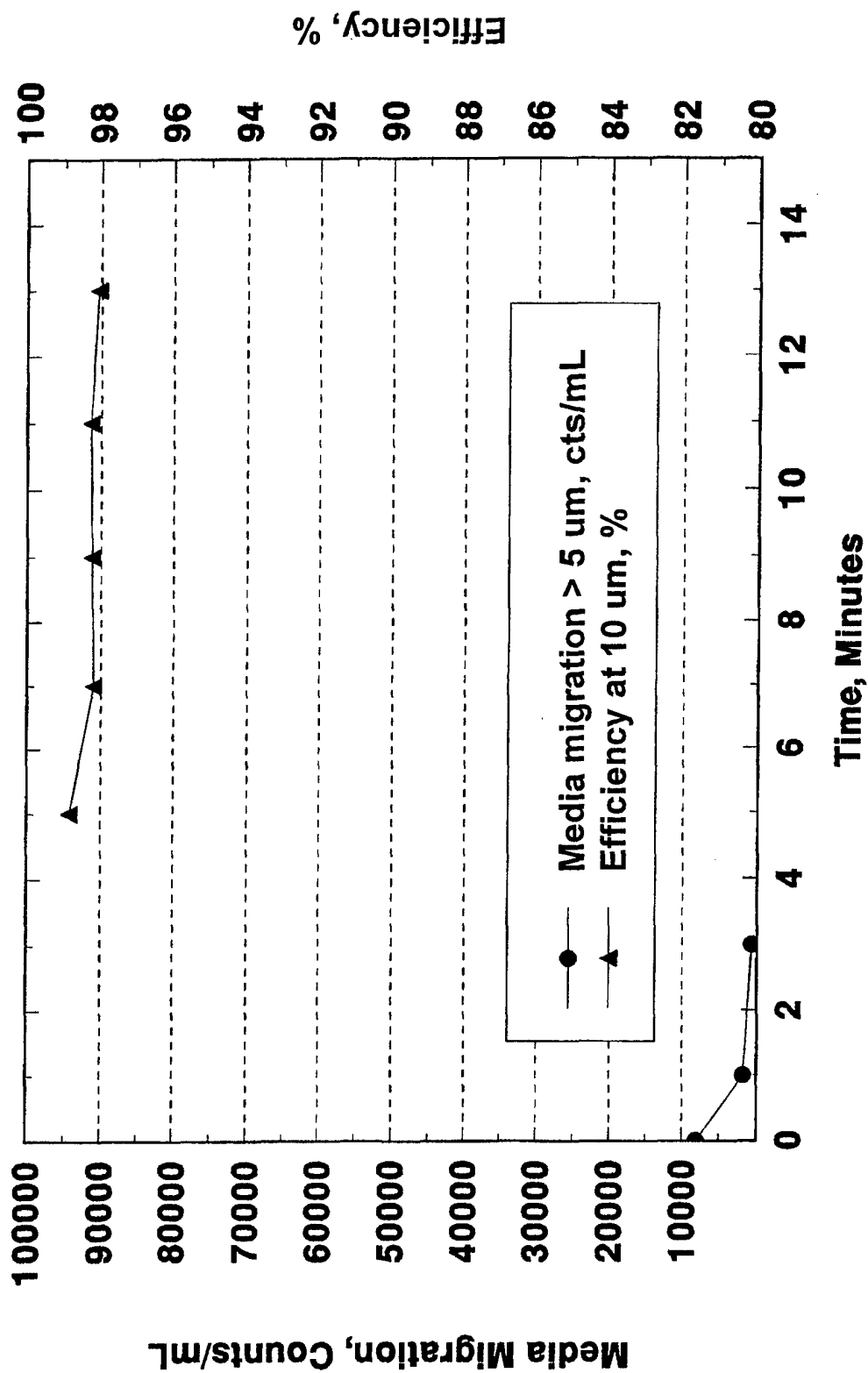
Biodiesel AC Fuel Filter Compatibility Evaluations **New Filter, No Storage**



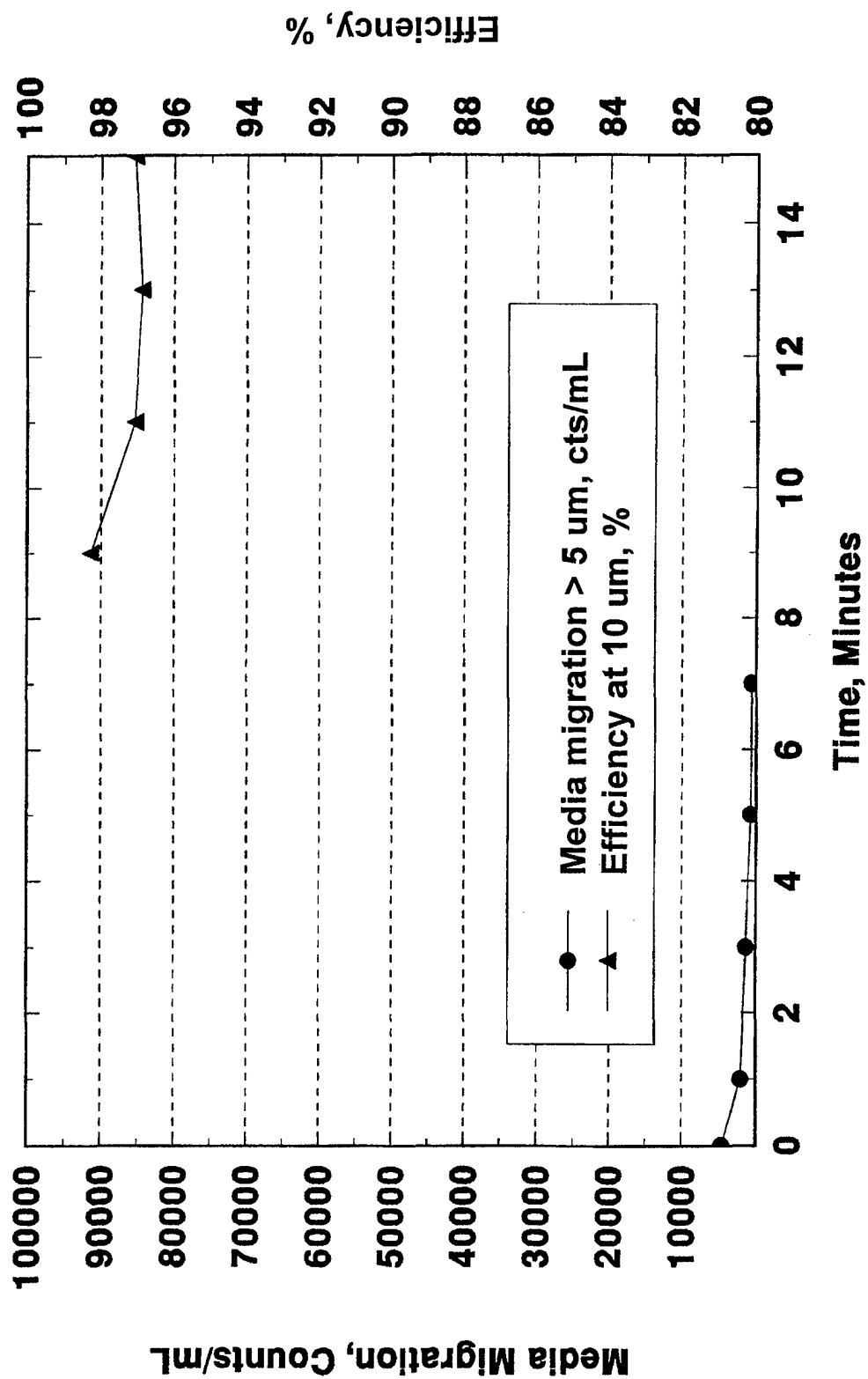
AC Fuel Filter Evaluation Baseline



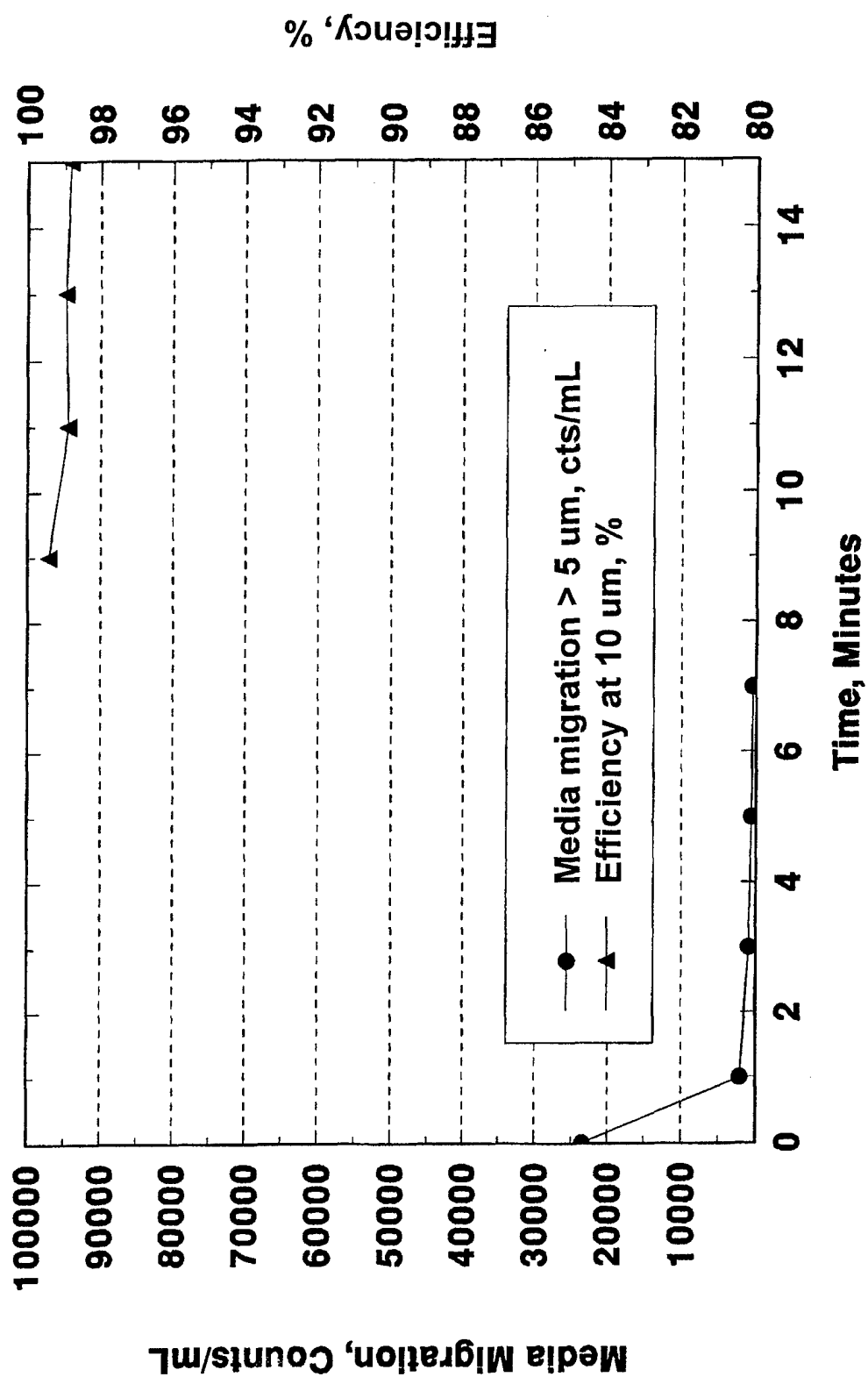
AC Fuel Filter Evaluation JP-8, 1 Month



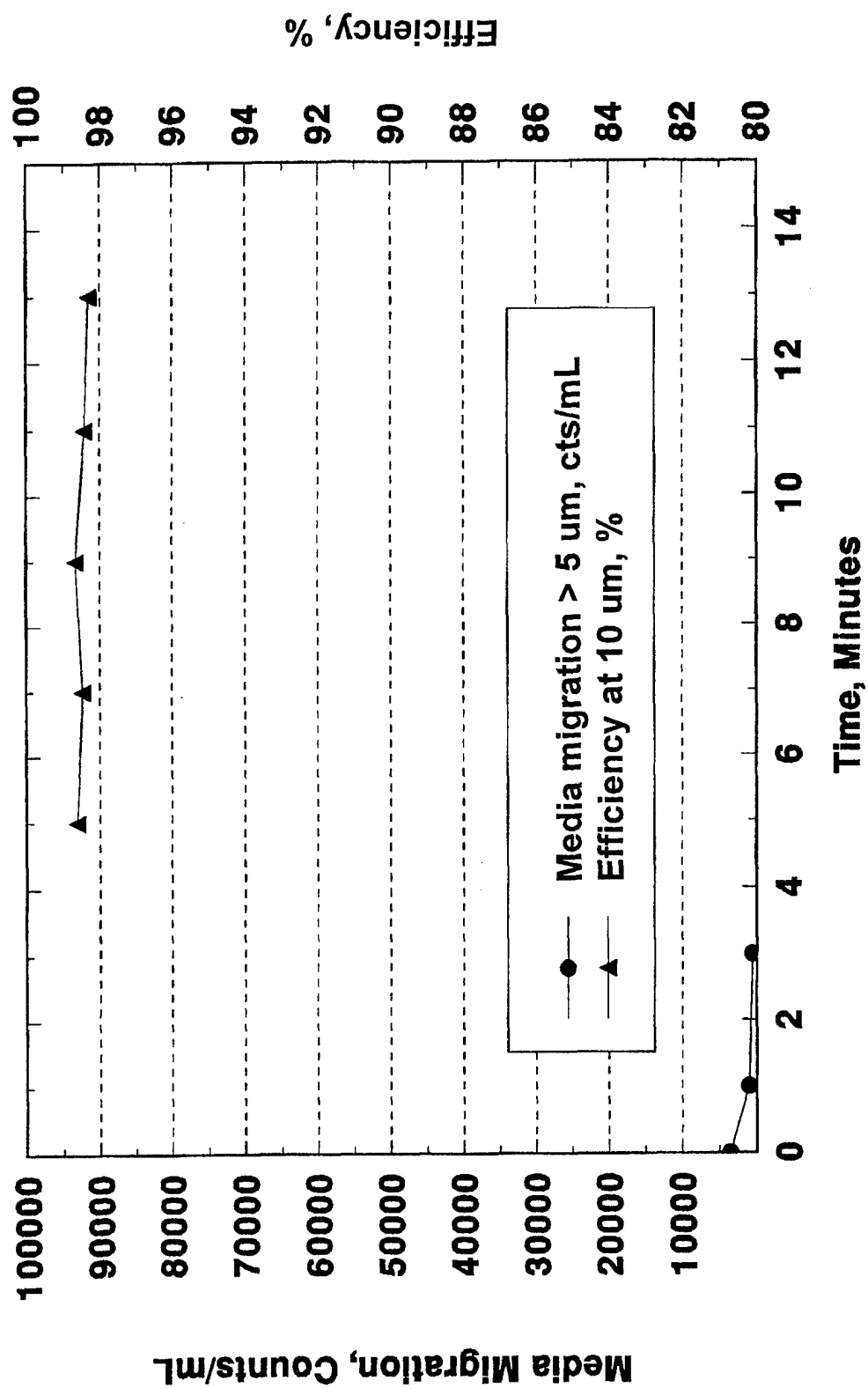
AC Fuel Filter Evaluation JP-8, 3 Month



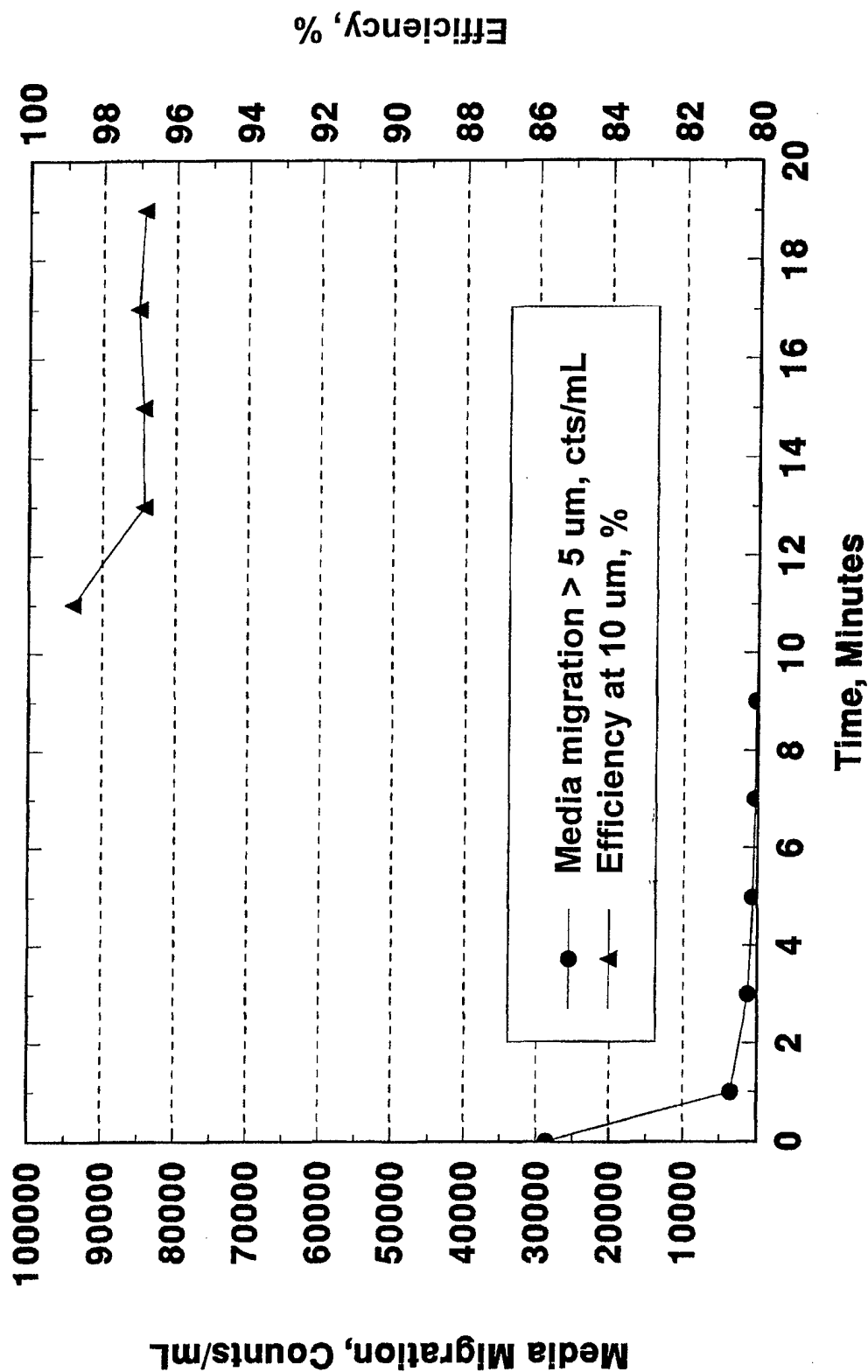
AC Fuel Filter Evaluation JP-8, 6 Months



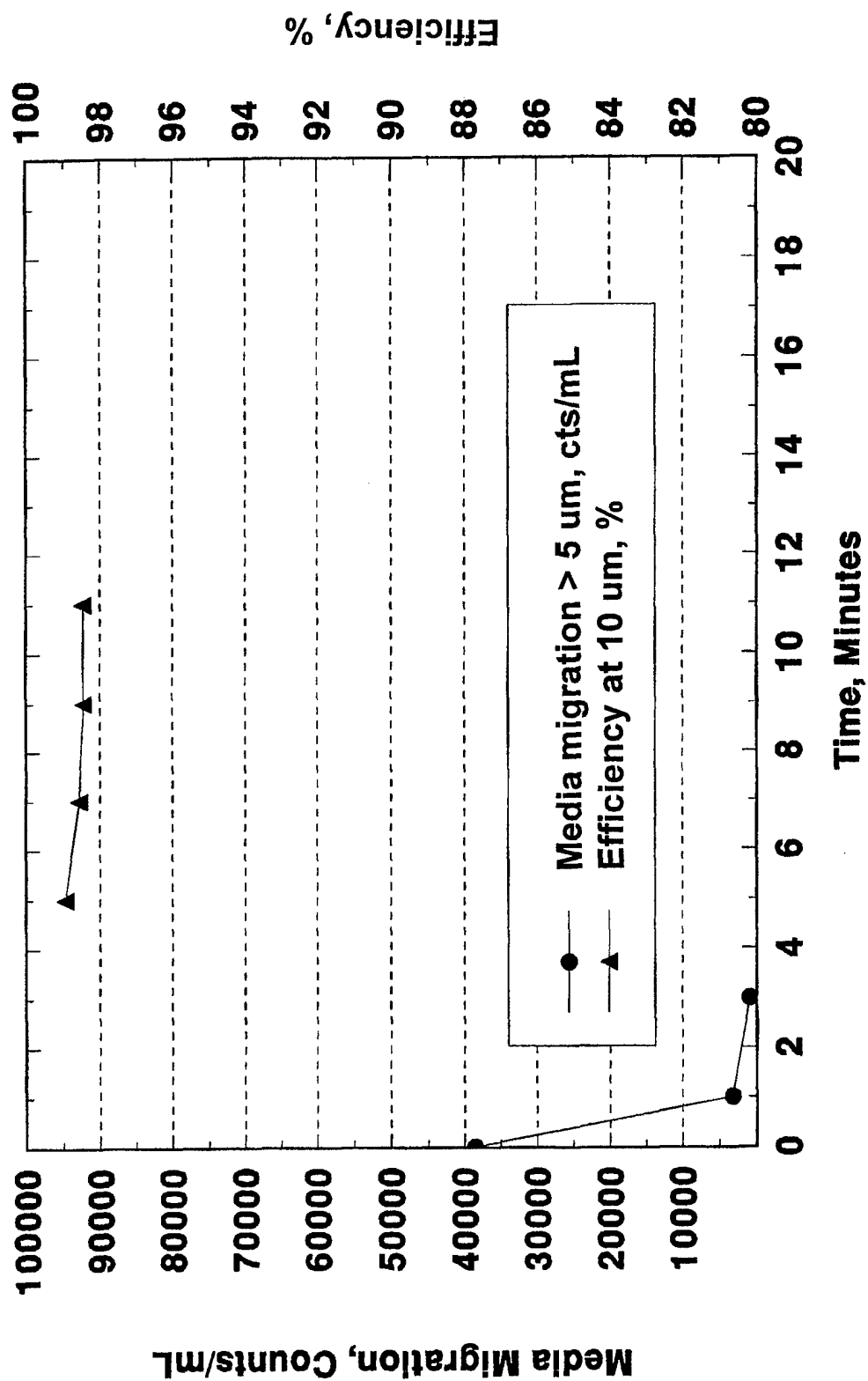
AC Fuel Filter Evaluation Biodiesel, 1 Month



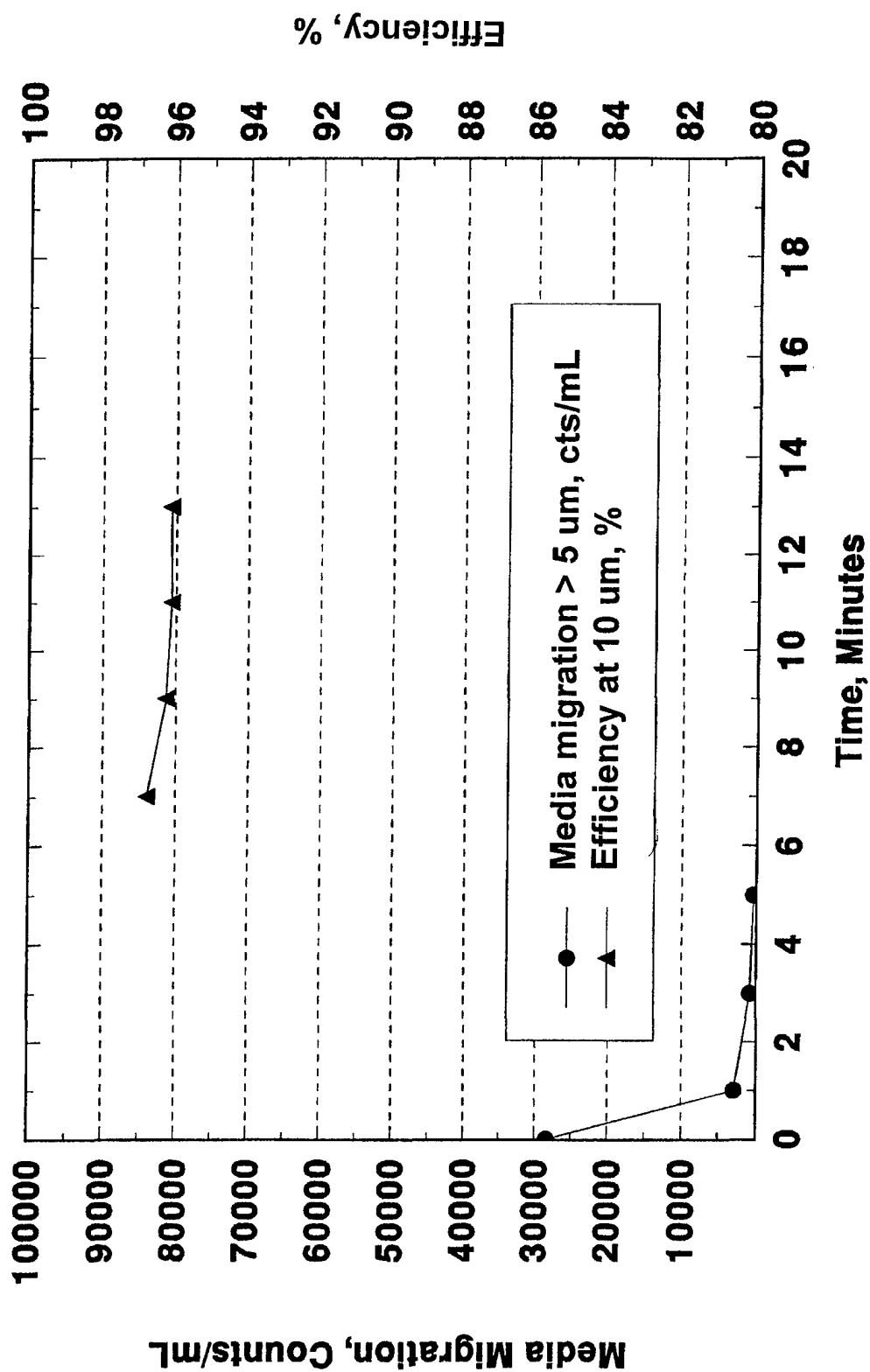
AC Fuel Filter Evaluation **Biodiesel, 3 Month**



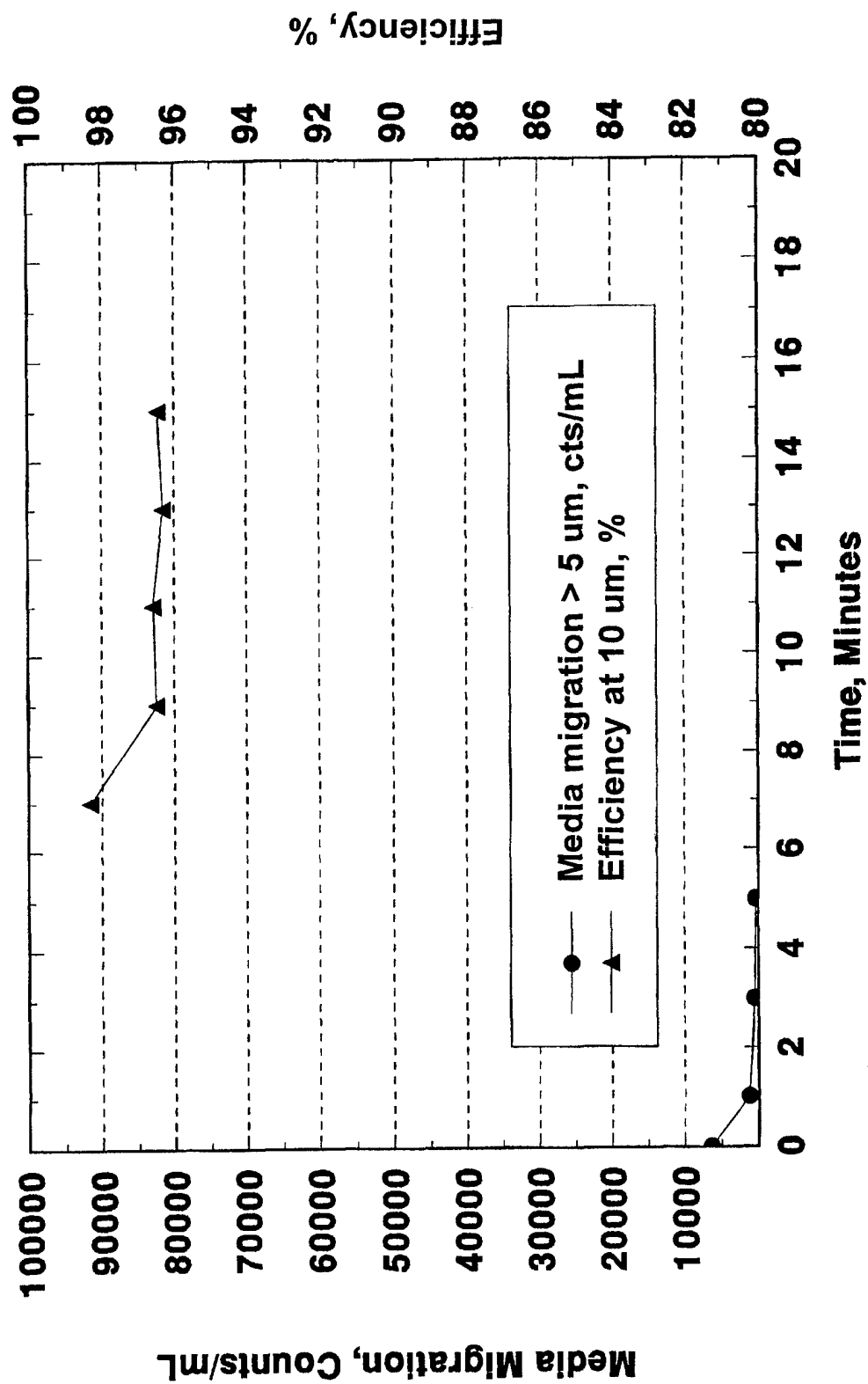
AC Fuel Filter Evaluation **Biodiesel, 6 Month**



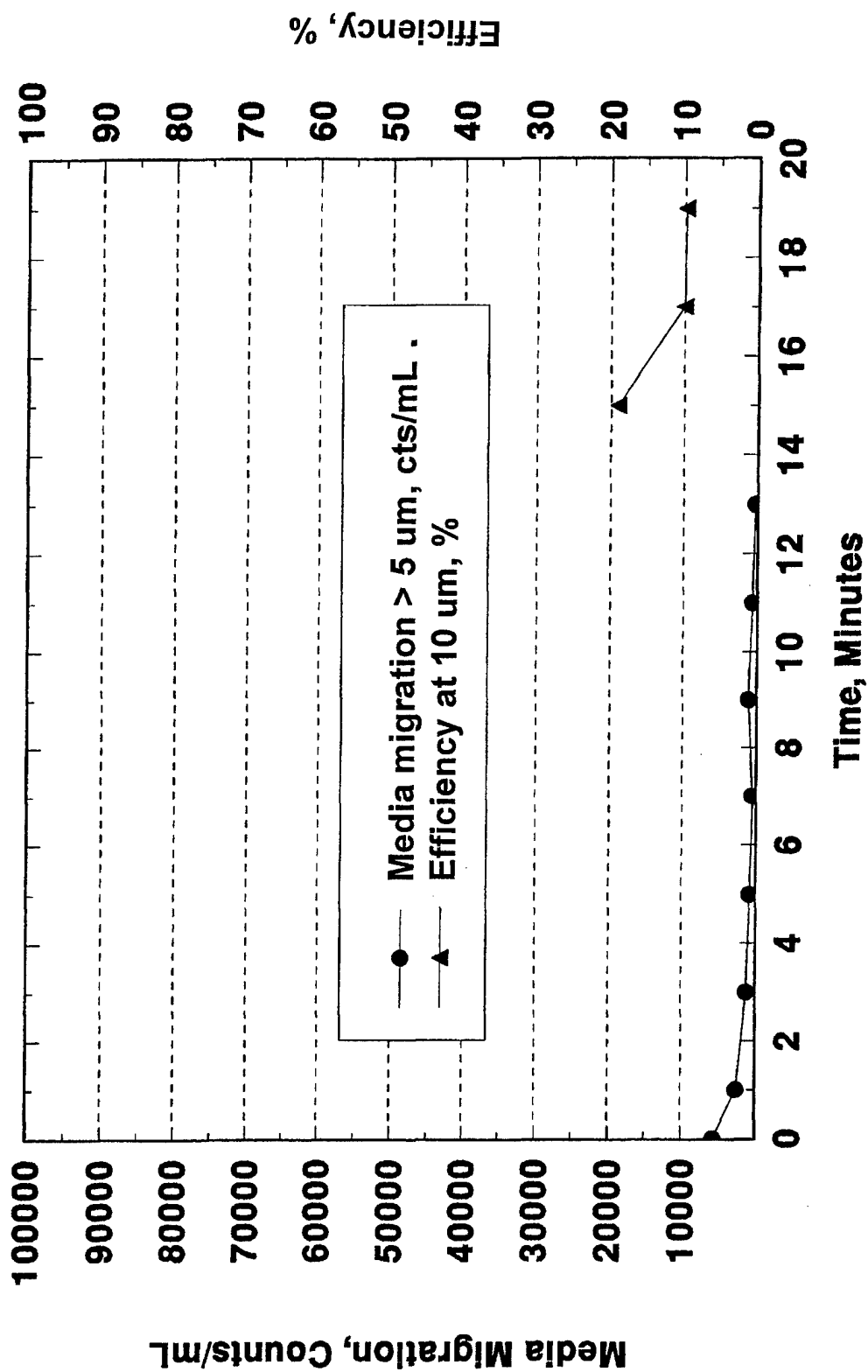
AC Fuel Filter Evaluation **Low Sulfur Diesel Fuel, 1 Month**



AC Fuel Filter Evaluation Low Sulfur Diesel Fuel, 3 Month

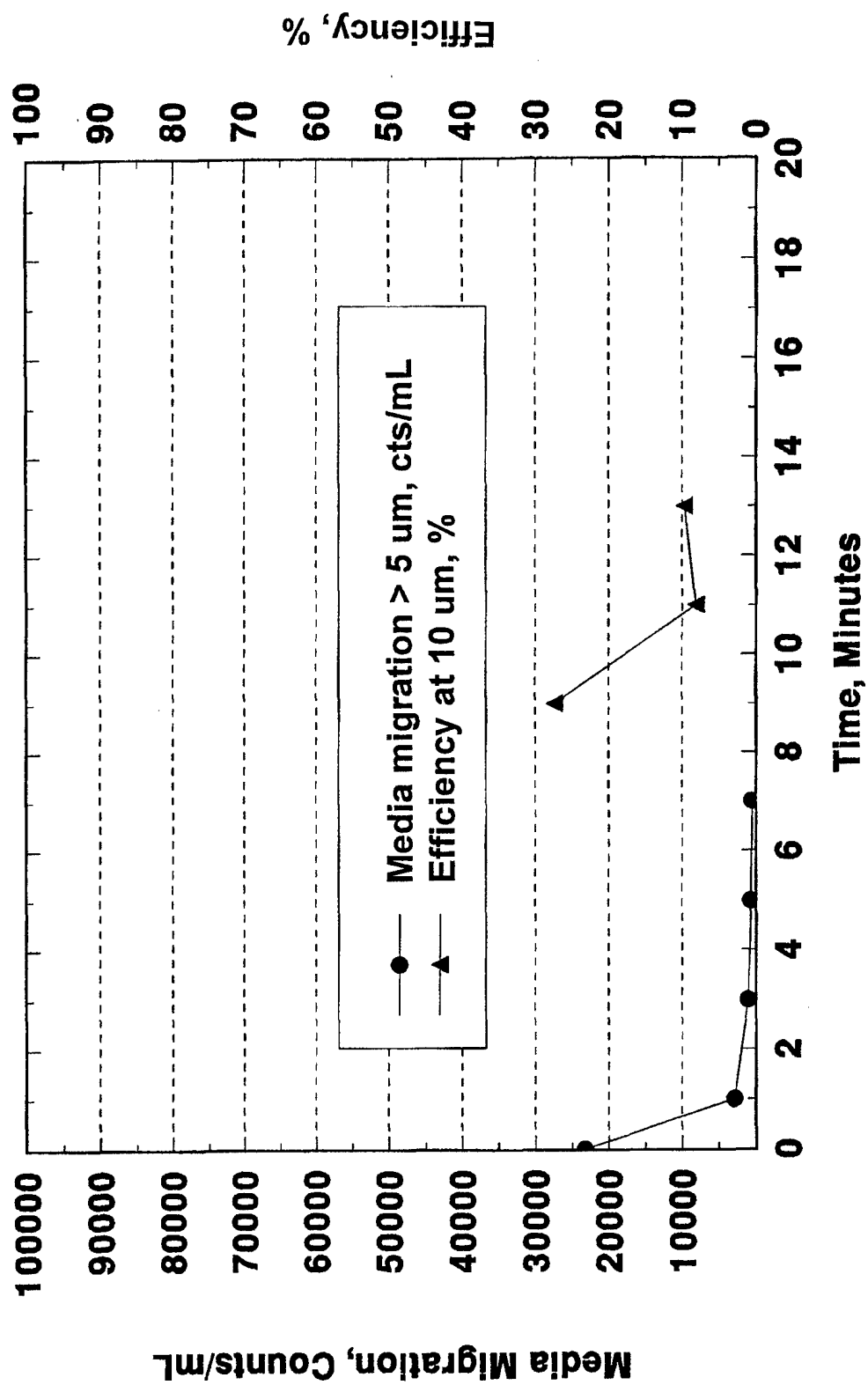


AC Fuel Filter Evaluation **Low Sulfur Diesel Fuel, 6 Month**

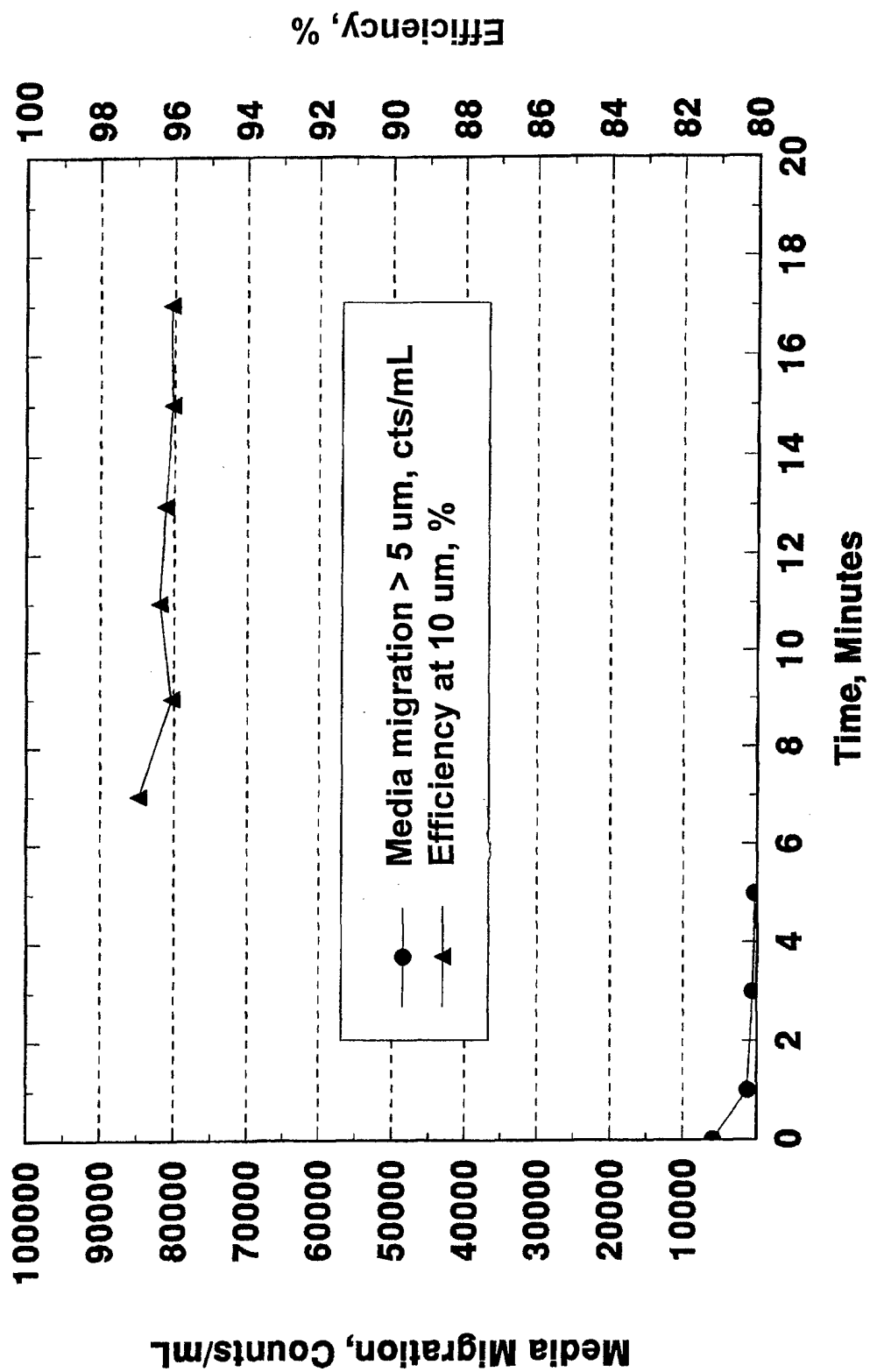


AC Fuel Filter Evaluation

Low Sulfur Diesel Fuel, 6 Month, Repeat

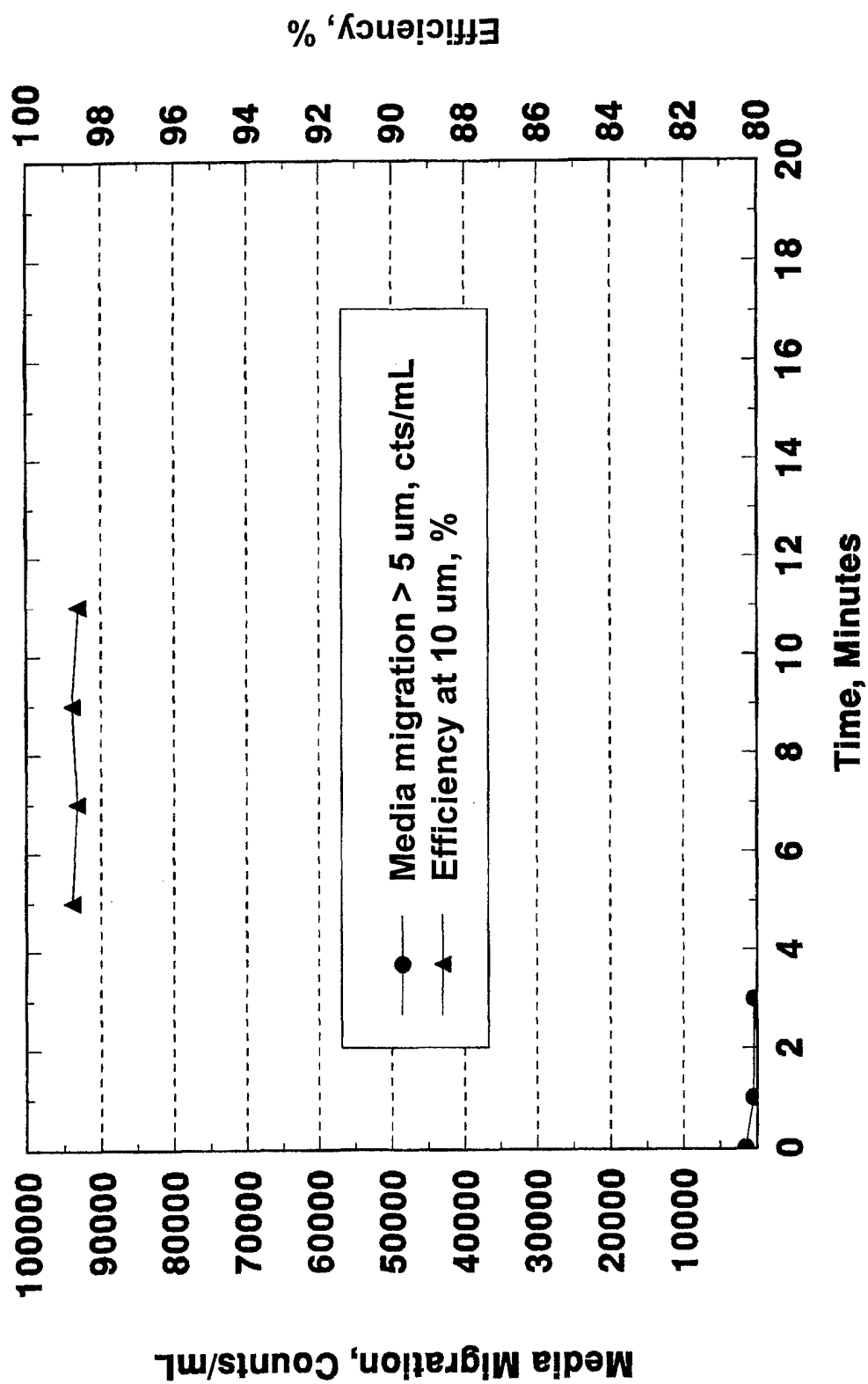


AC Fuel Filter Evaluation Cat 1-H, 1 Month

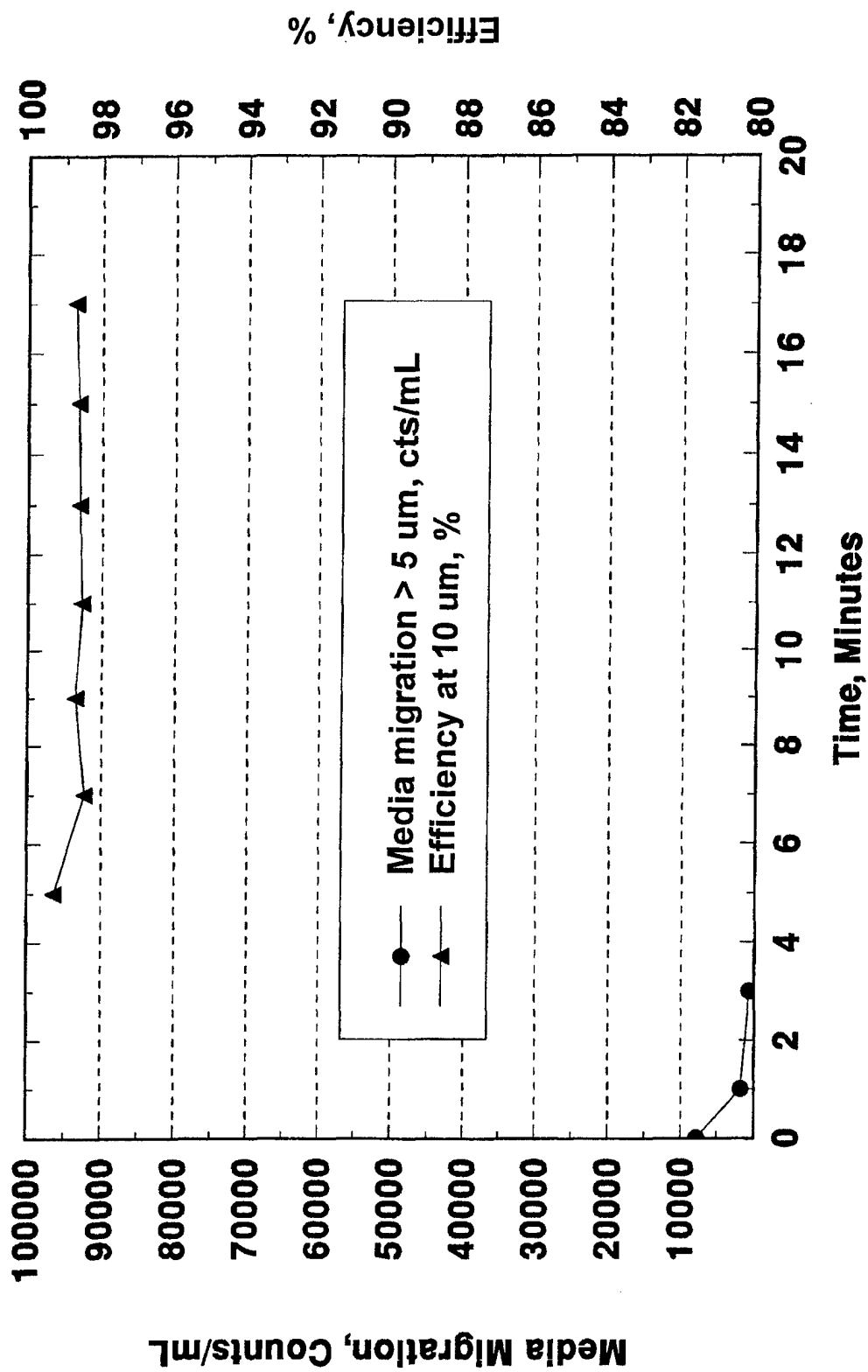


AC Fuel Filter Evaluation

Cat 1-H, 3 Month

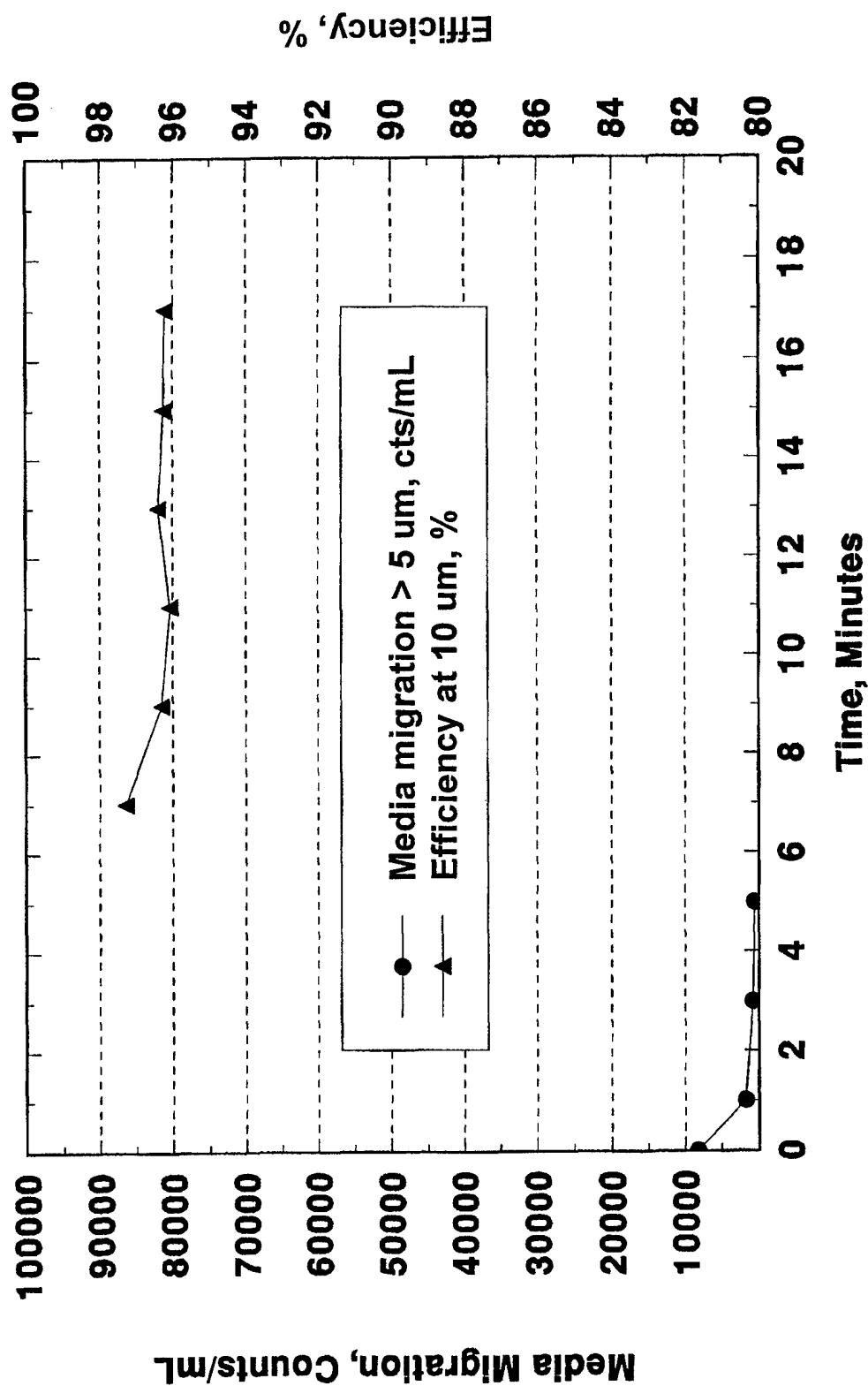


AC Fuel Filter Evaluation **Cat 1-H, 6 Month**



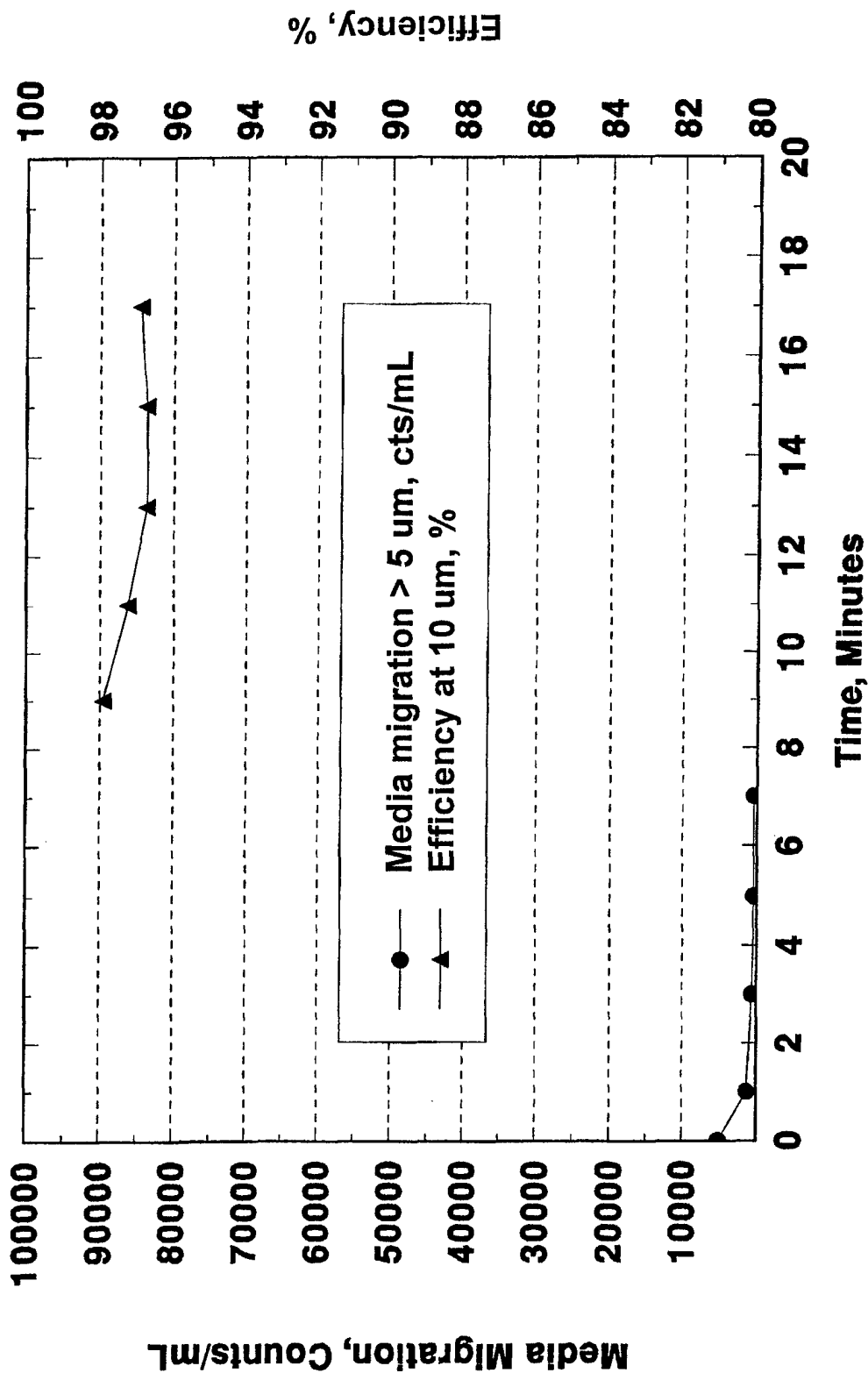
AC Fuel Filter Evaluation

20% Biodiesel/80% Low Sulfur Diesel Fuel, 1 Month

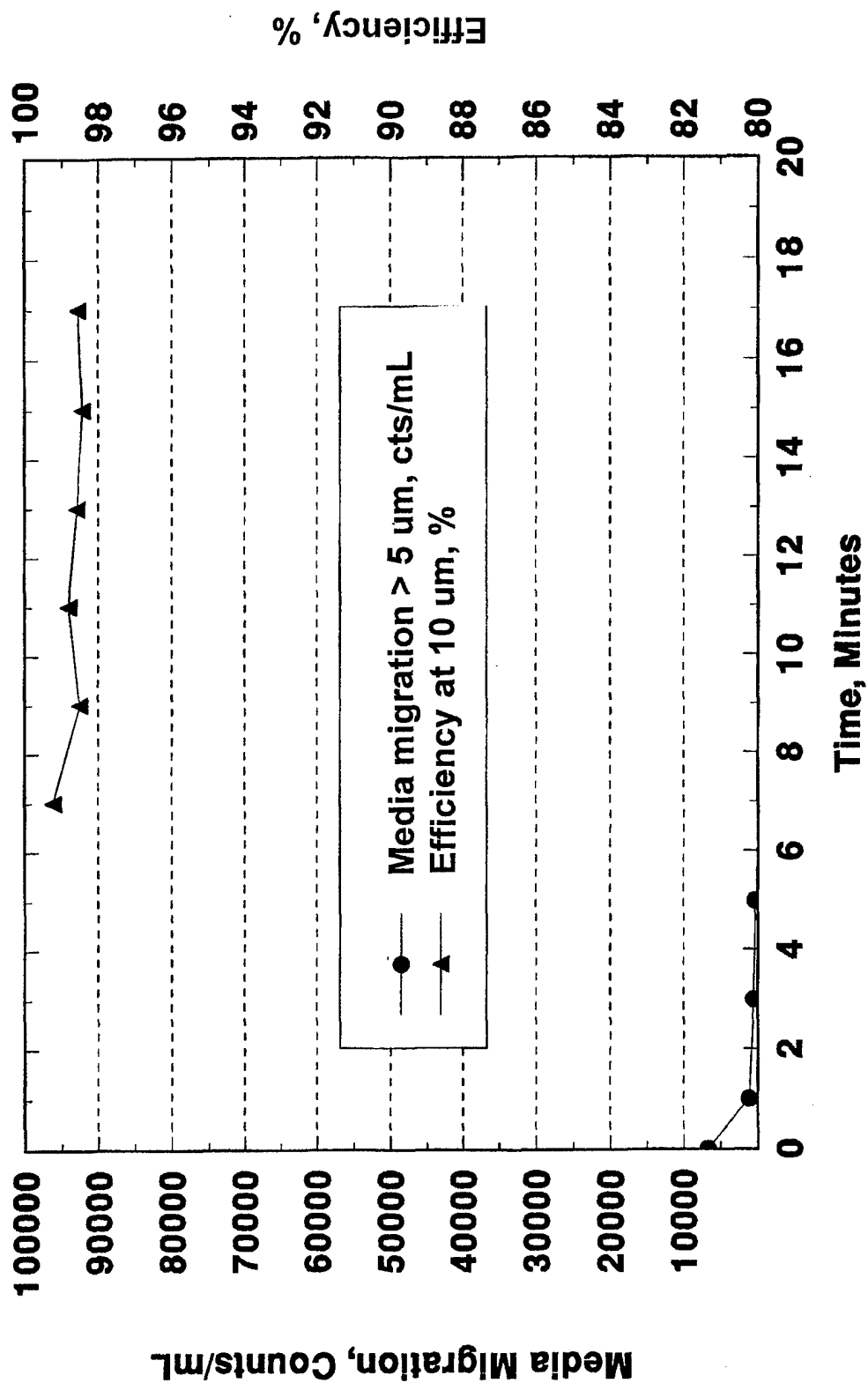


AC Fuel Filter Evaluation

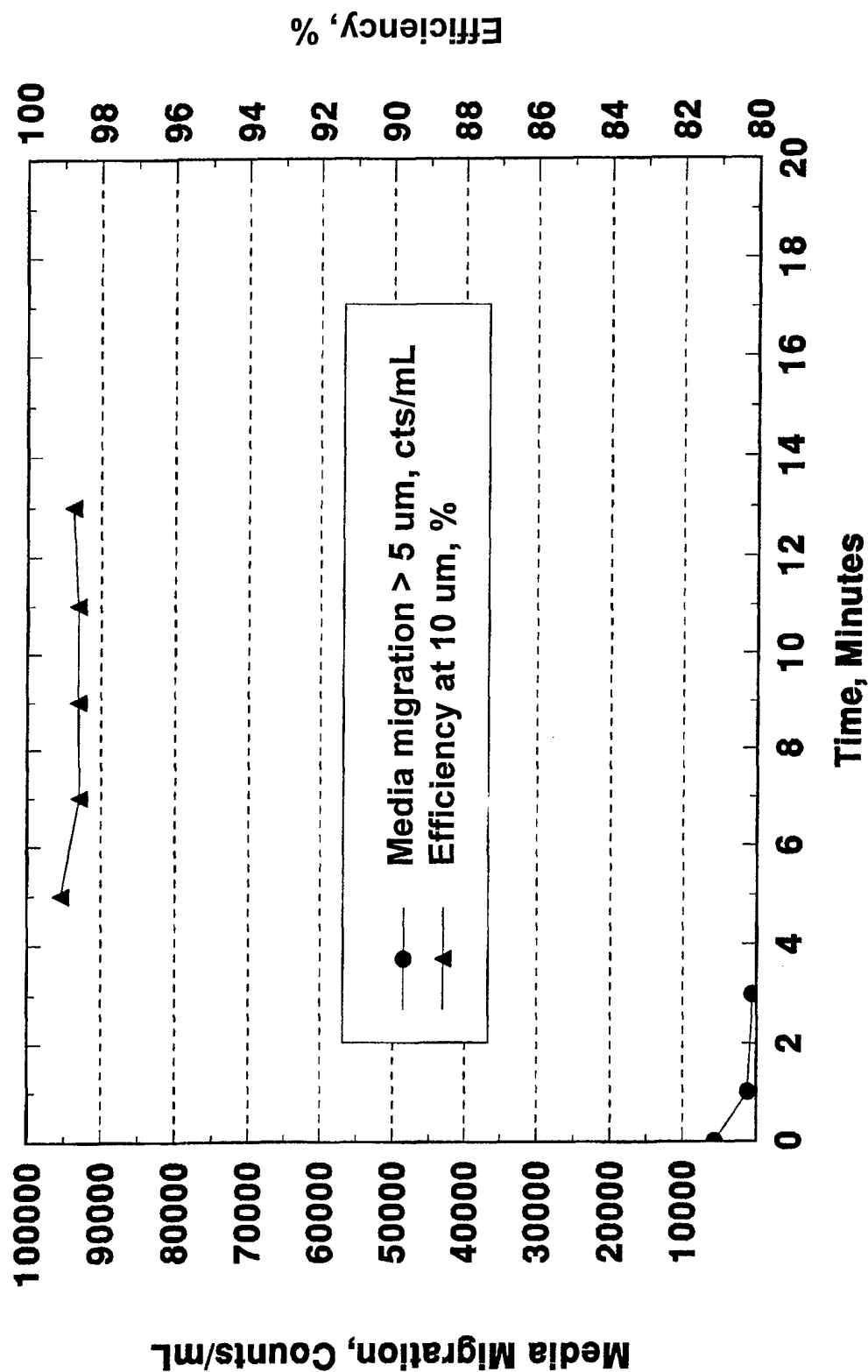
20% Biodiesel/80% Low Sulfur Diesel Fuel, 3 Month



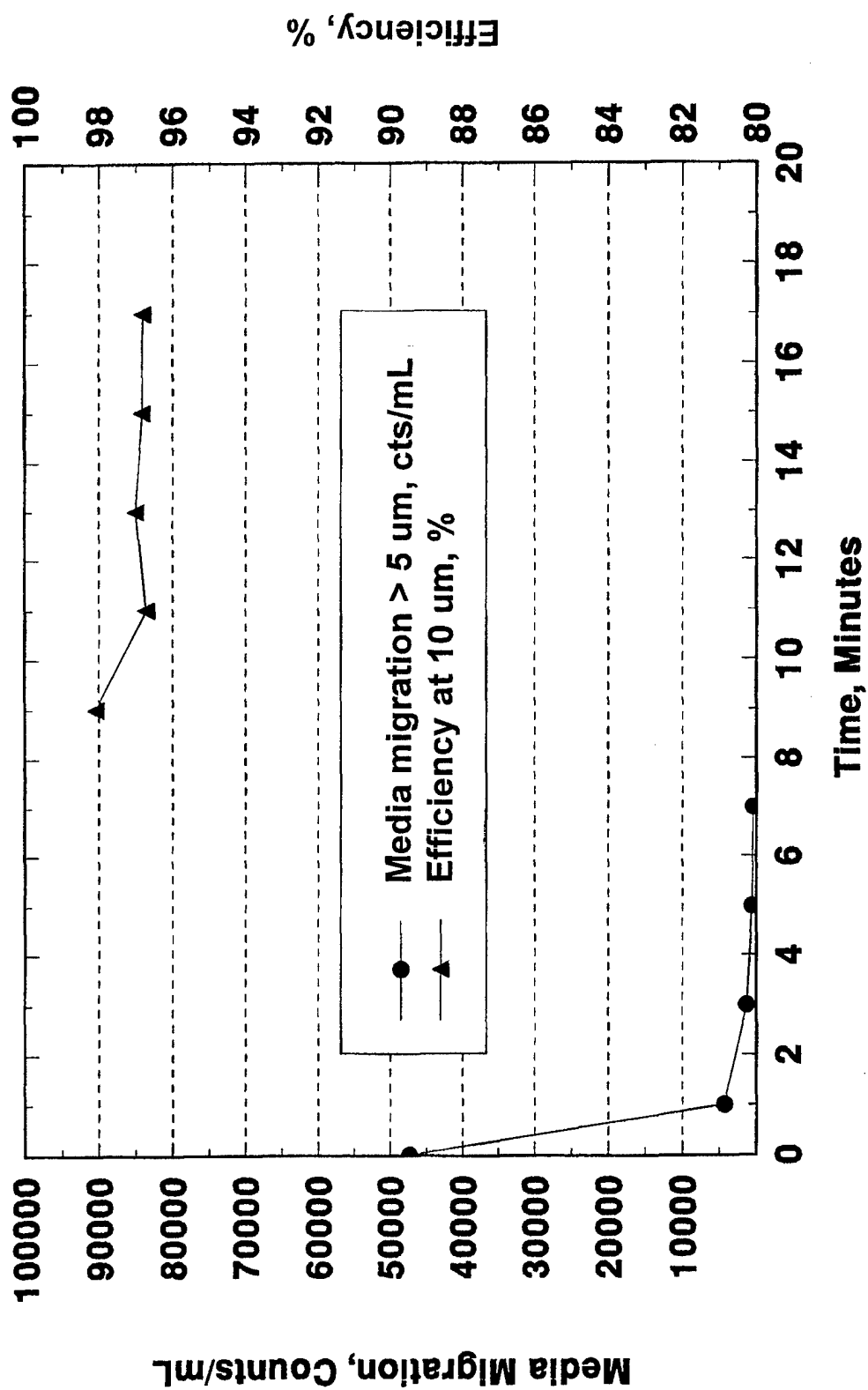
AC Fuel Filter Evaluation **20% Biodiesel/80% Low Sulfur Diesel Fuel, 6 Month**



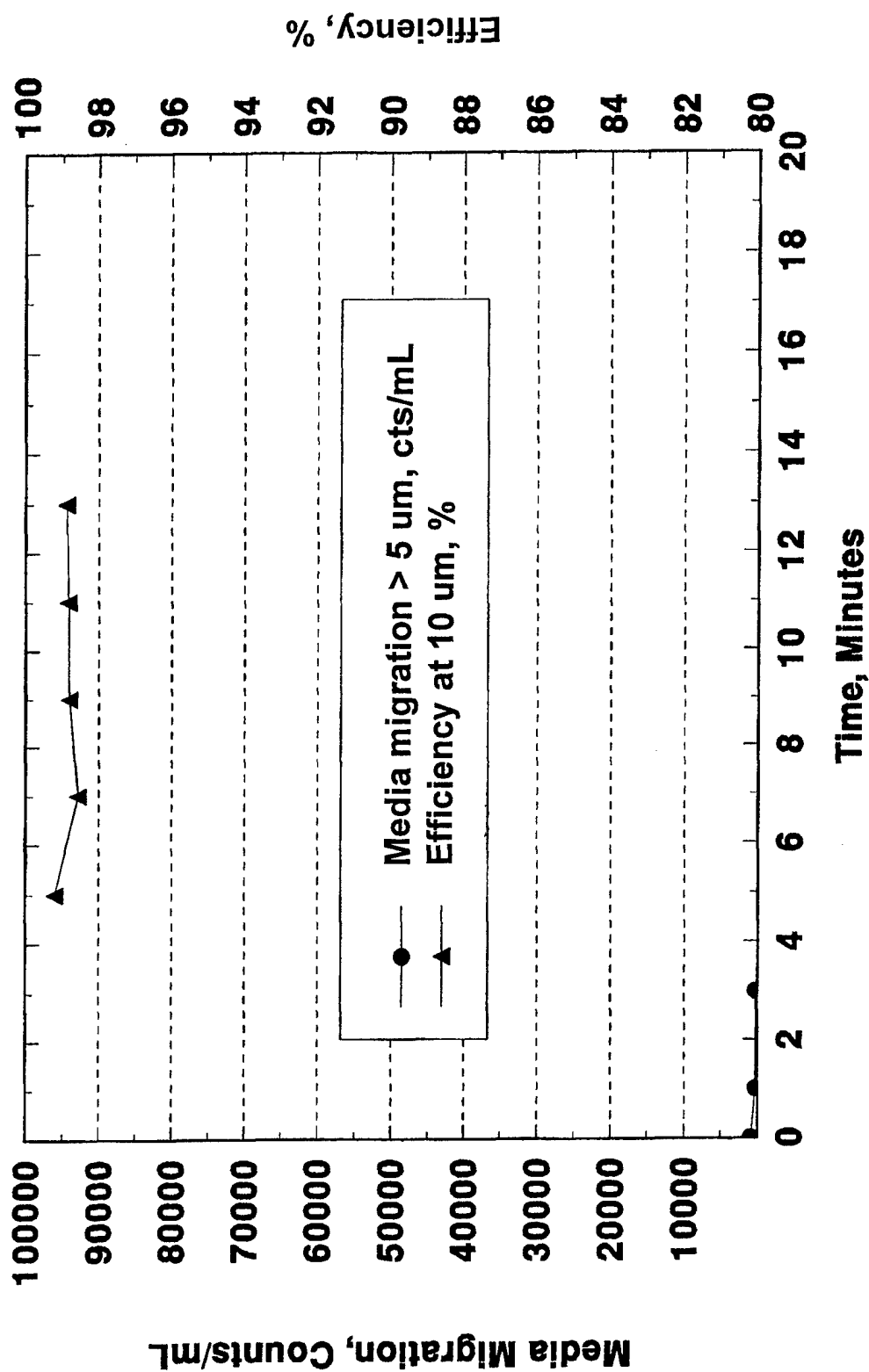
AC Fuel Filter Evaluation **30% Biodiesel/70% Low Sulfur Diesel Fuel, 1 Month**



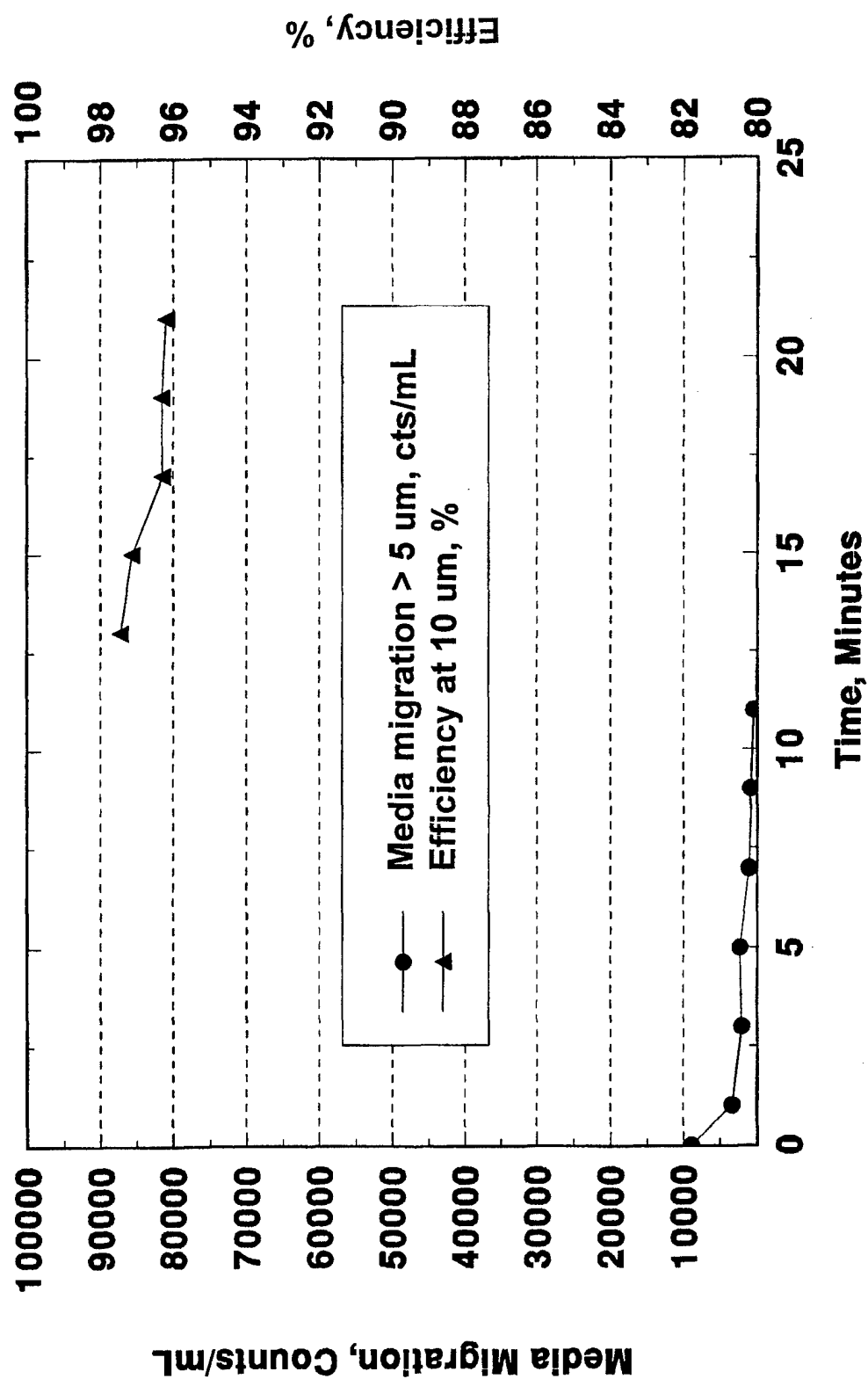
AC Fuel Filter Evaluation **30% Biodiesel/70% Low Sulfur Diesel Fuel, 3 Month**



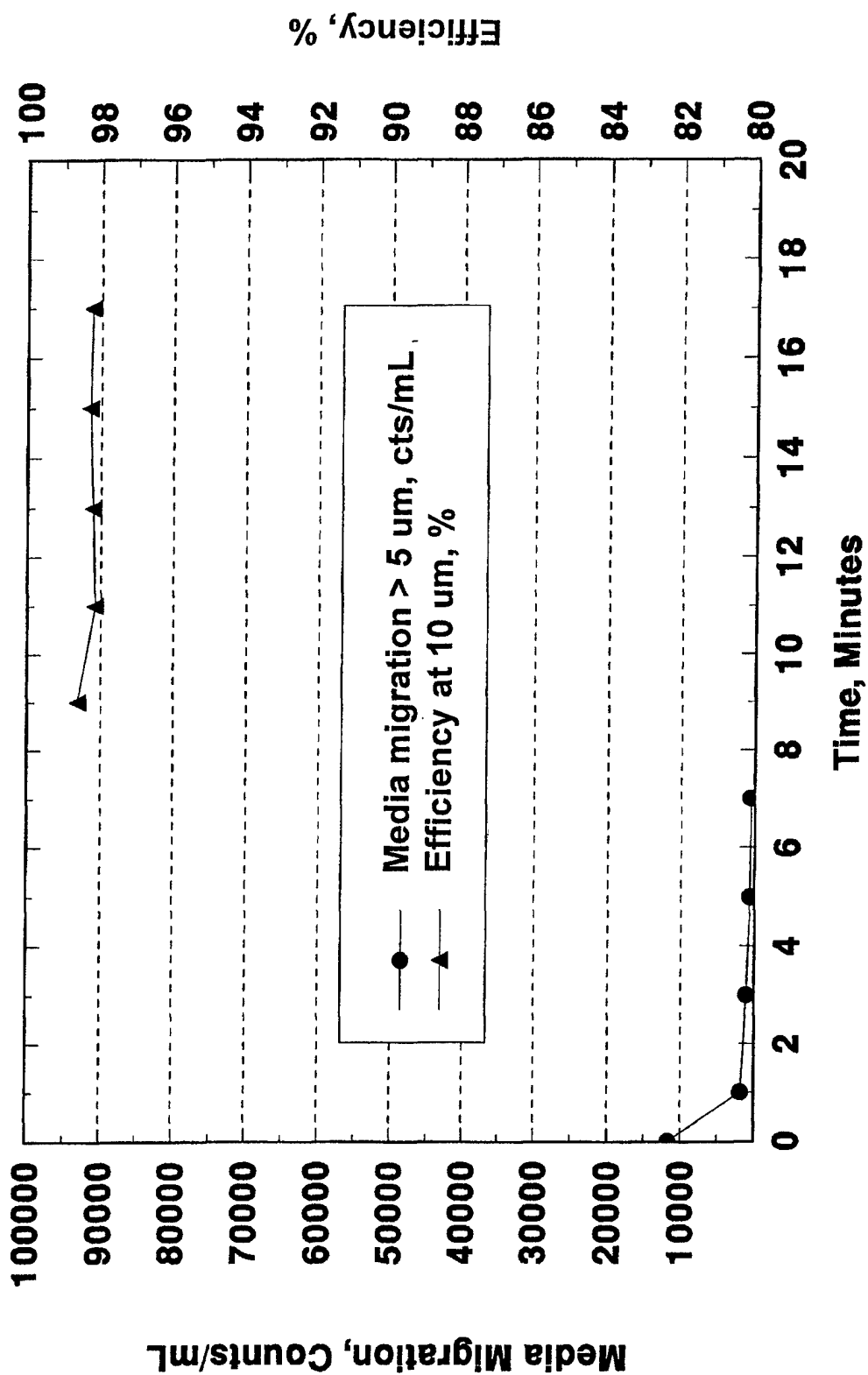
AC Fuel Filter Evaluation **30% Biodiesel/70% Low Sulfur Diesel Fuel, 6 Month**



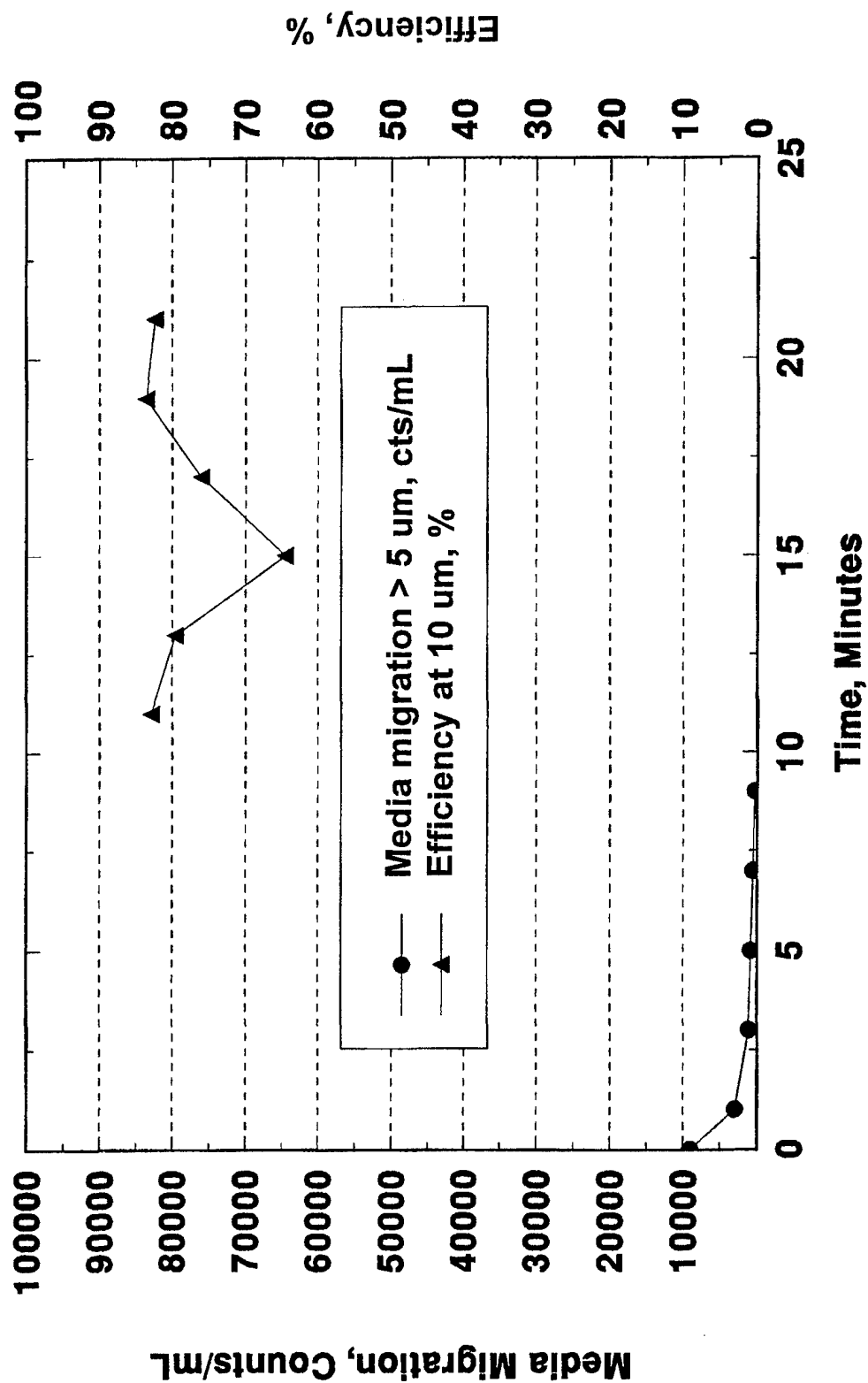
AC Fuel Filter Evaluation 20% Biodiesel/80% Cat 1-H, 1 Month



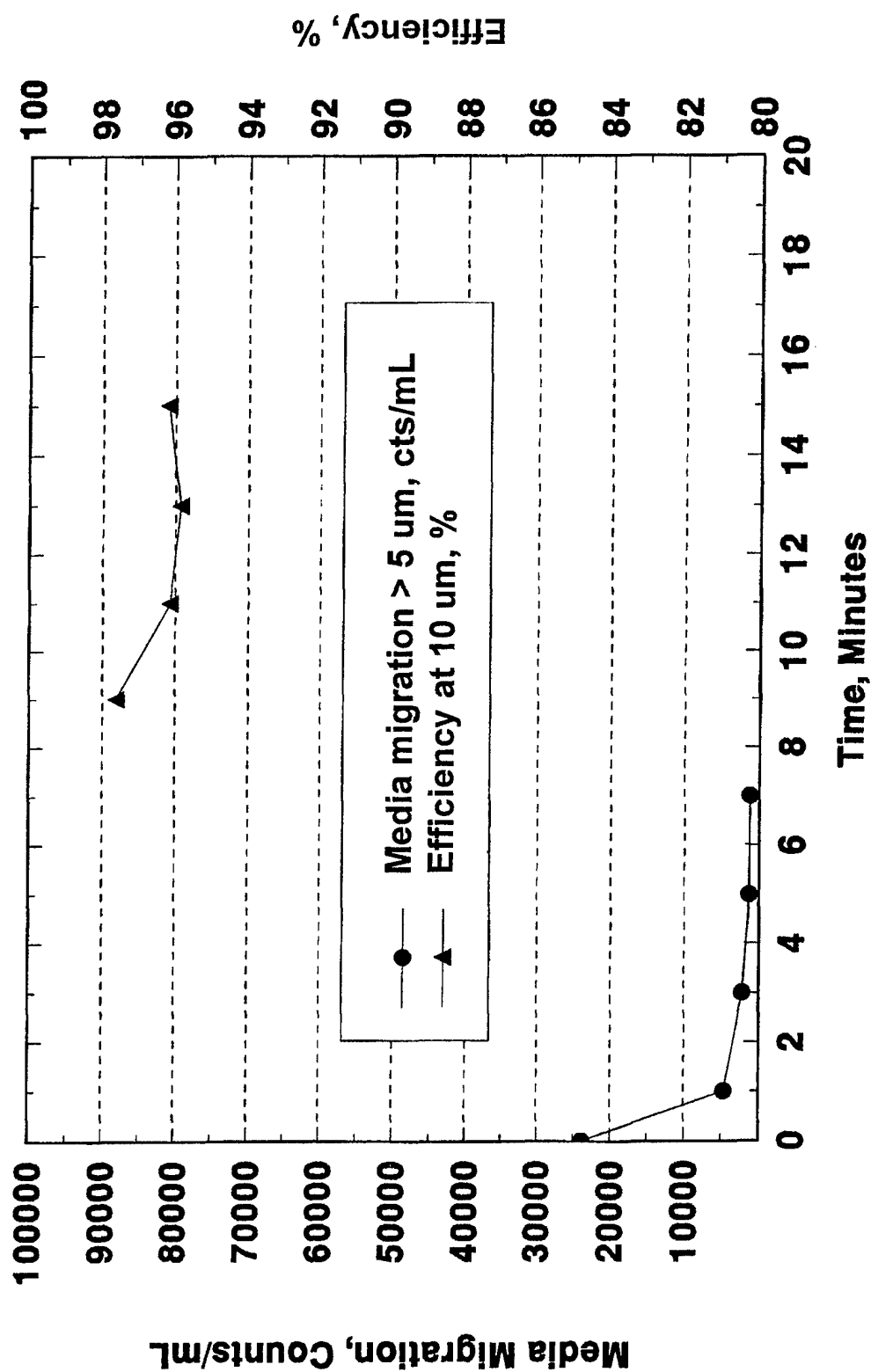
AC Fuel Filter Evaluation **20% Biodiesel/80% Cat 1-H, 3 Month**



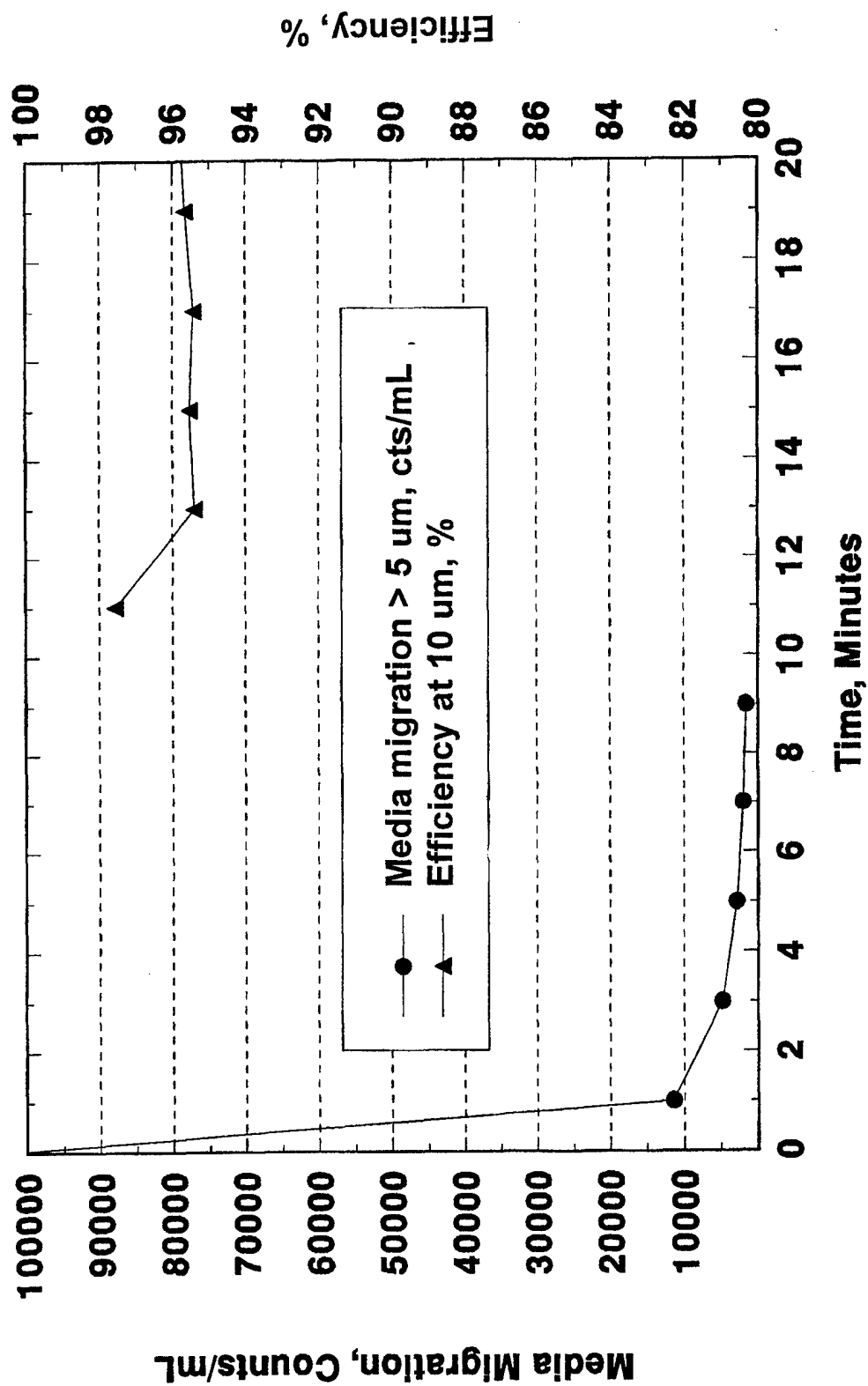
AC Fuel Filter Evaluation 20% Biodiesel/80% Cat 1-H, 6 Month



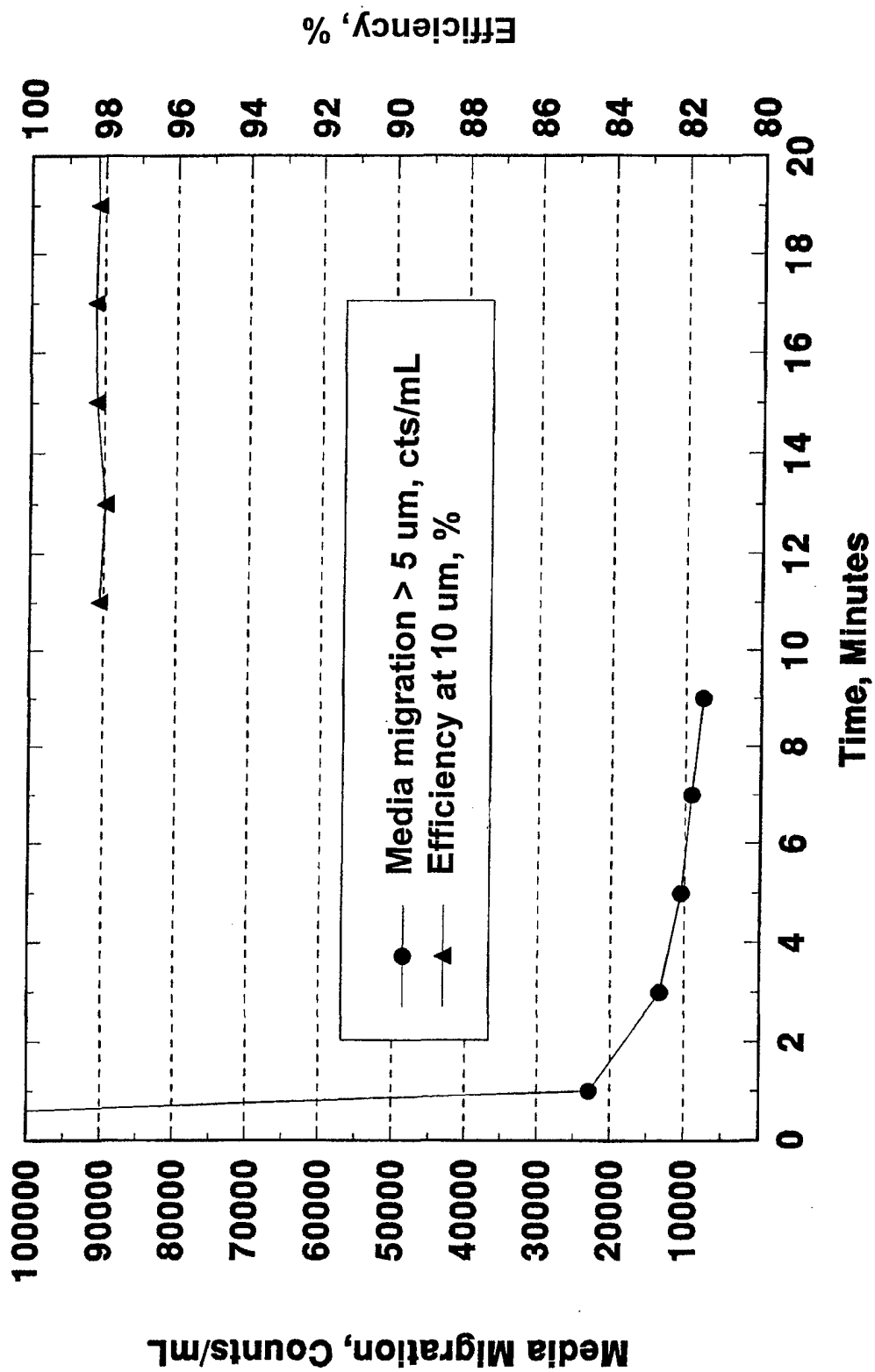
AC Fuel Filter Evaluation **30% Biodiesel 70% Cat 1-H, 1 Month**



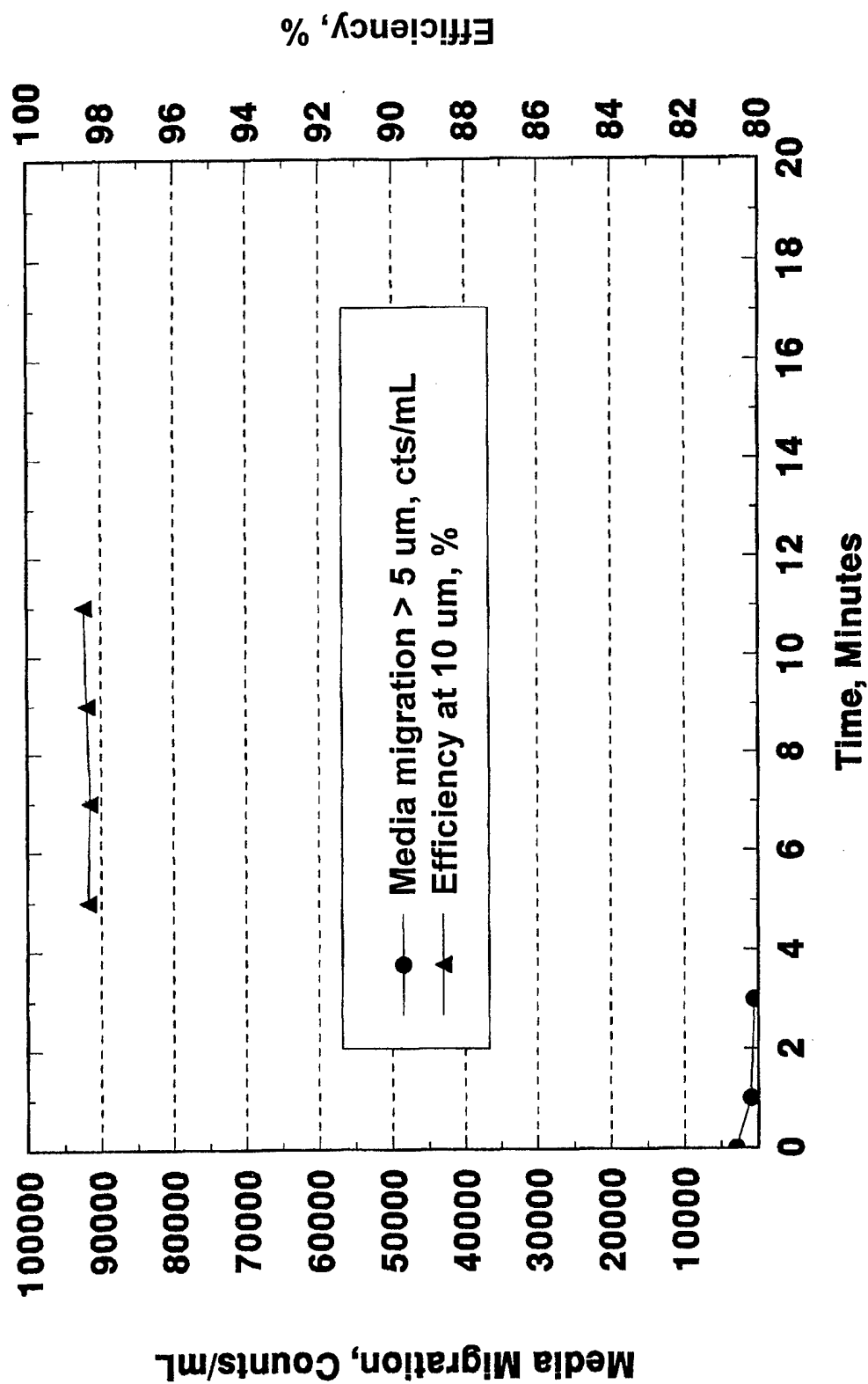
AC Fuel Filter Evaluation 30% Biodiesel 70% Cat 1-H, 3 Month



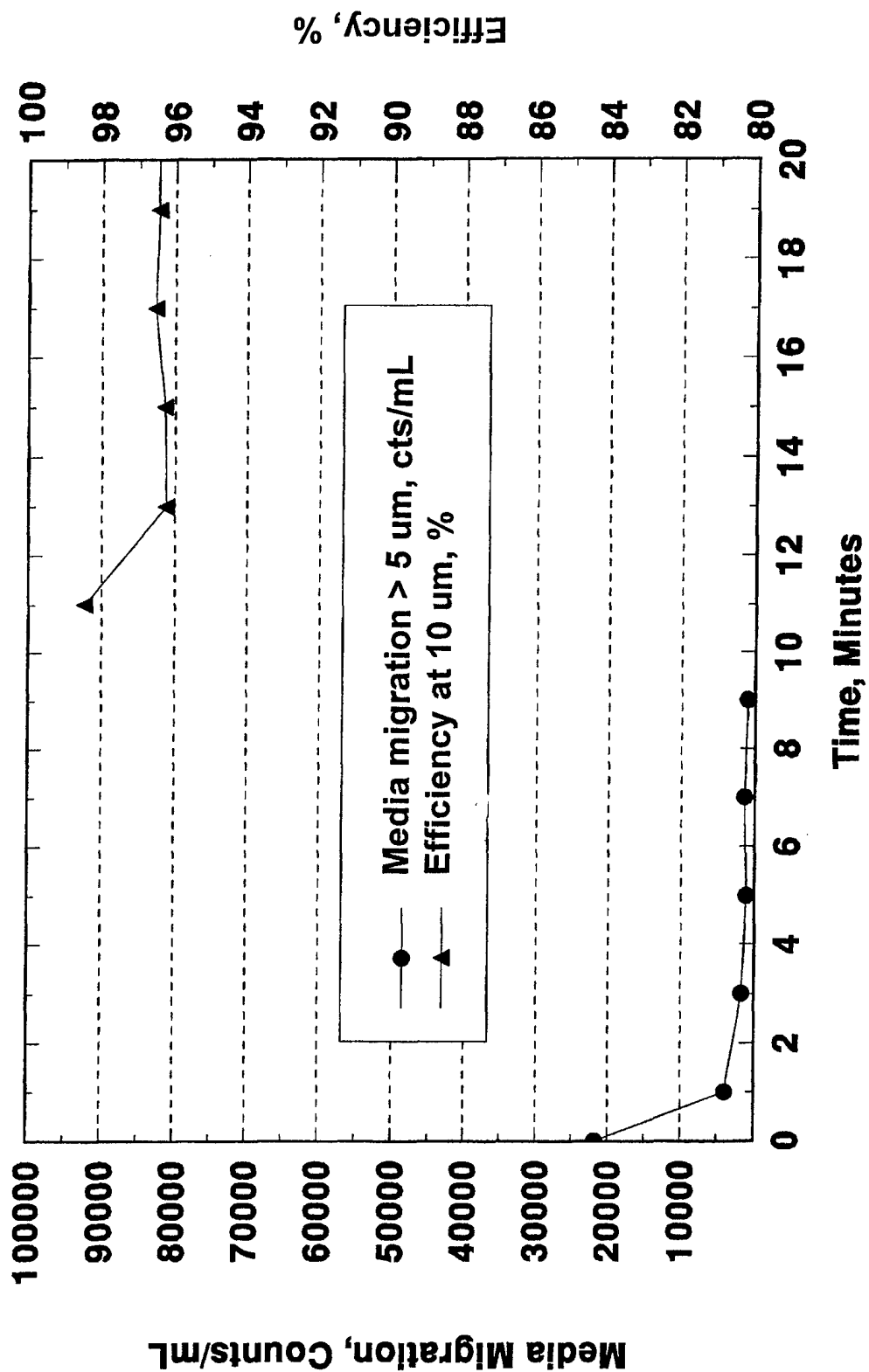
AC Fuel Filter Evaluation 30% Biodiesel 70% Cat 1-H, 6 Month



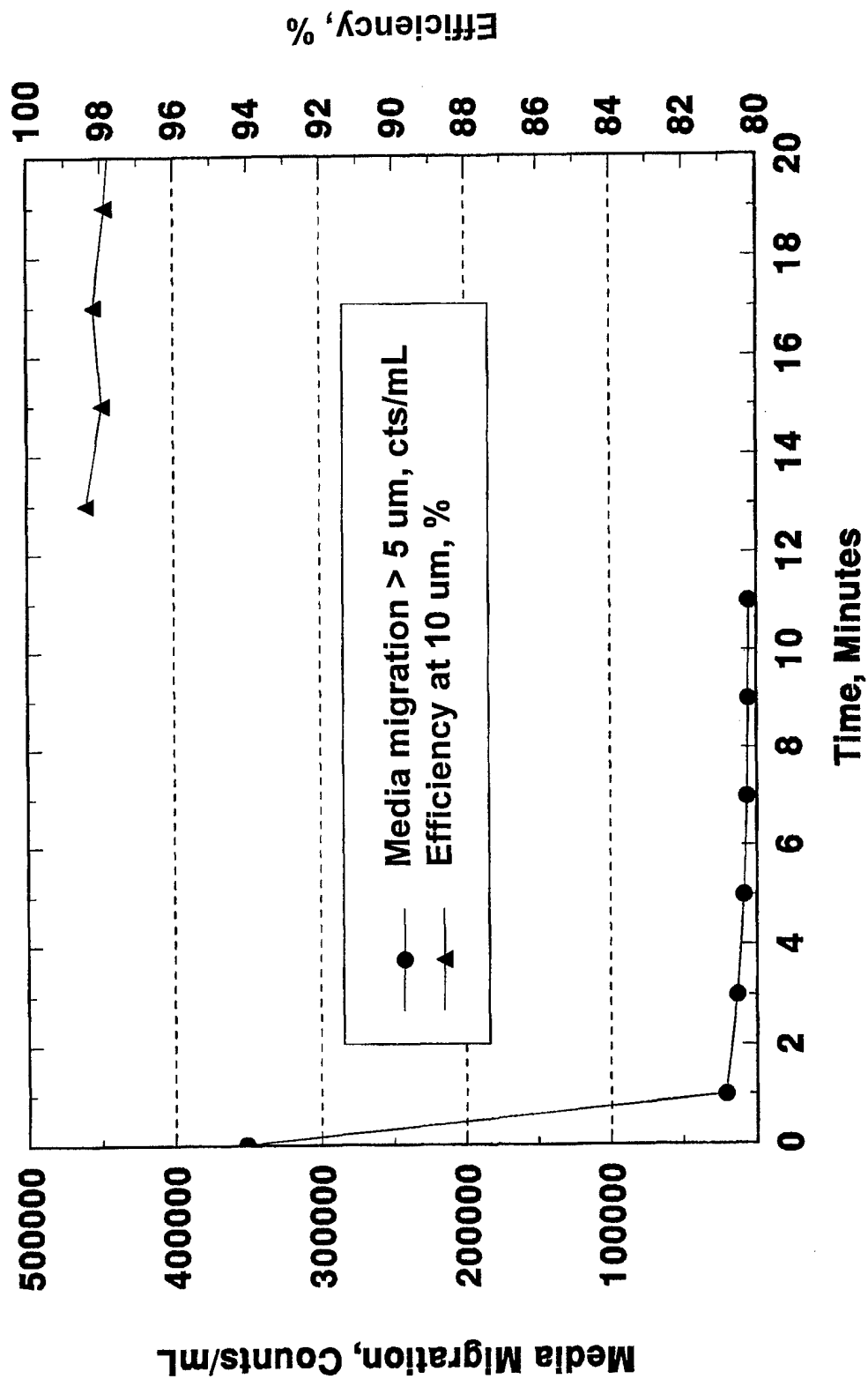
AC Fuel Filter Evaluation **20% Biodiesel/80% JP-8, 1 Month**



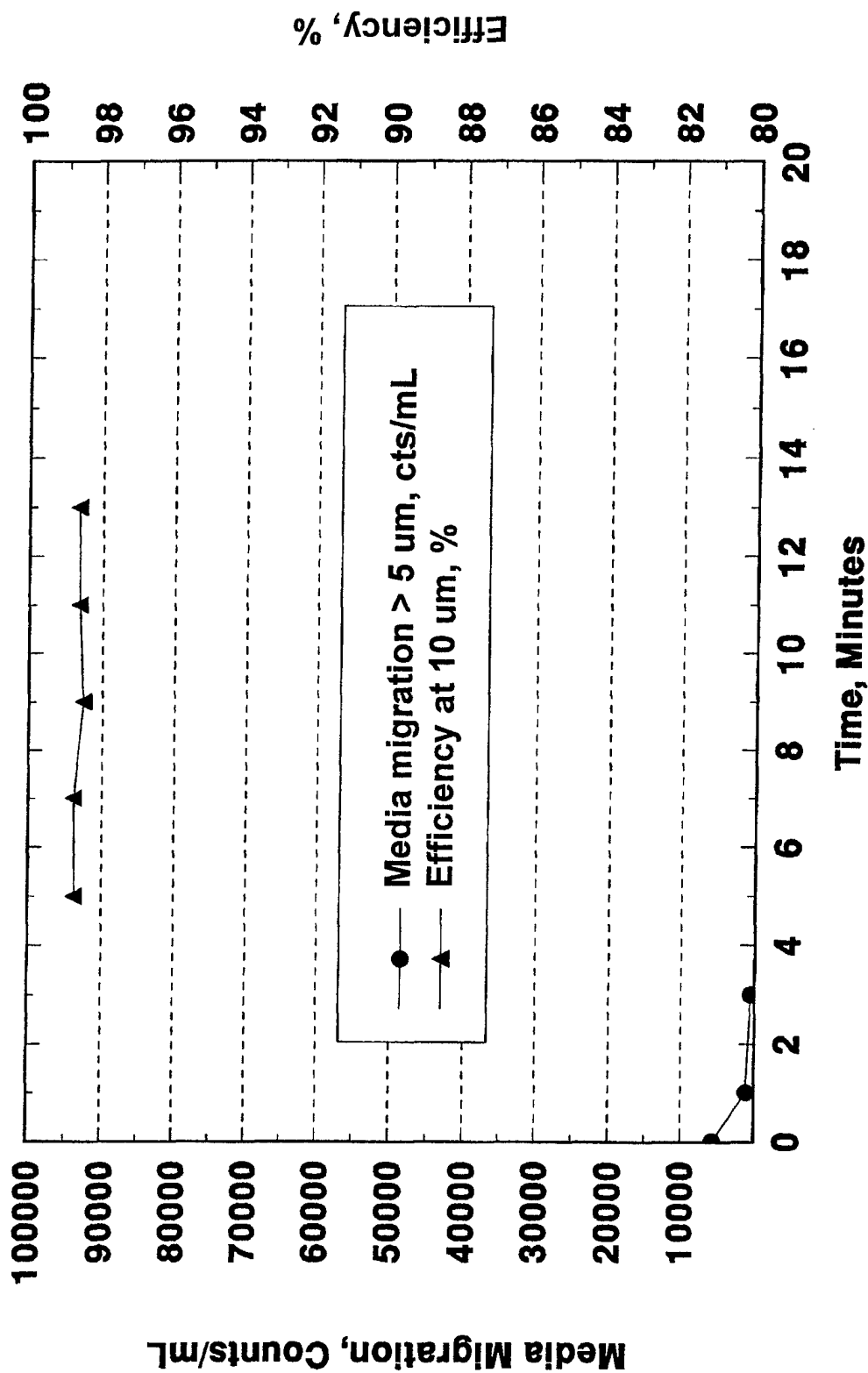
AC Fuel Filter Evaluation **20% Biodiesel/80% JP-8, 3 Month**



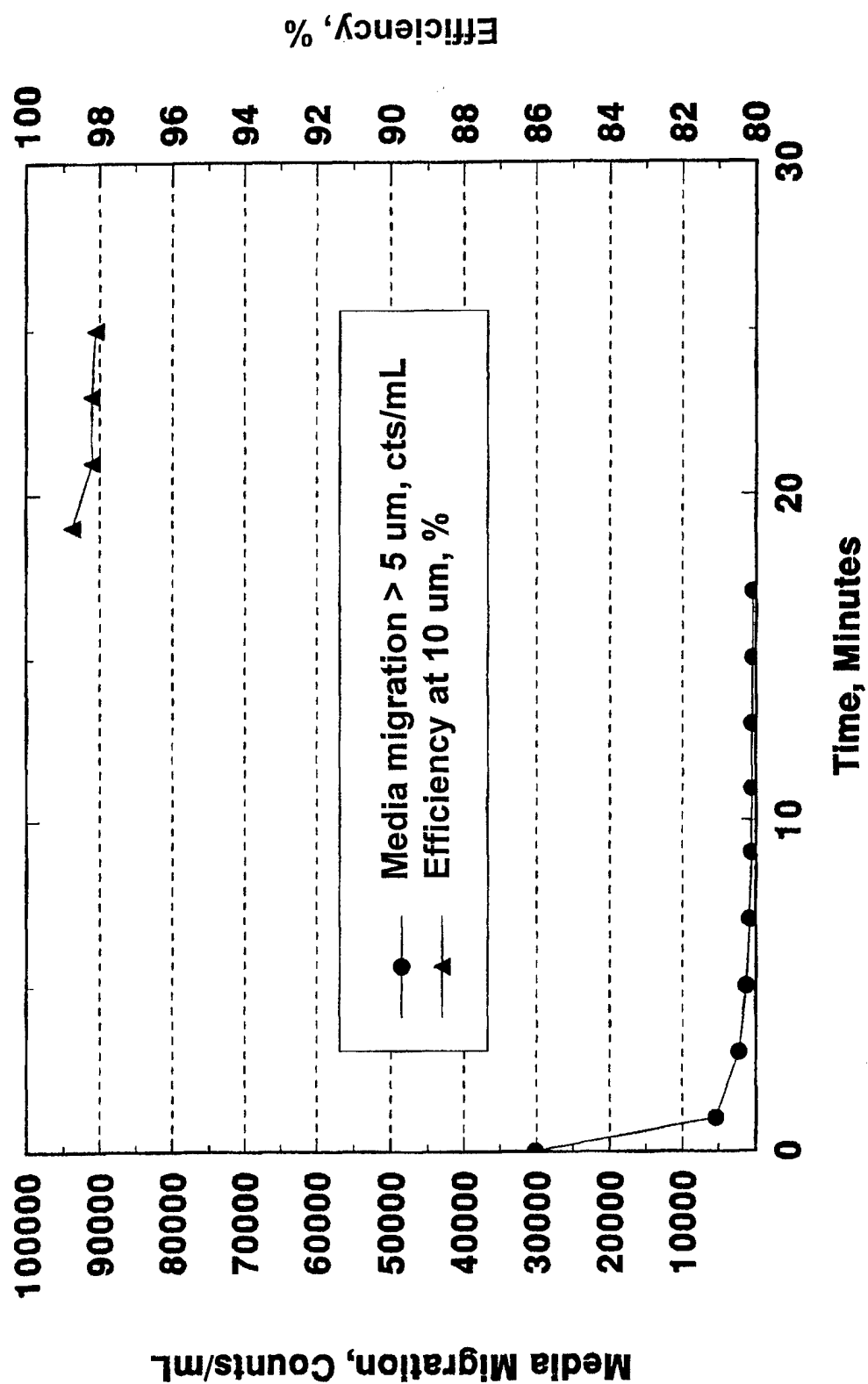
AC Fuel Filter Evaluation **20% Biodiesel/80% JP-8, 6 Month**



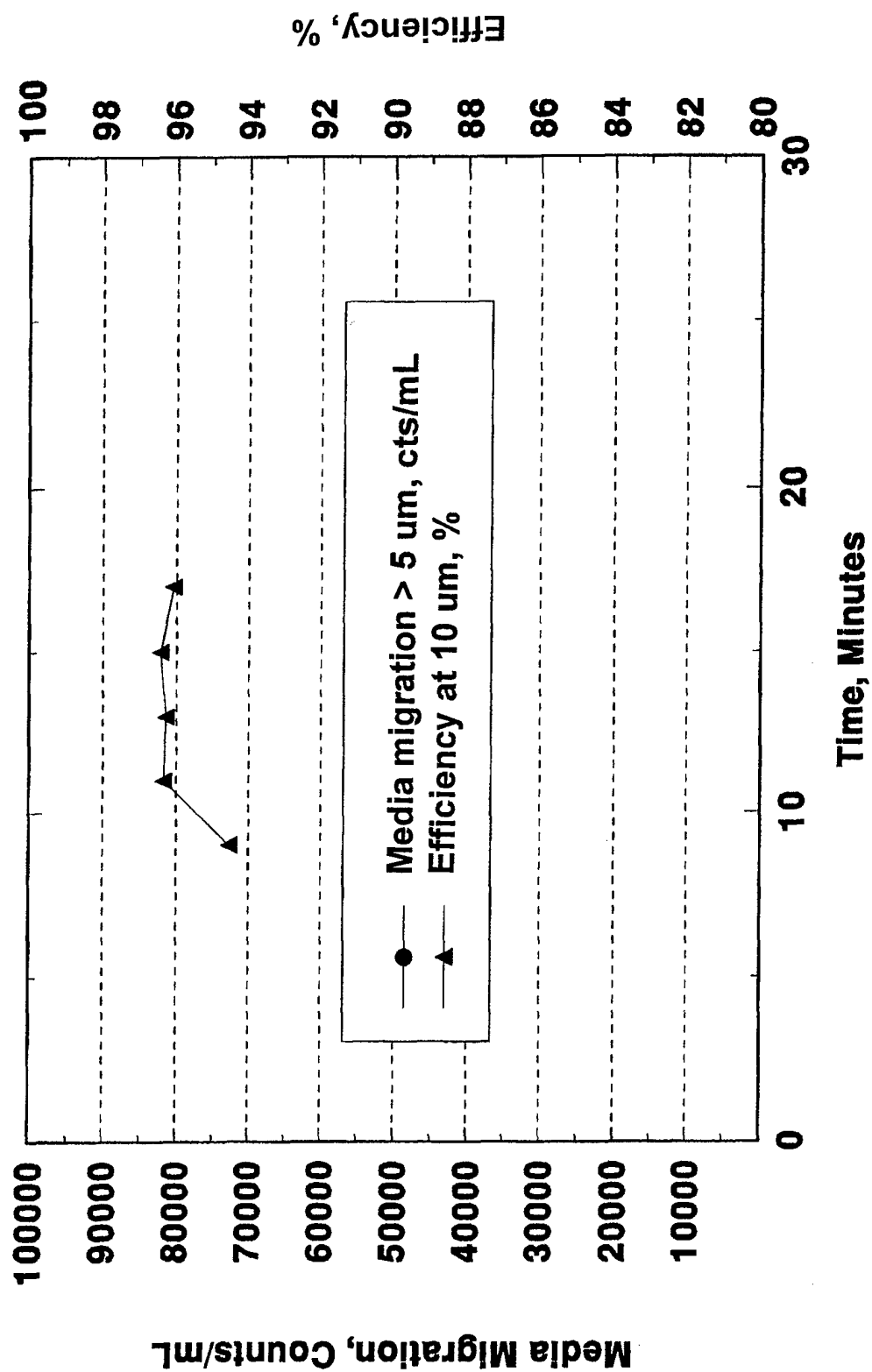
AC Fuel Filter Evaluation 30% Biodiesel/70% JP-8, 1 Month



AC Fuel Filter Evaluation **30% Biodiesel/70% JP-8, 3 Month**



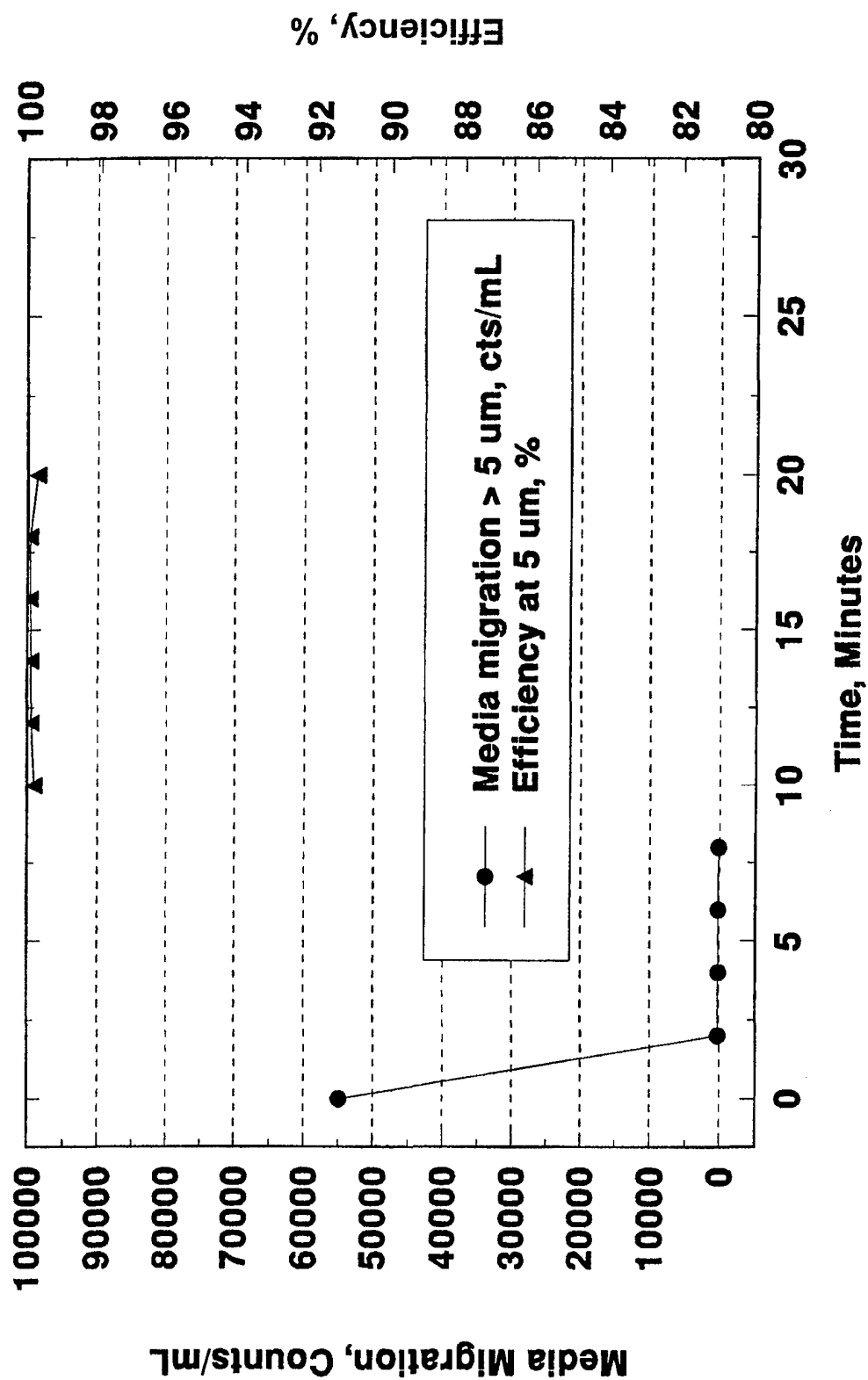
AC Fuel Filter Evaluation 30% Biodiesel/70% JP-8, 6 Month



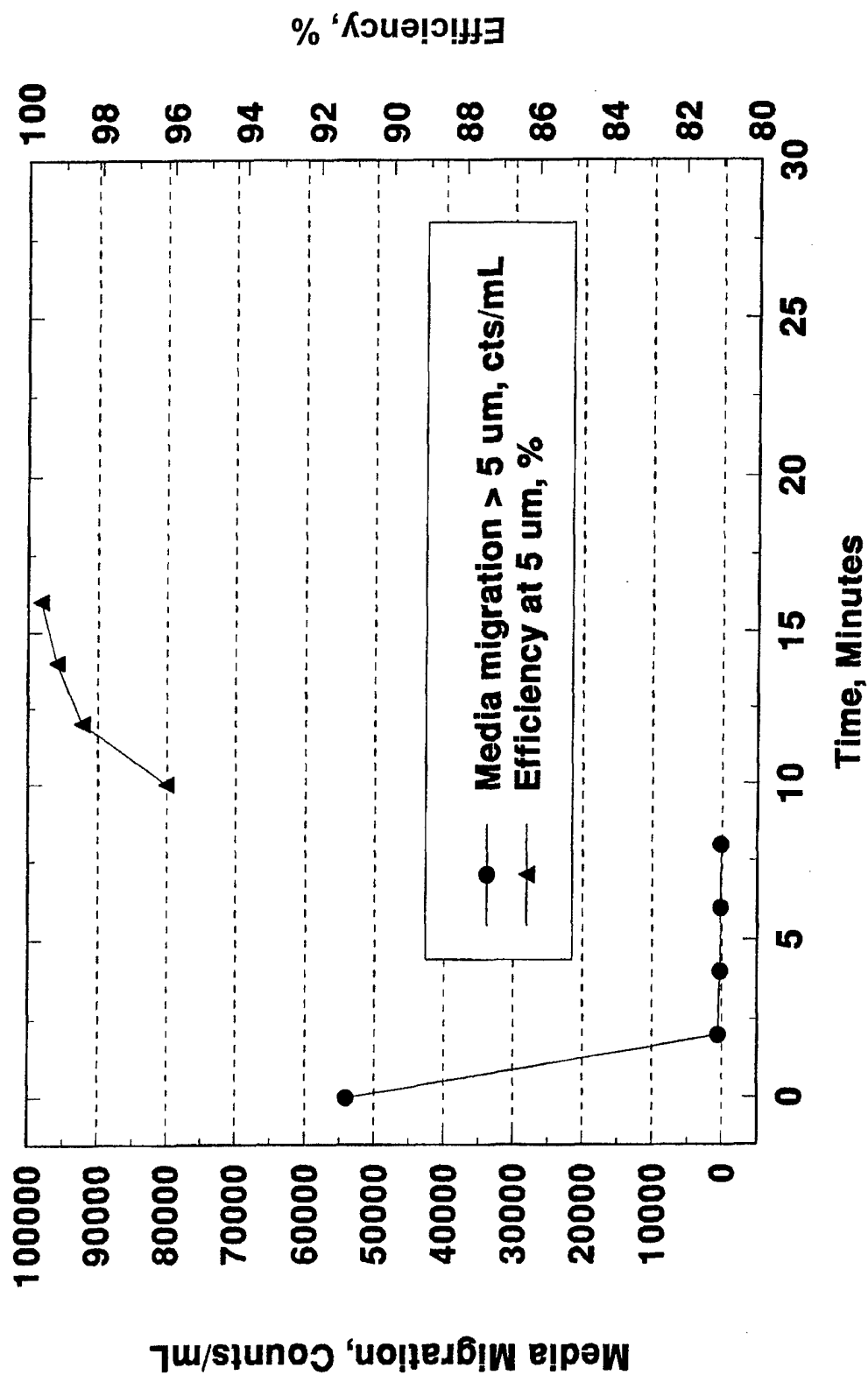
APPENDIX G

HMMWV Single-Pass Filter Evaluation

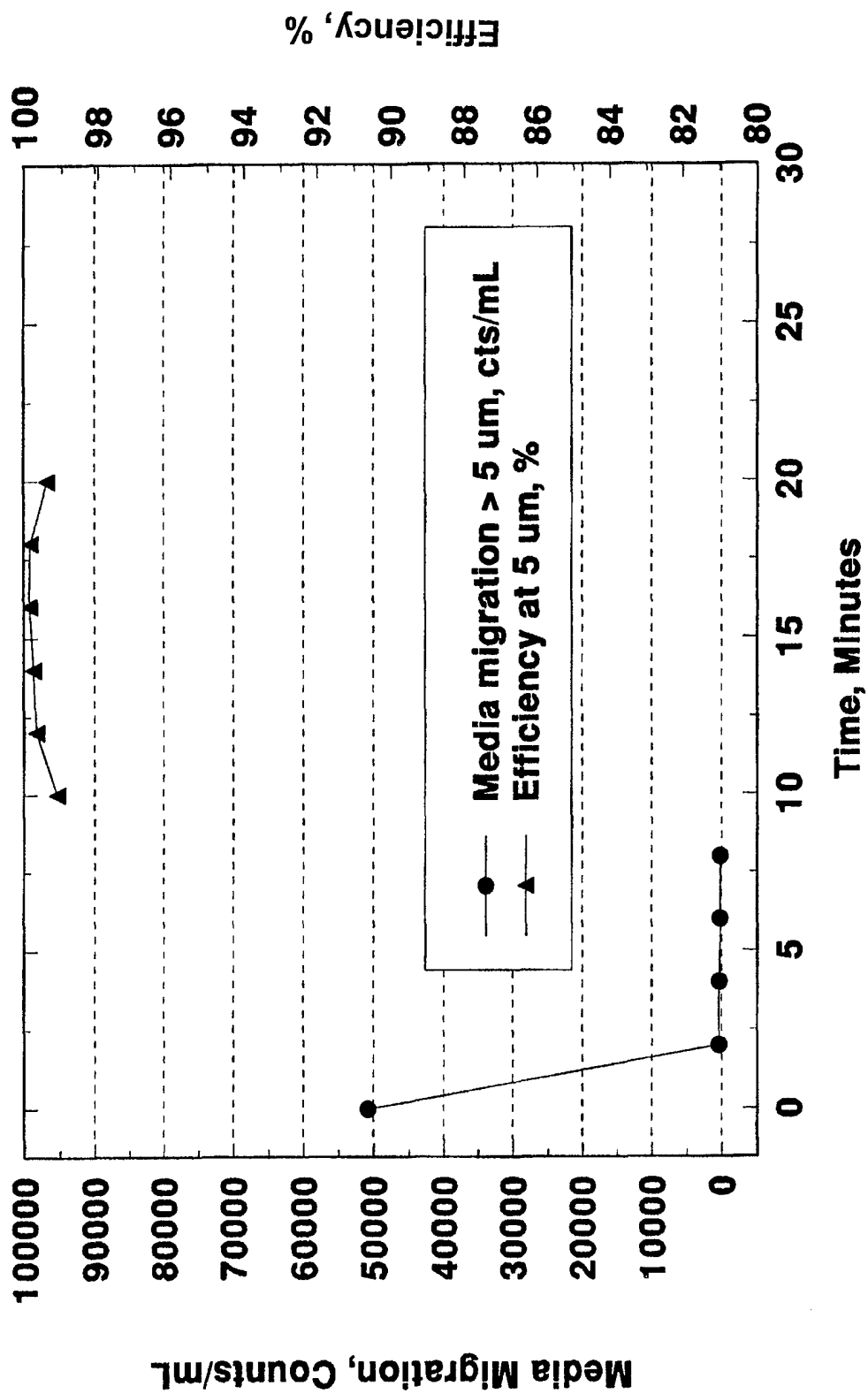
Kaydon Fuel Filter Evaluation **JP-8, 3 Month**



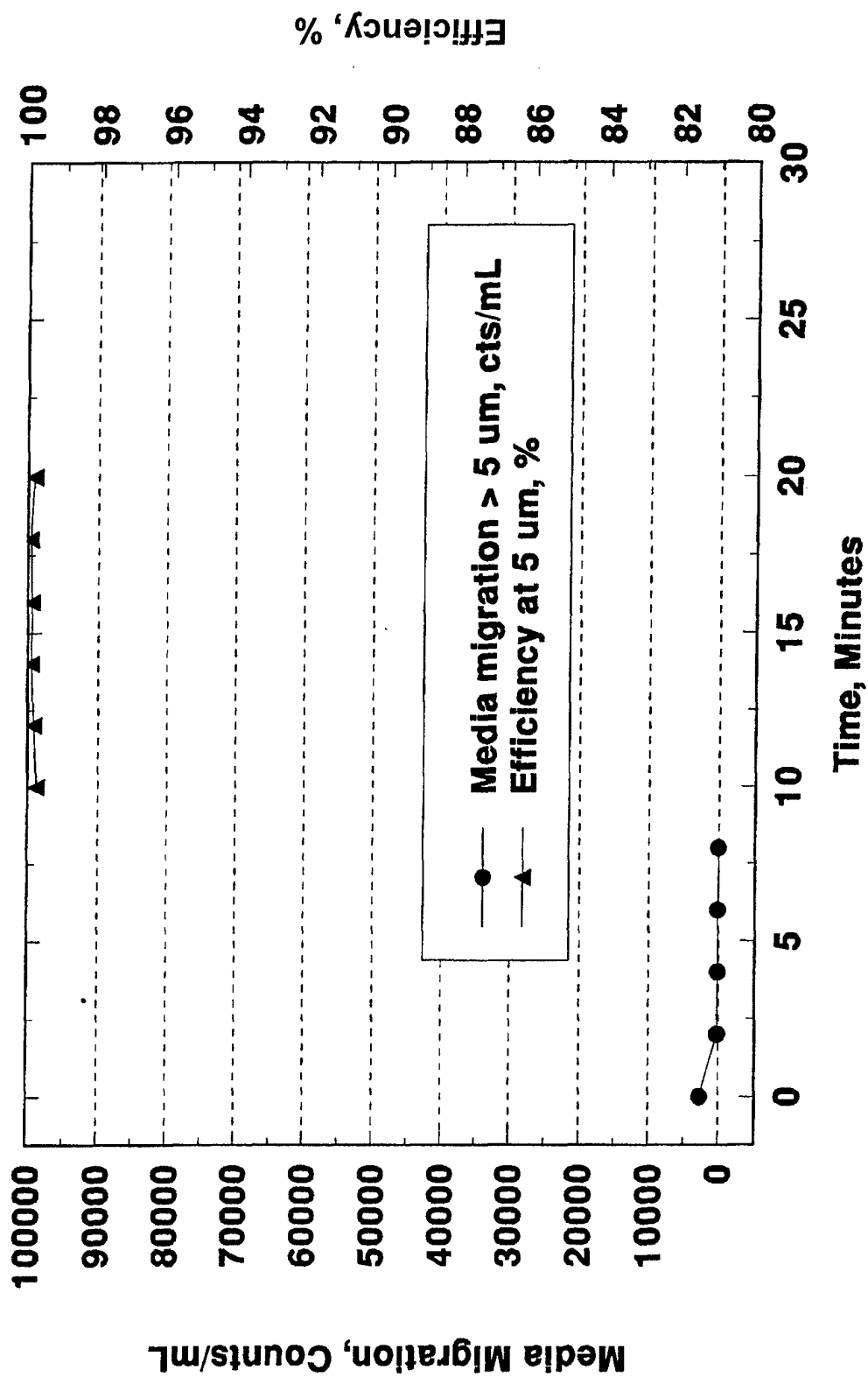
Kaydon Fuel Filter Evaluation Baseline



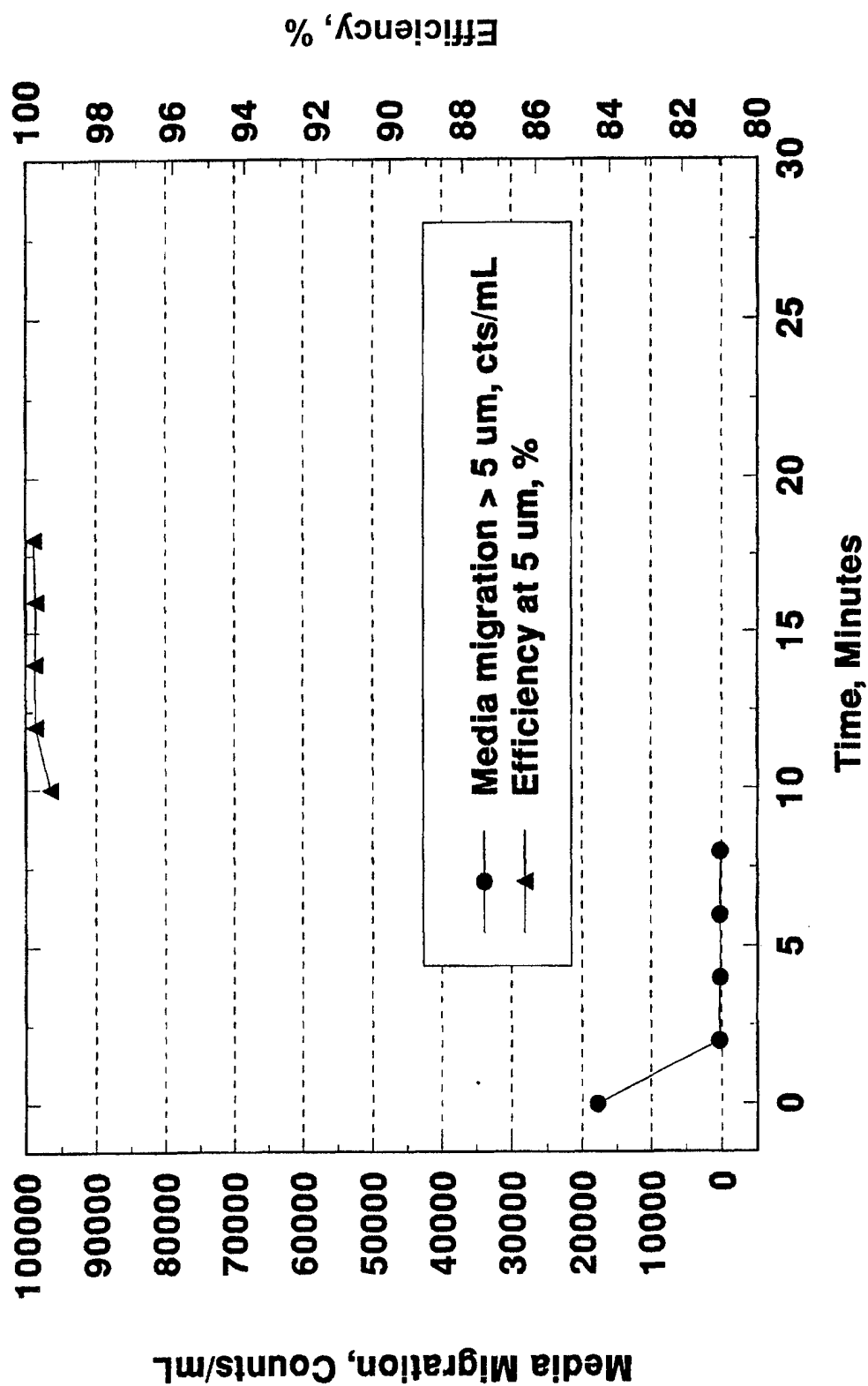
Kaydon Fuel Filter Evaluation **JP-8, 1 Month**



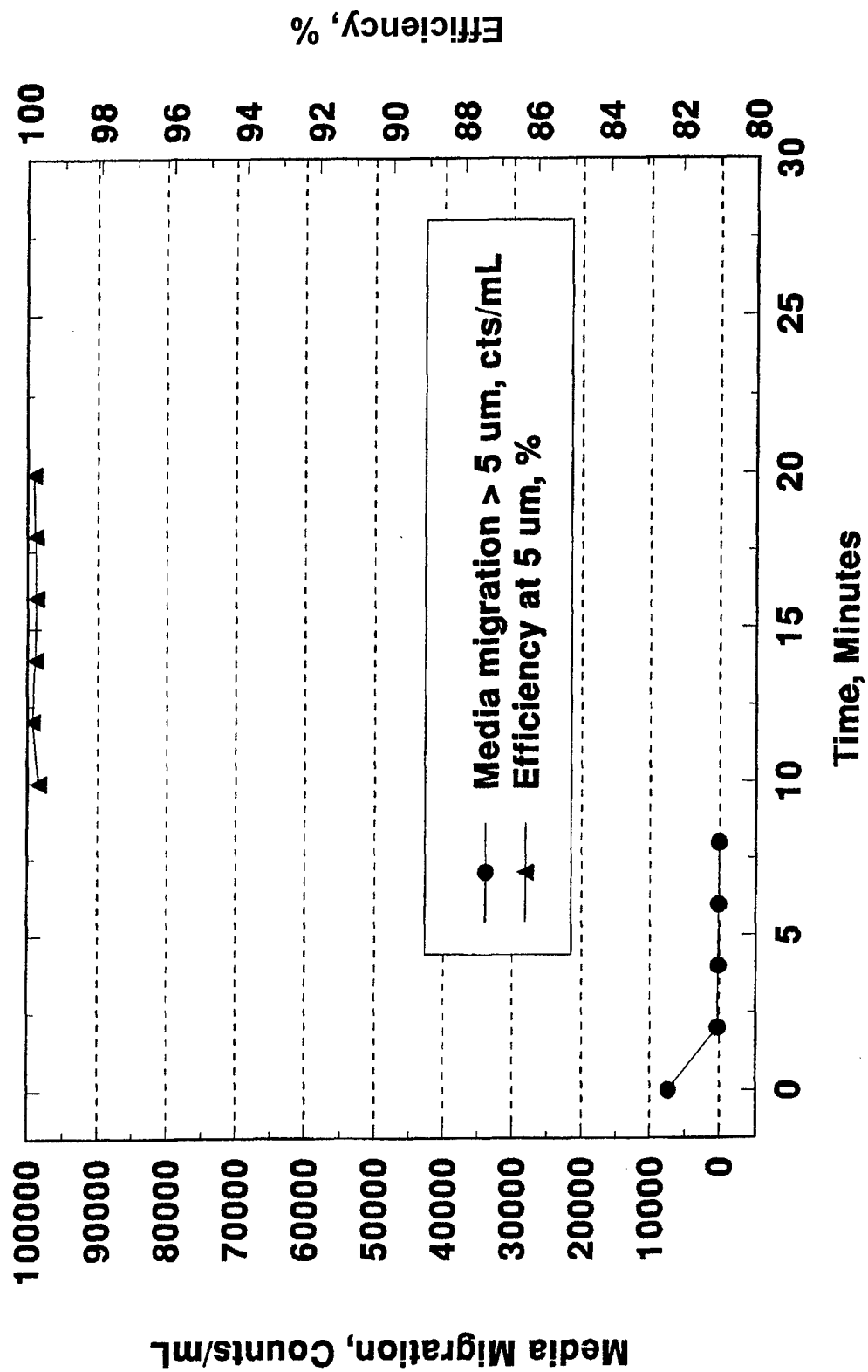
Kaydon Fuel Filter Evaluation **JP-8, 6 Month**



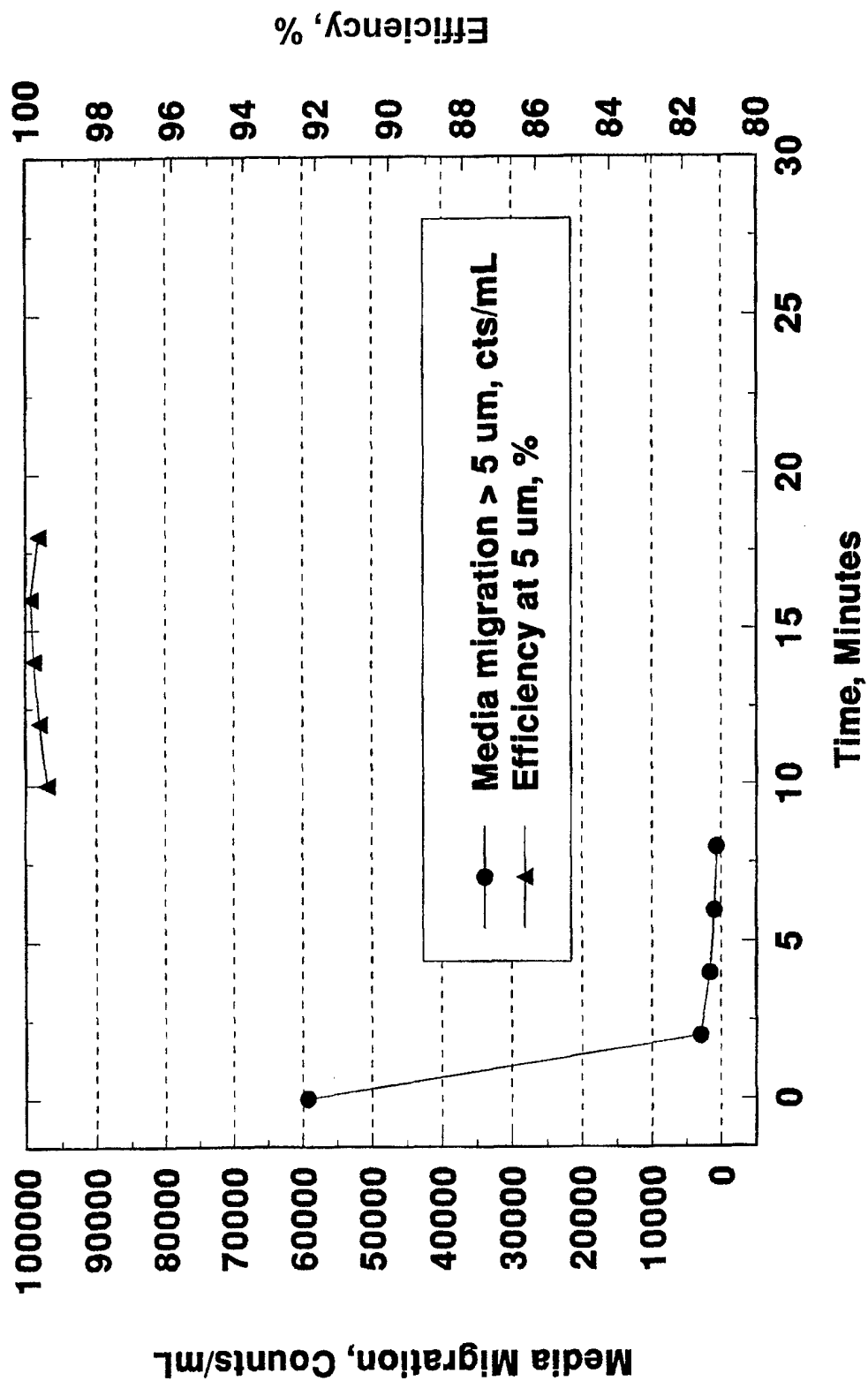
Kaydon Fuel Filter Evaluation **Biodiesel, 1 Month**



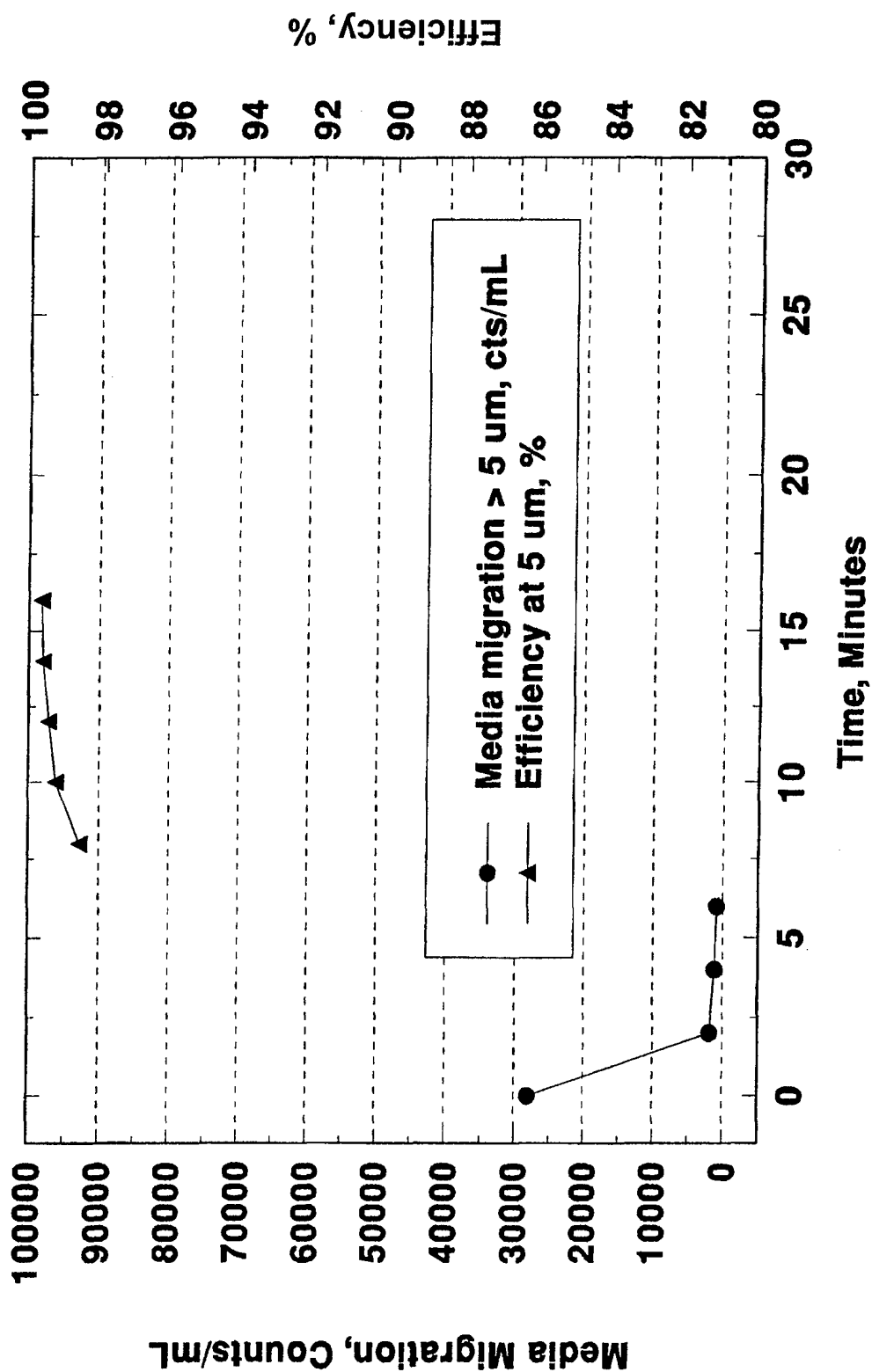
Kaydon Fuel Filter Evaluation **Biodiesel, 3 Month**



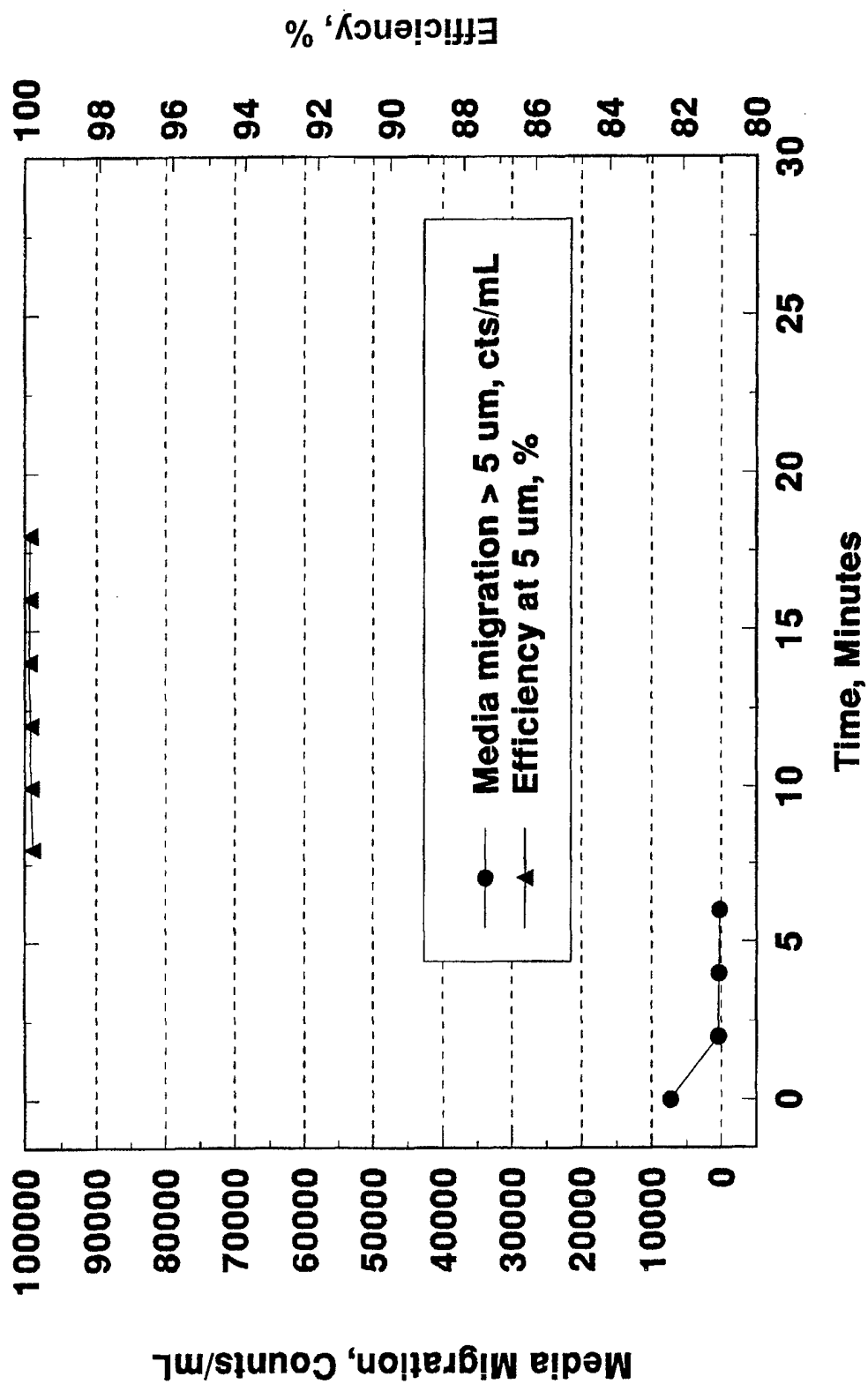
Kaydon Fuel Filter Evaluation **Biodiesel, 6 Month**



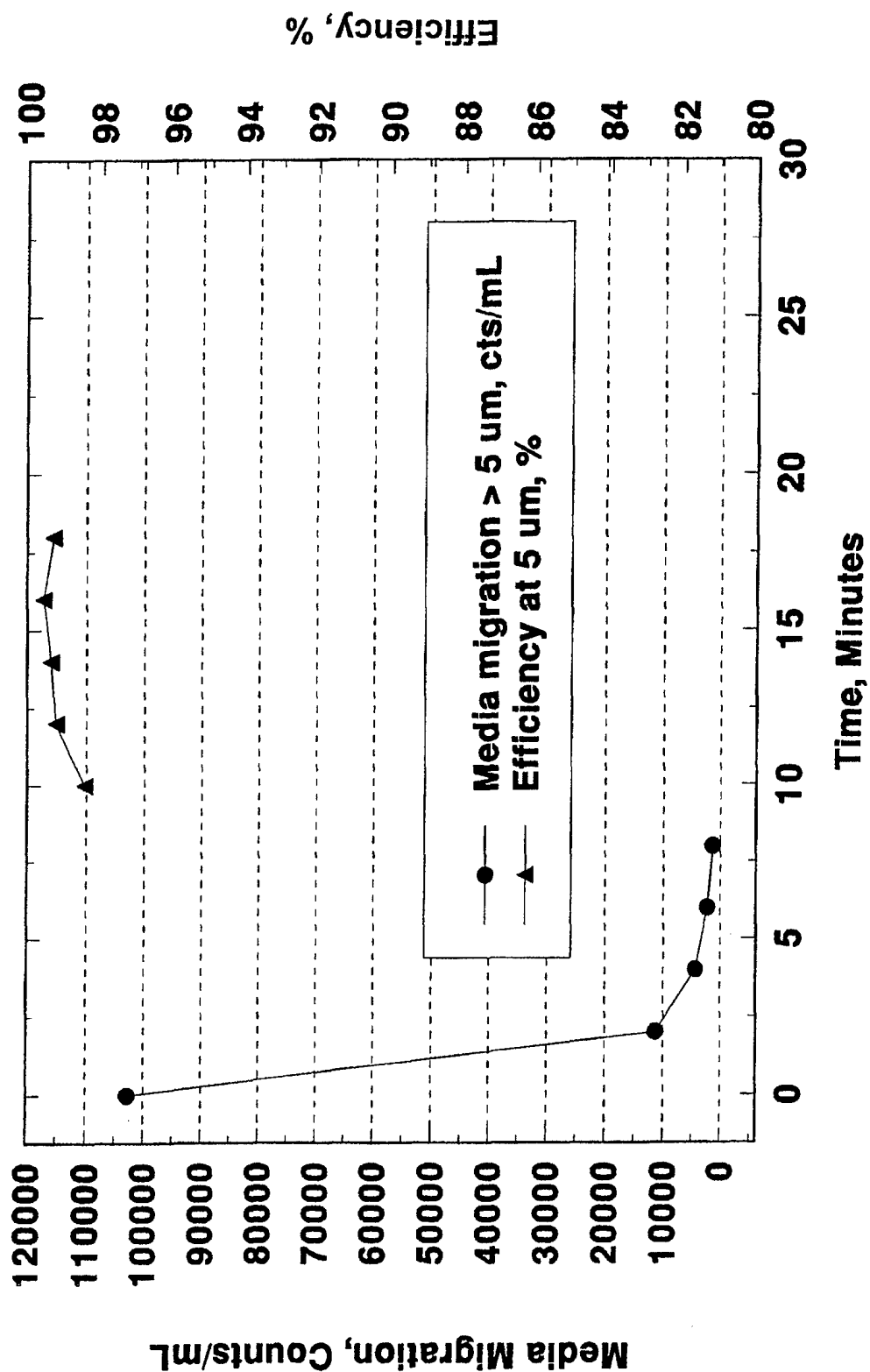
Kaydon Fuel Filter Evaluation **Low-Sulfur Diesel Fuel, 1 Month**



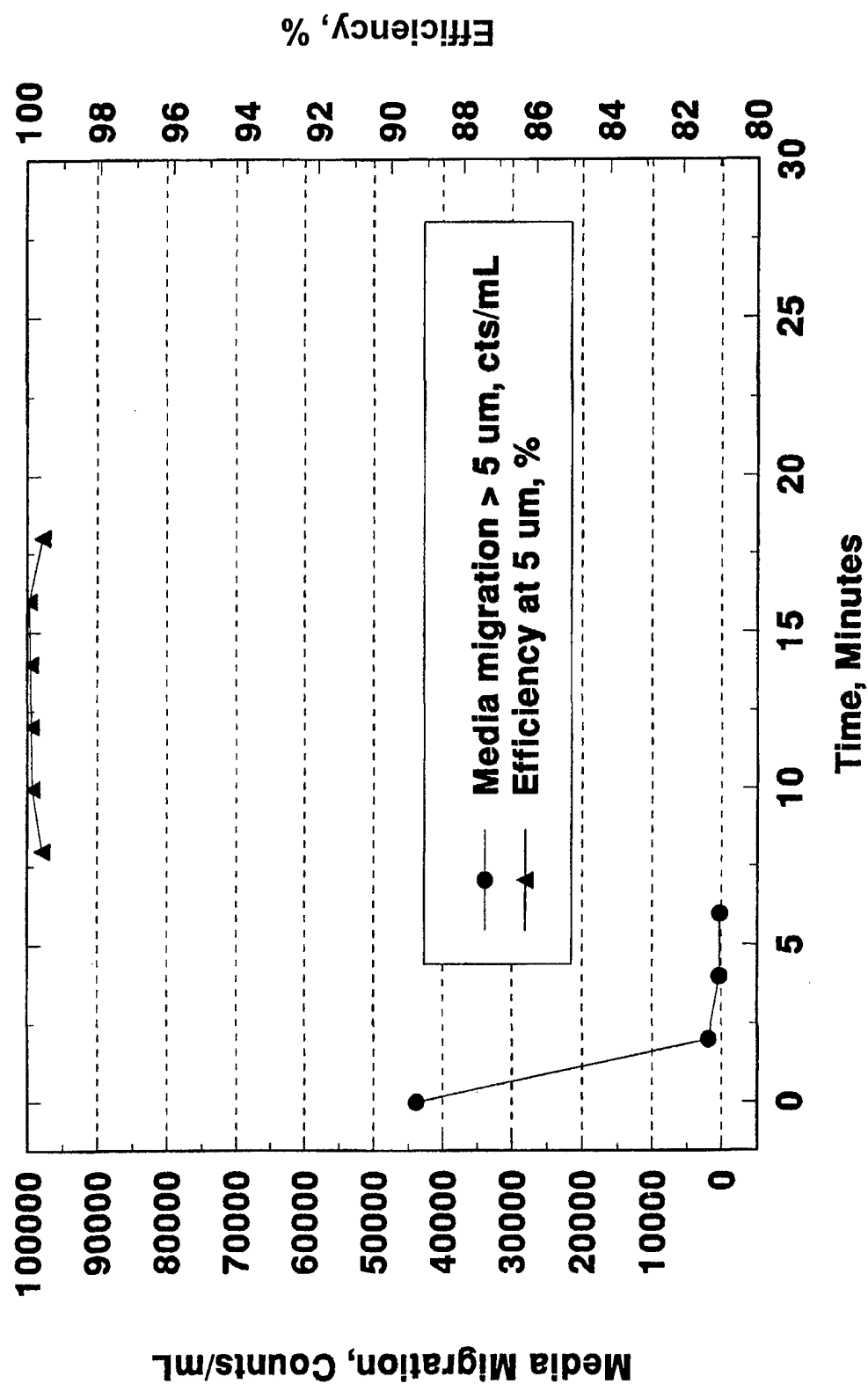
Kaydon Fuel Filter Evaluation **Low-Sulfur Diesel Fuel, 3 Months**



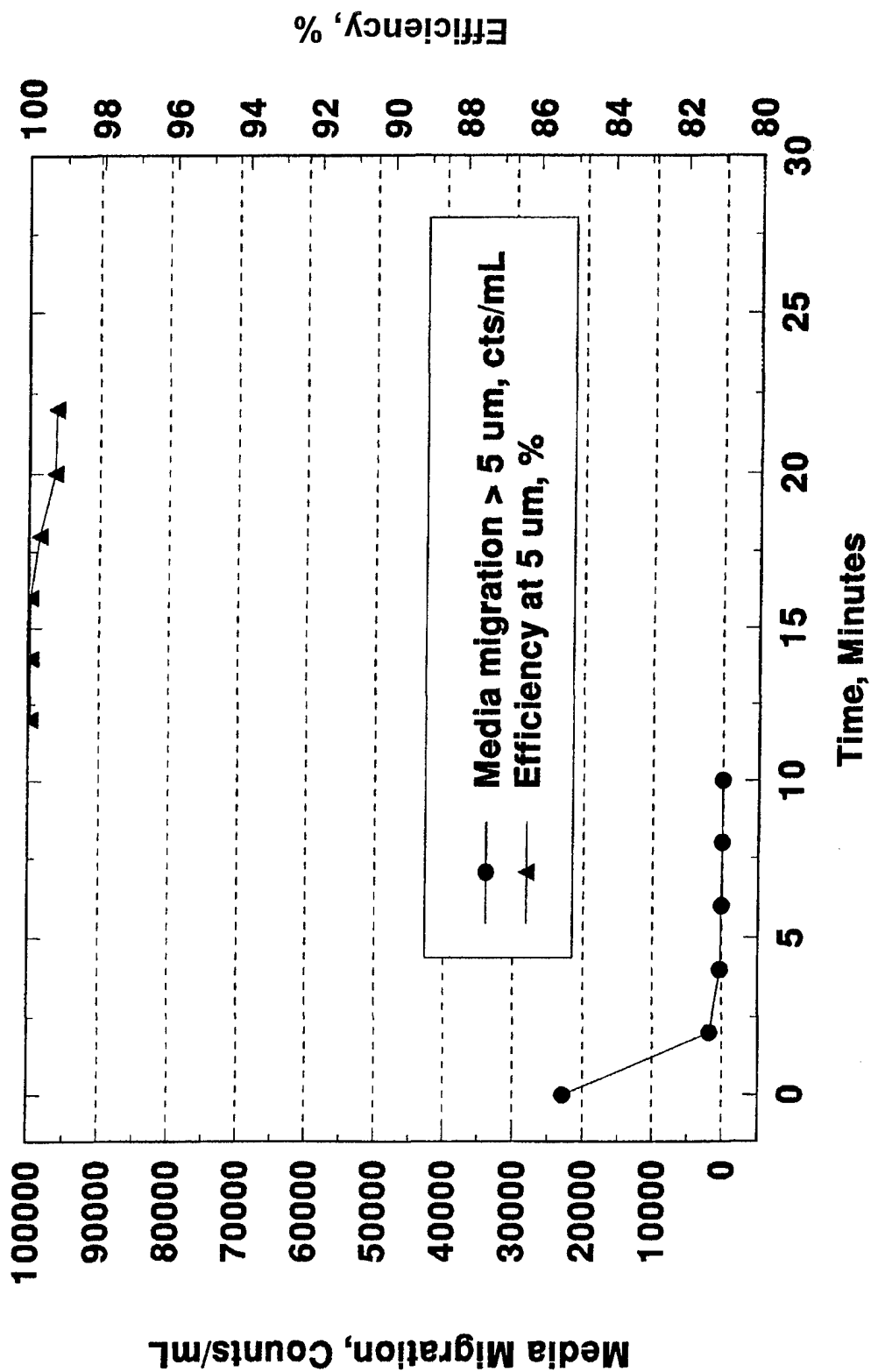
Kaydon Fuel Filter Evaluation **Low-Sulfur Diesel Fuel, 6 Month**



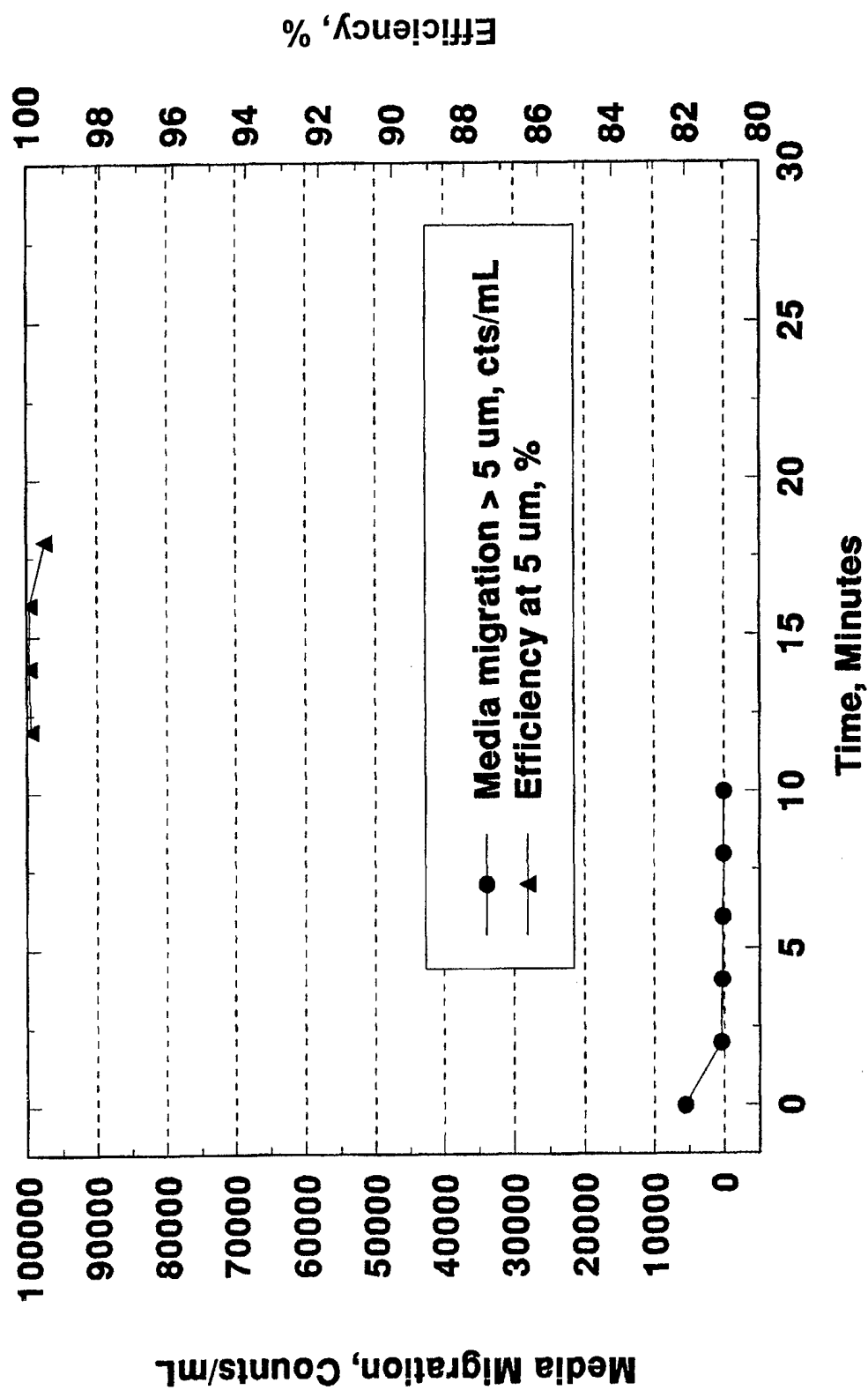
Kaydon Fuel Filter Evaluation **Cat 1-H, 1 Month**



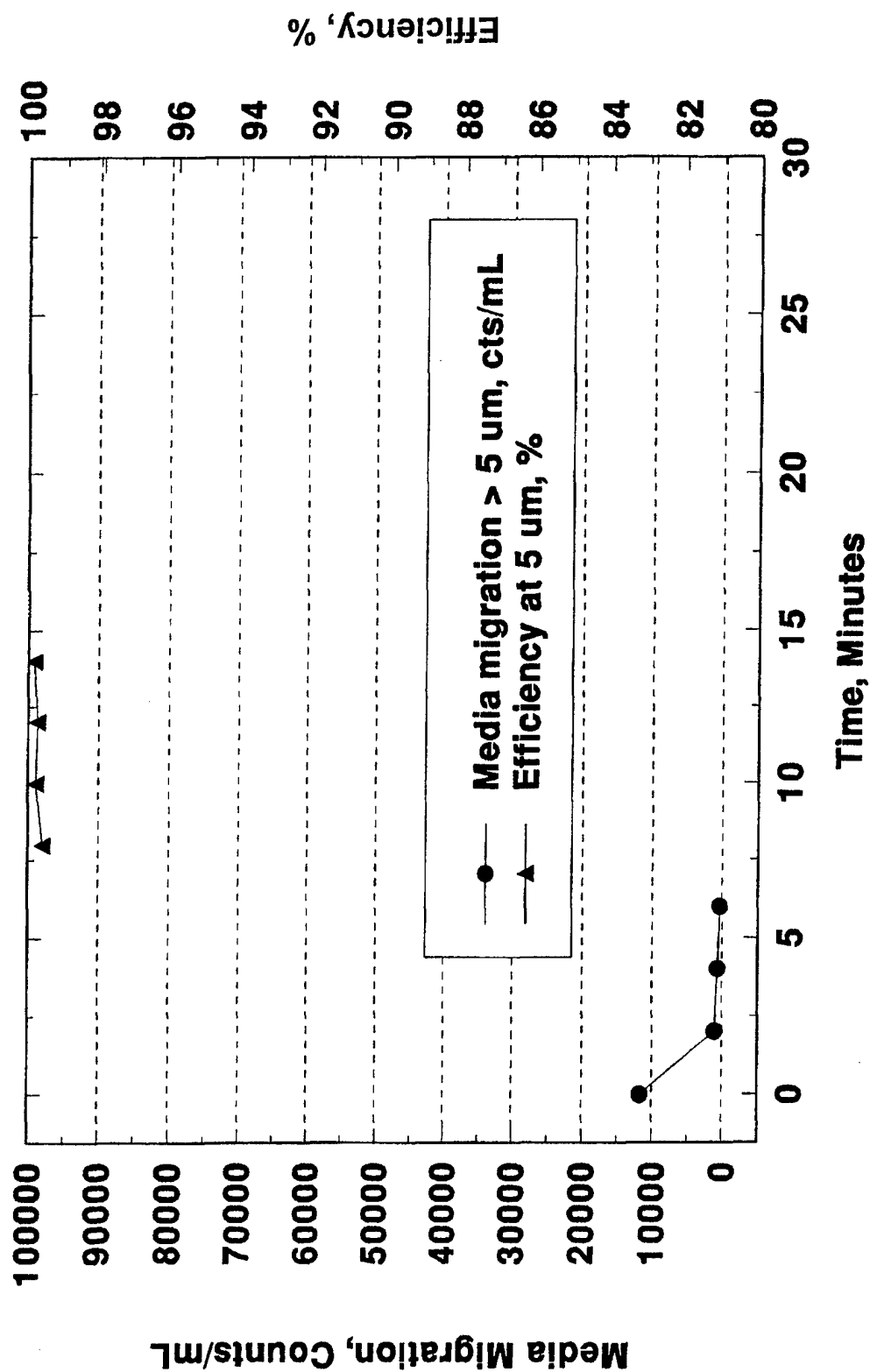
Kaydon Fuel Filter Evaluation **Cat 1-H, 3 Month**



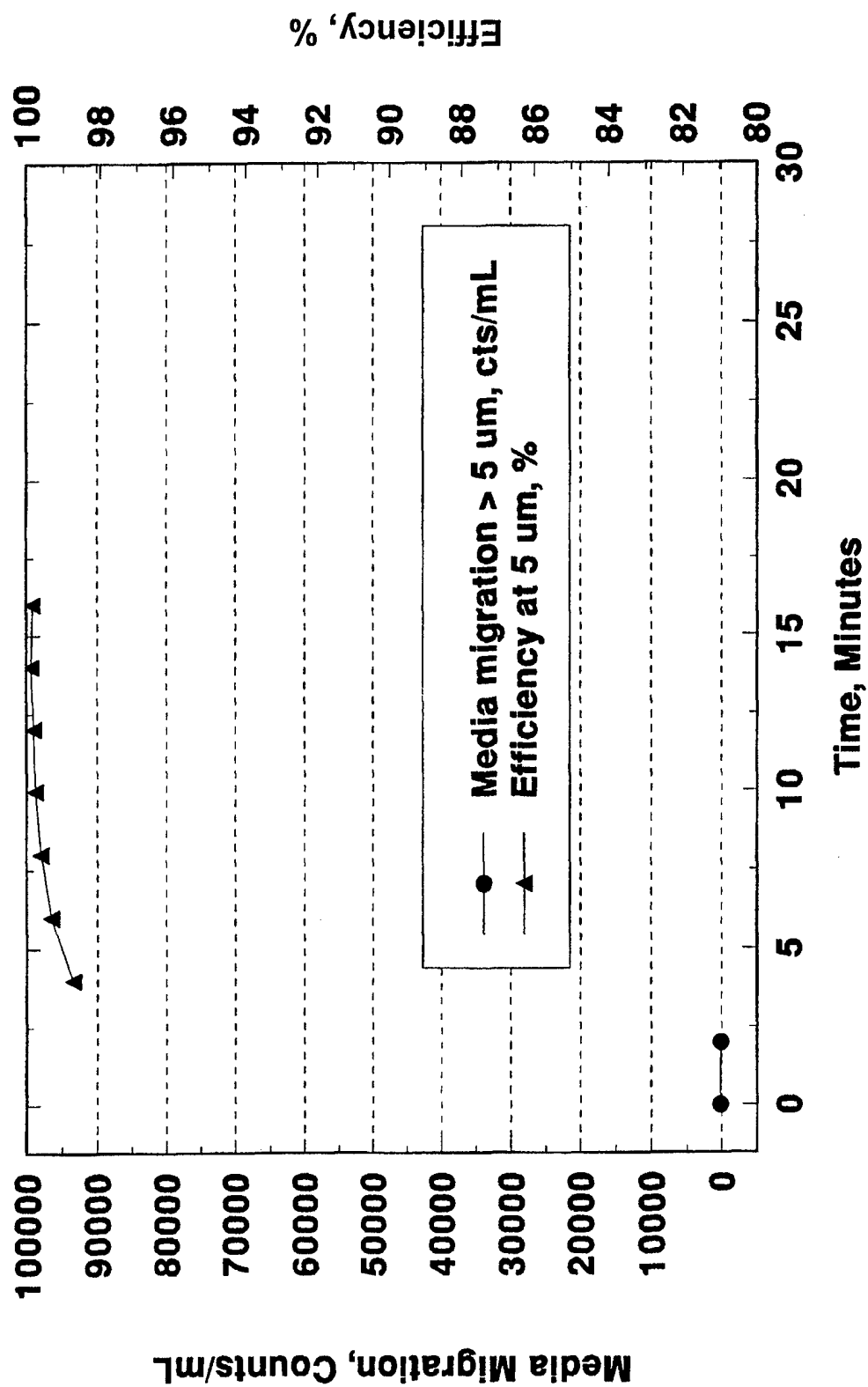
Kaydon Fuel Filter Evaluation **Cat 1-H, 6 Month**



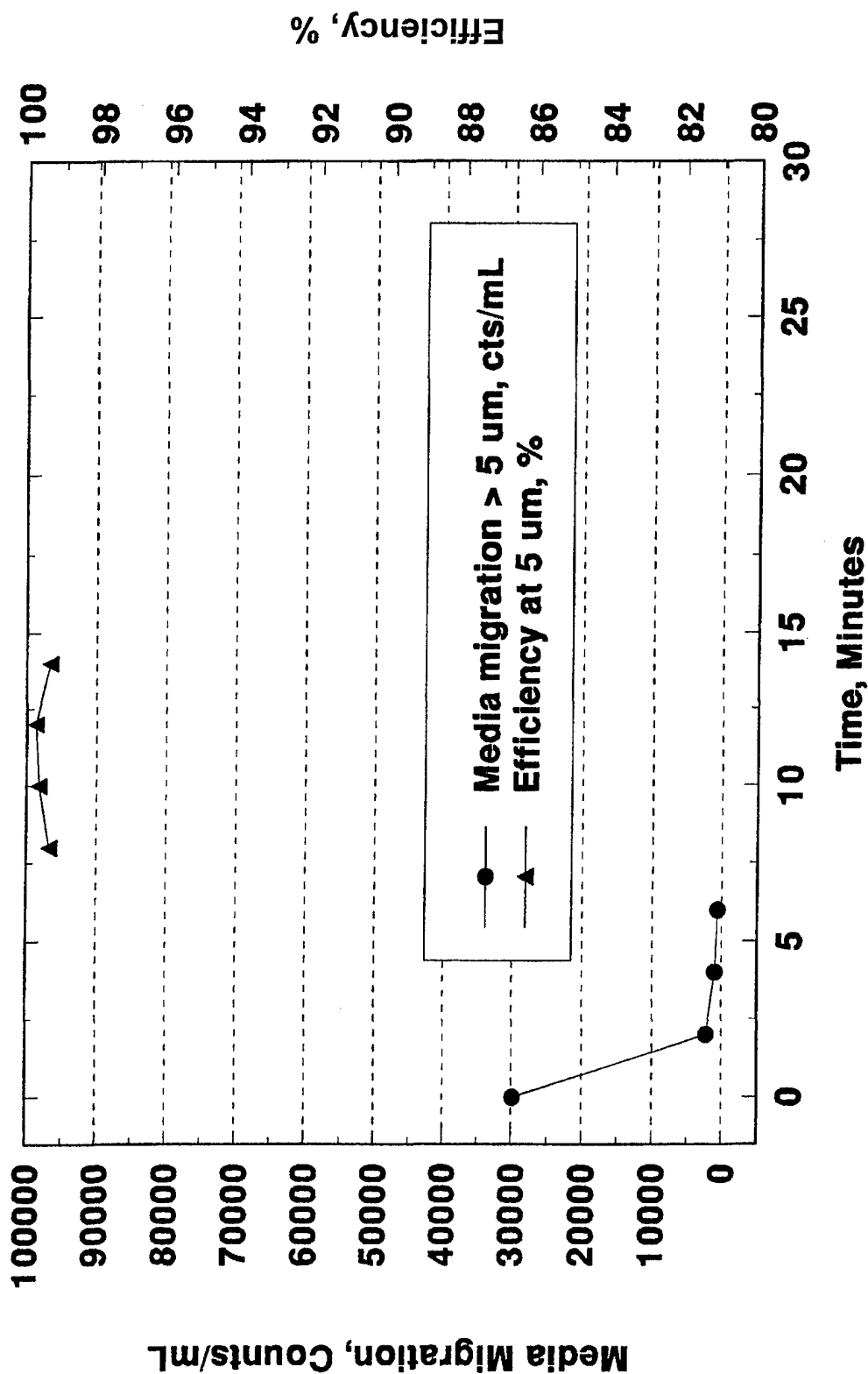
Kaydon Fuel Filter Evaluation **20% Biodiesel/80% Low-Sulfur Diesel Fuel, 1 Month**



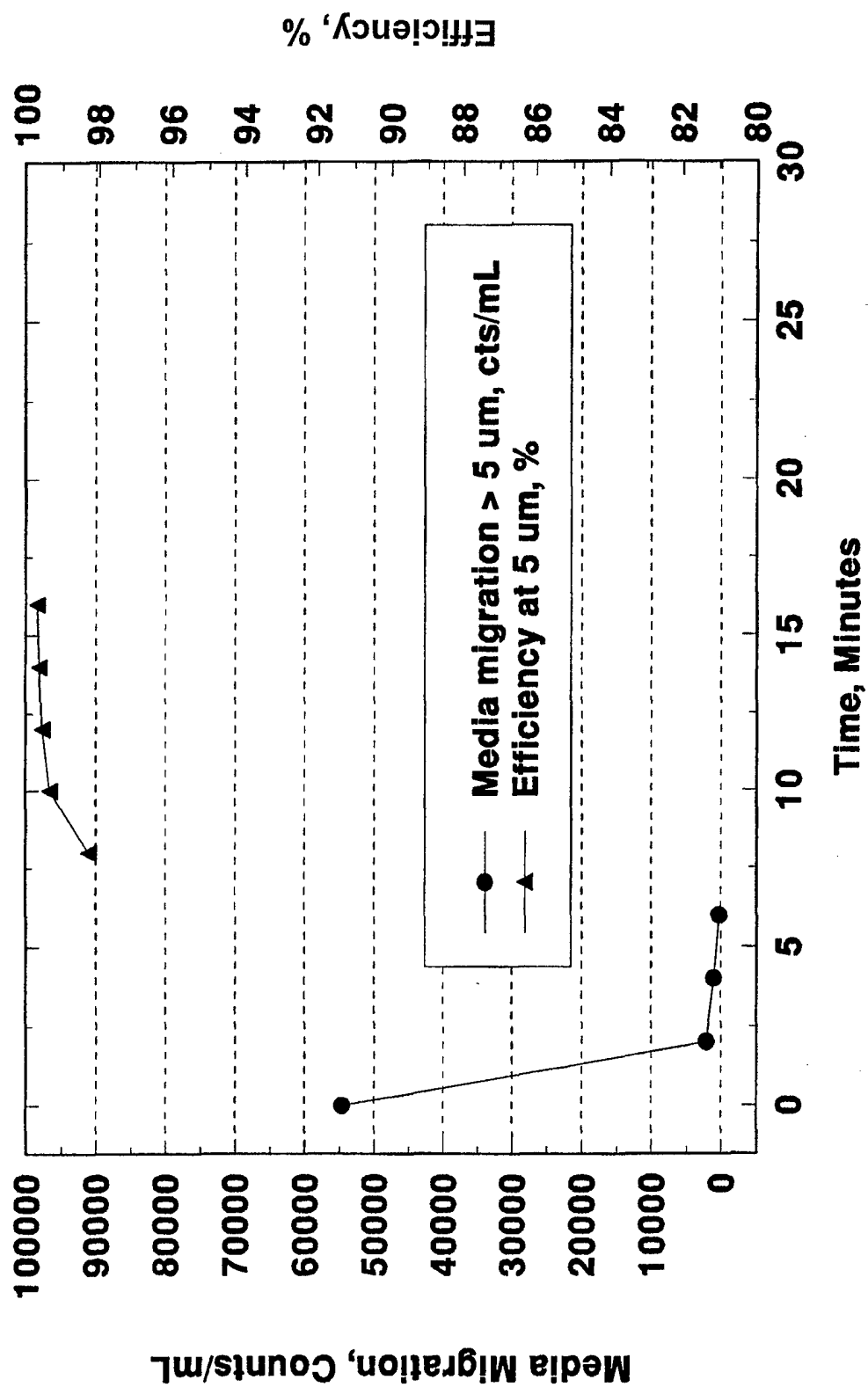
Kaydon Fuel Filter Evaluation **20% Biodiesel/80% Low-Sulfur Diesel Fuel, 3 Month**



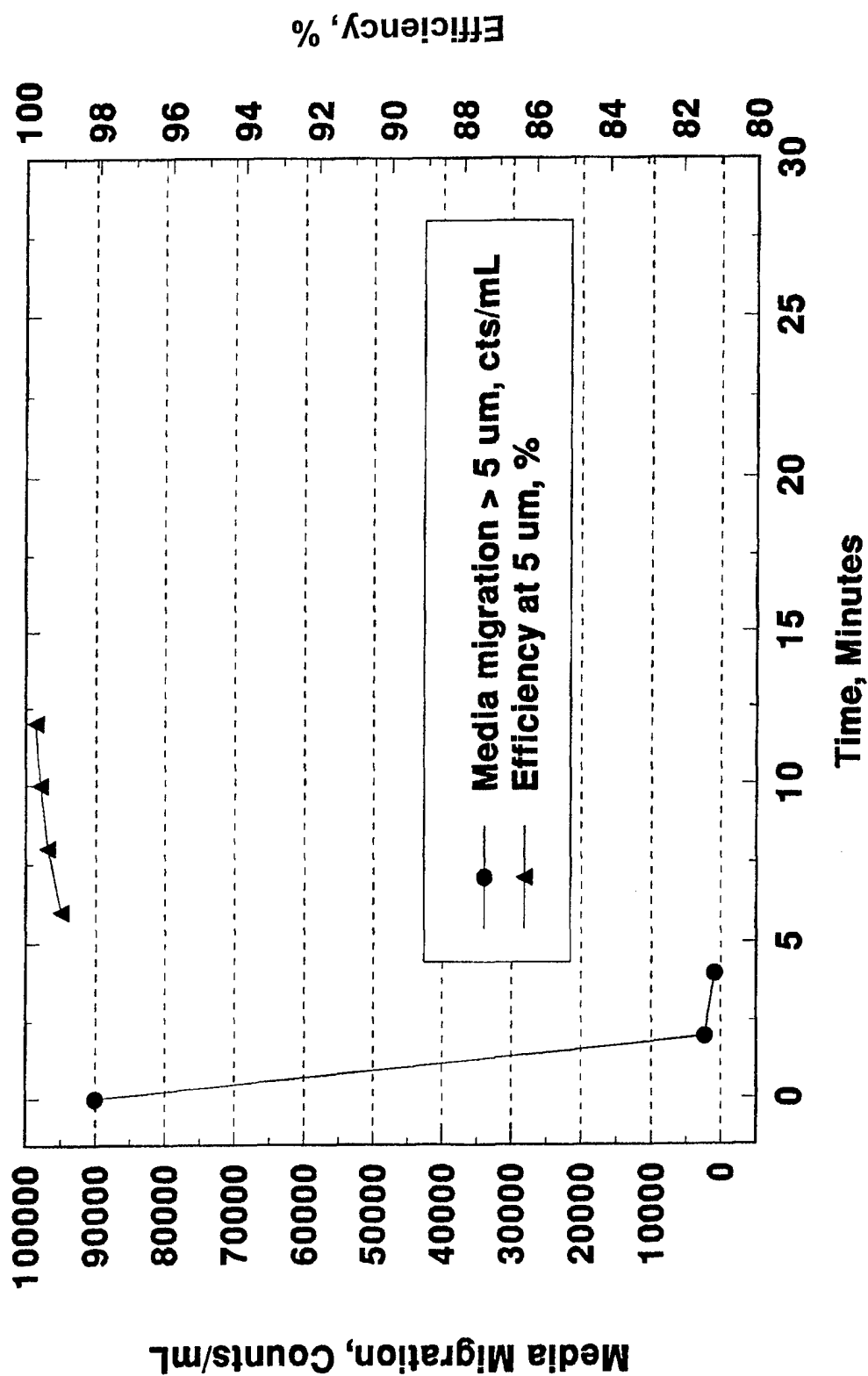
Kaydon Fuel Filter Evaluation **20% Biodiesel/80% Low-Sulfur Diesel Fuel, 6 Month**



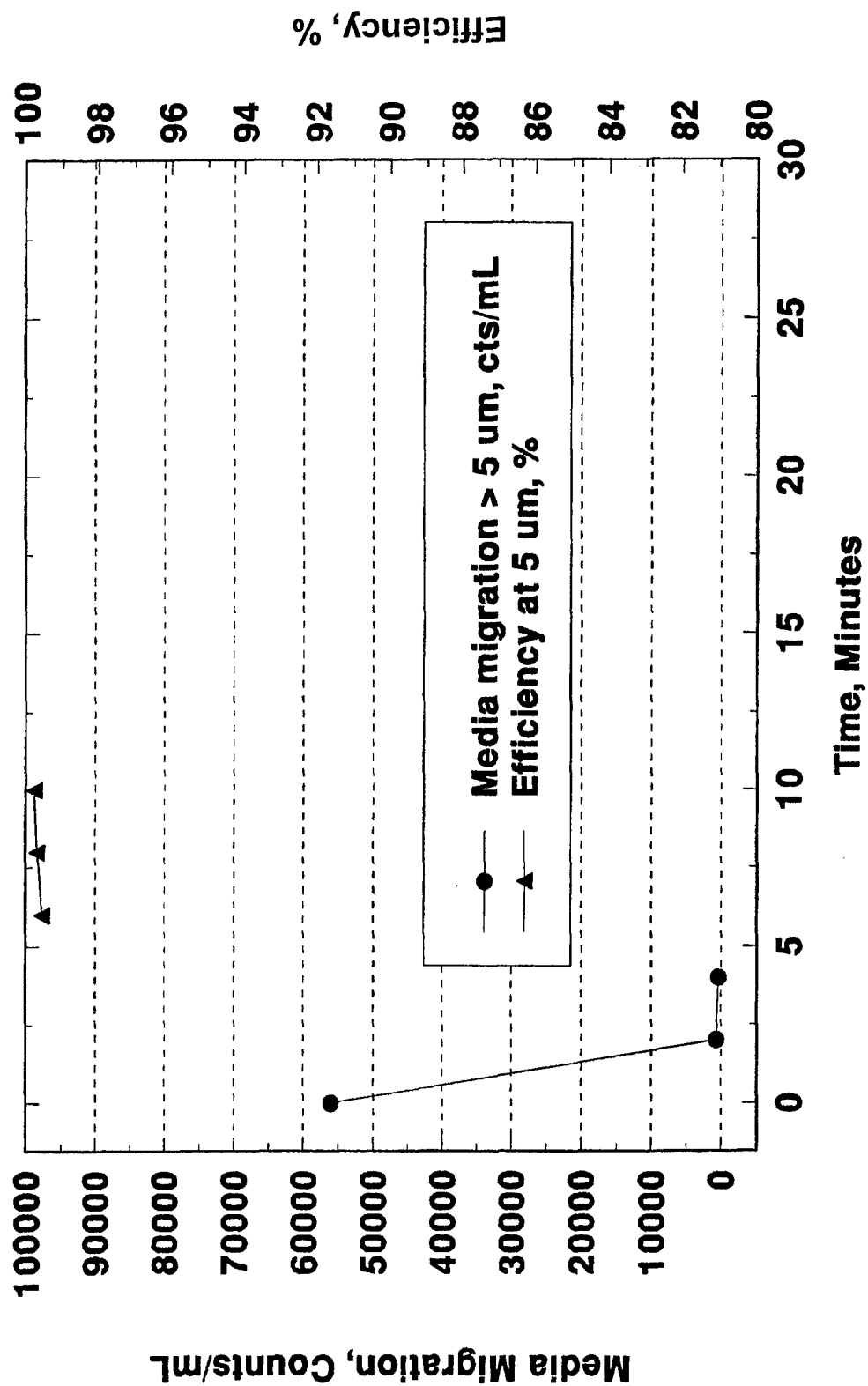
Kaydon Fuel Filter Evaluation **30% Biodiesel/70% Low-Sulfur Diesel Fuel, 1 Month**



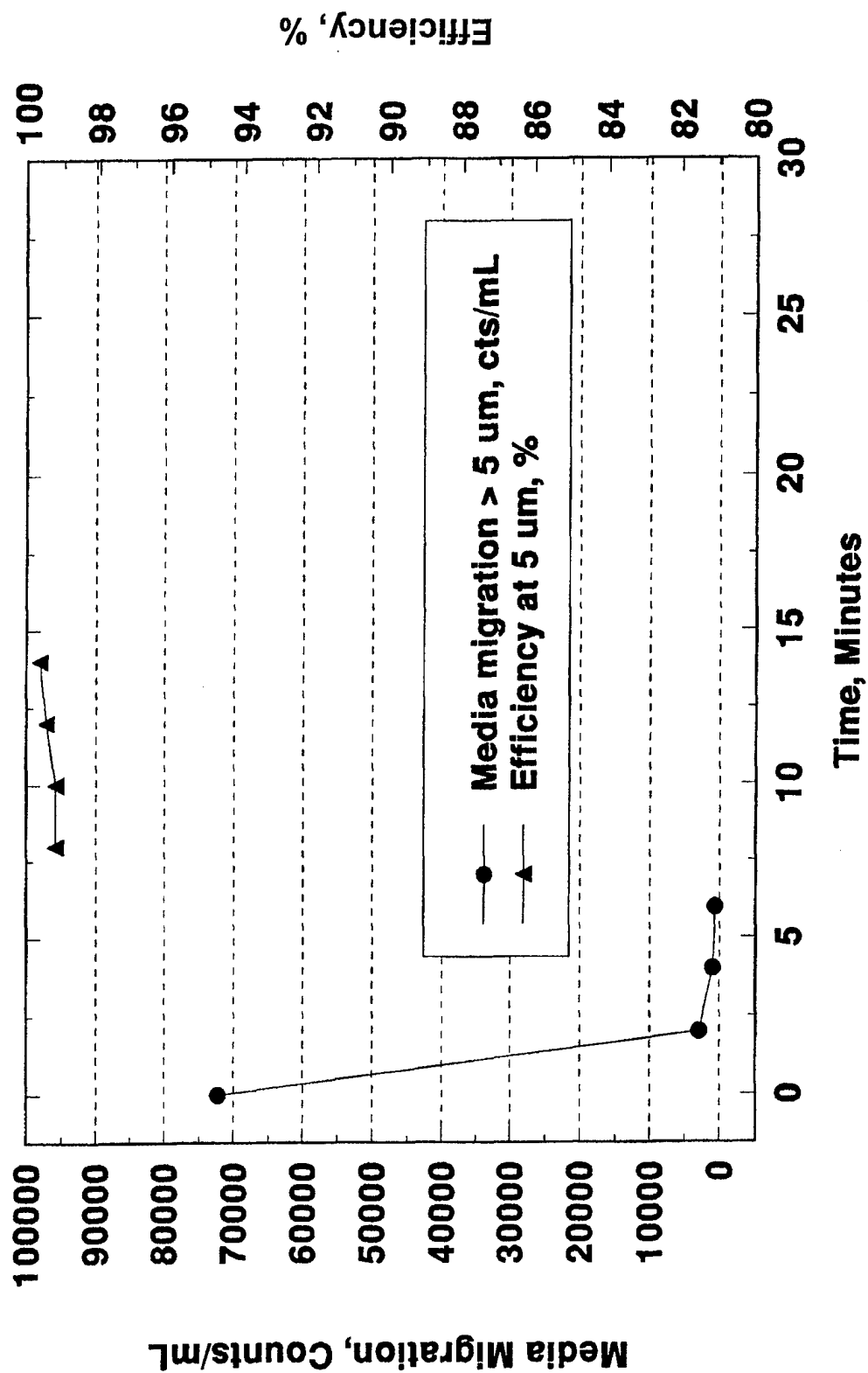
Kaydon Fuel Filter Evaluation **30% Biodiesel/70% Low-Sulfur Diesel Fuel, 3 Month**



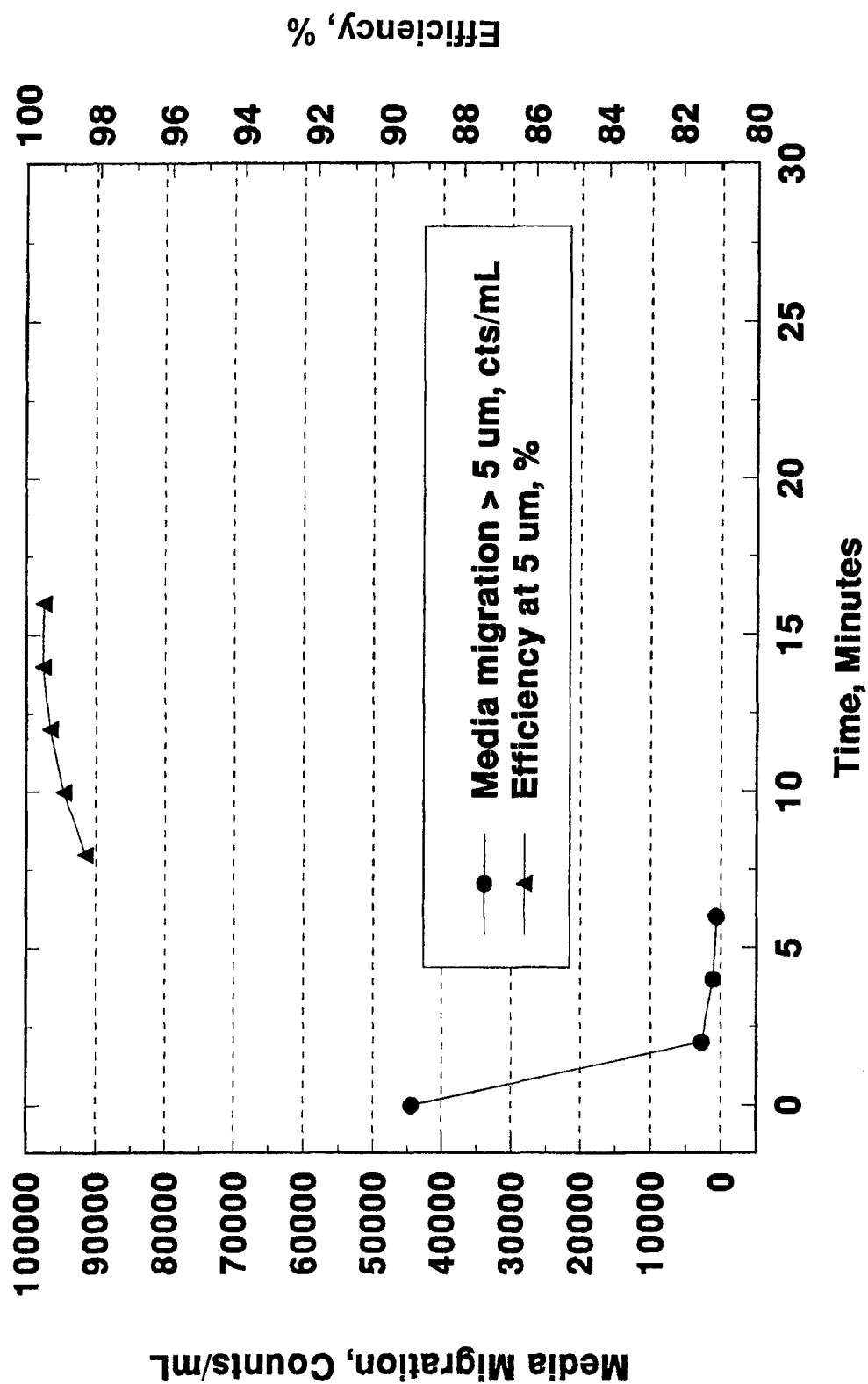
Kaydon Fuel Filter Evaluation **30% Biodiesel/70% Low-Sulfur Diesel Fuel, 6 Month**



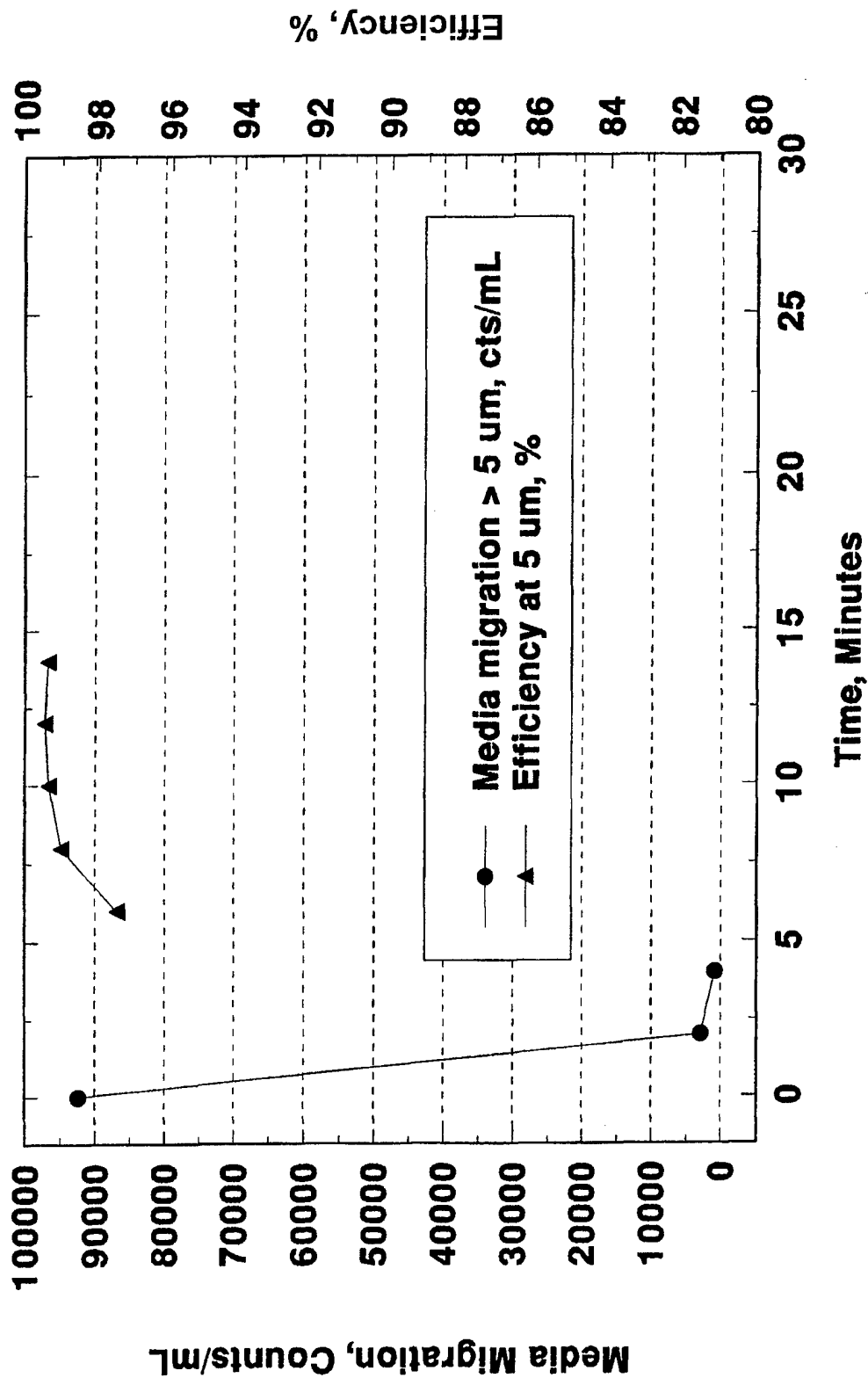
Kaydon Fuel Filter Evaluation **20% Biodiesel/80% Cat 1-H, 1 Month**



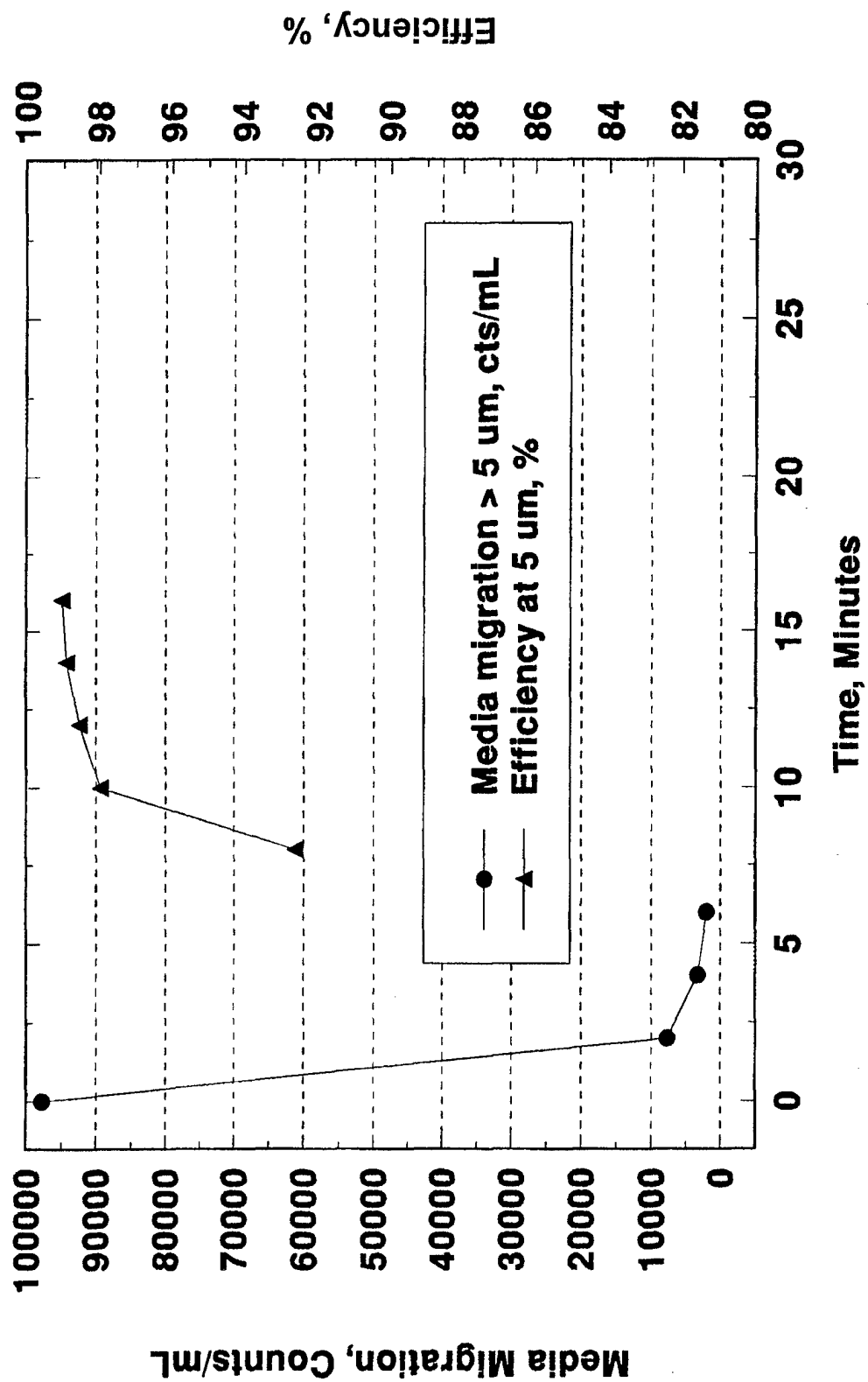
Kaydon Fuel Filter Evaluation **20% Biodiesel/80% Cat 1-H, 3 Month**



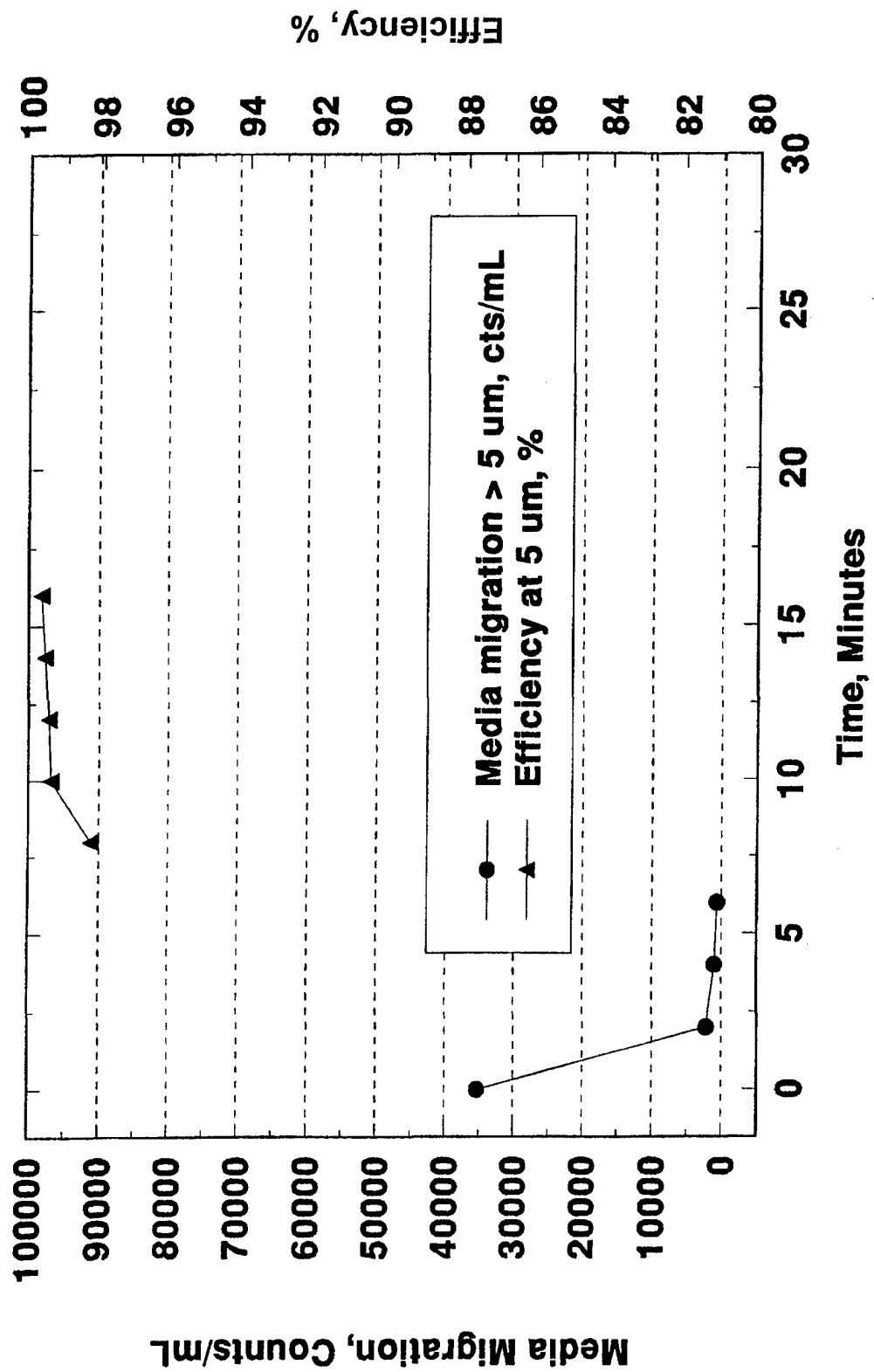
Kaydon Fuel Filter Evaluation **20% Biodiesel/80% Cat 1-H, 6 Month**



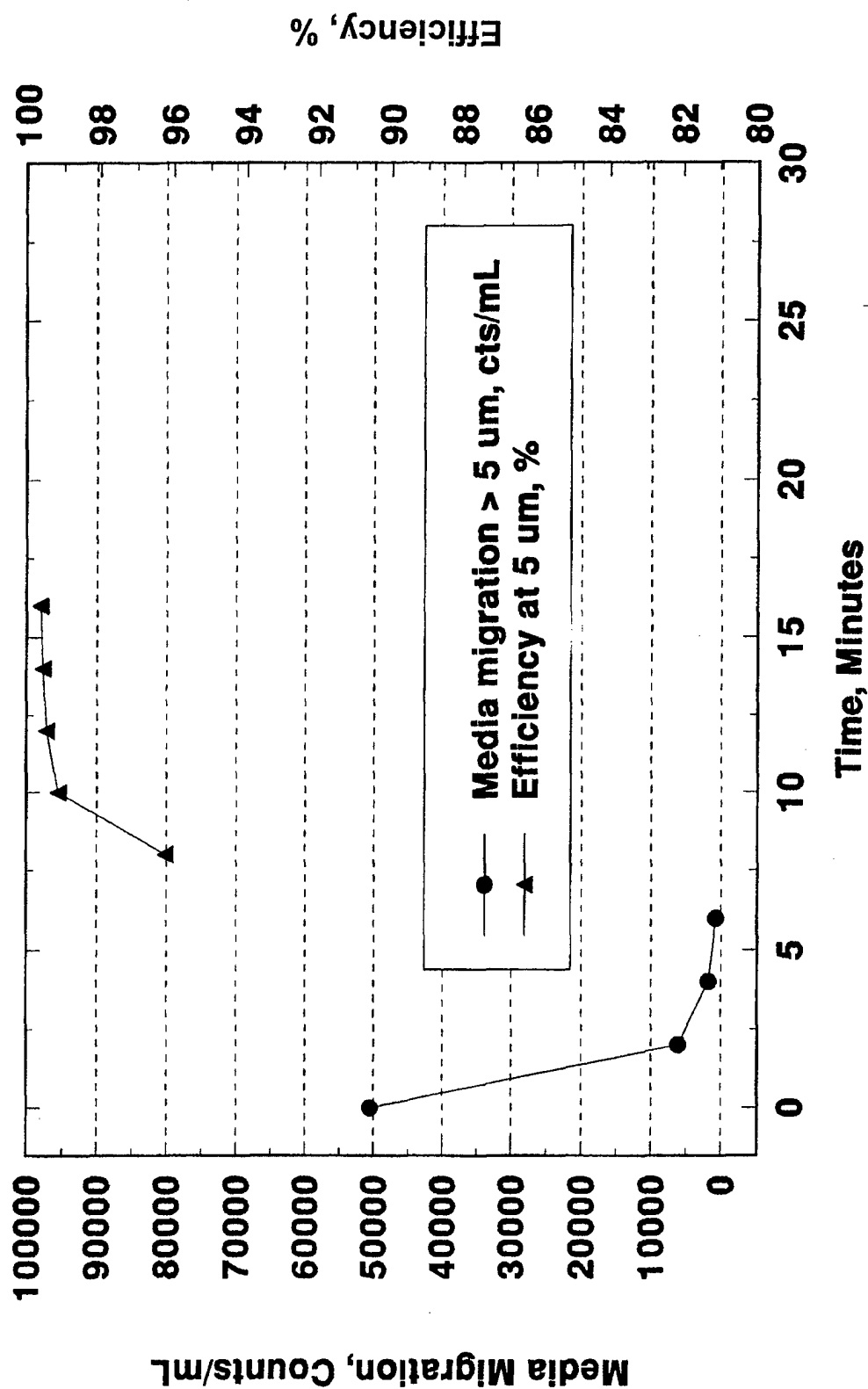
Kaydon Fuel Filter Evaluation **30% Biodiesel/70% Cat 1-H, 1 Month**



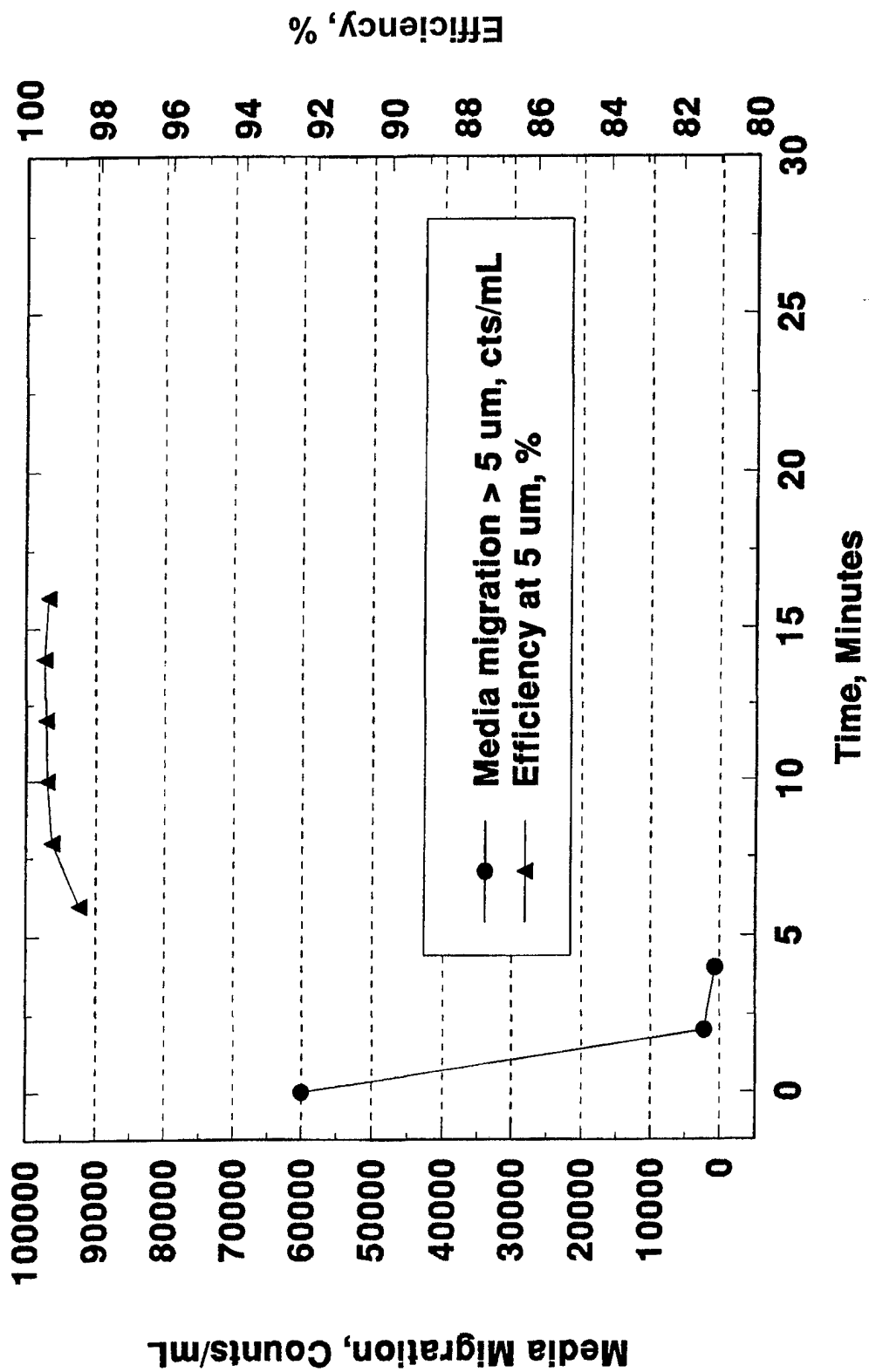
Kaydon Fuel Filter Evaluation **30% Biodiesel/70% Cat 1-H, 3 Month**



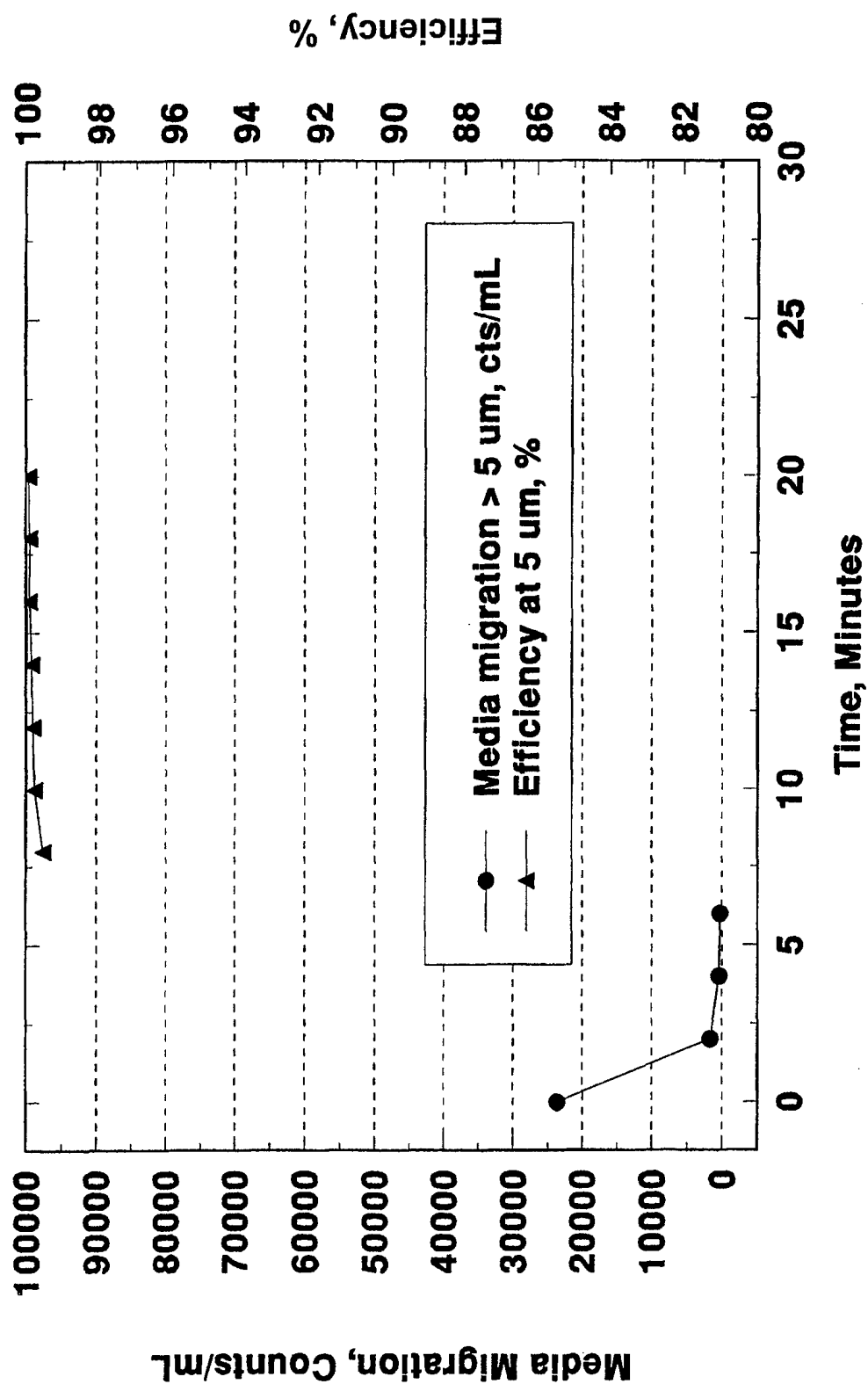
Kaydon Fuel Filter Evaluation **30% Biodiesel/70% Cat 1-H, 6 Month**



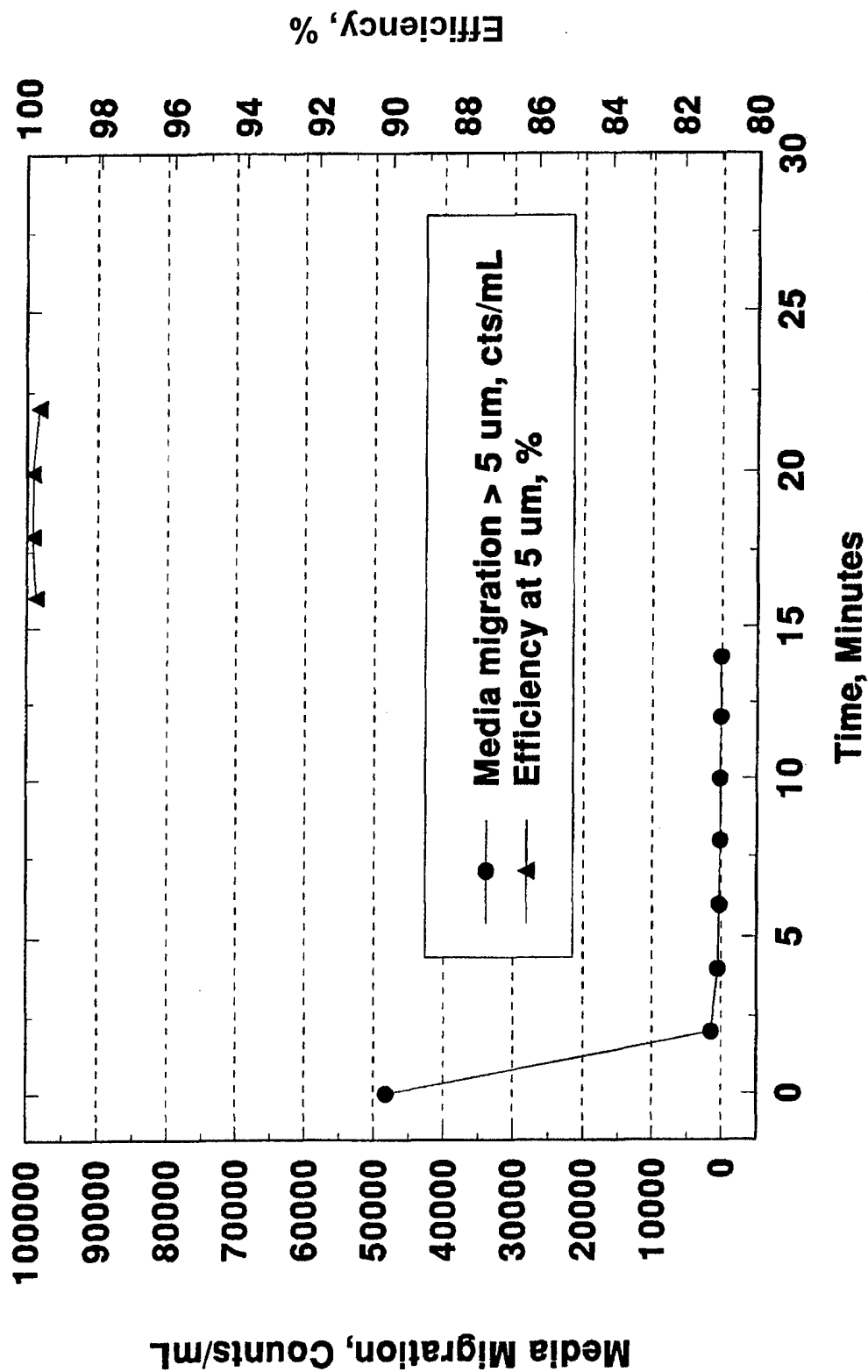
Kaydon Fuel Filter Evaluation 20% Biodiesel/80% JP-8, 1 Month



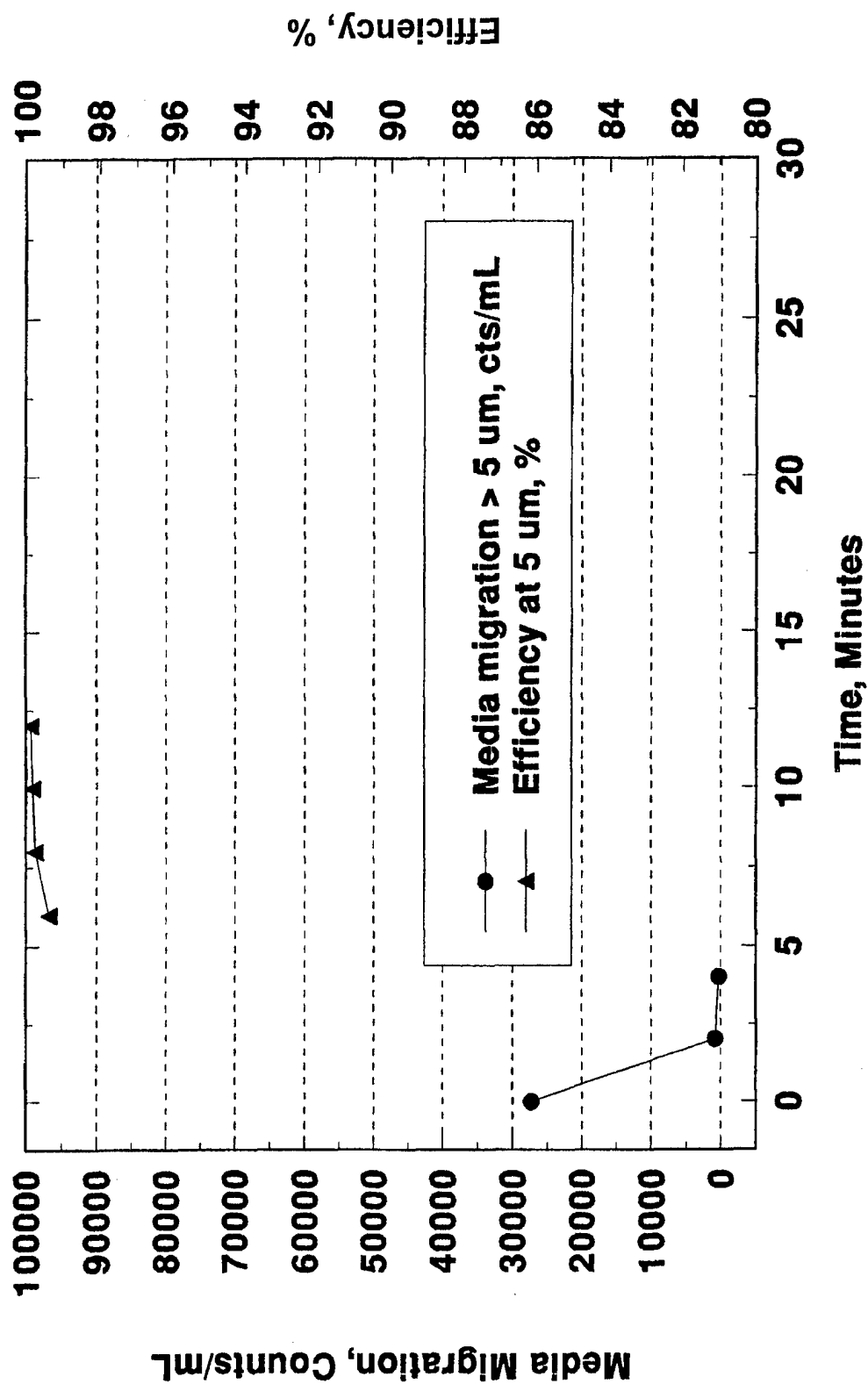
Kaydon Fuel Filter Evaluation **20% Biodiesel/80% JP-8, 3 Month**



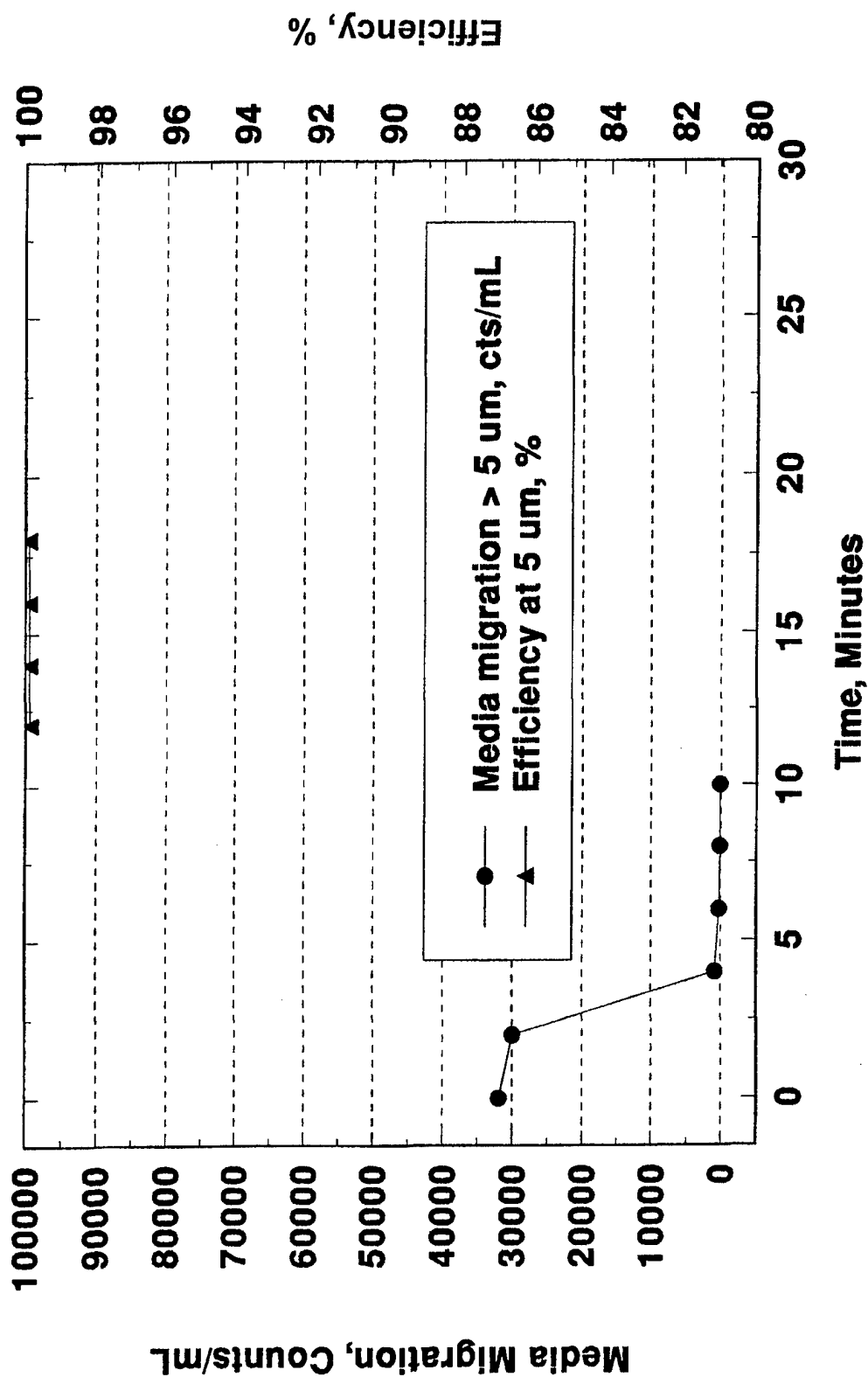
Kaydon Fuel Filter Evaluation **20% Biodiesel/80% JP-8, 6 Month**



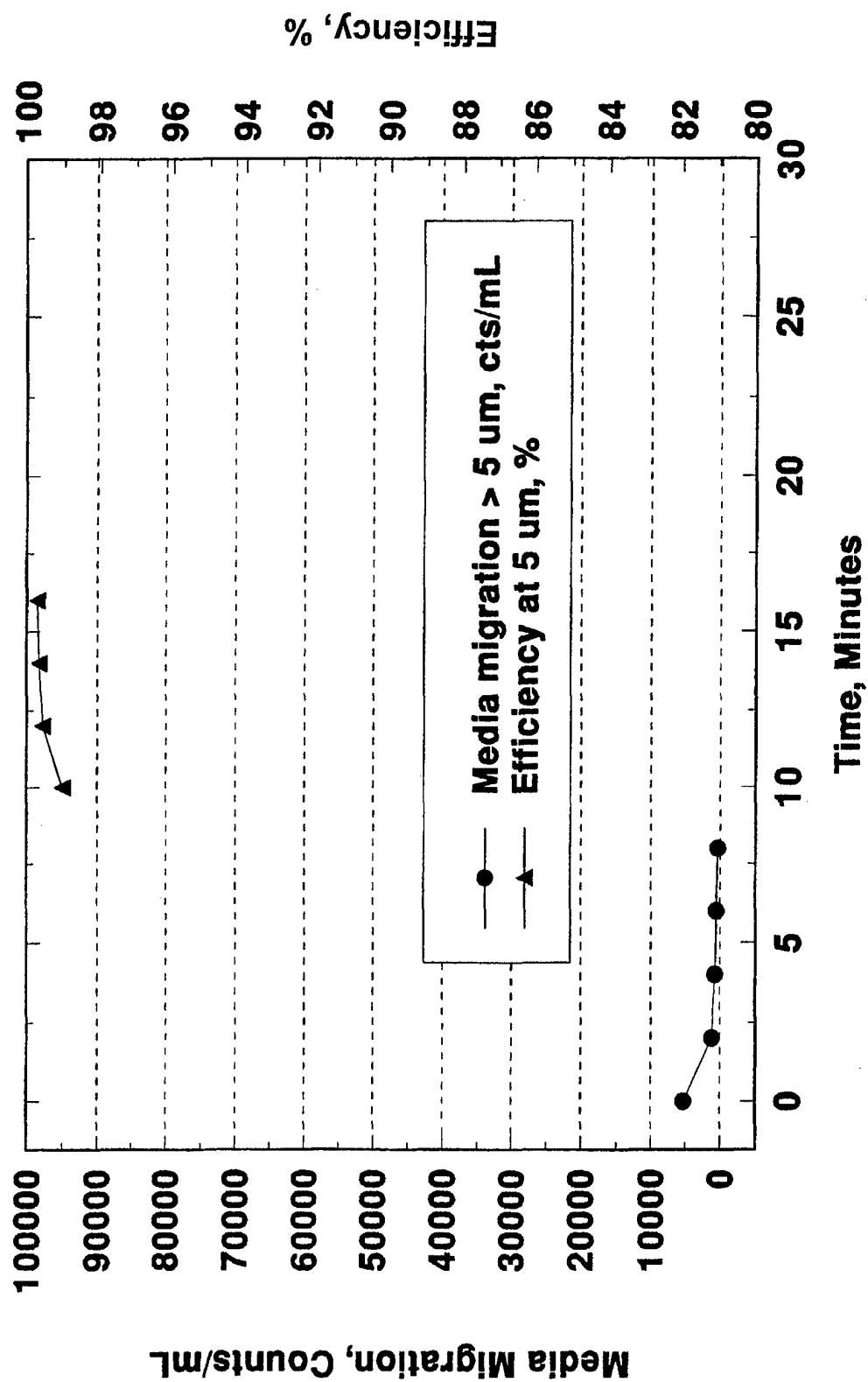
Kaydon Fuel Filter Evaluation **30% Biodiesel/70% JP-8, 1 Month**



Kaydon Fuel Filter Evaluation **30% Biodiesel/70% JP-8, 3 Month**



Kaydon Fuel Filter Evaluation **30% Biodiesel/70% JP-8, 6 Month**

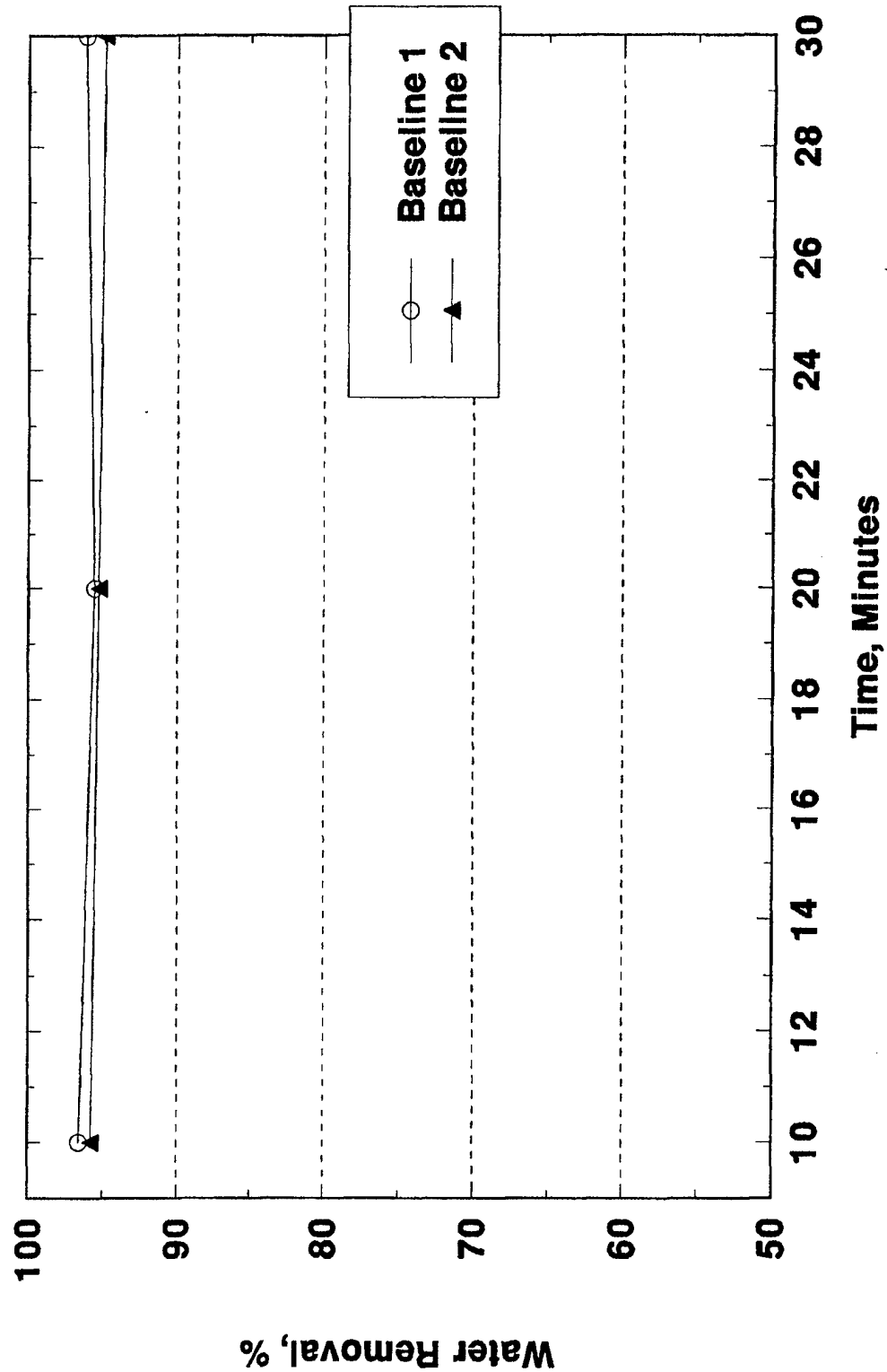


APPENDIX H

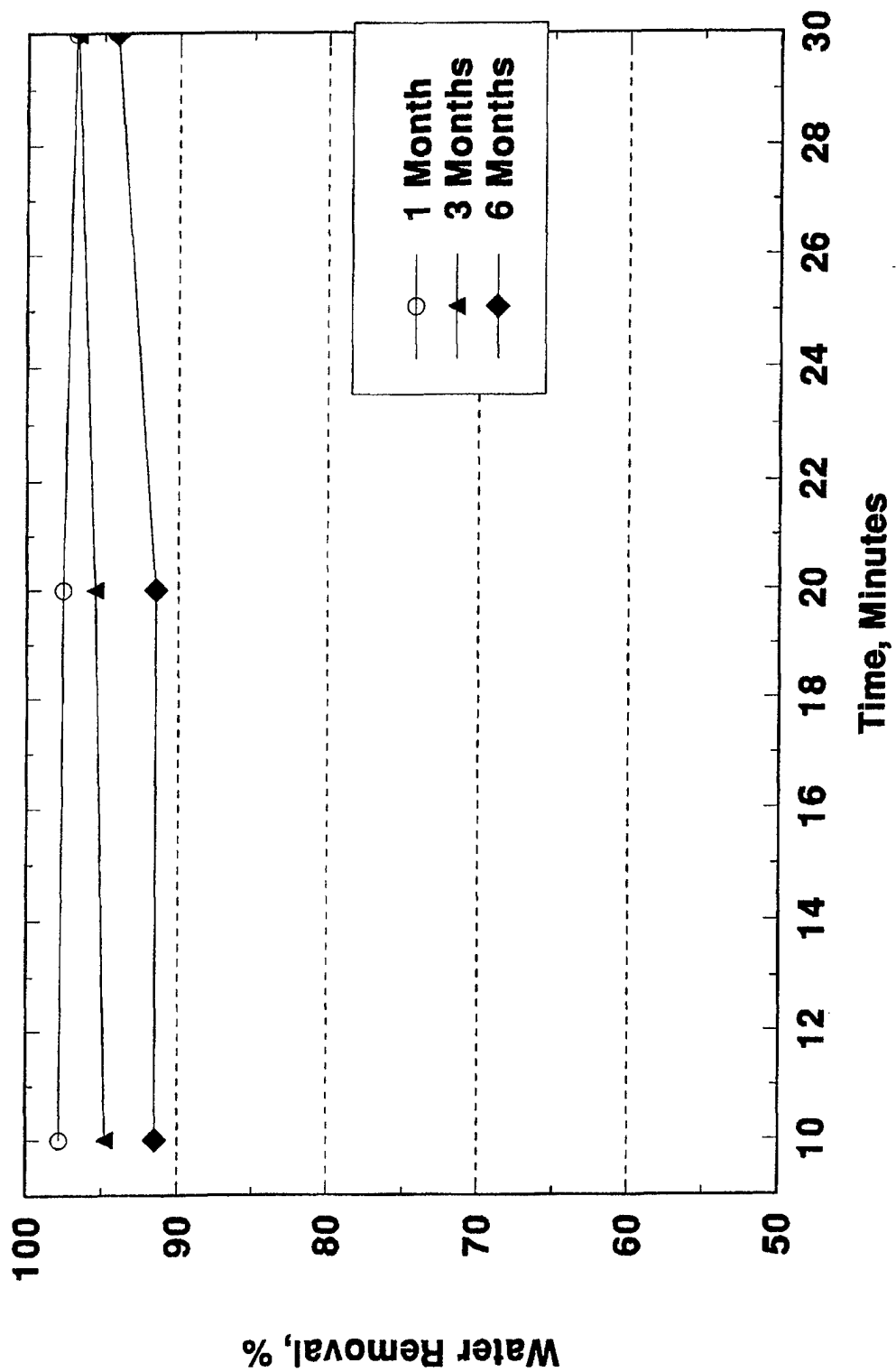
SAE J1839 Coarse Droplet Fuel/Water Separation Evaluations

Preceding Page Blank

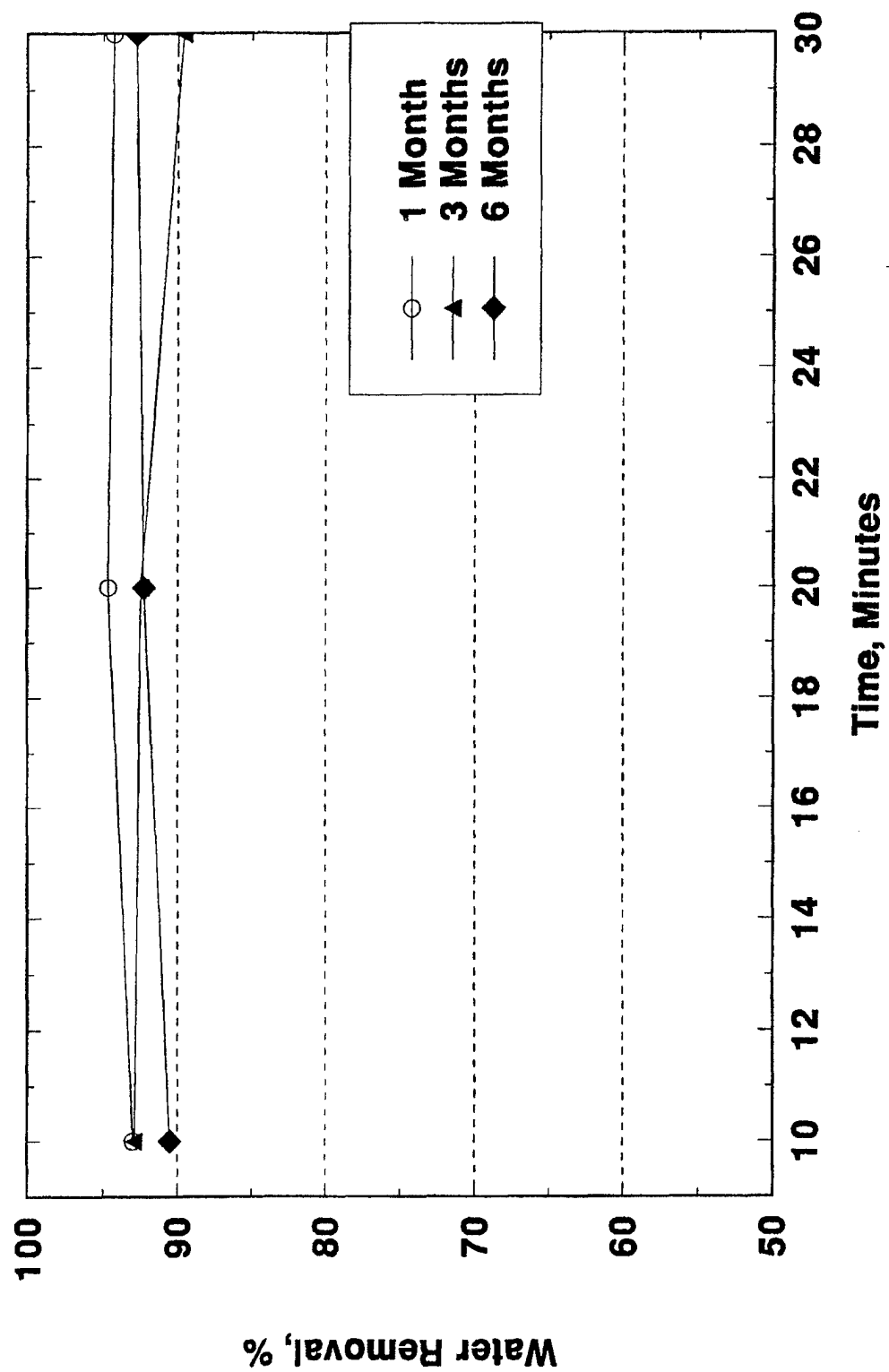
M1 Separation System SAE J1839



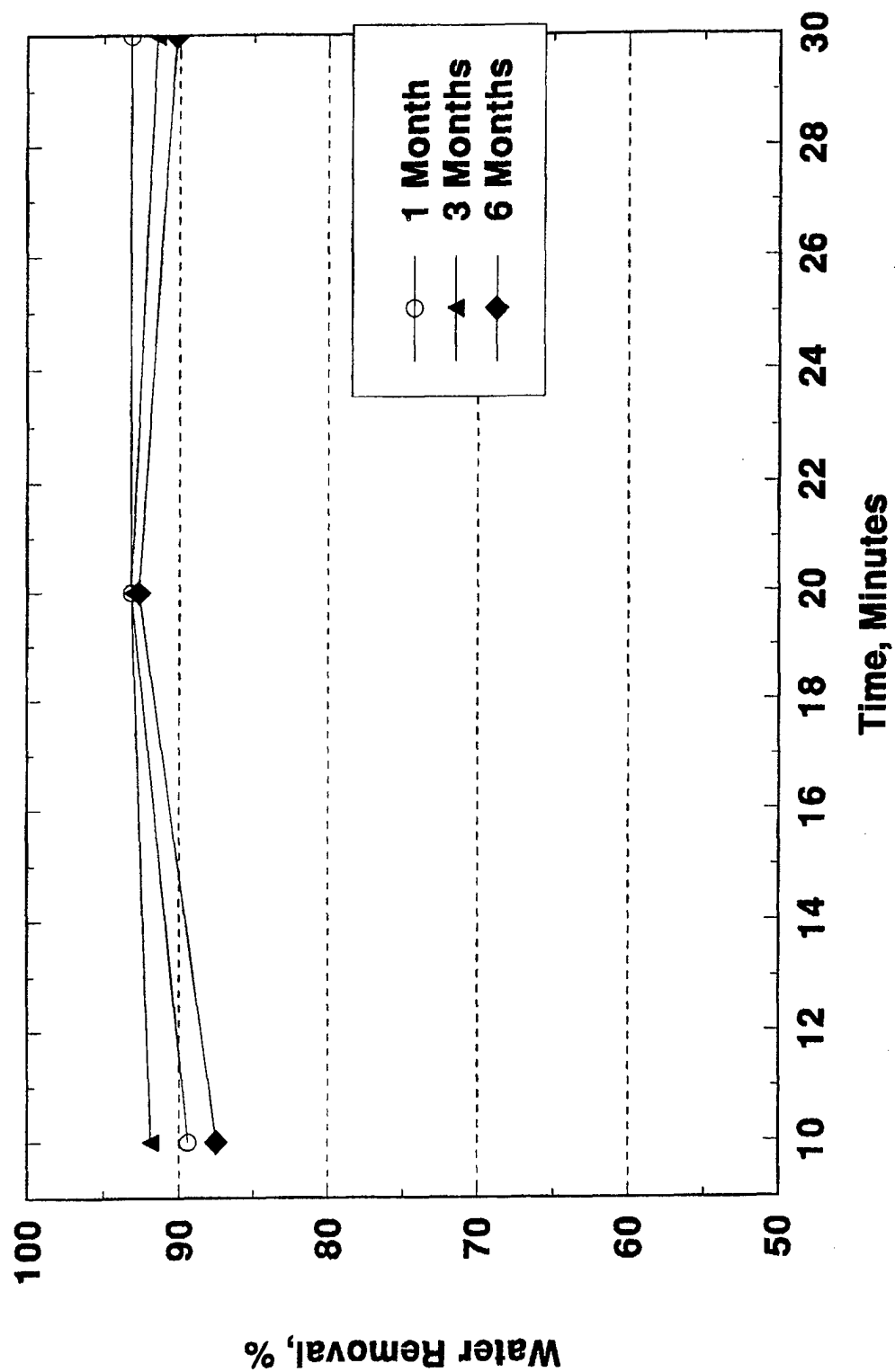
M1 Separation System JP-8



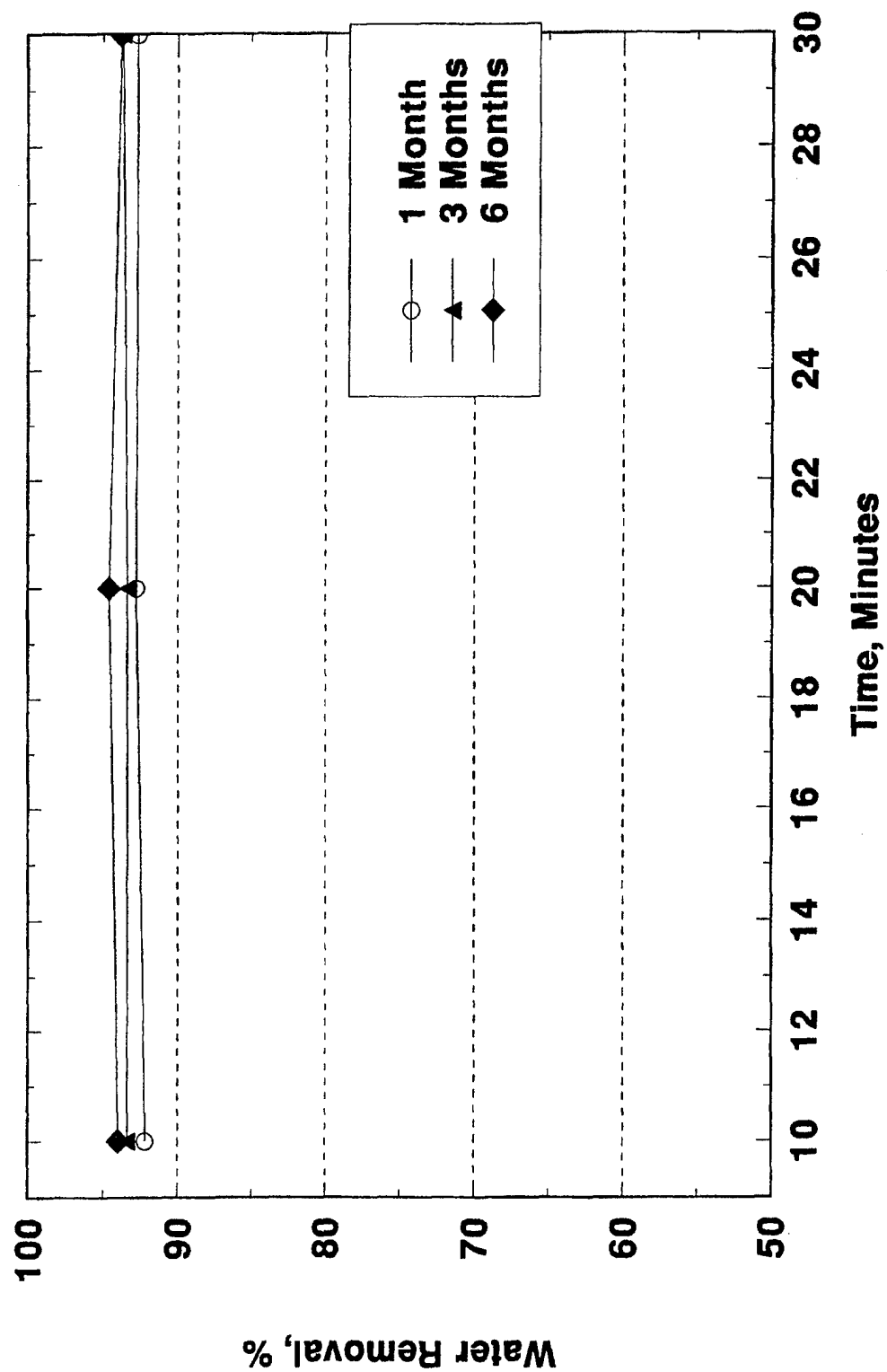
M1 Separation System Biodiesel



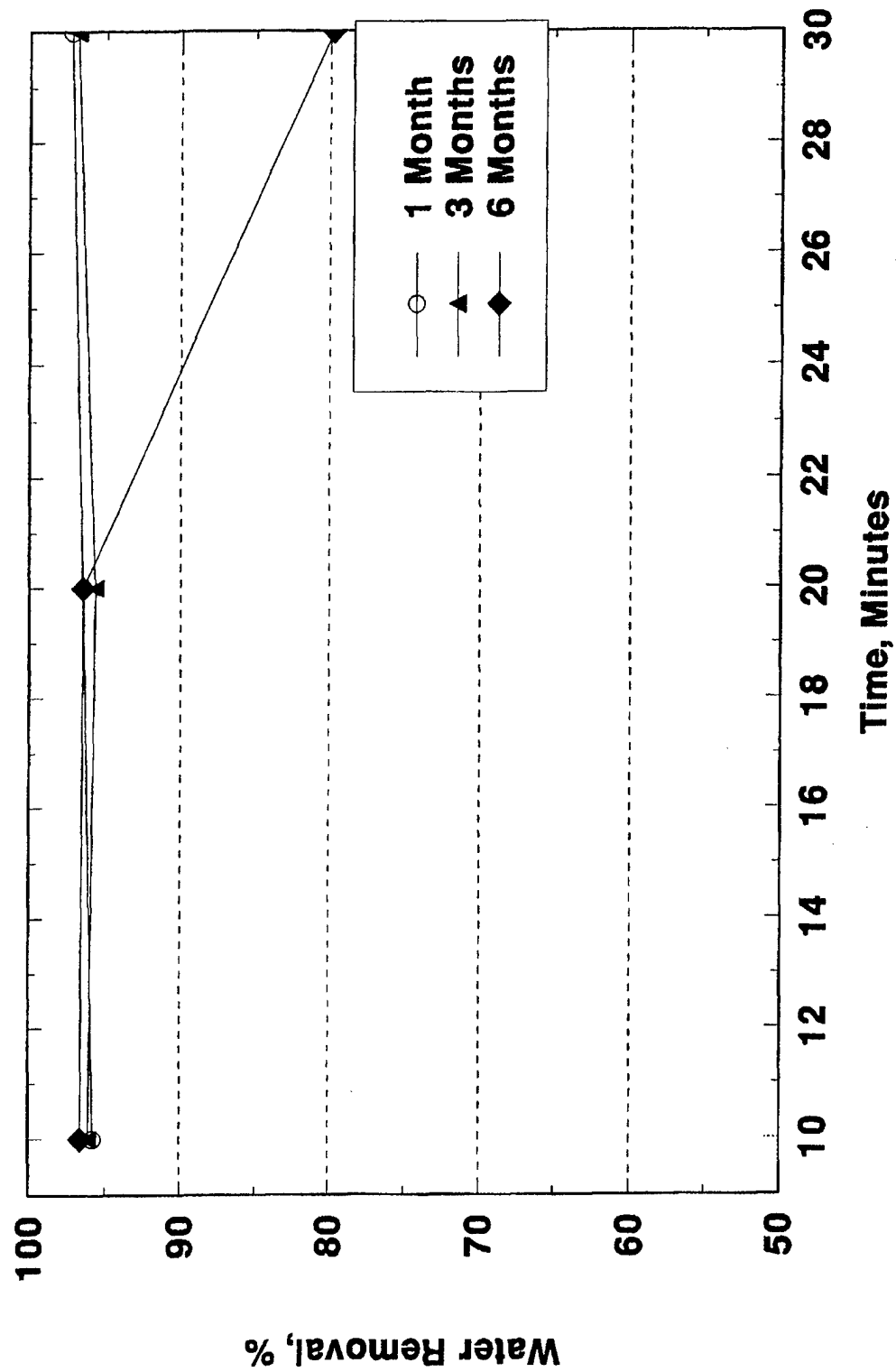
M1 Separation System Low-Sulfur Diesel Fuel



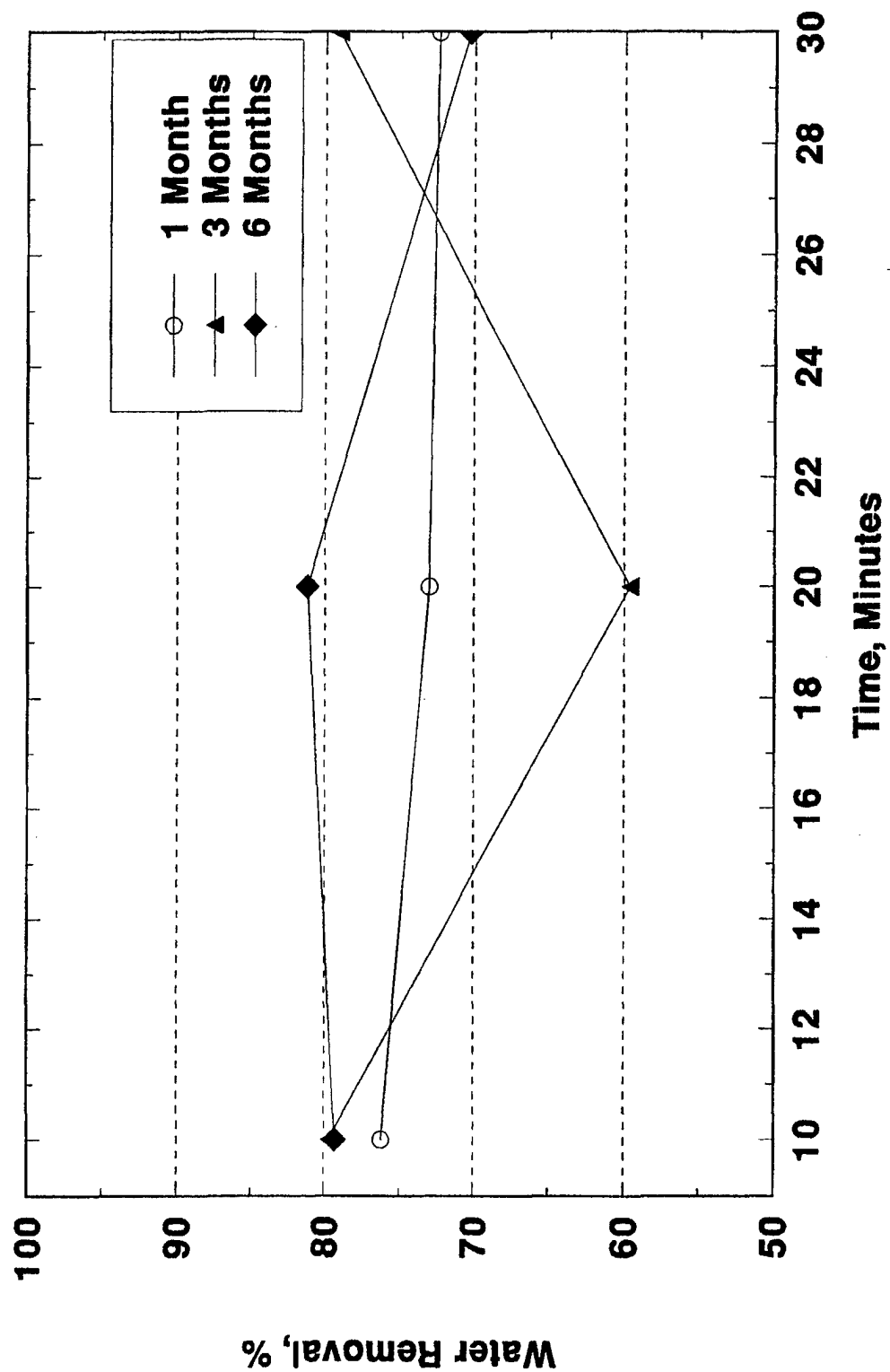
M1 Separation System Ref DF-2



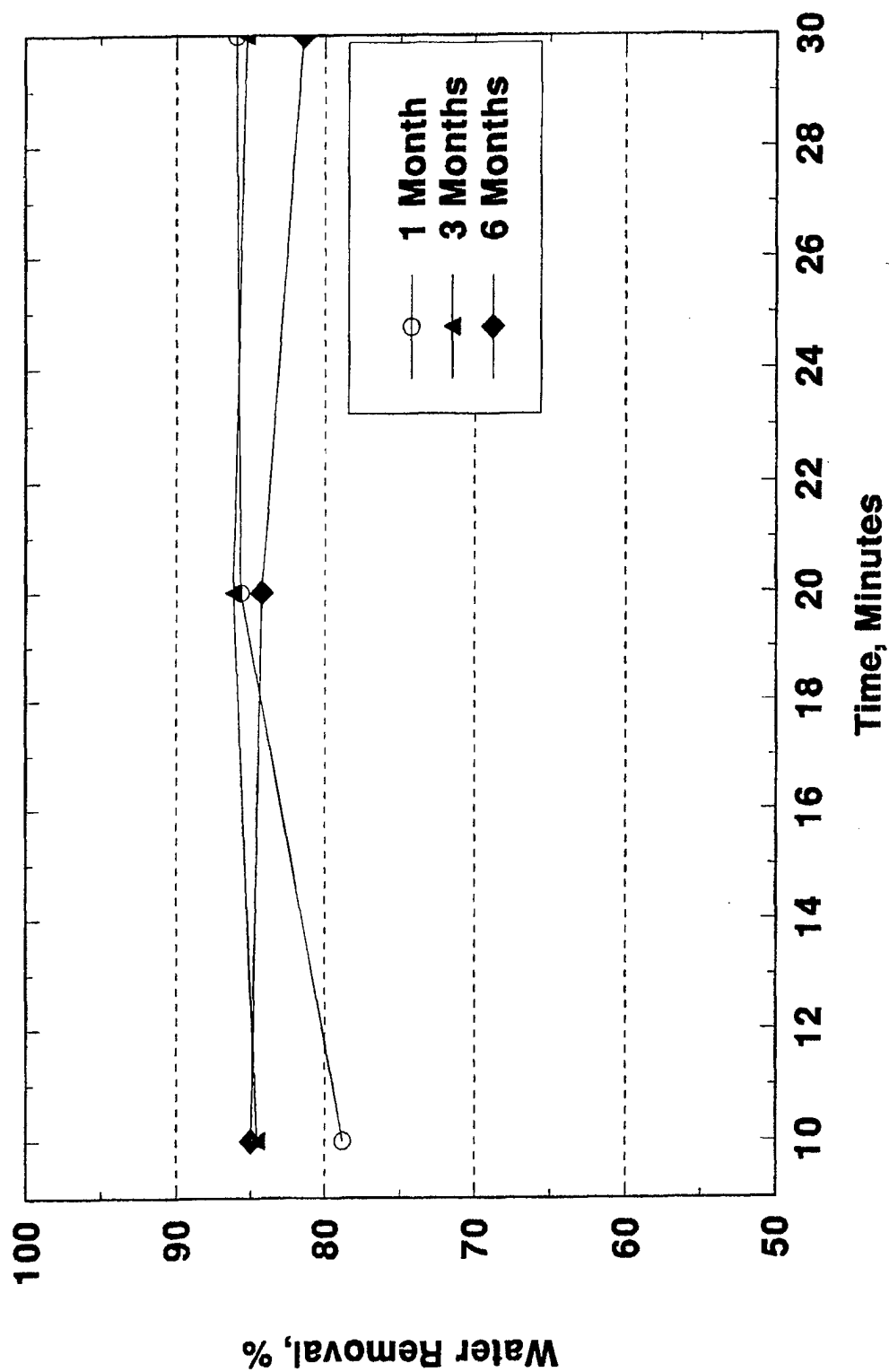
M1 Separation System
20% Biodiesel/80% Low-Sulfur Diesel Fuel



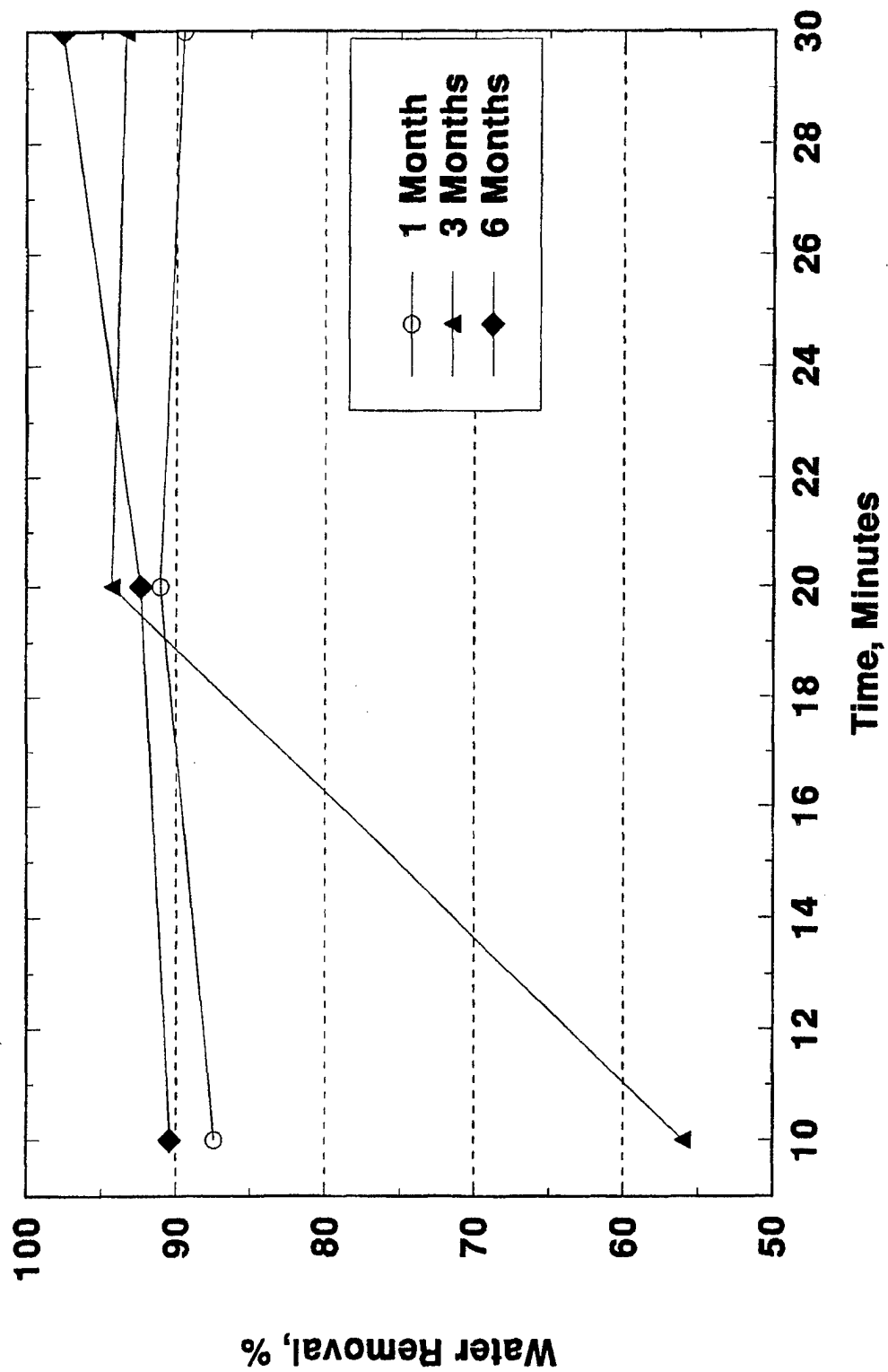
M1 Separation System
30% Biodiesel/70% Low-Sulfur Diesel Fuel



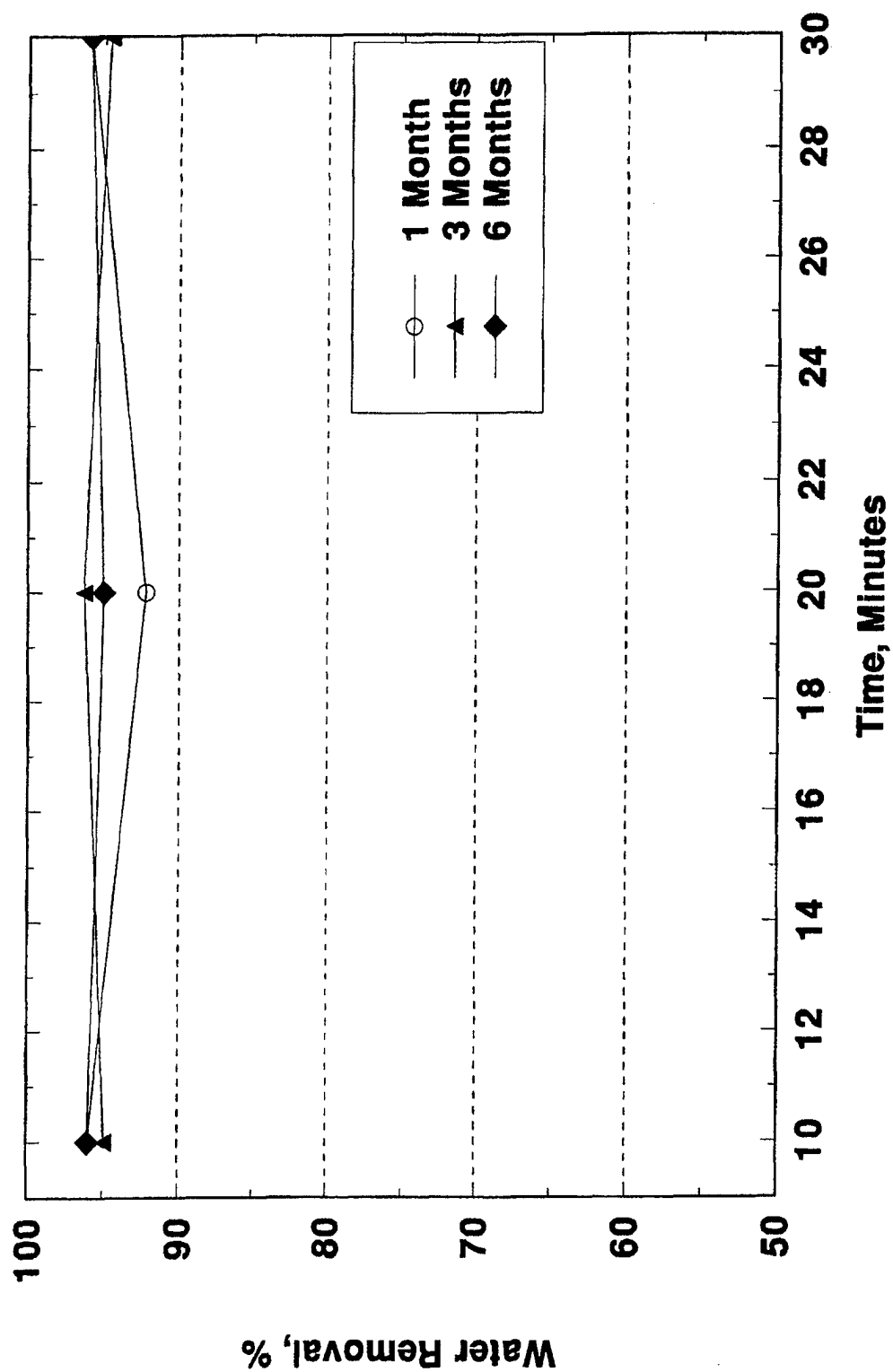
M1 Separation System
20% Biodiesel/80% Ref DF-2



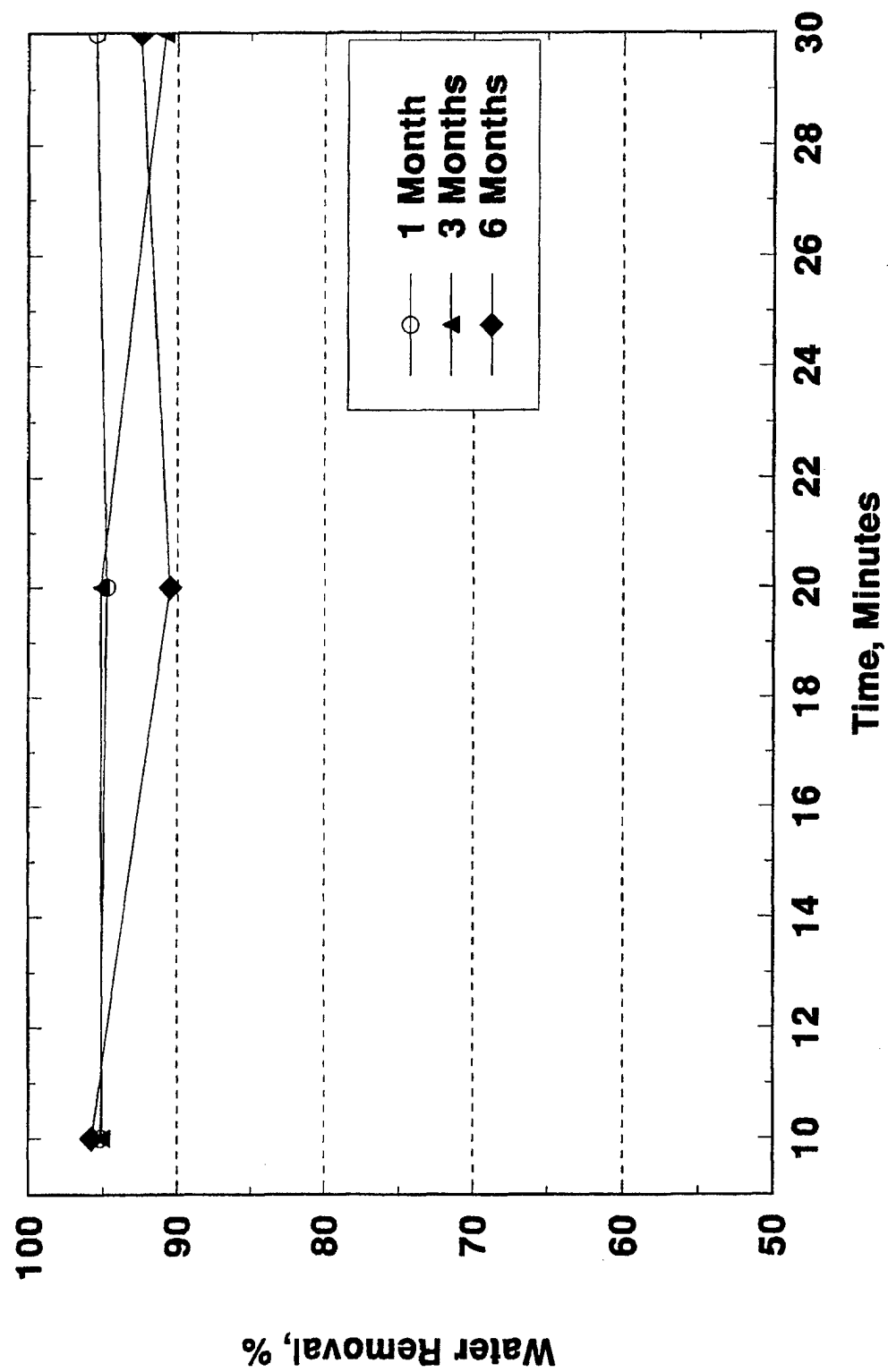
M1 Separation System
30% Biodiesel/70% Ref DF-2



**M1 Separation System
20% Biodiesel/80% JP-8**



**M1 Separation System
30% Biodiesel/70% JP-8**



APPENDIX I
Fuel Properties

Preceding Page Blank

APPENDIX
Fuel Properties
Table A-1 - U.S. Jet A-1 Turbine Fuel

Test	Specifications		
	Minimum	Maximum	Result
Gravity, °API	37.0		51.0
Density, kg/m	0.775		0.840
Color	Report		+25
Distillation, °C			
IBP			160
5%			165
10%		204	167
20%			169
30%			170
40%			172
50%			175
60%			178
70%			182
80%			187
90%			195
95%			207
EP		300	218
Recovery, vol%			99.1
Residue, vol%		1.5	0.9
Loss, vol%		1.5	0.0
Sulfur, wt%		0.300	0.002
Doctor test		Neg.	Neg.
Freeze point, °C		-47.0	-59.5
Flash point, °C	38		44
Viscosity, cSt at -34°C		8.0	4.2
Viscosity, sSt at 40°C			1.07
Copper Corrosion		1B	1B
Existent Gum, mg/100 mL		7.0	3.4
Particulates, mg/L		1.0	0.8
Smoke point, mm	20.0		29.0
WSIM	Report		00
Hydrocarbon Composition, vol%			
Aromatics		20.0	8.1
Olefins		5.0	0.0
Saturates	Report		91.9
Acidity, total (mg KOH/g)		0.015	0.004
Net Heat of Combustion, Btu/lb	18,400		18721
JFTOT, mm Hg		25.0	0.0
JFTOT, TDR		12	1
Water Reaction		1B	1A
Separation rating, max.		2.0	0.0
Interfacing rating, max.		1B	1A

Preceding Page Blank

920824

APPENDIX
Fuel Properties

Table A-2 - Reference No. 2 Diesel Fuel

Test	Specifications		
	Minimum	Maximum	Result
Gravity, °API	33.0	35.0	34.1
Distillation, °F (°C)			
IBP			400 (204)
5%			449 (232)
10%			462 (239)
20%			476 (247)
30%			489 (254)
40%			501 (261)
50%	500	530	515 (268)
60%			531 (277)
70%			550 (288)
80%			573 (301)
90%	590	620	611 (322)
95%			642 (339)
EP	650	690	669 (354)
Recovery, vol%			99.0
Residue, vol%			1.0
Loss, vol%			0.0
Cetane number	47.0	53.0	50.0
Flash, °F (°C)	140 (60)		188 (87)
Cloud point, °F (°C)			24 (-4)
Pour point, °F (°C)		20 (-7)	15 (-9)
Water and sediment, vol%		0.05	<0.05
Sulfur, wt%	0.38	0.42	0.39
Ash, wt%		0.010	0.001
Viscosity, cSt at 104°F	2.00	4.00	3.00
Copper Corrosion		2	1A
Neutralization No., mgKOH/g		0.15	0.07
Ramsbottom, 10% residium, wt%		0.20	0.10

APPENDIX J

200-Hour Pump Stand Evaluation of Stanadyne Fuel Injection Pumps Using Fuel AL-24252

Conducted by TFLRF
September 1995

Fuel Analysis
AL-24252

Fuel Composition

Jet A-1	92%
Biodiesel	8%

Properties

Kvis, 40°C, cSt, D445	1.14
-----------------------	------

Water, Karl Fischer, ppm	180
--------------------------	-----

TAN, D664	0.02
-----------	------

Distillation, D86

°C@ % off

1	163
10	169
20	172
30	175
40	177
50	180
60	183
70	186
80	192
90	215
95	334

Residue, %v	1.2
-------------	-----

Lubricity, HFRR Wear, mm	0.28
--------------------------	------

Preceding Page Blank

Pump Stand Test Conditions

Duration, hours	200
Speed, RPM, Full Rack	1800
Inlet Fuel Pressure, psi	3.0 max
Inlet Fuel Temperature, °F	165-170 max
Reservoir Fuel Temperature, °F	100 max

**Pump Calibration
Additive Evaluation Project**

Pump Type: DB2-4524 (STD.) "A" left pump	SN: 8239195
Test description: CT-JET A-1+8% BIODIESEL (200hrs)	AL: 23889

RPM	Parameter/Spec	Before	After	Change (After - Before)
1000	TPP 70-76 psi	75	75	
	Hsg. 8-12 psi	10	10	
	Adv. 1.5 deg.	1.5	1.5	
	Ret. Fuel 225-375 cc	300	300	
	Fuel Del. 51-55 cc	54.5	53.5	-1cc
325	Low Idle 12-116 cc	15	18	+3cc
	Adv. 1.5 min	4	3.5	-.5deg.
	CAS 0-1 deg.	0	0	
	Adv. 2.75 deg. min	5	5	
750	FC 21.5 - 23.5 cc	22	22	
	Adv. 3.5 deg.	3.5	3.5	
1800	Fuel Del. 46 cc min.	53.5	54	+.5cc
	TPP	108	110	+2psi
	Housing psi	10	10	
1950	Fuel Del. 44 cc min.	51	52	+1cc
2100	High Idle 8 cc max.	0	0	
	TPP 135 psi max.	132	140	+8cc
200	Fuel Del. 47 cc min.	48.5	48.5	
	Shut-Off 4 cc max.	0	0	
75	Fuel Del. 29 cc min.	38.5	38.5	
	TPP 12 psi min.	24	26	+2psi
	Airtime + 0.25	+ 0.25	+ 0.25	
	Deg. C	44	43	
	Date	09/04/95	10/12/95	

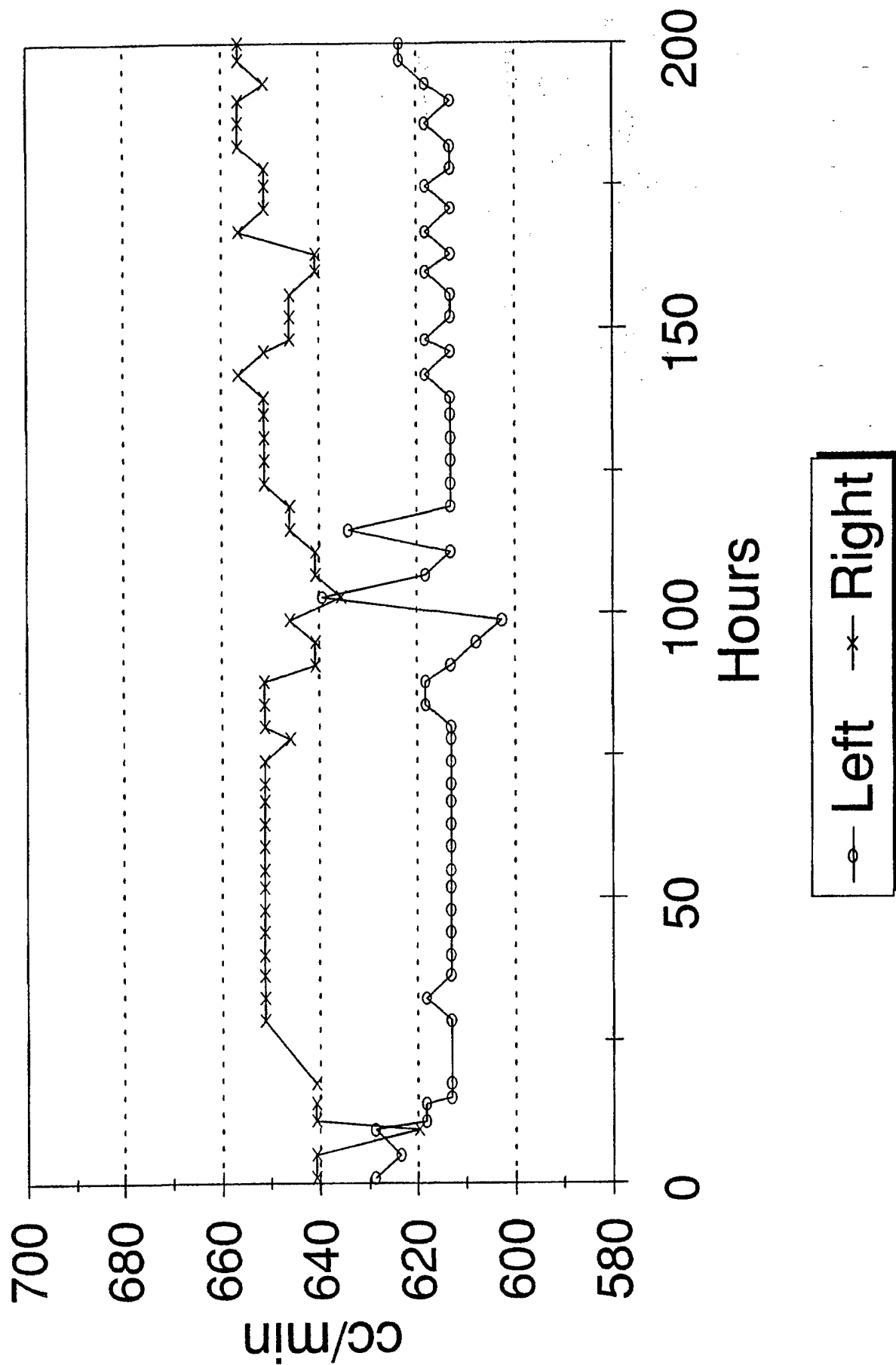
**Pump Calibration
Additive Evaluation Project**

Pump Type: DB2-4523 (ARC.) "B" right pump	SN: 8164638
Test description: CT-JET A-1+8% BIODIESEL (200hrs)	AL: 23886

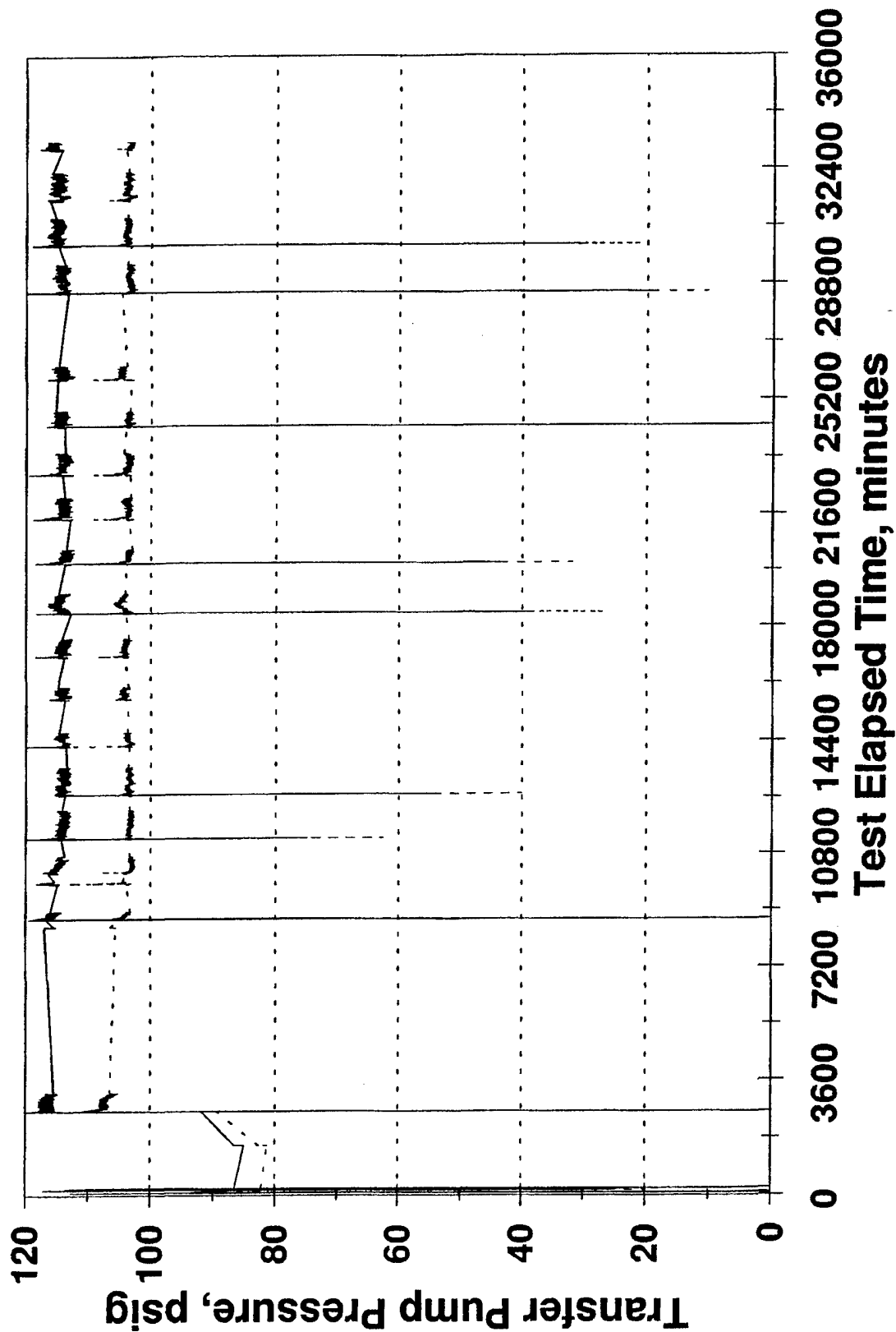
<i>RPM</i>	<i>Parameter/Spec</i>	<i>Before</i>	<i>After</i>	<i>Change (After - Before)</i>
1000	TPP 70-76 psi	74	72	-2psi
	Hsg. 8-12 psi	10	10	
	Adv. 1.5 deg.	1.5	1.25	
	Ret. Fuel 225-375 cc	375	400	+25cc
	Fuel Del. 51-55 cc	54	53	-1cc
325	Low Idle 12-16 cc	15.5	18	+2.5cc
	Adv. 1.5 min	3	3	
	CAS 0-1 deg.	0	0	
	Adv. 2.75 deg. min	4.5	4.5	
750	FC 21.5 - 23.5 cc	23	23	
	Adv. 3.5 deg.	3.5	3.75	+.25deg
1800	Fuel Del. 46 cc min.	52.5	53.5	+1cc
	TPP	110	110	
	Housing psi	10	10	
1950	Fuel Del. 44 cc min.	50.5	51	+.5cc
2100	High Idle 8 cc max.	0	0	
	TPP 135 psi max.	140	140	
200	Fuel Del. 47 cc min.	49.5	48.5	-1cc
	Shut-Off 4 cc max.	0	0	
75	Fuel Del. 29 cc min.	38.5	37	-1.5cc
	TPP 12 psi min.	19	18	-1cc
	Airtime + 0.25	+ 0.25	+ 0.25	
	Deg. C	44.5	44	
	Date	09/04/95	10/12/95	

PUMP FUEL FLOW

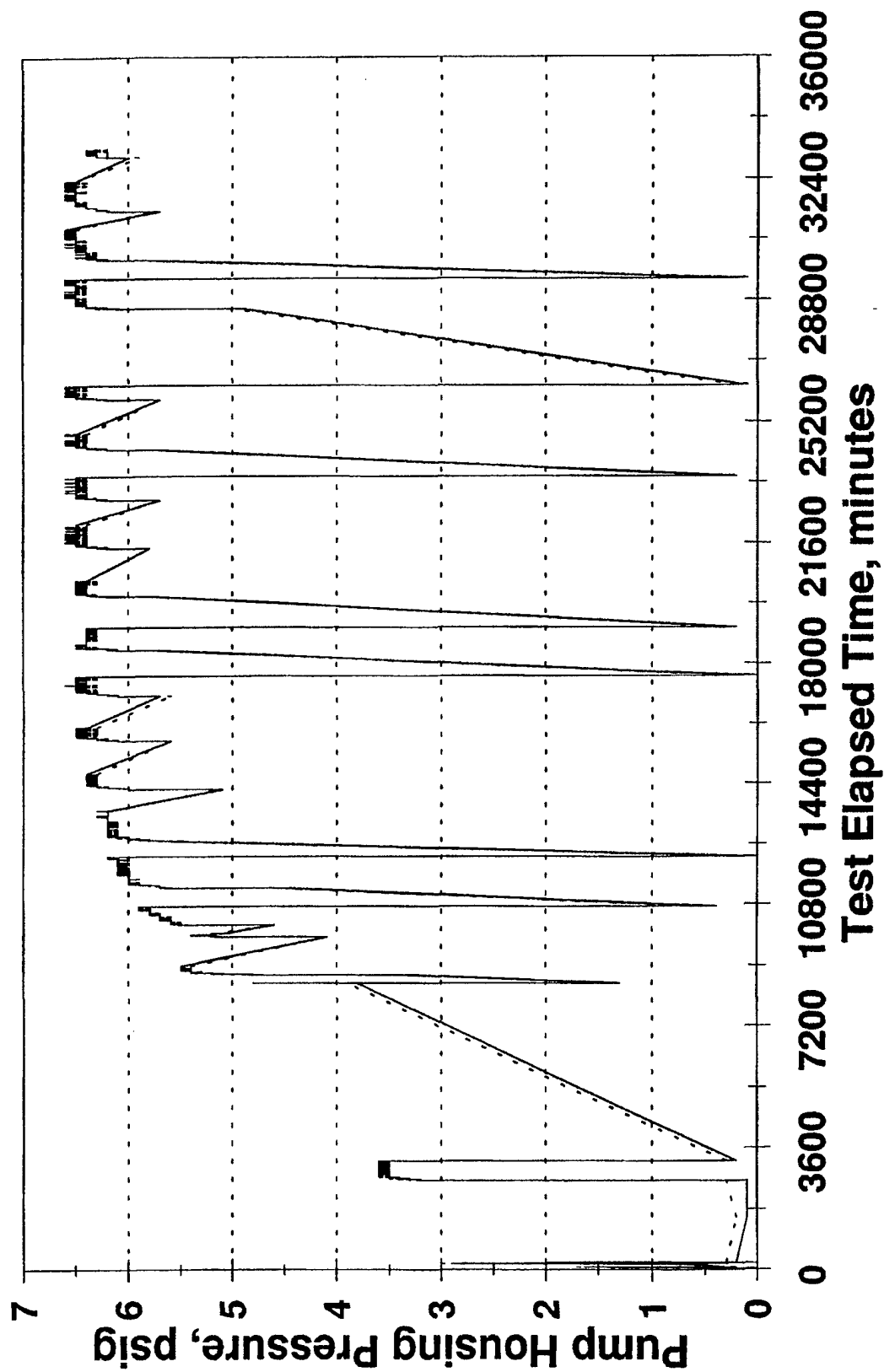
8% Biodiesel in neat Jet-A1



Transfer Pump Pressure 8% BioDiesel in Jet A-1



Pump Housing Pressure **8% Biodiesel in Jet A-1**



Wear Measurements on Transfer Pump Blades

A reciprocating action is formed between the rotor and the transfer pump blade. This action forms a wear scar with a sharp step at the limit of the cycle. The depth of the wear scar was measured at this step using a Talysurf 10 profilometer. Scar depth was assumed to decrease linearly across the contact area, and the wear volume was calculated accordingly. An improved metallurgy is available in the arctic pump vanes and the appropriate indentation hardness was used in calculating Archards wear coefficient. The cumulative sliding distance was calculated for an eccentricity of 4 mm.

Note: Hardness of Arctic Pump Vanes (Hv) = 750
 Hardness of Standard Pump Vanes (Hv) = 460
 Sliding Distance in 200 Hours = 173 km
 Approximate Contact Load = 0.36 kg

TABLE J-1. Wear Measurements on Transfer Pump Blades

Pump	Wear Scar Dimensions			Wear Coefficient, K x 10 ⁻⁹
	Max Depth, mm x 10 ⁻³	Final Area, mm ²	Volume, mm ³ x 10 ⁻³	
Std (No. 3)	1.33	9	5.99	10.9
Arctic (No. 4)	1.46	12	8.76	37.5

Wear Measurements on Governor Thrust Washer

This is a wear ring formed by the action of the six governor weights on the governor thrust washer. The average depth of the wear scar was measured using a Talysurf profilometer and was found to be approximately constant around the complete circumference. The applied load was derived from the thrust required to counteract centripetal force on each governor weight at 1800 rpm. The indentation hardness of both the arctic and standard components were similar.

Note: Hardness of Both Arctic and Standard Parts (Hv) = 670

Cumulative Sliding Distance	= 388 km
Approximate Contact Load	= 2 kg
Circumference of Contact	= 83.2 mm

TABLE J-2. Wear Measurements on Governor Thrust Washer

<u>Pump</u>	<u>Scar Depth,</u> <u>mm x 10⁻³</u>	<u>Scar Width,</u> <u>mm</u>	<u>Volume,</u> <u>mm³ x 10⁻³</u>	<u>Wear Coefficient,</u> <u>K x 10⁻⁹</u>
Std (No. 3)	0.6	1.8	89.9	25.6
Arctic (No. 4)	1.3	1.8	195	55.8

Wear Measurements on Governor Weights

The six governor weights mate with the thrust washer described in the previous section. A narrow wear scar is formed across the 12-mm width of each weight. The wear scar is triangular in cross section and was measured using a Talysurf surface profilometer. The tabulated results are the average derived from three individual traces along each wear scar.

Note: Approximate Contact Load = 2 kg

Vickers Hardness = 410

TABLE J-3. Wear Measurements on Governor Weights

<u>Pump</u>	<u>Wear Scar Dimensions</u>			<u>Wear Coefficient, K x 10⁻⁹</u>
	<u>Max Depth, mm x 10⁻³</u>	<u>Width, mm</u>	<u>Volume, mm³ x 10⁻³</u>	
Std (No. 3)	19	0.25	28.5	1.1
Arctic (No. 4)	19	0.325	37	1.4

Wear Measurements on Cam Roller Shoe

This wear scar is formed by a counterformal contact between the cam roller shoe and the pumping plunger. Little relative motion should occur other than due to vibration. The approximate sliding distance was calculated by assuming that the shoe vibrated once each time the roller strikes the cam ring. The amplitude of the movement is equal to the tolerance between the shoe and the slot in the hydraulic head after testing. The wear volume was approximated by assuming that pumping plunger is cone-shaped close to the area of contact. The tabulated result is an average value derived from both shoes on each pump. It should be noted that considerable variation existed between the two shoes on many of the pumps.

Note: Vickers Hardness = 730
Approximate Sliding Distance = 8.5 km
Total Contact Load During Injection = 57 kg

TABLE J-4. Wear Measurements on Cam Roller Shoe

<u>Pump</u>	<u>Scar Depth, mm x 10⁻³</u>	<u>Scar Diameter, mm</u>	<u>Volume, mm³ x 10⁻³</u>	<u>Wear Coefficient, K x 10⁻⁹</u>
Std (No. 3)	4.4	3.0	10.37	5
Arctic (No. 4)	4.0	3.15	10.39	5

Wear Measurements on Rotor Retainers

The wear scar is a circular ring and was formed by the motion of the pump rotor. The depth of the wear scar was measured using the Talysurf profilometer and the tabulated result is the average of four individual measurements. The depth of the wear scar was relatively constant in each measurement. The radial width of the wear scar was normally 2 mm, corresponding to the overlap between the pump rotor and the washers. However, only a portion of the apparent contact area was worn in the two pumps that operated with diesel fuel. The applied load was approximated from the end loading on the shaft due to the transfer pump pressure and opposing reaction force from the governor weights. End loading from the drive shaft will also be a contributing factor.

Note: Sliding Distance = 1425 km
Approximate Applied Load = 4 kg
Vickers Hardness = 560
Average Circumference = 66 mm

TABLE J-5. Wear Measurements on Rotor Retainers

<u>Pump</u>	<u>Max Depth, mm x 10⁻³</u>	<u>Width, mm²</u>	<u>Volume, mm³ x 10⁻³</u>	<u>Wear Coefficient, K x 10⁻⁹</u>
Std (No. 3)	0.6	1.8	71	2.3
Arctic (No. 4)	5.0	2.2	72.6	23.2

Wear Measurements on Drive Tang

A wedge-shaped wear scar is formed where the drive tang mates with the pump rotor. The maximum wear scar depth (at the deepest portion of the wedge) was measured using a micrometer and compared with unworn portions of the drive tang. The depth of the wear scar was then assumed to decrease linearly to zero at the opposite edge of the scar. The tabulated value is an average calculated from measurements taken from each side of the drive tang.

A single deviation of 0.1 mm is assumed to occur at the drive tang for each injection cycle, i.e., eight times per revolution. The contact load is calculated for an average radius of 0.25 inches at a torque of 250-inch pounds.*

Note: Approximate Applied Load = 250 kg
Sliding Distance = 17.2 km
Vickers Hardness = 650

TABLE J-6. Wear Measurements on Drive Tang

<u>Pump</u>	<u>Max Depth,</u> <u>mm x 10⁻³</u>	<u>Cont. Area,</u> <u>mm²</u>	<u>Volume,</u> <u>mm³ x 10⁻³</u>	<u>Wear Coefficient,</u> <u>K x 10⁻⁹</u>
Std (No. 3)	30	9.6	144	6.5
Arctic (No. 4)	25	3.69	46.1	1.2

* Hess, T. and Salzgeber, D., "The Stanadyne DB2 Distributor Pump for Medium Duty Diesels," Off-Highway Vehicle Meeting and Exposition MECCA, Milwaukee, WI 10-13 September 1979.

Wear Measurements on Drive Slot

The drive slot mates with the drive tang, the wear measurements for which are described in TABLE F-7. The maximum depth of each wear scar was measured using a Talysurf surface profilometer. The tabulated result is an average value derived from readings obtained on both sides of the slot. The contact area in each instance was taken from TABLE F-6. The depth of the wear scar was then assumed to decrease linearly to zero at the opposite edge of the scar and the wear volume calculated accordingly.

TABLE J-7. Wear Measurements on Drive Slot

<u>Pump</u>	<u>Max Depth, mm x 10⁻³</u>	<u>Final Area, mm²</u>	<u>Volume, mm³ x 10⁻³</u>	<u>Wear Coefficient, K x 10⁻⁹</u>
Std (No. 3)	13	9.6	124	4.8
Arctic (No. 4)	6	3.69	22.1	0.8

TABLE J-8. Visual Wear Level* on Critical Pump Components

<u>Component</u>	Standard	Arctic
	<u>8% Biodiesel</u>	<u>8% Biodiesel</u>
Distributor rotor	1	0
Delivery Valve	1	1
Pumping Plungers	4	4
Cam rollers & Shoes	2	2
Leaf Spring	1	1
Drive Shaft Tang	2	1
Cam	1	1
Governor Weights	1	1
Governur Thrust Sleeve	1	1
Pressure Regulator	1	2
Pressure Regulator Piston	2	2
Transfer Pump Blades	1	1
Liner	1	1
Rotor Retainers	1	1
Metering Valve	1	1
Advance Piston	2	2
Average:	1.35	1.29

* 0 = No Wear; 5 = Failure.

APPENDIX K

200-Hour Pump Stand Evaluation of Stanadyne Fuel Injection Pumps Using Fuel AL-24322

Preceding Page Blank

**Conducted by TFLRF
December 1995**

Fuel Analysis
AL-24322

Fuel Composition

Jet A-1 99%
Biodiesel 1%

Properties

Kvis, 40°C, cSt, D445 1.04

Water, Karl Fischer, ppm 114

TAN, D664 0.05

Distillation, D86

°C@ % off

1	165
10	169
20	172
30	175
40	177
50	179
60	181
70	184
80	187
90	193
95	198

Residue, %v 1.4

Lubricity, HFRR Wear, mm 0.34

Preceding Page Blank

Pump Stand Test Conditions

Duration, hours	200
Speed, RPM, Full Rack	1800
Inlet Fuel Pressure, psi	3.0 max
Inlet Fuel Temperature, °F	165-170 max
Reservoir Fuel Temperature, °F	100 max

Test Operation Notes

Both pumps seized on startup after 46 hours, due to improper startup procedure. The head, rotor assembly, and drive tang were replaced with used parts that had accumulated 200 hours in previous tests. These replacement parts were in "as-new" condition. The 200 hour test was completed without further interruption.

**Pump Calibration
Additive Evaluation Project**

Pump Type: DB2-4524 (STD.) "C" left pump	SN: 8239196
Test description: CT-JET A-1+1% BIODIESEL (200hrs)	AL: 23890

<i>RPM</i>	<i>Parameter/Spec</i>	<i>Before</i>	<i>After</i>	<i>Change (After - Before)</i>
1000	TPP 70-76 psi	75	72	-3
	Hsg. 8-12 psi	10	10	0
	Adv. 1.5 deg.	1.5	.75	-.75
	Ret. Fuel 225-375 cc	300	300	0
	Fuel Del. 51-55 cc	55	51	-4
325	Low Idle 12-116 cc	15	40	+25
	Adv. 1.5 min	3.75	2	-1.75
	CAS 0-1 deg.	0	0	0
	Adv. 2.75 deg. min	5	4°	-1
750	FC 21.5 - 23.5 cc	22	22	0
	Adv. 3.5 deg.	3.5	4°	+0.5
1800	Fuel Del. 46 cc min.	54.5	52	-2.5
	TPP	112	100	-12
	Housing psi	10	10	0
1950	Fuel Del. 44 cc min.	51.5	52	0.5
2100	High Idle 8 cc max.	0	0	0
	TPP 135 psi max.	136	122	-14
200	Fuel Del. 47 cc min.	48.5	46	-2.5
	Shut-Off 4 cc max.	0	0	0
75	Fuel Del. 29 cc min.	37.5	35	-2.5
	TPP 12 psi min.	30	24	-6
	Airtime + 0.25	+ 0.25	+ 0.25	0
	Deg. C	45	45	
	Date	09/04/95	12/13/95	

**Pump Calibration
Additive Evaluation Project**

Pump Type: DB2-4523 (ARC.) "D" right pump	SN: 8164639
Test description: CT-JET A-1+1% BIODIESEL (200hrs)	AL: 23887

<i>RPM</i>	<i>Parameter/Spec</i>	<i>Before</i>	<i>After</i>	<i>Change (After - Before)</i>
1000	TPP 70-76 psi	75	74	-1
	Hsg. 8-12 psi	10	10	0
	Adv. 1.5 deg.	1.5	1.5	0
	Ret. Fuel 225-375 cc	325	300	-25
	Fuel Del. 51-55 cc	54	54	-1
325	Low Idle 12-16 cc	15	50	+35
	Adv. 1.5 min	3.5	2.5	-1.0
	CAS 0-1 deg.	0	0	0
	Adv. 2.75 deg. min	5°	4°	-1
750	FC 21.5 - 23.5 cc	22.5	22	- 0.5
	Adv. 3.5 deg.	3.5	4	+0.5
1800	Fuel Del. 46 cc min.	55.5	54	-1.5
	TPP	110	105	-5
	Housing psi	10	10	0
1950	Fuel Del. 44 cc min.	53	55	+2
2100	High Idle 8 cc max.	0	0	0
	TPP 135 psi max.	138	126	-12
200	Fuel Del. 47 cc min.	49.5	50	+0.5
	Shut-Off 4 cc max.	0	0	0
75	Fuel Del. 29 cc min.	37.5	44	+6.5
	TPP 12 psi min.	22	22	-0
	Airtime + 0.25	+ 0.25	+ 0.25	0
	Deg. C	44.5	43	
	Date	09/04/95	12/13/95	

Wear Measurements on Transfer Pump Blades

A reciprocating action is formed between the rotor and the transfer pump blade. This action forms a wear scar with a sharp step at the limit of the cycle. The depth of the wear scar was measured at this step using a Talysurf 10 profilometer. Scar depth was assumed to decrease linearly across the contact area, and the wear volume was calculated accordingly. An improved metallurgy is available in the arctic pump vanes and the appropriate indentation hardness was used in calculating Archards wear coefficient. The cumulative sliding distance was calculated for an eccentricity of 4 mm.

Note:	Hardness of Arctic Pump Vanes (Hv)	=	750
	Hardness of Standard Pump Vanes (Hv)	=	460
	Sliding Distance in 200 Hours	=	173 km
	Approximate Contact Load	=	0.36 kg

TABLE K-1. Wear Measurements on Transfer Pump Blades

<u>Pump</u>	<u>Wear Scar Dimensions</u>			<u>Wear Coefficient, K x 10⁻⁹</u>
	<u>Max Depth, mm x 10⁻³</u>	<u>Final Area, mm²</u>	<u>Volume, mm³ x 10⁻³</u>	
STD (No. 5)	0	--	0	0
Arctic (No. 6)	1.4	11	7.7	33

Wear Measurements on Governor Thrust Washer

This is a wear ring formed by the action of the six governor weights on the governor thrust washer. The average depth of the wear scar was measured using a Talysurf profilometer and was found to be approximately constant around the complete circumference. The applied load was derived from the thrust required to counteract centripetal force on each governor weight at 1800 rpm. The indentation hardness of both the arctic and standard components were similar.

Note: Hardness of Both Arctic and Standard Parts (Hv) = 670

Cumulative Sliding Distance	= 388 km
Approximate Contact Load	= 2 kg
Circumference of Contact	= 83.2 mm

TABLE K-2. Wear Measurements on Governor Thrust Washer

<u>Pump</u>	<u>Scar Depth, mm x 10⁻³</u>	<u>Scar Width, mm²</u>	<u>Volume, mm³ x 10⁻³</u>	<u>Wear Coefficient, K x 10⁻⁹</u>
STD (No. 5)	0.7	2.0	116.6	33.2
Arctic (No. 6)	0.2	1.8	29.99	8.6

Wear Measurements on Governor Weights

The six governor weights mate with the thrust washer described in the previous section. A narrow wear scar is formed across the 12-mm width of each weight. The wear scar is triangular in cross section and was measured using a Talysurf surface profilometer. The tabulated results are the average derived from three individual traces along each wear scar.

Note: Approximate Contact Load = 2 kg

Vickers Hardness = 410

TABLE K-3. Wear Measurements on Governor Weights

Pump	Wear Scar Dimensions			Wear Coefficient, K x 10 ⁻⁹
	Max Depth, mm x 10 ⁻³	Width, mm ²	Volume, mm ³ x 10 ⁻³	
STD (No. 5)	13	0.225	17.55	0.6
Arctic (No. 6)	22	0.375	49.5	1.8

Wear Measurements on Cam Roller Shoe

This wear scar is formed by a counterformal contact between the cam roller shoe and the pumping plunger. Little relative motion should occur other than due to vibration. The approximate sliding distance was calculated by assuming that the shoe vibrated once each time the roller strikes the cam ring. The amplitude of the movement is equal to the tolerance between the shoe and the slot in the hydraulic head after testing. The wear volume was approximated by assuming that pumping plunger is cone-shaped close to the area of contact. The tabulated result is an average value derived from both shoes on each pump. It should be noted that considerable variation existed between the two shoes on many of the pumps.

Note: Vickers Hardness = 730
Approximate Sliding Distance = 8.5 km
Total Contact Load During Injection = 57 kg

TABLE K-4. Wear Measurements on Cam Roller Shoe

<u>Pump</u>	<u>Scar Depth,</u> <u>mm x 10⁻³</u>	<u>Scar Diameter,</u> <u>mm²</u>	<u>Volume,</u> <u>mm³ x 10⁻³</u>	<u>Wear Coefficient,</u> <u>K x 10⁻⁹</u>
STD (No. 5)	3.6	2.55	6.13	3
Arctic (No. 6)	8.0	2.75	16.19	8

Wear Measurements on Rotor Retainers

The wear scar is a circular ring and was formed by the motion of the pump rotor. The depth of the wear scar was measured using the Talysurf profilometer and the tabulated result is the average of four individual measurements. The depth of the wear scar was relatively constant in each measurement. The radial width of the wear scar was normally 2 mm, corresponding to the overlap between the pump rotor and the washers. The applied load was approximated from the end loading on the shaft due to the transfer pump pressure and opposing reaction force from the governor weights. End loading from the drive shaft will also be a contributing factor.

Note: Sliding Distance = 1425 km
Approximate Applied Load = 4 kg
Vickers Hardness = 560
Average Circumference = 66 mm

TABLE K-5. Wear Measurements on Rotor Retainers

<u>Pump</u>	<u>Max Depth,</u> <u>mm x 10⁻³</u>	<u>Width,</u> <u>mm</u>	<u>Volume,</u> <u>mm³ x 10⁻³</u>	<u>Wear Coefficient,</u> <u>K x 10⁻⁹</u>
STD (No. 5)	11.5	2.3	1745	55.8
Arctic (No. 6)	5.0	2.1	693	22.1

Wear Measurements on Drive Tang

A wedge-shaped wear scar is formed where the drive tang mates with the pump rotor. The maximum wear scar depth (at the deepest portion of the wedge) was measured using a micrometer and compared with unworn portions of the drive tang. The depth of the wear scar was then assumed to decrease linearly to zero at the opposite edge of the scar. The tabulated value is an average calculated from measurements taken from each side of the drive tang.

A single deviation of 0.1 mm is assumed to occur at the drive tang for each injection cycle, i.e., eight times per revolution. The contact load is calculated for an average radius of 0.25 inches at a torque of 250-inch pounds.*

Note: Approximate Applied Load = 250 kg
Sliding Distance = 17.2 km
Vickers Hardness = 650

TABLE K-6. Wear Measurements on Drive Tang

<u>Pump</u>	<u>Max Depth, mm x 10⁻³</u>	<u>Cont. Area, mm²</u>	<u>Volume, mm³ x 10⁻³</u>	<u>Wear Coefficient, K x 10⁻⁹</u>
STD (No. 5)	20	8.97	90	3.8
Arctic (No. 6)	40	11.33	226	5.6

* Hess, T. and Salzgeber, D., "The Stanadyne DB2 Distributor Pump for Medium Duty Diesels," Off-Highway Vehicle Meeting and Exposition MECCA, Milwaukee, WI, 10-13 September 1979.

Wear Measurements on Drive Slot

The drive slot mates with the drive tang, the wear measurements for which are described in TABLE F-7. The maximum depth of each wear scar was measured using a Talysurf surface profilometer. The tabulated result is an average value derived from readings obtained on both sides of the slot. The contact area in each instance was taken from TABLE F-6. The depth of the wear scar was then assumed to decrease linearly to zero at the opposite edge of the scar and the wear volume calculated accordingly.

TABLE K-7. Wear Measurements on Drive Slot

<u>Pump</u>	<u>Max Depth, mm x 10⁻³</u>	<u>Cont. Area, mm²</u>	<u>Volume, mm³ x 10⁻³</u>	<u>Wear Coefficient, K x 10⁻⁹</u>
STD (No. 5)	8	8.97	71.7	2.7
Arctic (No. 6)	25	11.33	283	10.8

TABLE K-8. Visual Wear Level^a on Critical Pump Components

<u>Biodiesel</u>	<u>Standard Component</u>	<u>Arctic 1% Biodiesel</u>	<u>1%</u>
	Distributor rotor	1*	1*
	Delivery Valve	1	1
	Pumping Plungers	4*	2*
	Cam rollers & Shoes	2	2
	Leaf Spring	1	1
	Drive Shaft Tang	1*	1*
	Cam	1	1
	Governor Weights	1	2
	Governor Thrust Washer	1	2
	Governor Thrust Sleeve	1	1
	Pressure Regulator	1	2
	Pressure Regulator Piston	3	2
	Transfer Pump Blades	2	1
	Liner	2	2
	Rotor Retainers	2	2
	Metering Valve	2	2
	Advance Piston	3	3
	Average:	1.70	1.64

a 0=No Wear; 5=Failure.

* Denotes used part

DISTRIBUTION LIST

Department of Defense

DEFENSE TECH INFO CTR ATTN: DTIC OCC 8725 JOHN J KINGMAN RD STE 0944 FT BELVOIR VA 22060-6218	12	JOAP TSC BLDG 780 NAVAL AIR STA PENSACOLA FL 32508-5300	1
ODUSD ATTN: (L) MRM PETROLEUM STAFF ANALYST PENTAGON WASHINGTON DC 20301-8000	1	DIR DLA ATTN: DLA MMSLP 8725 JOHN J KINGMAN RD STE 2533 FT BELVOIR VA 22060-6221	1
ODUSD ATTN: (ES) CI 400 ARMY NAVY DR STE 206 ARLINGTON VA 22202	1	CDR DEFENSE FUEL SUPPLY CTR ATTN: DFSC I (C MARTIN) DFSC IT (R GRAY) DFSC IQ (L OPPENHEIM) 8725 JOHN J KINGMAN RD STE 2941 FT BELVOIR VA 22060-6222	1 1 1
HQ USEUCOM ATTN: ECJU LIJ UNIT 30400 BOX 1000 APO AE 09128-4209	1	DIR DEFENSE ADV RSCH PROJ AGENCY ATTN: ARPA/ASTO 3701 N FAIRFAX DR ARLINGTON VA 22203-1714	1
US CINCPAC ATTN: J422 BOX 64020 CAMP H M SMITH HI 96861-4020	1		

Department of the Army

HQDA ATTN: DALO TSE DALO SM 500 PENTAGON WASHINGTON DC 20310-0500	1 1	CDR ARMY TACOM ATTN: AMSTA IM LMM AMSTA IM LMB AMSTA IM LMT AMSTA TR NAC MS 002 AMSTA TR R MS 202 AMSTA TR D MS 201A AMSTA TR M AMSTA TR R MS 121 (C RAFFA) AMSTA TR R MS 158 (D HERRERA) AMSTA TR R MS 121 (R MUNT) AMCPM ATP MS 271 AMSTA TR E MS 203 AMSTA TR K AMSTA IM KP AMSTA IM MM AMSTA IM MT AMSTA IM MC AMSTA IM GTL AMSTA CL NG USMC LNO AMCPM LAV AMCPM M113 AMCPM CCE WARREN MI 48397-5000	1 1
SARDA ATTN: SARD TT PENTAGON WASHINGTON DC 20310-0103	1		
CDR AMC ATTN: AMCRD S AMCRD E AMCRD IT AMCEN A AMCLG M AMXLS H 5001 EISENHOWER AVE ALEXANDRIA VA 22333-0001	1 1 1 1 1 1		
CDR U S ARMY SOLDIER SYSTEM COMMAND ATTN AMSS YM (H SCHREUDER-GIBSON) NATICK MA 01760-5018			

U.S. Army TACOM		VEHICLE PROPULSION DIR	
ATTN: AMSTA TR-R/210 (Luis Villahermosa)	10	ATTN: AMSRL VP (MS 77 12)	1
AMSTA TR-R/210 (T. Bagwell)	1	NASA LEWIS RSCH CTR	
10115 GRIDLEY RD STE 128		21000 BROOKPARK RD	
FT BELVOIR VA 22060-5843		CLEVELAND OH 44135	
MOBILITY TECH CTR BELVOIR		CDR AMSAA	
ATTN AMSTA RBFF (TOM BOWEN)		ATTN: AMXSY CM	1
10115 GRIDLEY RD STE 128		AMXSY L	1
FT. BELVOIR VA 22060-5843		APG MD 21005-5071	
PROG EXEC OFFICER		CDR ARO	
ARMORED SYS MODERNIZATION		ATTN: AMXRO EN (D MANN)	1
ATTN: SFAE ASM S	1	RSCH TRIANGLE PK	
SFAE ASM H	1	NC 27709-2211	
SFAE ASM AB	1	CDR AEC	
SFAE ASM BV	1	ATTN: SFIM AEC ECC (T ECCLES)	1
SFAE ASM CV	1	APG MD 21010-5401	
SFAE ASM AG	1	CDR ARMY ATCOM	
CDR TACOM		ATTN: AMSAT I WM	1
WARREN MI 48397-5000		AMSAT I ME (L HEPLER)	1
PROG EXEC OFFICER		AMSAT I LA (V SALISBURY)	1
ARMORED SYS MODERNIZATION		AMSAT R EP (V EDWARD)	1
ATTN: SFAE FAS AL	1	4300 GOODFELLOW BLVD	
SFAE FAS PAL	1	ST LOUIS MO 63120-1798	
PICATINNY ARSENAL		CDR ARMY SOLDIER SPT CMD	
NJ 07806-5000		ATTN: SATNC US (J SIEGEL)	1
PROG EXEC OFFICER		SATNC UE	1
TACTICAL WHEELED VEHICLES		SATNC-YM	3
ATTN: SFAE TWV TVSP	1	NATICK MA 01760-5018	
SFAE TWV FMTV	1	CDR ARMY ARDEC	
SFAE TWV PLS	1	ATTN: AMSTA AR EDE S	1
CDR TACOM		PICATINNY ARSENAL	
WARREN MI 48397-5000		NJ 07808-5000	
PROG EXEC OFFICER		CDR ARMY WATERVLIET ARSN	
ARMAMENTS		ATTN: SARWY RDD	1
ATTN: SFAE AR HIP	1	WATERVLIET NY 12189	
SFAE AR TMA	1	CDR APC	
PICATINNY ARSENAL		ATTN: SATPC L	1
NJ 07806-5000		SATPC Q	1
PROG MGR		NEW CUMBERLAND PA 17070-5005	
UNMANNED GROUND VEH		PETROL TEST FAC WEST	1
ATTN: AMCPM UG	1	BLDG 247 TRACEY LOC	
REDSTONE ARSENAL		DDRW	
AL 35898-8060		P O BOX 96001	
DIR		STOCKTON CA 95296-0960	
ARMY RSCH LAB		CDR ARMY LEA	
ATTN: AMSRL PB P	1	ATTN: LOEA PL	1
2800 POWDER MILL RD		NEW CUMBERLAND PA 17070-5007	
ADELPHIA MD 20783-1145			

CDR ARMY TECOM		CDR ARMY TRANS SCHOOL	
ATTN: AMSTE TA R	1	ATTN: ATSP CD MS	1
AMSTE TC D	1	FT EUSTIS VA 23604-5000	
AMSTE EQ	1		
APG MD 21005-5006		CDR ARMY INF SCHOOL	
		ATTN: ATSH CD	1
		ATSH AT	1
		FT BENNING GA 31905-5000	
PROJ MGR PETROL WATER LOG			
ATTN: AMCPM PWL	1	CDR ARMY AVIA CTR	
4300 GOODFELLOW BLVD		ATTN: ATZQ DOL M	1
ST LOUIS MO 63120-1798		ATZQ DI	1
		FT RUCKER AL 36362-5115	
PROJ MGR MOBILE ELEC PWR			
ATTN: AMCPM MEP T	1	CDR ARMY ENGR SCHOOL	
AMCPM MEP L	1	ATTN: ATSE CD	1
7798 CISSNA RD STE 200		FT LEONARD WOOD	
SPRINGFIELD VA 22150-3199		MO 65473-5000	
CDR		CDR 49TH QM GROUP	
ARMY COLD REGION TEST CTR		ATTN: AFFL GC	1
ATTN: STECR TM	1	FT LEE VA 23801-5119	
STECR LG	1		
APO AP 96508-7850			
		CDR ARMY ORDN CTR	
CDR		ATTN: ATSL CD CS	1
ARMY BIOMED RSCH DEV LAB		APG MD 21005	
ATTN: SGRD UBZ A	1		
FT DETRICK MD 21702-5010		CDR ARMY SAFETY CTR	
		ATTN: CSSC PMG	1
CDR FORSCOM		CSSC SPS	1
ATTN: AFLG TRS	1	FT RUCKER AL 36362-5363	
FT MCPHERSON GA 30330-6000			
		CDR ARMY ABERDEEN TEST CTR	
CDR TRADOC		ATTN: STEAC EN	1
ATTN: ATCD SL 5	1	STEAC LI	1
INGALLS RD BLDG 163		STEAC AE	1
FT MONROE VA 23651-5194		STEAC AA	1
		APG MD 21005-5059	
CDR ARMY ARMOR CTR			
ATTN: ATSB CD ML	1	CDR ARMY YPG	
ATSB TSM T	1	ATTN: STEYP MT TL M	1
FT KNOX KY 40121-5000		YUMA AZ 85365-9130	
CDR ARMY QM SCHOOL		CDR ARMY CERL	
ATTN: ATSM PWD	1	ATTN: CECER EN	1
FT LEE VA 23001-5000		P O BOX 9005	
		CHAMPAIGN IL 61826-9005	
ARMY COMBINED ARMS SPT CMD			
ATTN: ATCL CD	1	DIR	1
ATCL MS	1	AMC FAST PROGRAM	
ATCL MES (C PARENT)	1	10101 GRIDLEY RD STE 104	
FT LEE VA 23801-6000		FT BELVOIR VA 22060-5818	
CDR ARMY FIELD ARTY SCH		CDR I CORPS AND FT LEWIS	
ATTN: ATSF CD	1	ATTN: AFZH CSS	1
FT SILL OK 73503		FT LEWIS WA 98433-5000	

CDR
RED RIVER ARMY DEPOT
ATTN: SDSRR M 1
SDSRR Q 1
TEXARKANA TX 75501-5000

PS MAGAZINE DIV
ATTN: AMXLS PS 1
DIR LOGSA
REDSTONE ARSENAL AL 35898-7466

CDR 6TH ID (L)
ATTN: APUR LG M 1
1060 GAFFNEY RD
FT WAINWRIGHT AK 99703

Department of the Navy

OFC CHIEF NAVAL OPER
ATTN: DR A ROBERTS (N420) 1
2000 NAVY PENTAGON
WASHINGTON DC 20350-2000

CDR
NAVAL SEA SYSTEMS CMD
ATTN: SEA 03M3 1
2531 JEFFERSON DAVIS HWY
ARLINGTON VA 22242-5160

CDR
NAVAL SURFACE WARFARE CTR
ATTN: CODE 63 1
CODE 632 1
CODE 859 1
3A LEGGETT CIRCLE
ANNAPOLIS MD 21402-5067

CDR
NAVAL RSCH LABORATORY
ATTN: CODE 6181 1
WASHINGTON DC 20375-5342

CDR
NAVAL AIR WARFARE CTR
ATTN: CODE PE33 AJD 1
P O BOX 7176
TRENTON NJ 08628-0176

CDR 1
NAVAL PETROLEUM OFFICE
8725 JOHN J KINGMAN RD
STE 3719
FT BELVOIR VA 22060-6224

CDR
NAVAL AIR SYSTEMS CMD
ATTN: AIR 4.4.5 (D MEARNES) 1
1421 JEFFERSON DAVIS HWY
ARLINGTON VA 22243-5360

Department of the Navy/U.S. Marine Corps

HQ USMC
ATTN: LPP 1
WASHINGTON DC 20380-0001

PROG MGR COMBAT SER SPT 1
MARINE CORPS SYS CMD
2033 BARNETT AVE STE 315
QUANTICO VA 22134-5080

PROG MGR GROUND WEAPONS 1
MARINE CORPS SYS CMD
2033 BARNETT AVE
QUANTICO VA 22134-5080

PROG MGR ENGR SYS 1
MARINE CORPS SYS CMD
2033 BARNETT AVE
QUANTICO VA 22134-5080

CDR
MARINE CORPS SYS CMD
ATTN: SSE 1
2030 BARNETT AVE STE 315
QUANTICO VA 22134-5010

CDR
BLOUNT ISLAND CMD
ATTN: CODE 922/1
5880 CHANNEL VIEW BLVD
JACKSONVILLE FL 32226-3404

1

CDR
MARINE CORPS LOGISTICS BA
ATTN: CODE 837
814 RADFORD BLVD
ALBANY GA 31704-1128

1

CDR
2ND MARINE DIV
PSC BOX 20090
CAMP LEJEUNE
NC 28542-0090

1

CDR
1ST MARINE DIV
CAMP PENDLETON
CA 92055-5702

1

CDR
FMFPAC G4
BOX 64118
CAMP H M SMITH
HI 96861-4118

1

Department of the Air Force

HQ USAF/LGSF
ATTN: FUELS POLICY
1030 AIR FORCE PENTAGON
WASHINGTON DC 20330-1030

1

SA ALC/SFT
1014 BILLY MITCHELL BLVD STE 1
KELLY AFB TX 78241-5603

1

HQ USAF/LGTV
ATTN: VEH EQUIP/FACILITY
1030 AIR FORCE PENTAGON
WASHINGTON DC 20330-1030

1

SA ALC/LDPG
ATTN: D ELLIOTT
580 PERRIN BLDG 329
KELLY AFB TX 78241-6439

1

AIR FORCE WRIGHT LAB
ATTN: WL/POS
WL/POSF
1790 LOOP RD N
WRIGHT PATTERSON AFB
OH 45433-7103

1

1

WR ALC/LVRS
225 OCMULGEE CT
ROBINS AFB
GA 31098-1647

1

AIR FORCE MEEP MGMT OFC
OL ZC AFMC LSO/LOT PM
201 BISCAYNE DR
BLDG 613 STE 2
ENGLIN AFB FL 32542-5303

1

Other Federal Agencies

NASA
LEWIS RESEARCH CENTER
CLEVELAND OH 44135

1

RAYMOND P. ANDERSON, PH.D., MANAGER
FUELS & ENGINE TESTING
BDM-OKLAHOMA, INC.
220 N. VIRGINIA
BARTLESVILLE OK 74003

1

DOT
FAA
AWS 110
800 INDEPENDENCE AVE SW
WASHINGTON DC 20590

1

DOE
CE 151 (MR RUSSELL)
1000 INDEPENDENCE AVE SW
WASHINGTON DC 20585

1

U S DEPARTMENT OF AGRICULTURE
ATTN USDA CSRS SP (MS CARMELA BAILEY) 10
901 D STREET SW STE 342
WASHINGTON DC 20250-2260

EPA
AIR POLLUTION CONTROL
2565 PLYMOUTH RD
ANN ARBOR MI 48105

1